Synthesis of Glycerol Based Fuel Additives to Reduce NO*x* Emissions from Diesel Engines Operated on Diesel and Biodiesel fuels by SNCR

Von der Fakultät für Lebenswissenschaften

der Technischen Universität Carolo-Wilhelmina

zu Braunschweig

zur Erlangung des Grades eines

Doktors der Naturwissenschaften

(Dr. rer. nat.)

genehmigte

D i s s e r t a t i o n

von **Shravan. Kumar Tanugula**

aus Karimnagar/Indian

1. Referent: Prof. Dr. Henning Hopf

2. Referent: Prof. Dr. Jürgen Krahl

eingereicht am: 07.06.2010

mündliche Prüfung (Disputation) am: 28.09.2010

Druckjahr: 2010

Dedicated to all those who provided me with

Social, Moral and Scientific education

It is my great pleasure to express my sincere gratitude to **Prof. Dr. Dr. h.c. Henning Hopf** for his support, encouragement and guidance throughout this research work. I thank him a lot for his invaluable ideas and remarks which made this study very interesting. I admire deep from my heart his energetic way of working and his brilliant ideas which made possible this research work to cover a vast area. I thank him for the freedom he gave and for the joy and satisfaction he shared with me during the course of my stay in Braunschweig.

I am deeply thankful to **Prof. Dr. Jürgen Krahl**, for his valuable discussions and help which made this study take a better shape. I am grateful to him for his invaluable advice, critical remarks and innumerable help that he rendered. I am thankful to him for agreeing to be the co-referee of my thesis. I am thankful to Mr. Olaf Schröder, from the Institute of Agricultural Technology and Biosystems Engineering**,** vTI, Braunschweig, for the engine experiments.

I offer my sincere thanks to the members of the Institute of Organic Chemistry, especially to Prof. Dr. P. G. Jones for the X-ray structure analyses; Prof. Dr. L. Ernst and Ms. P. Holba-Schulz for high resolution and 2D NMR spectra; Ms. K. Kadim for UV and IR spectra; Ms. D. Döring and Dr. U. Papke for MS; Dr. T. Beuerle for GC/MS, Dr. J. Grunenberg for theoretical calculations and Dr. U. Jahn for his valuable discussions. I also thank all the non-teaching staff members of the chemistry department for their help.

My sincere thanks to my colleagues and friends, especially to Mr. M. Szmatola, Ms. A. Carjila, Mr. H. Berger, Dr. P. Tankam, Dr. Z. Hussain, Dr. A. Keecherikunnel and Dr. R. Menon for all their help and valuable discussions and making my stay in Braunschweig a pleasant one. I sincerely thank Ms. Salomon and Ms. Weiss for their care and support.

I sincerely express my indebtedness to **VDB** for their financial support.

Contents *Page*

Page

Chapter 1: Introduction

1.1: History of glycerol

Nature makes glycerol (1,2,3-propanetriol) as a widely distributed hydroxylic alcohol in combination with fats and other lipids which are essential for life processes. Glycerol has been known to humans as early as 2800 BC from the saponification of fats.[1, 2] Chemically glycerol was discovered in 1779 by the Swedish chemist C. W. Scheele, during the saponification of olive oil with lead oxide. Until the 20th century, glycerol was obtained almost always as a byproduct from the manufacture of soap. In 1811, the French chemist Michel Eugène Chevreul, a pioneer in the chemical analysis of fats, introduced the name "glycerol", which is derived from the Greek (*glycos*) meaning sweet.[3, 4] Chevreul was the first scientist to note that glycerol could be obtained by saponification of fats and oils. He discovered that all animal fats break down into fatty acids and glycerol by hydrolysis. Coconut and palm oils, tallow and Soya oil contain 17 %, 11 %, 10 % and 10 % glycerol respectively, making it a part and parcel of our daily dietary intake. It also occurs in egg yolk, brain tissue, blood cells, bile and neural tissue. Glycerol is also formed to a lesser extent during alcoholic fermentation.

Although most glycerol is still produced along with soap, large quantities are synthesized from propylene.[5] In 1836, Pelouze came up with the empirical composition and in 1871, Charles Friedel who conducted the first thorough research on alcohols, discovered a method for synthesizing glycerol from propylene.[6, 7] Since the late 1940ies when synthetic detergents dominated the market, particularly in the USA, there was no longer enough fatty acid-based glycerol to meet the demand, and glycerol **(2)** was produced synthetically from epichlorohydrin **(1)** obtained from propylene (Scheme 1).[7]

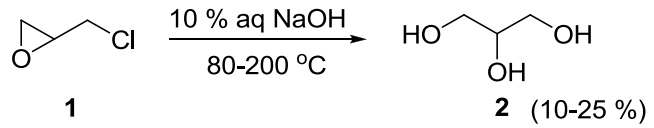

1 **2** (10-25 %)

Scheme 1: Synthesis of glycerol **(2)** from epichlorohydrin

1.2: Physical properties[3, 4]

Glycerol **(2)** is a sweet-tasting hygroscopic, colorless, odorless viscous liquid. The extreme wide range of uses for glycerol is due to its large measure of unique combination of physical properties, which made it possible to end up virtually in every field of research and technology.

Boiling point: The boiling point of glycerol **(2)** is 290 ^{o}C at atmospheric pressure. With some liquids, glycerol forms azeotropic solutions (e.g. water). The freezing point of glycerol is 18 ^{o}C. Because of its strong tendency of supercooling the crystalline state is hardly ever reached. However, a glassy state can be reached at -70 to -100 ^{o}C;[8] glycerol can be crystallized at 0 ^{o}C by seeding with glycerol crystals.

Specific Gravity: specific gravity is the means by which glycerol purity is determined using a pycnometer; for 100 % pure glycerol at 15.4 ^{o}C Bostart and Snoddy have found the following specific gravity: 1.26415.[9]

Density: Bostart and Snoddy[10] have calculated the density of glycerol at various concentrations from the specific gravity data, for 100 % glycerol at 0 ^{o}C (1.27269 g/mL), at 20 ^{o}C (1.26134 g/mL) and at its boiling point (1.05969 g/mL) has been obtained, respectively.[11]

Vapor Pressure: Due to the molecular association characteristic of alcohols, glycerol **(2)** shows much lower vapor pressure than expected from its molecular weight. The vapor pressure of pure glycerol at room temperature is below 0.001 mmHg and at 100 ^{o}C it is below 0.2 mmHg.[12] The most accurate vapor pressure of pure glycerol was calculated by extrapolation of the partial pressure in solution to the point where partial pressure equals the total pressure with an error of 1 %.[13] The vapor pressure of glycerol in aqueous solutions can be calculated according to Duhring's rule.[14]

Hygroscopicity: Glycerol solutions at any concentration can accumulate moisture until equilibrium is reached with its surrounding. Different case studies were made corresponding to the relative moisture content and amount of water absorbed or released by glycerol solution. In one case when a glycerol solution with 80 % glycerol and water was introduced into a chamber with 40 % relative humidity,[3] the total concentration of glycerol reached 86 %, releasing water to the atmosphere. When pure glycerol (100 g) was introduced into a

chamber with 80 % relative humidity, 28 % water was absorbed from the atmosphere achieving a total weight of 128 g. Temperature change has very little impact on the equilibrium. Pure glycerol has a high affinity towards moisture which makes it suitable to use as plasticizer and as a humectants.

Viscosity: The viscosity of pure glycerol at 20 ^{o}C amounts to 1410 centipoises; a very precise study was performed by Segar and Oberstar[15] covering a whole range of measurements from 0-100 ^{o}C and concentration of 0-100 wt % of glycerol in water.[16]

Refractive Index: The refractive index of pure glycerol n_D^{20} is 1.47399,[3] which is mostly used for the determination of concentration of glycerol up to 0.1 % accuracy.

Solubility: The solubility of glycerol is dominated by the hydroxyl groups. The work by Jackson and Drury[17] covers a wide range of organic solvents and their miscibility with glycerol and it concludes that introduction of amine or hydroxyl group into aliphatic or aromatic hydrocarbon increases the solubility of glycerol. In most of the organic solvents glycerol is immiscible including acetone; it is soluble in *o*-cresol, diethylenetriamine, DMF, diisopropylamine, ethanol, *o*-methylbenzylamine, pyridine etc. and partially soluble in di-*n*-amylamine and di-*n*-butylamine.

Surface Tension: The surface tension of pure glycerol amounts to 63.4 dynes/cm at 20 ^{o}C and 51.9 dynes/cm at 150 ^{o}C, which is less than that of water.[3]

Flash and fire point, auto ignition temperature: The flash point of 99 % glycerol is 177 ^{o}C and the fire point is 204 ^{o}C. According to the procedure described in test D 92-33 of the American Society for Testing Materials (ASTM) the auto ignition temperature of glycerol is 523 ^{o}C on platinum and 429 ^{o}C on glass.[18]

1.3: Production of glycerol

1.3.1: Glycerol from fats and oils

The glycerol content of fats and oils varies between 8 and 14 wt %, depending on the proportion of free acid and on the chain length distribution of the fatty acid esters.[2] Glycerol is obtained by hydrolysis of oils and fats, by either of the following methods.

1.3.1.1: Fat splitting

Natural glycerol today is mainly produced by high-pressure splitting and transesterification. High-pressure splitting has been known since 1854; glycerol from the saponification of oils is performed only in small quantities. Continuous process reactors are used presently where water and fat are fed in counter current into a splitting column at 20-60 bar and 220-260 ^{o}C. The hydrolysis occurs in homogenous fashion by the dissolved water, separating glycerol and fatty acids. The reaction takes place in step wise fashion forming glycerol, monoglycerides and diglycerides, as shown in Fig. 1. Using different distillation methods the free fatty acid is separated from the glycerol water mixture, the remaining glycerol water mixture is commercially known as "sweet water", a 15 % solution of glycerol in water.[19]

1.3.1.2: Transesterification

Natural crude glycerol can be obtained by transesterification of oils and fats to their methyl esters (biodiesel).[20] Glycerol from the low pressure transesterification process has a much higher salt content (2–5 %). The crude glycerol is obtained directly in a concentration of ca. 90–92 %.

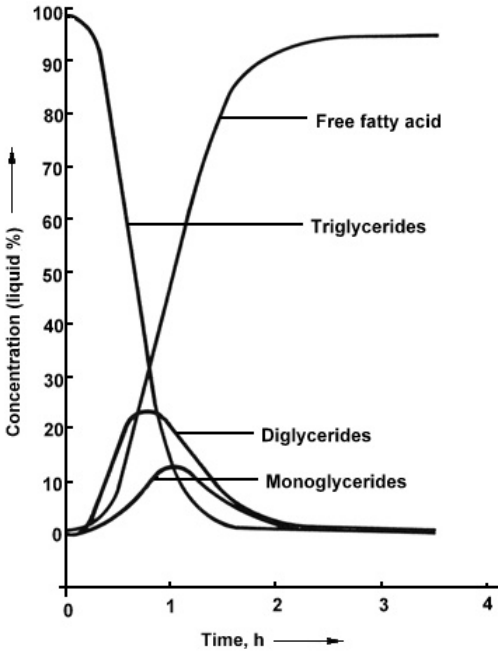

Fig. 1: Typical course of a fat hydrolysis at 235 ^{o}C and 35 bar using oil and water in 1:2 ratio.[4]

Today the production of glycerol by transesterification of fats and oils to the corresponding methyl esters has reached a pinnacle and has become a major source of glycerol production.[4]

1.3.1.3: Pretreatment and concentration of crude glycerol (2)

The most important step for the trouble free production of glycerol **(2)** ensuring high quality of the final product **2** involves pretreatment of glycerol water. The slightly acidic glycerol water produced by high-pressure hydrolysis contains dispersed fat and fatty acid components which are largely removed by settling or by centrifugation. In a subsequent step the concentration is increased to 70-90 % of **2** to avoid decomposition.[1] This main pretreatment takes place directly before final purification and refining following the addition of activated charcoal for bleaching and sodium hydroxide to saponify any remaining fat components. A separation by filtration follows each step. The soda-lime process is an age old process used for the pretreatment of crude glycerol.[2] Thus treated crude glycerol is further concentrated by distillation. Single or multiple-step plants are used applying a vacuum of 0.1-0.15 bar.

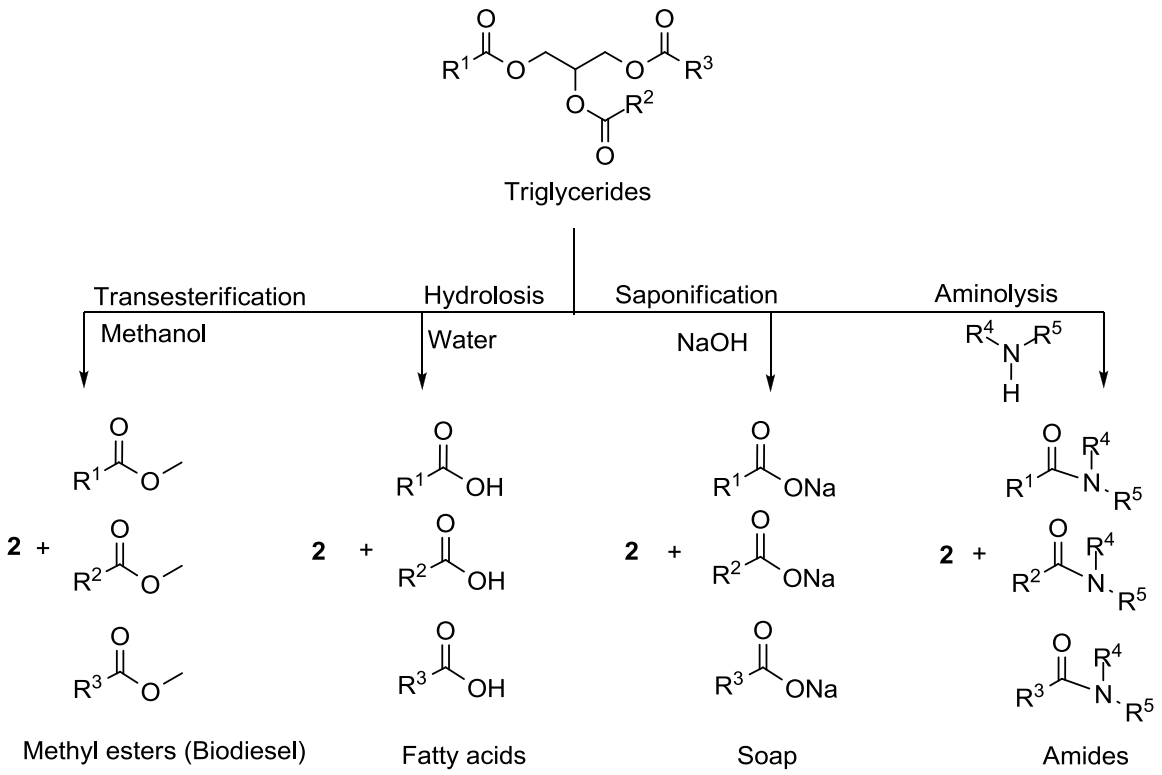

Scheme 2: Glycerol **(2)** from fats and oils.[4]

Purification of crude glycerol is also possible by ion exclusion chromatography, using a cationic, strongly acidic ion exchanger. The technique was originally developed in the sugar industry. The resin column is first fed with a certain amount of glycerol, the ionic substances

remain in the liquid volume between the resin particles (Gibbs-Donnan effect), where the charged molecules starting on one side of a semi-permeable membrane sometimes will not evenly distribute themselves by diffusion on both sides of the membrane.[21, 22] When the resin column is rinsed with water in the second step, the ionic substances are eluted first, followed by the nonionic compounds.

1.3.2: Chemical synthesis

As mentioned above, glycerol is obtained as a byproduct in the conversion of fats and oils to fatty acids or fatty acid alkyl esters. This type of glycerol is known as natural or native glycerol. In contrast synthetic glycerol is produced from propene (propene → allylchloride → epichlorohydrin → glycerol)[23, 24] where epichlorohydrin is hydrolysed to glycerol at 80-200 ^{o}C with 10-15 % of aqueous sodium hydroxide or sodium carbonate to obtain 10-25 % of glycerol solution, or from acrolein (Shell process) (propene → acrolein → 2,3-epoxy-1-propanol → glycerol);[25] acrolein is first reduced to allylalcohol by the MPV (Meerwein-Ponndorf-Verley) reduction method. The alcohol is then epoxidised to 2,3-epoxy-1-propanol (glycedol) and this hydrolysed to glycerol **(2)**. Alternatively allyl alcohol **(3)** can be oxidized by the Upjohn process (Scheme 3) in the presence of osmium tetroxide and *N*-methylmorpholine-*N*-oxide (NMO) as an oxidation reagent.[25, 26]

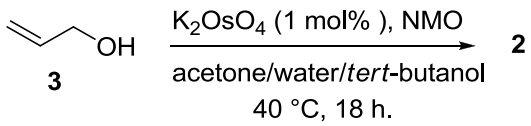

Scheme 3: Upjohn process used for converting allyl alcohol **(3)** to glycerol **(2)**

The first two methods are industrially important processes. Other methods of production (e.g., fermentation of sugar or hydrogenation of carbohydrates) do not show much industrial significance. Presently, the fastest growing source of glycerol is from the production of biodiesel.

Chapter 2: Biodiesel

2.1: History of Biodiesel

The term "Biodiesel" commonly also known as FAME (Fatty Acid Methyl Ester) refers to monoalkyl esters of long chain fatty acids derived from vegetable or animal fats which meet (a) the registration requirements for fuels and fuel additives established by the Environmental Protection Agency under section 211 of the Clean Air Act (42 U.S.C. 7545), and (b) the requirements of The German Standard Institute (Deutsches Institut für Normung e. V.) DIN EN 14214.[27] The Belgian patent 422,877 ("Procédé de Transformation d'Huiles Végétales en Vue de Leur utilisation comme Carburants") granted to Chavanne in 1937 constitutes the first report on the acid catalyzed transesterification of vegetable oils (using ethanol or methanol) and their use as fuel in internal combustion engines. In the early 20th century due to the plentiful availability of mineral oil the market shifted to the use of mineral oils as a source of fuel. But when the cost of mineral oils increased in the 1970s the scenario shifted again, and the interest in biodiesel renewed again. The first commercial production of biodiesel was started in South-Africa in 1981 followed by Austria, Germany and New-Zealand in 1982. In 1985 RME was first produced on a pilot plant scale in Austria, and in 1990 the farmer's co-operative started commercial production of biodiesel.[28] Another important milestone was the allocation of the first fuel standard ON C 1190 for biodiesel in 1991 by the Austrian standardization institute assuring a high quality of the fuel. However, the history of biodiesel as presented by most of authors is taken from the biography of Diesel by Nitske and Wilson, on page 139.[29a] It reads: "As the nineteenth century ended, it was obvious that the fate and scope of the internal-combustion engine were dependent on its fuel or fuels. At the Paris exposition of 1900, a Diesel engine, built by the French Otto Company, ran wholly on peanut oil. Eventually, none of the onlookers was aware of this. The engine, built especially for that type of fuel, operated exactly like those powered by other oils".[30] Apparently, this quotation is not consistent with Diesel´s book.[29b, 30] It may be considered that the idea of operating diesel engine on peanut oil was the idea of the French government rather than the idea of Diesel himself.[30]

From 2006-2008 (Fig. 2) the production of biodiesel in Germany has almost doubled: from 2662000 tons to 5102000 tons. RME (Rapeseed oil Methyl Ester) is mainly used in Europe, where it is commercially available as B100 (100 % biodiesel) or B2, B5 and B20 corresponding for 2, 5 and 20 % of biodiesel blended with petroleum diesel, respectively.[31, 33]

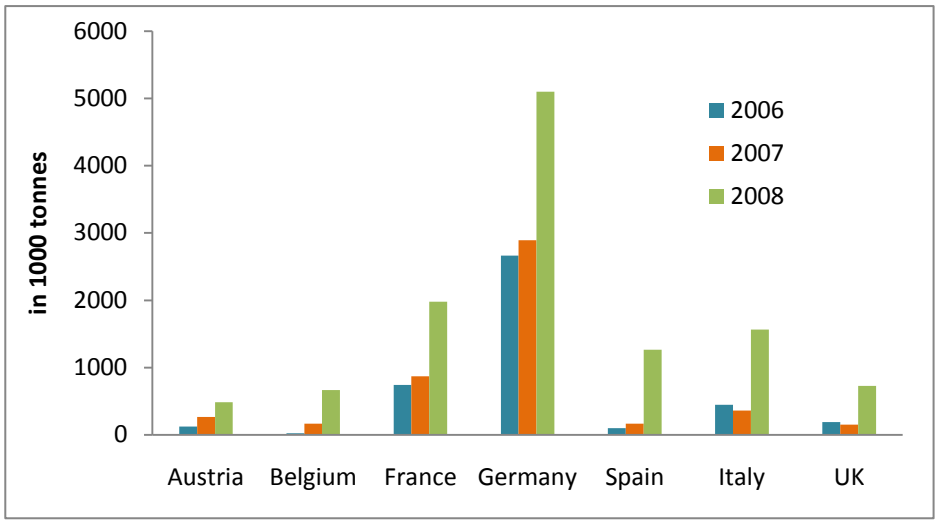

Fig. 2: Biodiesel production in major EU countries from 2006-2008.[33]

2.2: Biodiesel production and market

In Europe legislation requires the use of renewable sources in fuels, according to EU Directive (2003/30/EG) (Biokraftstoffquotengesetz, 2006)[34] on the promotion of biofuels, which enables the use of 4.4 % of biofuels blended with fossil fuels, as well as the Energy Taxation Directive (2003/96/EG), which restructured the framework for the taxation of energy products to promote biofuels as a strategic element of fuel supply.[35] The other important factor is that biofuels that are produced from domestic raw materials reduce the dependence on imported oil. Biodiesel production in Germany has sky-rocketed from 2004 onwards, and according to the UFOP report Germany is the largest biodiesel producer followed by Netherlands in the European Union states today. Biofuels are an environmentally friendly source of energy due to the fact that CO_2 emission from biofuel is partially carbon neutral, apart from the use of methanol and the process and technical energy invested in its production.[37] The introduction of biodiesel created an increase in crude glycerol reserves leading to the closedown of many industries producing glycerol synthetically. The cost of biodiesel production in Germany is comparatively lower than the petroleum diesel price due to a substantial subsidy given by the German government on the production of biofuels.

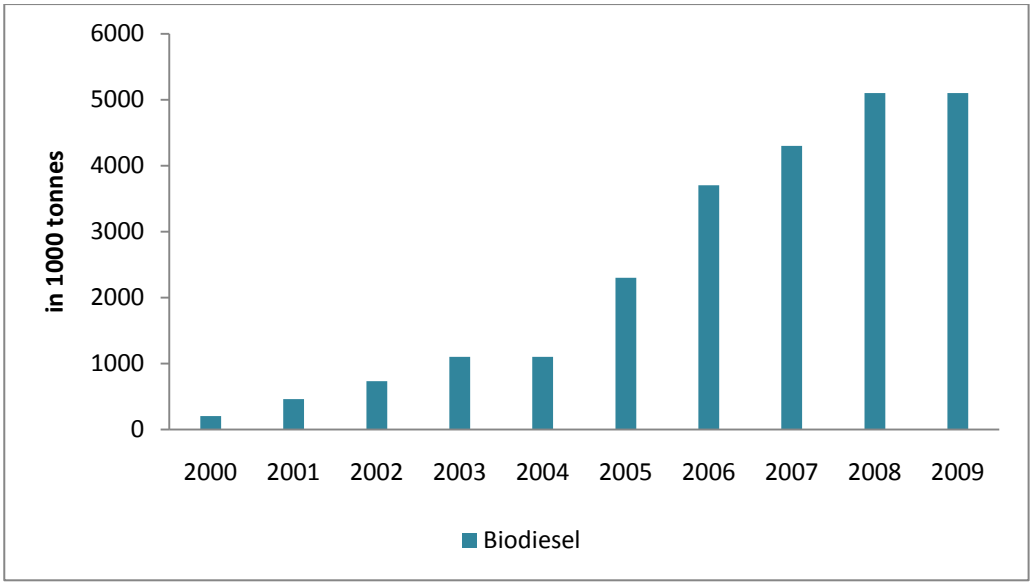

Fig 3: Biodiesel production in Germany from 2000 to 2009.

However, the increase in taxation from 0.09 €/L to 0.18 €/L in 2009 by the German government increased the price of biodiesel (Fig 4). Presently a close difference of 2-5 cents/L is maintained between the tank prices of diesel and biodiesel fuels.[38]

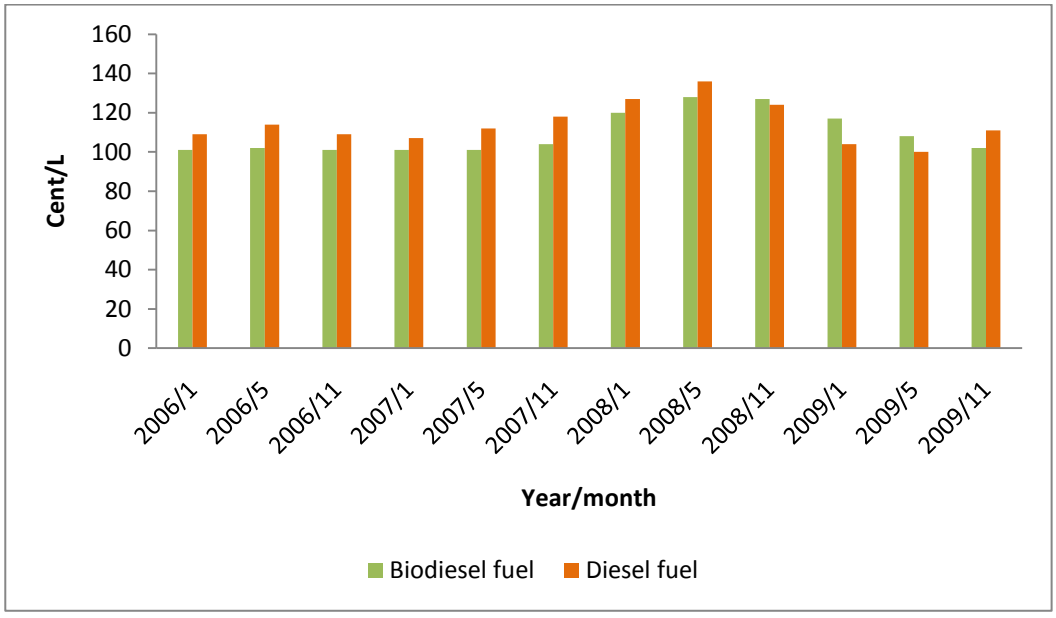

Fig 4: Comparison of diesel and biodiesel prices in Germany (price at the tank inclusive taxes) from 2006-2009.[38]

2.2.1: Advantages and disadvantages of biodiesel (FAMEs)

Advantages: Biodiesel is a fuel which is extracted from renewable resources of energy, making it partially carbon neutral upon combustion. One of the most important characteristics of diesel fuel is its ability towards auto-ignition. U.S diesel typically has a cetane index in the low 40s, and European diesel typically has a cetane index in the low 50s.[31] Biodiesel possesses a cetane number of 48-61.8 which enables it to be used as fuel. Biodiesel improves combustion and therefore reduces CO emissions compared to petroleum diesel. It could be due to the lower carbon content of the biodiesel compared to petroleum diesel fuel or due to the presence of higher oxygen content.

Disadvantages: Currently Biodiesel is blended in 5% to fossil diesel fuel according to EN 14214 and EN 590. By an increase of RME blend to the petroleum diesel fuel to 10 %, there is a concern regarding the long life of RME to a difference in its physicochemical properties in comparison to commercial diesel fuel.[34] Another known problem with biodiesel is that it causes an irreversible oil dilution in the engine lubrication system due to the regeneration mode of current automobile diesel engines with particulate filters. This is caused by the higher distillation characteristic of RME compared to the fossil diesel fuel. In the case when unburnt RME reaches the lubricant in the oil sump through the piston-cylinder assembly during the regeneration of the particulate filter, the fuel fraction that entered the oil sump cannot be evaporated from the engine oil due to its high boiling character compared to diesel fuel. As a result of oil dilution, the viscosity of the engine oil is decreased irreversibly leading to the risk of increasing wear.[36a] However, McCormick *et al*. have shown that the oil dilution caused by B20 has no effect on performance of engine or lube oil properties.[36b]

Generally a good diesel fuel must possess a wide “distillation window”. The distillation window of a fuel is termed as the boiling behavior of a fuel which is an important factor determining fuel quality. Most of the biodiesel fuels have a narrow distillation window (Fig. 5) due to the higher percentage of one of the fatty acid esters (Table 1), which confines biodiesel to a narrow distillation window in comparison to petroleum diesel with a boiling range of 135–350 ^{o}C.[40]

FAME (Fatty acid methyl ester)	RME (%)	SME (%)	m.p. (°C)	b.p. (°C)
Palmitic acid methyl ester	5.39	10.39	+ 30	+ 299
Stearic acid methyl ester	1.90	4.39	+ 39.1	+ 323
Oleic acid methyl ester	56.0	23.17	- 19.9	+ 318
Linoleic acid methyl ester	23.96	53.19	- 35.0	+ 317
Linolenic acid methyl ester	12.32	7.68	- 46.0	+ 318

Table 1: Contents of FAME in RME (rapeseed oil methyl ester) and SME (soybean oil methyl ester) and their melting and boiling points.[34, 40]

In cold countries B100 suffer from its cold filter plugging point (CFPP).[41] The CFPP is the temperature below which under defined conditions a specified fuel cannot flow through a metal sieve within a specified period of time (EN 116) (ASTM D6371).[42] At this temperature the fuel appears cloudy indicating the formation of waxy crystals.

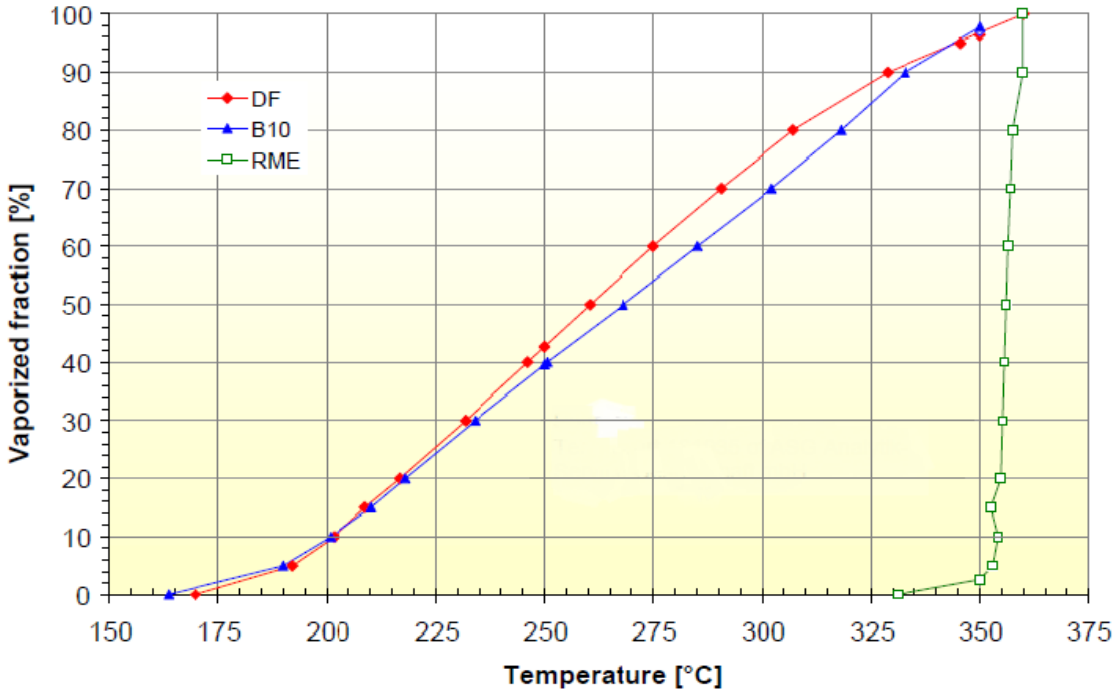

Fig. 5: Boiling point curves of B100 (RME), B10 and Diesel fuel (Source data ASG Analytic Service GmbH).[36]

The introduction of biodiesel could also imbalance the world food markets due to the overproduction of oilseeds. It has a dramatic effect on environment; in countries like

Indonesia thousands of hectares of carbon rich peat lands are being destroyed to provide free land for palm tree plantations threatening the environment and wild life.[43] However, the introduction of biodiesel triggered a swing in the glycerol market as the glycerol is a byproduct of biodiesel industry.

2.2.2: Recent improvements in biodiesel fuel

Due to the drawbacks mentioned above a second generation of biodiesel fuels has been proposed. In an article by Krahl, Munack and Bockey in 2007[34] about the demands of the future biodiesel the advantages of HVO (Hydrogenated Vegetable Oils) over RME has been proposed. HVO has a high cetane number (101) and higher calorific value but it also has the disadvantage of higher NO*x* emissions as proposed by Koyama.[44] Canoira *et al.*[45] have proposed a modification where nitrated FAMEs could be used as additives to enhance the cetane number of the fuel (Scheme 4).

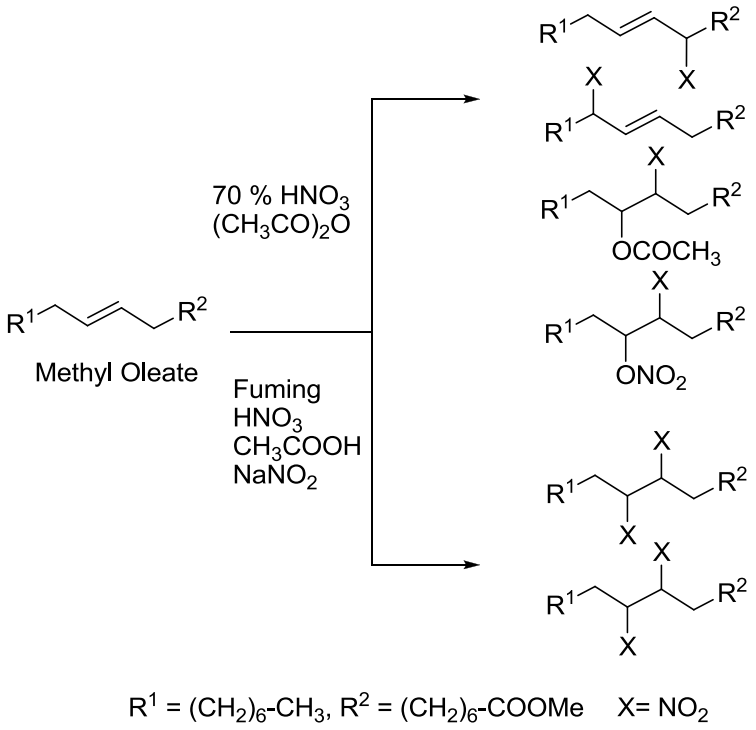

Scheme 4: Nitration products of FAME to be used as cetane enhancers.[45]

However, presently biodiesel (RME) such as B100 cannot be used for passenger cars due to the problem of engine oil dilution. Other favorable modification that can be performed on fats and oils to be used as fuel additives is ozonization. Ozonization of fats and oils is a known process where the use of 1-1.5 % ozonised vegetable oils as pour point depressants was

proposed by Soriano *et al*.[46] Furthermore the addition of ozonized oils effects the thermodynamics and kinetics of biodiesel crystal formation and has an influence on CFPP.[47]

A better solution could either be the fragmentation of the ester groups to obtain straight chain alkenes and alkanes or the fragmentation of FAMEs by breaking of the double bond. Thus, fragmentation of the FAMEs could be performed by different methods (metathesis, oxidation followed by fragmentation, and ozonolysis). Metathesis may not be a cost efficient process to produce fuel industrially presently. whereas ozonolysis is an established[48,49] process which can be performed on both oils and FAMEs.[50] Fragmentation of double bonds leads to further smaller molecules as shown in Scheme 5. Proper chemical modification of fragmented molecules could then provide fuel or fuel additives. If the process is performed in a cost efficient manner it could probably be used to produce biofuels and also value added precursors for many industrial chemicals (*green chemicals*).

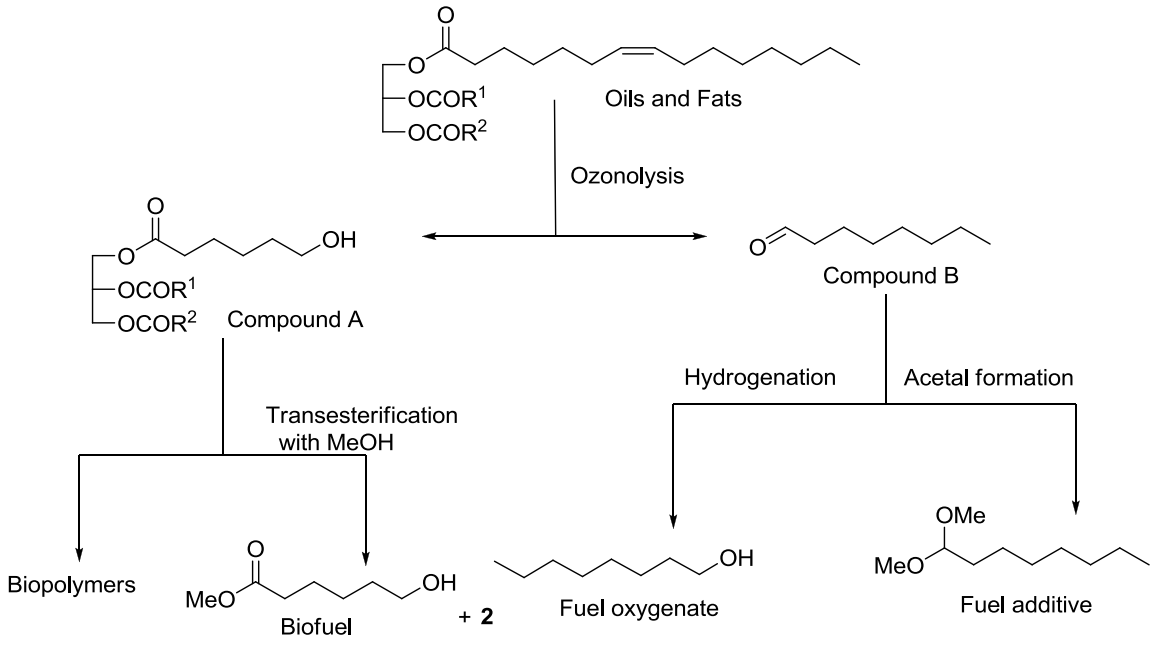

Scheme 5: Proposed alternatives for FAMEs as fuel

The advanced automobile technology demands the necessity for further chemical modification of present day biodiesel (FAME) in order to withstand future demands. Industry of course has to sustain the costs of such modifications. However, the drastic increase in the production of biodiesel in the past few years has changed the glycerol markets, and it also created a necessity to find value added outlets for the over-produced glycerol.

Chapter 3: Conversion of glycerol to value added chemicals *(green chemicals)*

3.1: Outlets of glycerol

Due to the consumer desire for eco-friendly "natural materials", the major outlets of glycerol (Fig. 6) are drugs and pharma and personal care products, the food & beverages industry contributing to 18, 16 and 11 % of total consumption.[51] Tobacco and resin production and other industries also contribute to the consumption of glycerol as such without major modifications. The majority of the present day market is relatively mature which makes it difficult to consume the surplus glycerol from the emerging biodiesel industry.

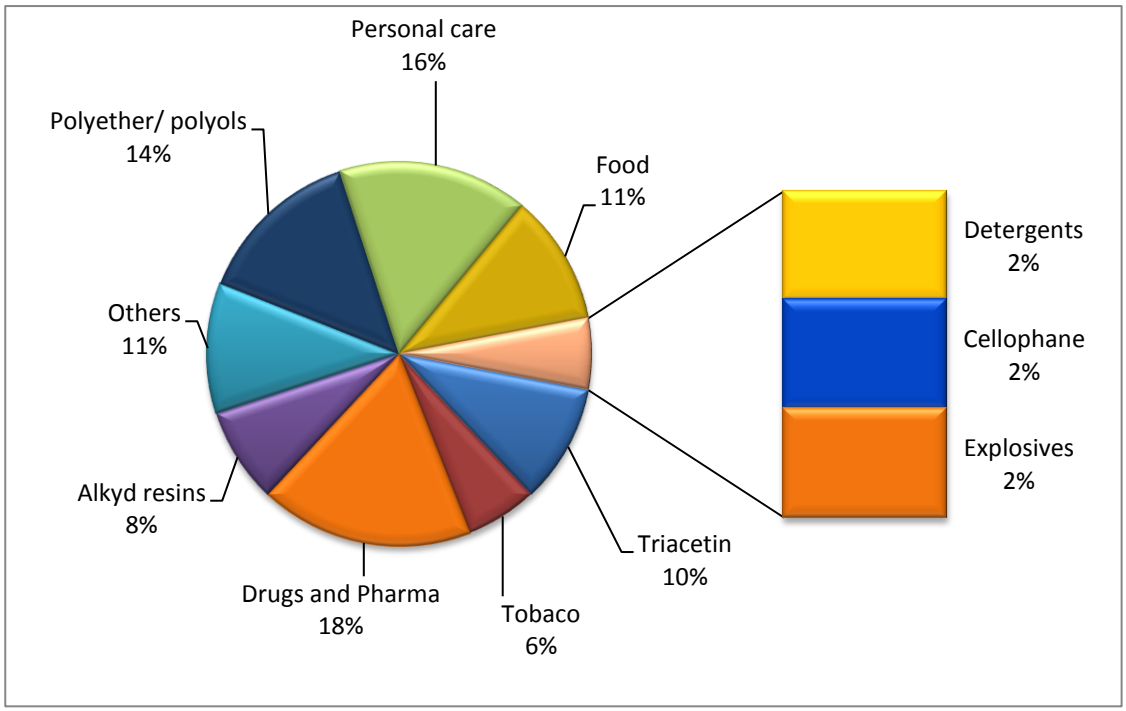

Fig. 6: Outlets of glycerol **(2)**.[52]

3.2: Chemical Transformations

To utilize excess glycerol produced from biodiesel production many industries are looking forward to develop innovative methods which can use glycerol as a building block for the production of value added chemicals. Scheme 6 depicts some important chemicals derived from glycerol chemistry.

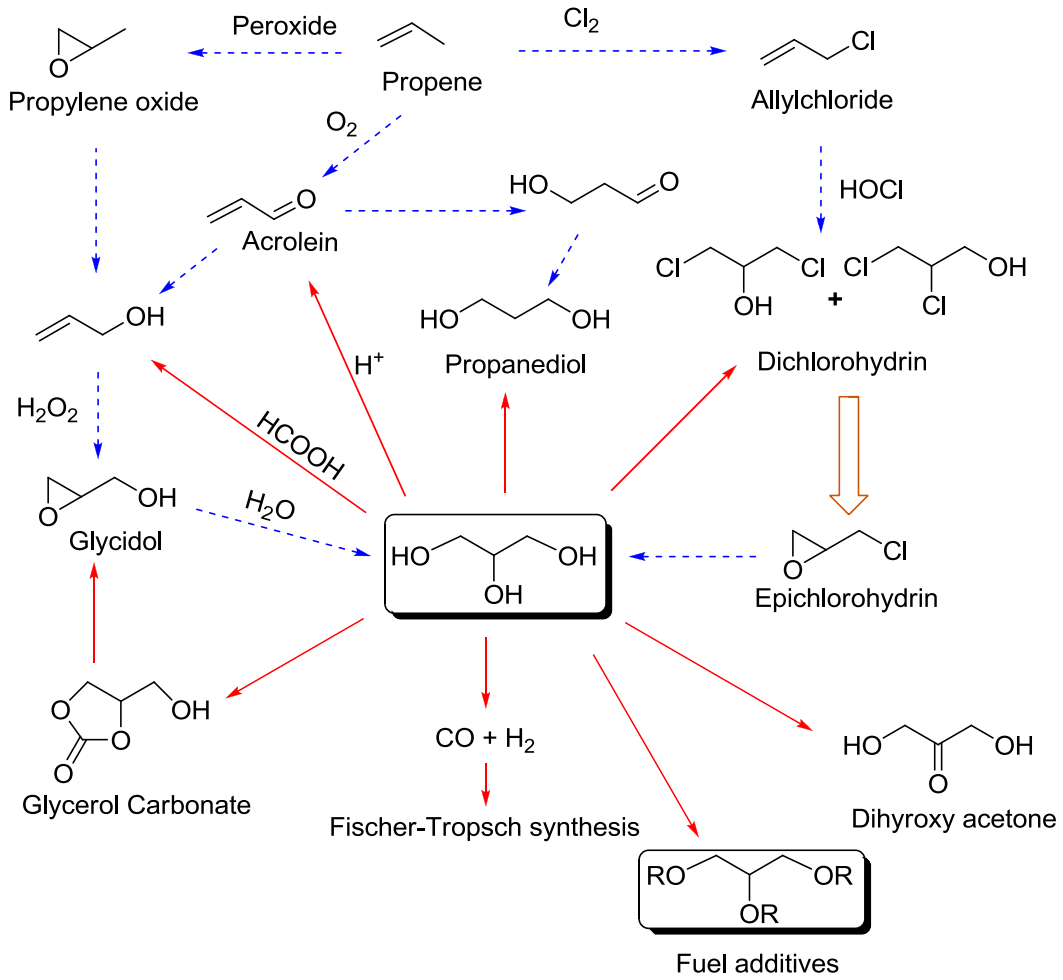

Scheme 6: Schematic representation of glycerol converted to value added products represented by arrows (*green chemicals*) and the chemicals produced from propene represented by dashed arrows (petrochemical source).

Presently, most of the above mentioned chemicals are produced from propene. Use of glycerol instead, provides a bright possibility towards fossil fuel independence. However, the above scheme clearly shows the cost competitiveness between the petroleum derived products and products obtained from glycerol, the balance can be maintained only when the cost price of glycerol is much lower than its petroleum based counterparts. Eventually, from all of the above possibilities this thesis mainly focuses on glycerol as a fuel additive.

3.3: Glycerol as a fuel additive

By definition a fuel additive can be any compound that is added to the fuel in a less than 1 % concentration to attain certain properties and to improve the quality of the base fuel. A wide range of additives has been added to fuel from the beginning of 19th century to generate a

higher and more improved grade of fuel.[53] The rapid growth of the automobile industry and improved technology lead to greater consumption of fuel which initiated the development of different kinds of additives to improve fuel quality. The most prominent of these are octane enhancers (anti-knocking agents). Even though an additive is often added in less than 1 % to the base fuel, it provides an advantage to the chemical industry to produce it in hundreds of tons with respect to fuel consumption. Glycerol as such is not well suited to be used as fuel additive due to its physical and chemical properties (see Chapter 1). The possible chemical transformations that facilitate glycerol to be used as fuel additive are discussed in the following chapters.

To understand the type of additives and their role played in the combustion chamber it is essential to understand the types of engines and fuels and the fuel combustion technology and the corresponding emissions.

There are technically two basic types of internal combustion engines, the Otto engine/ spark ignition engine or petrol engine and the Diesel engine. These are the most commonly used engines in our daily life.

3.4: Otto engine (gasoline engine, petrol engine)

The Otto engine or spark ignition engine was invented by Nikolaus August Otto in 1876; it operated on coal gas. The engine was adapted by the French engineer Edouard Delamare-Debouteville and by Gottlieb Daimler and was modified to use gasoline as fuel.[54, 55] In the most frequently used gasoline four stroke engine the gas exchange process of the four stroke cycle is controlled by valves. The cycle is carried out in a sequence of four steps 1) intake, 2) compression, 3) ignition and 4) exhaust as depicted in Fig. 7.[56, 57] In a petrol engine fuel is primarily diluted with air (in a stoichiometric ratio under normal load) in an electronically controlled fuel injection system and throttled into the cylinder, which is compressed and ignited by a spark plug.

The compression ratio, which is the ratio between the cylinder volume at the beginning and end of the compression stroke, limits the efficiency of engine. The greater the compression ratio the greater is the efficiency of the engine. Higher compression ratio is limited by the octane number of the base fuel.[53]

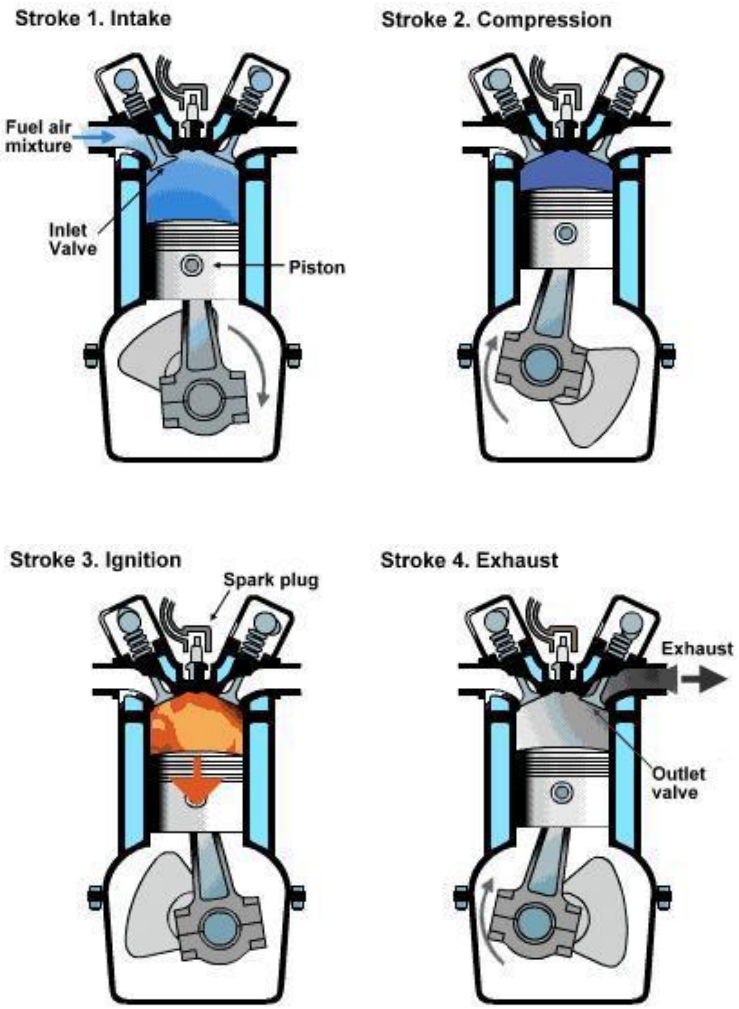

Fig. 7: Schematic representation of a four stroke gasoline engine.[58]

However, the knock sensors in modern engines avoid knocking even with a varying octane number of the fuels. Low quality octane fuels causes loss in engine efficiency, octane enhancers are added to improve the octane number of the fuel, enhance the engine efficiency and avoid knocking.

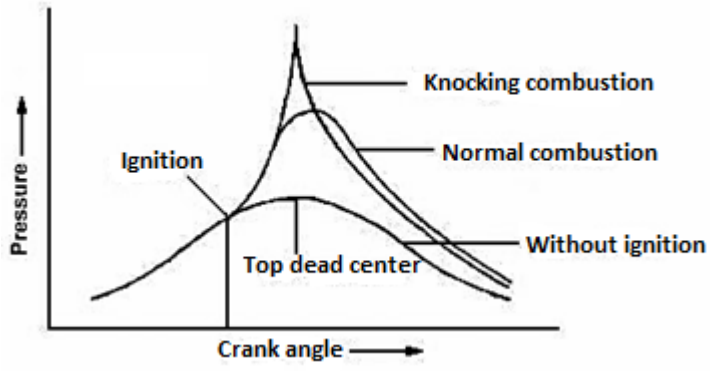

Fig. 8: Combustion in a petrol engine.[53]

3.5: Quality requirements of gasoline

Gasoline used for Otto engines is a blended product with a boiling range from 40-150 ^{o}C. Typical gasoline components consist of light and heavy fractions; the most important property to be fulfilled by motor gasoline is its knock rating (Octane number) (RON super gasoline 95-100), other aspects like boiling character, volatility, flash point (minimum -40 ^{o}C), density (at 15 ^{o}C, minimum 725 kg/ m^3, maximum 780 kg/ m^3) and oxidation stability (ASTM D 4814, minimum 240 min) are also important factors which influence the engine performance.

3.5.1: Anti-knocking agents (octane enhancers)

Anti-knocking agents are compounds which are added to the base fuel to promote cleaner fuel combustion. They boost fuel octane values and reduce carbon monoxide and particulate matter emissions. Today the most widely used anti-knocking agents which replaced tetra ethyl lead due to lead pollution and toxicity are (Fig. 9), methyl *tert*-butyl ether (MTBE) **(4)**, ethyl *tert*-butyl ether (ETBE) **(5)**, *tert*-amyl methyl ether (TAME) **(6)**, di-isopropyl ether (DIPE) **(7)**, isopropyl alcohol (IPA) **(8)**, isobutyl alcohol (IBA) **(9)**, and *tert*-butyl alcohol (TBA) **(10)**.[59, 60]

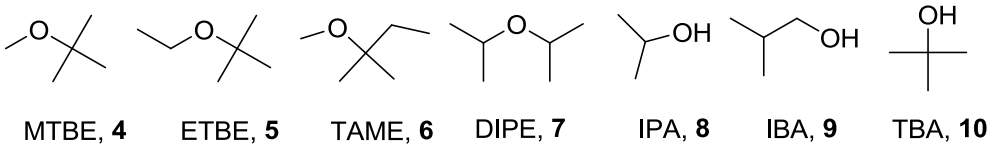

Fig. 9: Commonly used anti-knocking agents.[59]

The introduction of organic anti-knocking agents started in 1970s with MTBE **4** which was followed by the other additives mentioned above. Oxygenated fuels are required to allow knock free combustion in high compression engines which enables optimum engine efficiency.

3.5.2: Octane number

According to EN 25164 / EN 25163 the octane number of a fuel is a comparative scale where *n*-heptane has an octane number of 0 and 2,2,4-trimethyl pentane has an octane number of 100. The basic concept behind the octane number measurement is that when a fuel is sprayed in to a petrol/gasoline engine,[53] the combustion initiated by the spark plug must proceed in a

controlled manner to avoid multiple ignitions. This enables the engine to achieve highest efficiency under "ideal" conditions. Ideal condition is achieved when isooctane (2,2,4-trimethyl pentane) is used as the fuel. In contrast when *n*-heptane is used as fuel under higher compression ratios it initiates a pre-flame reaction where portions of fuel self-initiate the combustion prior to the advancing flame from the spark plug. This leads to an explosion or knock in the engine. Antiknocking agents facilitate slow and uniform burning of the fuel. Addition of anti-knocking agents to the ground fuels promotes higher compression ratios, avoids multiple ignition points, and act as fire extinguishers to reduce knocking.[56, 57]

The octane number is determined in specially designed single cylinder, four stroke test engines which have a mechanically adjustable compression ratio; generally the cooperative fuel research (CFR) engine is used worldwide.[61] During the octane number measurement of fuel the compression ratio is raised until a standardized knock is shown by the knock meter. Fuel octane numbers are technically determined under two different running conditions.

3.5.2.1: Research octane number (RON)

The so called research octane number (RON)[53, 62] determination is performed under comparatively mild conditions, at 600 rpm, constant ignition timing and cold start according to the test standards EN-25164, ASTM D 2699.

3.5.2.2: Motor octane number (MON)

The motor octane number (MON)[53, 62] is determined at higher mechanical (900 rpm) and thermal loads under variable ignition timing, warm start at 150 ^{o}C according to the test standards EN-25163, ASTM D 2700.

RON provides the acceleration knocking of the fuel and MON high speed knocking. Due to the harsh conditions MON is normally lower than RON and the difference is called sensitivity. The third component is road octane number which specifically depends on the type of vehicle and weather conditions. The road octane number is evaluated by a formula "a RON + b MON + c", where a, b, and c are vehicle dependent constants. The road octane number normally lies between RON and MON, starting with RON and slowly approaching MON under constant acceleration. For German standards the RON minimum is 91.0 while the MON minimum amounts to 82.5.[63, 64]

3.6: Diesel engines

Unlike gasoline engines diesel engines lack an external source of ignition (Fig. 10), since the fuel has to autoignite under pressure, a good ignition performance is an important criterium for fuel quality. In a four stroke diesel engine which is the most commonly used engine, the air is taken into the cylinder unthrottled and compressed to obtain a pressure of 30 to 55 bars which generates a temperature up to 700 ^{o}C.[53, 65] Fuel is injected into the heated air shortly before the end of the compression stroke.[66] Depending on the injection of fuel two types of diesel engines have been designed 1) direct injection (DI) engines and 2) indirect injection engines (IDI).

In modern cars DI engines are used with an electronically controlled common rail fuel injection system developed by Bosch which can generates a pressure up to 1800 bars; the high pressure injection systems reduces engine noise and pollution up to 20 %.[68] Highly compressed fuel also reduces the ignition delay in the combustion chamber.

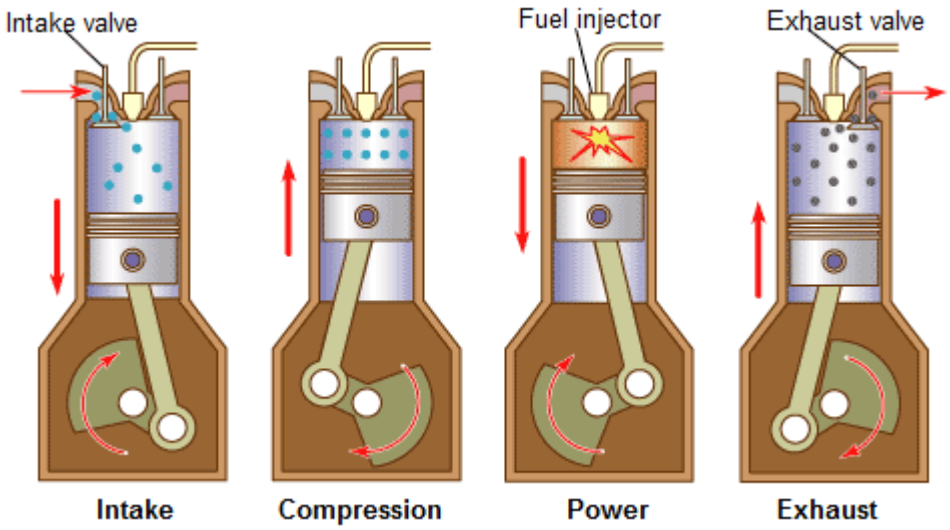

Fig. 10: Schematic diagram of diesel engine.[67]

Ignition delay is the time delay between the injection and the beginning of combustion of the fuel (Fig. 11), which mainly depends on the ignition quality of the diesel fuel. For optimal operation of an engine with low noise and emissions, shorter ignition delay is essential which in-turn requires high diesel fuel quality i.e. high cetane number fuel.

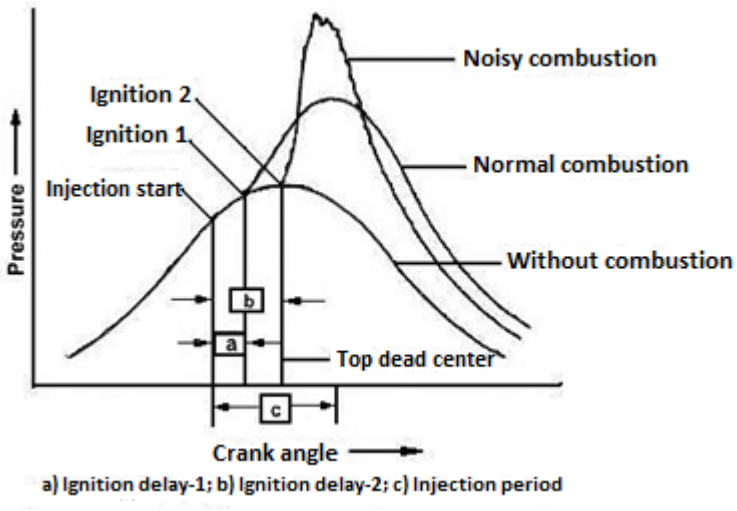

Fig. 11: Combustion in the diesel engine [53]

3.6.1: Quality requirements of diesel fuel

Diesel fuel or gas oil is a blend of light and heavy gas oil fractions with a boiling range of 135-350 ^{o}C which is normally used as automotive fuel and as fuel for heating. The most important property of diesel fuel is its ignition quality. In contrast to gasoline, diesel fuel must ignite readily in the engine which implicates its cetane rating (minimum 51 EU standard and 40 U.S standard).[53] Other aspects like density (min. 820 kg/m^3, max. 860 kg/m^3), flash point (min. 55 ^{o}C), the cold flow property (CFPP between + 5 ^{o}C and −20 ^{o}C, (specified according to the seasonal and regional standards), the fuel lubricity and viscosity (min. 2.0 mm^2/s, max. 4.5 mm^2/s) are also important factors which influence engine performance.[69]

3.6.2: Cetane enhancers

Cetane boosters are compounds that are added to the base fuel to improve the ignition quality or to reduce the ignition delay of the base fuel. The effect of cetane enhancers is based on free radical formation by rapid decomposition to propagate the flame. It is well-known that cetane improvers enhance ignition quality by generating a radical pool at low temperatures. Yonei *et al.*[70] have demonstrated by quantum mechanical calculations that compounds that promote the generation of alkyl peroxy radical through an oxygen addition reaction are the best cetane enhancers. The most common cetane enhancers are nitrates and peroxides. Many other cetane enhancers have been proposed but 2-ethylhexyl nitrate (EHN **11)** is the only industrially successful chemical used presently.

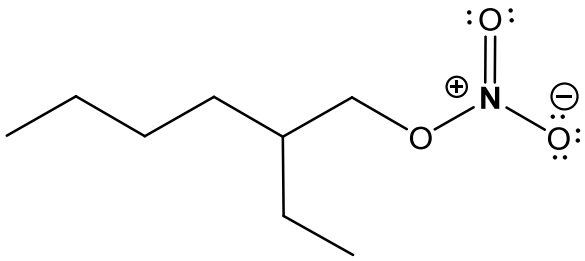

11

Fig. 12: Additive 2-ethylhexyl nitrate **(11)** a cetane enhancer used in diesel fuel.

3.6.3: Cetane number

The cetane number is a quantitative measure for diesel fuel combustion. Like the octane number the cetane number measurement is performed in a single cylinder test engine (Waukesha CFR Swirl Chamber Cetane Rating Engine). To determine the ignition quality of the fuel the test engine allows varying the compression ratio of the engine depending on the quality of test fuel by keeping the ignition delay constant. A reference mixture of α-methylnaphthalene which has very low ignition quality with a cetane number 0 and *n*-hexadecane with a cetane number 100 are used as reference. The cetane number of reference mixture is given by the volume % of cetane in α-methyl naphthalene.[53] However, it is also possible to calculate the cetane number of a fuel by using the cetane index method (ENISO 4264, ASTM D 4737). The calculated cetane index is used to estimate the cetane number when a test engine is not available or if the quantity of a sample is too small for an engine rating. In cases where the cetane number of a fuel has been initially established, the index is useful as a cetane number check on subsequent samples of established fuel, provided its source and mode of manufacture remain unchanged. The cetane index is, however, an indication of ignition quality of a fuel without an added cetane booster. The cetane number provides a qualitative measurement of a fuel; this is essential for the starting behavior, engine noise and for emissions reduction of a diesel engine.[71]

Chapter 4: Emissions and pollution

4.1: Chemistry of emission and pollution control

In an internal combustion engine hydrocarbon fuel is burned in the presence of air. Under ideal conditions the hydrocarbons burn to produce carbon dioxide, water, heat.[72]

$$C_mH_n + (m + 0.25n)\ O_2 \rightarrow mCO_2 + 0.5n\ H_2O + \text{heat}$$

Even in technologically most modern and advanced engines it is impossible to achieve ideal conditions, due to lack of a homogenous gas phase and chemical equilibrium. This leads to an incomplete combustion, and hence to pollution. In general the more efficient the engine becomes the smaller are the emissions. Advanced technologies such as closed loop engine control systems and common rail fuel injection system increase fuel economy and emission control, making the present day engines more efficient than their predecessors in the 1970ies and 80ies.

4.1.2: Fuel-Air ratio

The fuel to air ratio plays an important role in the combustion process. In a gasoline engine fuel intake is throttled to obtain an ideal fuel-air ratio for optimum emission, fuel economy, and good engine performance. In spark-ignition engines the ideal air to fuel ratio (A/F ratio) is 14.7:1 at 50 % humidity and a pressure of 1013.2 millibar, which is referred to as stoichiometry. An air to fuel ratio higher than stoichiometry has an impact on fuel economy and emissions and an A/F ratio lower than stoichiometry influences the power, drivability and emissions. Variations from the stoichiometric ratio are characterized by the term *lambda* (Fig. 13).[66, 73] Lambda less than 1 means a rich mixture (excess fuel), and lambda greater than 1 means a lean mixture (excess air). Under rich conditions the exhaust gas contains more reduced reactants (CO, HC) than oxidized reactants (O_2, NO*x*). The reduction reactions of NO*x* are favored under rich conditions or stoichiometric conditions, whereas lean conditions favor the catalytic oxidation reactions of CO and hydrocarbons. Before 1975 engines were run under slightly rich conditions (λ= 0.9, 10% excess fuel) to reduce NO*x* emissions. An excess of HC and CO was produced which was treated by using catalytic converters. Presently, advanced engines are run under stoichiometric conditions (λ=1) to promote fuel economy and efficient functioning of the three way catalyst used in the exhaust (λ = $AFR/AFR_{\text{stoichiometry}}$).

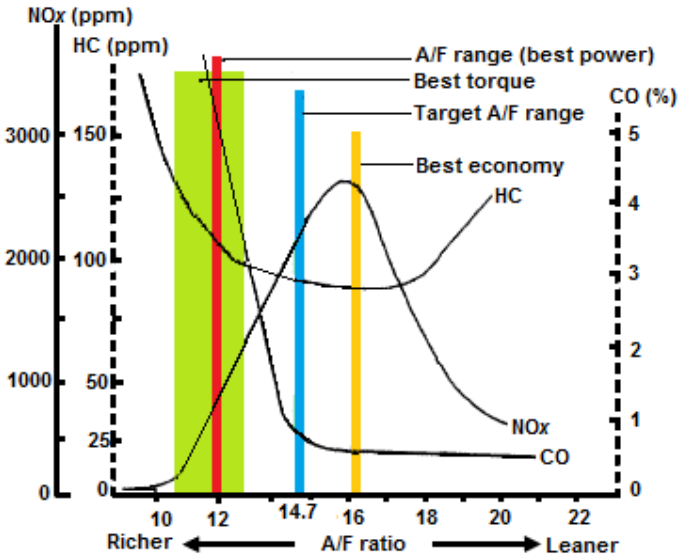

Fig. 13: Lambda window of a gasoline engine.[74]

There is a very lean window for the engine to be operated under optimal emission conditions. A slight variation of the λ window in either direction can increase the concentration of some of the pollutants dramatically. To avoid this situation most of modern engines use the λ sensors. These monitor the amount of oxygen in the exhaust and send a signal to an OBC (on board computer) which throttles the flow of fuel into the combustion chamber accordingly.

4.2: Pollution causing elements

As mentioned before if the fuel is burnt completely under ideal conditions only CO_2 and water are released which are not hazardous. However, the following major pollutants are generated in an internal combustion engine due to incomplete combustion of fuel.[73] Eventually, NO*x* emissions are the side products of fuel combustion where components of fuel are scarcely involved.

- Carbon monoxide (CO)
- Unburned or partially oxidized hydrocarbons (HC)
- Particulate matter (PM)
- Oxides of nitrogen (NO*x*)

4.2.1: Carbon monoxide (CO)

It is a known that any carbon containing compound upon incomplete oxidation produces carbon monoxide. Incomplete oxidation in the combustion process can be due to richer

stoichiometric conditions. This can occur during cold operation, warm up or power enrichment or can be due to the influence of mechanical failures.

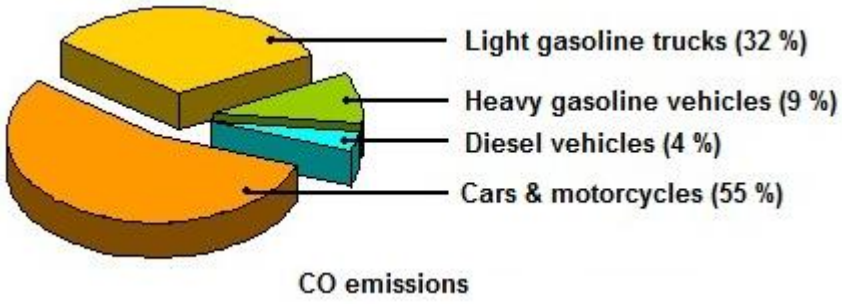

Fig. 14: Carbon monoxide emissions of different vehicles.[75]

High fuel injection pressure can also lead to higher carbon monoxide emissions. Automobile emissions are the major source of carbon monoxide pollution in the atmosphere from which spark ignition engines contribute the larger part. According to an EPA as much as 95 % of carbon monoxide pollution is contributed by automobiles in USA (Fig. 14).[76, 77]

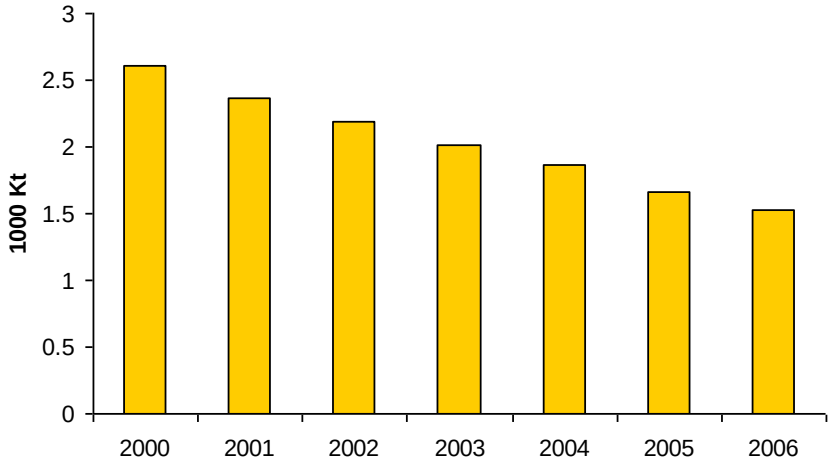

Fig 15: Carbon monoxide pollution from automobiles (related to road traffic only) in Germany from 2000-2006.[78]

The major part of it (55 %) is contributed by cars and motorcycles which run on gasoline, followed by light gasoline trucks. The data provided by the Umweltbundesamt,[78] on carbon monoxide pollution by road traffic in Germany is represented Fig 15. Due to stringent federal pollution laws adopted by the German government and also due to the advanced technology developed by automobile industries, the amount of CO pollution has considerably decreased in recent years.

4.2.1.1: Environmental and health effects

Carbon monoxide indirectly affects other greenhouse gases like methane causing "climate change". Inhalation of the low levels of carbon monoxide (200 ppm for 2-3 hours) can cause headache, dizziness, light-headedness and fatigue. Exposure to higher concentrations (400 ppm) of carbon monoxide causes sleepiness, hallucinations, convulsions, collapse, loss of consciousness and ultimately death. It can also cause personality and memory changes, mental confusion and loss of vision. At very high levels carbon monoxide will be life threatening. Long term (chronic) exposure to low levels of carbon monoxide may produce heart diseases and damages the nervous system.[79] Exposure of pregnant animals to carbon monoxide may cause low birth-rates and nervous system damage of the offspring. Extremely high exposures to carbon monoxide can cause the formation of carboxyhaemoglobin and decrease the body's ability to carry oxygen. This can cause a bright red color of the skin and mucous membranes causing trouble breathing, collapse, convulsions, coma and death. Long term (chronic) health effects can occur from exposure to low levels of carbon monoxide.

4.2.2: Hydrocarbon emissions (HC)

Hydrocarbon (HC) emissions are mainly due to incomplete combustion of injected fuel which leads to partially oxidized or unburned fuel emission.[80] In spark ignition engines which contribute to the major part (Fig. 16), most hydrocarbons originate from the regions not reached by the flame (quench zones). Wall quenching is a process where fire is extinguished by the cold walls of the engine during the cold start. Almost 60 % of total HC emissions are contributed to wall quenching. Flame quenching is a process where a very lean mixture of air to fuel ratio can extinguish the flame before complete combustion; it also occurs due to relatively low gas temperature.

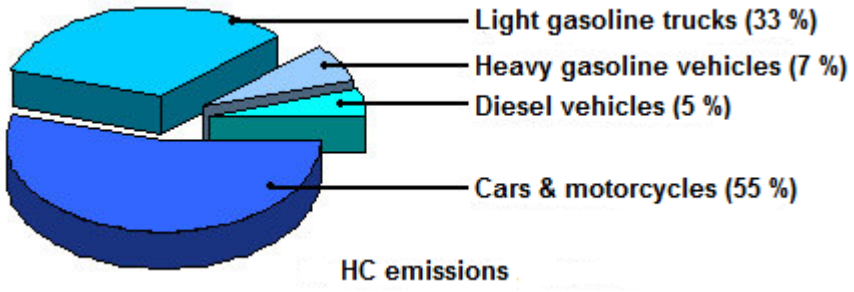

Fig. 16: Hydrocarbon emissions by different vehicles.[75]

In diesel engines under high and low fuel-air mixtures incomplete combustion may occur leading to HC emissions. The composition of HC emissions mostly depends on the quality of the fuel used, operation conditions and system of combustion. According to the Umweltbundesamt[78] statistics (Fig. 17) about 144 kilotons of HC were produced by road traffic in Germany in 2006.

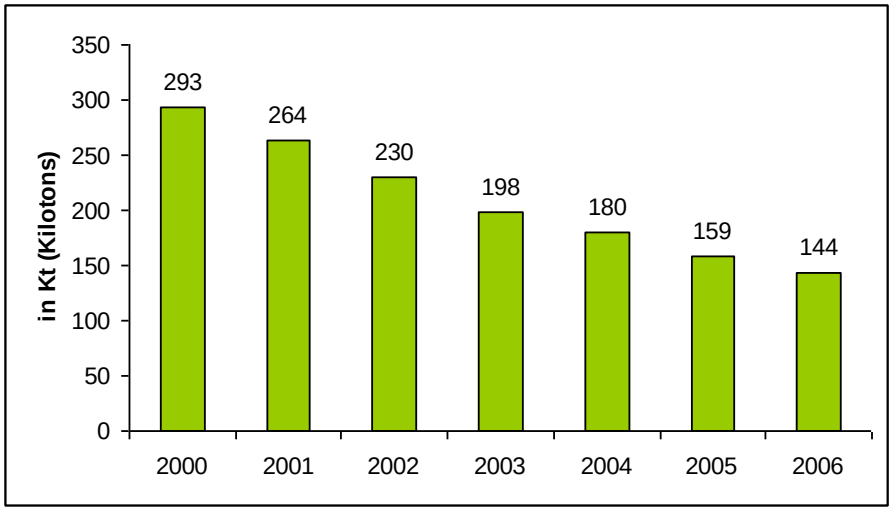

Fig. 17: HC pollution from automobiles (related only to road traffic) in Germany from 2000-2006.[78]

4.2.2.1: Environmental and health effects

HC pollution is a major environmental concern in big cities all around the globe. Volatile organic compounds are associated to troposphere ozone formation relating to formation of smog. According to the EPA, 47 % of hydrocarbon emissions in the atmosphere can be attributed to on-road and off-road vehicles in USA.[75] The strong odor associated with diesel emissions is associated with the presence of volatile organic compounds. Formation of smog by VOCs is a serious form of air pollution. Smog which is differentiated into summer and winter smog in many urban areas causes irritation and damage to eyes, skin and lungs. It dries out the protective membranes of the nose and throat, interfering with the body's ability to fight infection. Some hydrocarbons are also considered toxic, causing serious health problems such as cancer or death. According to WHO reports European daily mortality raised by 0.3% and that for heart diseases by 0.4 % / 10 µg/m^3 increase in exposure to troposphere ozone (ground level ozone).[79]

4.2.3: Particulate matter (PM) emissions

Particulate matter is a cluster of solid or liquid particles that are emitted from the exhaust. The size of the particles matter emissions from diesel engines varies from D_p = 0.05-0.5 micrometers from which 90 % are attributed to 0.05 microns according to Kittelson´s generalized distribution. However, the particulate matter from the exhaust gets accumulated in the atmosphere, and depending on the size they are differentiated to $PM_{2.5}$ where the particle size is less than 2.5 microns in aerodynamic diameter and PM_{10} for a particle size with an aerodynamic diameter of 10 microns.[81] The visibility of smoke is due to the larger particulates. Particulate matter is mainly formed in low air to fuel ratio zones leading to the formation of soot. Soot emissions are strongly increased if the air-fuel ratio is near stoichiometry.

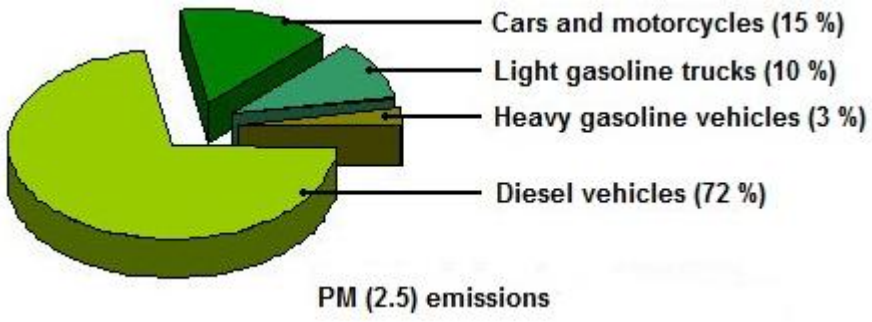

Fig. 18: Particulate matter emissions by different vehicles.[81]

Particulate matter with size of 0-50 microns is suspended in air and is called TSP (Total Suspended Particles). Particulate matter greater than 10 microns does not enter the body and is considered to be harmless. Particulate matter ranging from 2.5-10 microns can enter through the mouth into the lungs and when it is less than 2.5 microns it enters the body through the nose. Diesel engines contribute to most of the PM pollution (Fig. 19).

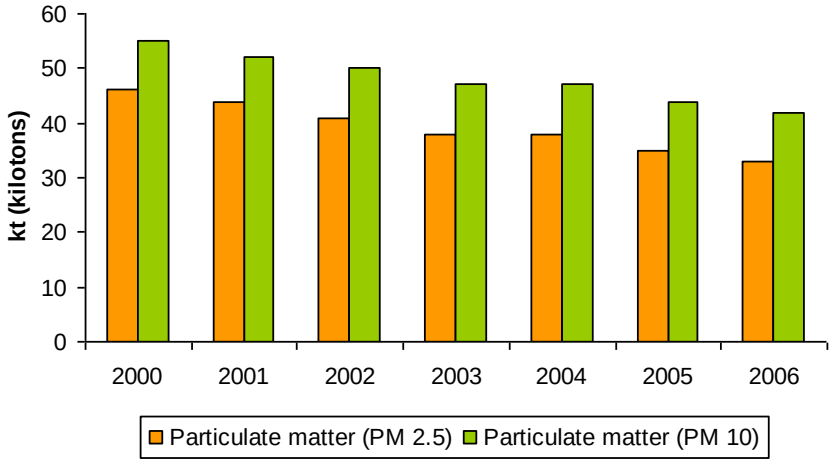

Fig 19: Particulate matter (PM $_{2.5}$, PM $_{10}$) pollution from automobiles (related only to road traffic) in Germany from 2000-2006.[78]

4.2.3.1: Environmental and health effects

Fine particulate matter is a health concern due to its capability of deeper penetration into the lungs. Health effects include asthma, difficult or painful breathing, and chronic bronchitis. Fine particulate matter associated with diesel exhaust is also thought to cause lung cancer. Fine particulate matter can travel long distances by air currents which is a major cause of haze. According to WHO the average annual levels of PM_{10} (from fossil fuels) exceed 70 micrograms per cubic meter. Reduction of particulate matter (PM_{10}) pollution from 70 to 20 micrograms per cubic meter can cut air quality related deaths by around 15 %.[79] According to WHO, the health effect of PM on human beings is higher than any other pollutants. New measures are being taken to introduce particle count per kilometer, where emissions are reported in number of particles emitted per kilometer.

4.2.4: Oxides of nitrogen (NO*x*) emissions

Oxides of nitrogen NO*x* are generally formed at high engine temperatures, by the oxidation of atmospheric nitrogen. Therefore, NO*x* emissions are considered as side products of fuel combustion in the engine (except fuel NO*x* emissions). NO*x* is a composition of different oxides of nitrogen which are mainly nitric oxide (NO), nitrogen dioxide (NO_2), nitrous oxide (N_2O), dinitrogen trioxide (N_2O_3), dinitrogen tetroxide (N_2O_4), dinitrogen pentoxide (N_2O_5). Among the emissions of NO*x*, nitric oxide (NO) comprises more than 90 % of the emitted oxides.

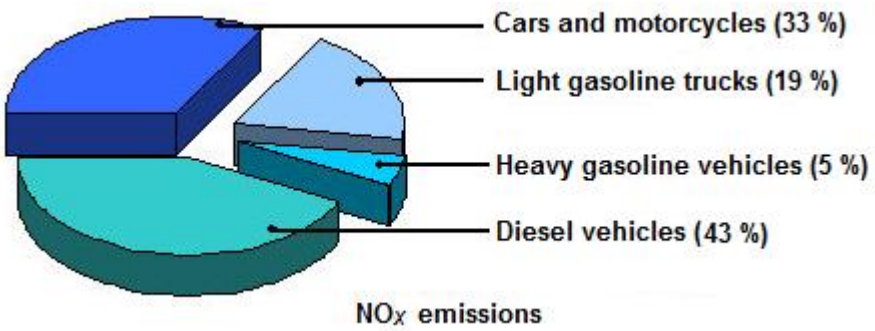

Fig. 20: NO*x* emissions by different vehicles.[82]

Road traffic contributes up to 50 % of NO*x* emissions in atmosphere from which diesel engines contribute the major percentage (Fig. 20). The formation of NO*x* during the combustion process can be attributed to many different factors, some of the most prominent are:

- Thermal NO*x*
- Prompt NO*x*
- Fuel NO*x*
- Oxygen content of the fuel

4.2.4.1: Thermal NOx

Thermal NO*x* is considered to be a major contributor; it is formed at temperatures above 1500 ^{o}C by the oxidation of atmospheric nitrogen by air.

$$N_2 + O_2 \rightleftharpoons 2\,NO$$

$$\Delta G^{o} = 86.596 \text{ kJ/mol}, \Delta H^{o} = 90.291 \text{ kJ/mol}.$$

The reaction shifts towards the right at higher temperatures.[83, 84] Thermal NO*x* formation is highly dependent on flame temperature. The dependence of NO*x* formation with respect to flame temperature and excess oxygen is shown in Fig. 21. The kinetics of the thermal NO*x* formation follows the so-called extended Zeldovich mechanism. At a temperature above 1500 ^{o}C NO is formed according to the reaction sequences 1 and 2 (global reactions).[85]

$$O + N_2 \rightleftharpoons N + NO \quad (1)$$

$$N + O_2 \rightleftharpoons N + NO \quad (2)$$

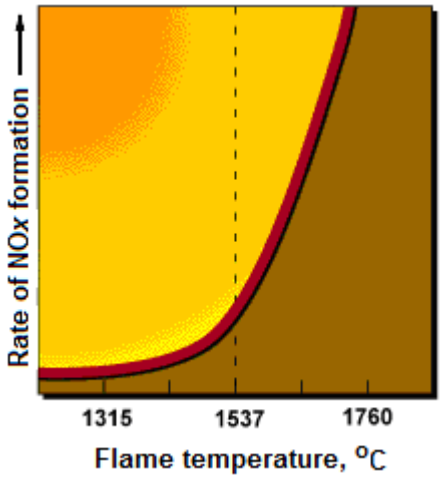

Fig 21: Thermal NO*x* formation as a function of temperature.[84]

A third reaction has been shown to contribute, particularly at near-stoichiometric conditions and in fuel-rich mixtures

$$N + OH \rightleftharpoons H + NO \quad (3)$$

The rate of formation of NO*x* is significant only at high temperatures (above 1500 ^{o}C) because to form reactive nitrogen species requires the breaking of the strong N_2 triple bond (dissociation energy of 941 k J/g mol). However, the activation energy for oxidation of free nitrogen species (N) is relatively low. In the presence of sufficient amounts of oxygen in a fuel-lean flame, the rate of consumption of free nitrogen atoms becomes equal to the rate of NO*x* formation and therefore a quasi-steady state is established[85, 86] (Fig. 22). This assumption is valid for most combustion cases except under extremely fuel-rich conditions.

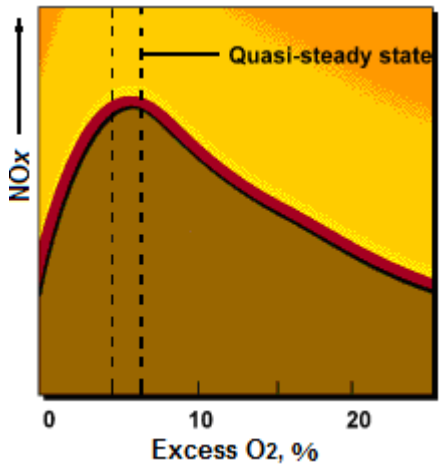

Fig. 22: Thermal NO*x* formation as a function of oxygen concentration.[84]

As most of the diesel engines run lean a quasi-steady state is unlikely to occur. Therefore the overall amount of NO formed depends largely on temperature, time of residence and air to fuel ratio.[87]

4.2.4.2: Prompt NO*x*

It is known that during the combustion of hydrocarbon fuels, the amount of nitrogen oxides formed is always higher than that is produced during the direct oxidation of atmospheric nitrogen (thermal NO*x*). The mechanism leading to the prompt NO*x* formation was first identified by Fenimore.[86] Prompt NO*x* provides an explanation for the formation of NO*x* at low temperatures, under fuel rich conditions and at shorter residence periods. Fenimore described a mechanism in which molecular nitrogen reacts with the radical species formed during the combustion of hydrocarbons according to the following reaction pathways (equation 1, 2, and 3 global reactions)

$$CH + N_2 \rightleftharpoons HCN + N \quad (1)$$

$$N + O_2 \rightleftharpoons NO + O \quad (2)$$

$$HCN + OH \rightleftharpoons CN + H_2O \quad (3)$$

From all the above equations the processes that contribute predominantly to the NO formation are equation 4 and 5 (global reactions).

$$CH_2 + N_2 \rightleftharpoons HCN + NH \quad (4)$$

$$HCN + CN + O \rightleftharpoons NO + \text{organic residue} \quad (5)$$

Prompt NO*x* formation is directly proportional to the number of carbon atoms present per unit volume. The concentration of HCN that is formed increases with the concentration of hydrocarbon radicals, which in turn increases with the equivalence ratio. As the equivalence ratio (λ) increases, prompt NO*x* formation increases at first, then passes a peak, and finally decreases due to a deficiency in oxygen (Fig. 23).[88]

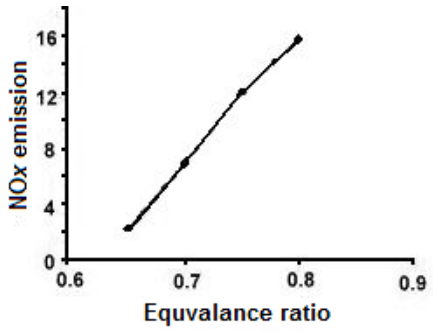

Fig. 23: Equivalence ratio (λ) vs NO*x* emissions (g/kWh)

In an internal combustion engine the flame reaction zone is extremely thin and residence time within this region is short because the combustion occurs at high pressure, and the burned gases produced early in the combustion are compressed to further higher temperatures in a shorter residential time, due to the rise in cylinder pressure immediately after combustion during most of the combustion process. This is termed as time of residence; all local and global reactions that lead to the formation of NO in initially stages mainly depend on the time of residence of a given ion at a particular temperature range.

4.2.4.3: Fuel NO*x*

Chemically bound nitrogen, when present in the fuel, can create nitrogen containing intermediates which are subsequently oxidized to NO*x*. This type of NO*x* formation is not prevalent for both diesel (>1 %) and biodiesel (0.02 %) emissions as the average nitrogen concentrations are too low. [83] However, fuel NO*x* strictly depends on the chemical structure and basicity of the nitrogen containing compound in the fuel (further explanation is presented in subsequent chapters).

4.2.4.4: Oxygen content of the fuel

The above three factors are well known as general causes for NO*x* emissions. The oxygen content of the fuel is one of the factors that plays an important role in NO*x* emissions, and also. fuel oxygen content is well known to reduce particulate matter emissions, but it also effects in the increase of NO*x* emissions which is a typical PM-NO*x* tradeoff behavior, i.e., the lower the PM emissions the higher the NO*x* emissions. The increase in oxygen content of the fuel thus increases the NO*x* emissions relative to the method in which oxygen is added (as chemically bond oxygen or enrichment of oxygen in intake air).[89] Li *et al.*[90] have studied the impact of enrichment of nitrogen on NO*x* emissions and shown that nitrogen enrichment of the intake air leads to a decrease in NO*x* emissions and a moderate increase in PM

emissions.[91] Song *et al.*[89] have shown that oxygen enrichment of the intake air increases the NO*x* emissions by 53 and 126 % with respect to the baseline oxygen concentration for 22 and 23 vol. %. The reduction of oxygen content in intake air hence reduces NO*x* emissions in one or the other way. A similar principle is applicable for fuels with enriched oxygen content.

The above discussion allows us to make a connection between the effects of oxygen on the NO*x* emissions. However, it does not provide a satisfactory explanation about the effect of chemically bond oxygen in the fuel. Eventually, any fuel that contains carbon and hydrogen when burned completely under stoichiometric conditions yields carbondioxide, water, and heat, as shown in equation (1).

$$C_mH_n + (m + 0.25n)\, O_2 \rightarrow m CO_2 + 0.5n\, H_2O + \text{heat} \quad (1)$$

The amount of oxygen required for a stoichiometric combustion of a fuel under ideal conditions is given by $m + 0.25n$ moles of oxygen per mole of fuel. A similar equation can be written for oxygen containing fuel (equation 2). The amount of atmospheric oxygen required by the fuel is given by $[(m - x/2) + 0.25n]$ moles of oxygen per mol oxygenated fuel, where *m*, *n* and *x* are number of carbon, hydrogen and oxygen atoms present in the fuel.

$$C_mH_nO_x + [(m - x/2) + 0.25n]\, O_2 \rightarrow m CO_2 + 0.5n\, H_2O + \text{heat} \quad (2)$$

From the equations 1 and 2 it is clear that when a fuel is burnt under stoichiometric conditions (ideal case) the amount of oxygen required by the fuel that contains chemically bond oxygen consumes a lower amount of atmospheric oxygen compared to the fossil fuel, irrespective of the chemical pathway involved in the combustion. The difference in the number of moles of atmospheric oxygen consumption by both the fuels can be given by a value "α" as shown in the equation (3).

$$\alpha = (m + 0.25n) - [(m\text{-}x/2) + 0.25n)] \quad (3)$$

The value of "α" can be positive or negative depending on the fuels that are compared. For example, when propane (C_3H_8) and methyl acetate ($C_3H_6O_2$) are used as fuels in an internal combustion engine, from equation (1) propane requires 5 mol of atmospheric oxygen for complete combustion under stoichiometric conditions, whereas methyl acetate according to equation (2) requires only 3.5 mol of atmospheric oxygen for its complete combustion. The difference can be given by the "α" value which is equal to + 1.5. That is 1.5 mol excess oxygen is consumed during the stoichiometric combustion of propane or 1.5 mol excess

oxygen is present in the engine cylinder during the stoichiometric combustion of methyl acetate.

In reality, oxygen is from the air and that every 4.76 equivalents of air contain 1 equivalent of oxygen. The equation to calculate the number of moles of air required for the combustion of a mol of fossil fuel $(A/F)_{ST}$ can be given by $4.76m + 1.19n$, and the number of mol of air required for the combustion of 1 mol of oxygenated fuel $(A/F)_{STO}$ can be given by the equation $4.76\ (m - x/2) + 1.19n$, where m, n and x are number of carbon, hydrogen and oxygen atoms present in the fuel. Considering that both fuels are burned in the same engine, under similar engine conditions, the difference in number of moles of air consumed is obtained by the difference between $(A/F)_{ST}$ and $(A/F)_{STO}$ which is given by a value "β"as shown in equation (4).

$$\beta = (4.76m + 1.19n) - [4.76\ (m - x/2) + 1.19n] \quad (4)$$

The value of "β" can be both positive and negative; a positive "β" conditions mean the engine is running lean with respect to the oxygenated fuel and a negative "β" value represents a fuel rich conditions. For example, when propane (C_3H_8) and methyl acetate ($C_3H_6O_2$) are used as fuels in an internal combustion engine, the difference in the consumption of air during stoichiometric combustion can be obtained by deducing the values in equation (4) which gives a "β" value of + 7.14. That means 7.14 equivalents of excess air is required for the combustion of 1 equivalent of propane compared to methyl acetate under stoichiometric conditions. Thus, when methyl acetate is burned under the same engine conditions as propane, the engine runs lean.

Similarly, the difference in the amount of air required during the stoichiometric combustion of two different fuels can be given by a value "η".

$$\eta = (A/F)_{ST} \text{ of non-oxygenated fuel} / (A/F)_{STO} \text{ of an oxygenated fuel} \quad (5)$$

$$\eta = (4.76m + 1.19n) / [4.76\ (m - x/2) + 1.19n]$$

For example, when propane (C_3H_8) and methyl acetate ($C_3H_6O_2$) are used as fuels in an internal combustion engine, from equation (5) the value of "η" is obtained as 1.428. The "η" value is significant in the comparison of fuel to air ratios of fossil fuels with that of oxygen containing fuels (mostly biofuels). For example, when propane (C_3H_8) and methyl propionate

($C_4H_8O_2$) are compared the value of η=1. In other words the fuel oxygen content has theoretically no effect on the fuel to air ratio or the number of equivalents of air required for a stoichiometric combustion. Thus when propane is blended with 10 % of methyl propionate, the oxygen content of methyl propionate does not have any effect on significant changes in the emissions, any variations in the emissions could be only associated to the physical factors of the fuel (Chapter-4.2.4.5) where the oxygen content of the fuel does not play any role, other than the difference in the ions generated during the combustion of the fuels.

However, most of the oxygenated fuels are used as additives or blends in the fossil fuel and also most of the fossil fuels are mixture of compounds which distill in certain temperature range. Under such conditions it is possible to calculate the number of equivalents of air required for the stoichiometric combustion of 100 grams of fuel or number of grams of air for the stoichiometric combustion of 1 grams of fuel is given by a value "ξ" by using equation (6).

$$\xi = 4.76\ (0.0833p - 0.031q) + 1.19\ r \text{ moles of air/100 g fuel} \quad (6)$$

$$\xi = 0.28\ [4.76\ (0.0833p - 0.031q) + 1.19\ r] \text{ grams of air/1 g fuel} \quad (6)$$

Where, *p*, *q* and *r* are the % of carbon, % of oxygen and % of hydrogen present in a given sample of a fuel. For example, when a fuel mixture of 50 % of propane (C_3H_8) and 50 % of methyl propionate ($C_4H_8O_2$) is burned in an internal combustion engine, by substituting the *p* (65.17 %), *q* (21.61 %) and *r* (13.22 %) values in equation (6) the "ξ" value is obtained as 38.33 moles of air/100 g fuel or ξ = 11.10 grams of air per gram fuel under stoichiometric conditions. It is easier to obtain the *p*, *q* and *r* values for any unknown fuel by a simple elemental analysis. When two different mixture of fuels that possess the same "ξ" value are burned under similar engine conditions and show significant changes in the emissions, then is only associated to the physical properties of the fuel (Chapter-4.2.4.5).

For example, equations (6) can be applied to compare diesel and biodiesel for their emissions. The No. 2 diesel fuel contains an average carbon content of 87 % (*p*), oxygen content of 0 % (*q*) and hydrogen content of 13 % (*r*). By substituting it in equation (6) yields ξ = 49.96 moles of air /100 g of diesel fuel or 13.98 grams of air/1 gram diesel fuel. The biodiesel fuel contains an average carbon content of 77 % (*p*), oxygen content of 11 % (*q*) and hydrogen content of 12 5 % (*r*) and with equation (6) ξ =43.187 moles of air/100 grams of biodiesel or 12 g of air required for the stoichiometric combustion of 1 g of biodiesel.

It is well known from most of the literature, that the emissions of biodiesel are compared with that of the diesel fuel. This is inappropriate because biodiesel has a lower "ξ" value compared to fossil diesel fuel. When biodiesel and diesel fuel are burned under similar engine conditions 1.98 grams of excess air per gram of biofuel is present in the engine cylinder compared to diesel fuel. Since NO*x* emissions increase with the increase in oxygen concentration of biodiesel and B100 produces almost 9.5-10 % excess NO*x* emissions than diesel fuel. Apart from other physical factors that influence NO*x* emissions, the increase in quantity of air or oxygen radicals during the combustion or lower "ξ" value provides a clear reasoning for the elevated NO*x* emissions shown by biodiesel. Similarly, biodiesel shows lower CO emissions as it has lower % of carbon or a lower "ξ" value compared to diesel fuel; the same is true with the PM emissions. Therefore, it is not appropriate to compare two fuels that do not possess the same "ξ" value.

In a diesel engine the air is taken into the cylinder unthrottled. However, the only variable factor that could affect the engine emissions for a given fuel is the amount of oxygen ions from air and chemically bond oxygen present in the cylinder during combustion. This is because the percentage of carbon, oxygen and hydrogen in a given fuel are constants, which also influence the CO, HC and PM emissions, even though the amount of air that is taken in to the engine cylinder is a variable factor. The percentage of NO*x* emissions produced by a certain fuel compared to the amount of nitrogen present in the air is almost negligible i. e. the NO*x* emissions depend on the variability of free oxygen ions or atoms present during the combustion.

As pointed out already any two fuels or mixtures of fuels can only be compared when they have the same "ξ" values. For example, a 70:30 % mixture of diesel fuel and ethanol or a 77.2:16:6.8 % mixture of RME, diesel fuel and ethanol has an "ξ" value of 12.42 to 12.5 which can be compared with the emissions of biodiesel (RME). When all three fuels or mixtures of fuels show (if any) variations in the emissions it can be concluded that the oxygen content of these fuels has no effect on these variations, but the chemical and physical properties of the fuel cause the respective differences. The "ξ" value facilitates a clear systematic study to know the effect of oxygen content of the fuel on engine emissions, especially NO*x* emissions, and also provides a common platform to design new additives and fuel blends in the future.

4.2.4.5: Other factors

Also several other factors are believed to influence NO*x* emissions. For example, fuel density, the so-called "heating valve effect", the cetane number and the concentration of aromatic compounds in the fuel are all known to affect NO*x* and PM emissions from diesel engines.[92] Parker *et al*.[93] have suggested other possible causes like loss of radiant heat transfer, alternation in spray properties in oxygenated fuels due to differences in viscosity, surface-tension and fuel boiling point. Furthermore, the spray properties are also influenced by droplet size, droplet momentum, degree of mixing and penetration, evaporation rate and radiant heat transfer rate.[92]

4.2.4.6: NO*x* emissions from biodiesel

The amount of NO*x* released by biodiesel (B100) is 9.5 % higher compared to normal diesel (Fig. 24), NO*x* emissions of biodiesel depends on various factors, advancement of ignition timing due to the difference in physical properties like higher bulk modules of biodiesel when used in normal diesel engines and combustion properties. Biodiesel has a lower volatility compared to diesel fuel, which causes ignition delay leading to premixed combustion. Some of the studies by McCormick[95] reported that cetane number and iodine number (Fig. 25a)[96] have a direct effect on NO*x* emissions. The greater the iodine number the greater is the NO*x* emission, and the greater the cetane number, the smaller is the NO*x* emission (Fig. 25b).[96]

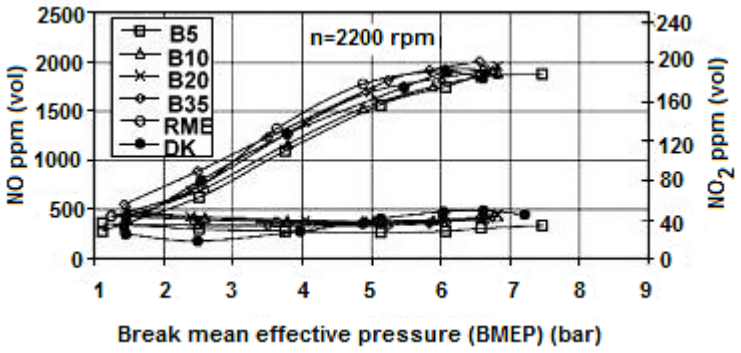

Fig. 24: Comparison of NO*x* emissions between biodiesel blends and Diesel fuel[94]

As mentioned above the fuel oxygen content also directly influences NO*x* emissions. The higher the fuel oxygen content (mass %) the higher are the NO*x* emissions (Table 2). In contrast, B100 (oxygen content 10.9 %) shows relatively low NO*x* emissions compared to B35 (oxygen content 4.08 %) blend which is associated with the aromatic content (up to 31.9

%) in petroleum diesel.[81] In order to reduce NO*x* from biodiesel an extensive study has to be done in the future to overcome the problems mentioned above.

Biodiesel blend (% oxygen content)	NO*x* emissions compared to diesel fuel
B 5 (0.925 %)	+ 5 %
B 10 (1.45 %)	+ 7.6 %
B 35 (4.075 %)	+ 9.1 %
B 100 (10.9 %)	+ 9.5 %

Table 2: Increase in NO*x* emissions with respect to biodiesel blends petroleum diesel [94]

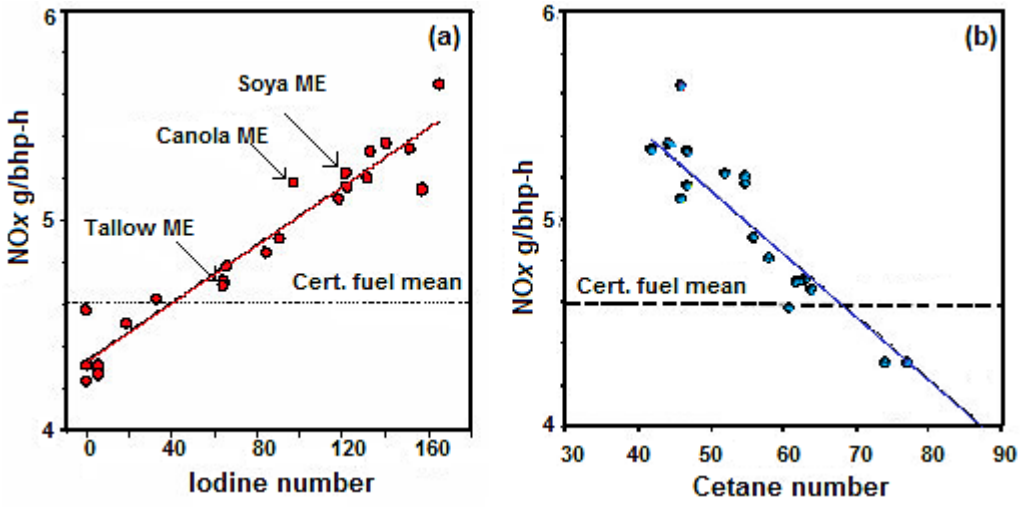

Fig. 25: Graph a) NO*x* emission vs iodine number, b) NO*x* emission vs cetane number

4.2.4.7: Environmental and health effects

Nitrogen oxides can travel long distances, causing a variety of health and environmental problems in locations far from their emissions source. These problems include ground level ozone and smog, which are created in the atmosphere by the reaction of nitrogen oxides and hydrocarbons (HC) in the presence of sunlight. The current levels set by a WHO guideline[79] have a value of 40 µg /m^3 (annual mean).

If the short term concentrations exceed 200 µg /m^3 they cause inflammation of the respiratory tract. NO_2 also leads to the formation of $PM_{2.5.}$ Epidemiological studies have shown that symptoms of bronchitis in asthmatic children increase with long-term exposure to NO_2.

Reduced lung function growth is also linked to NO_2 at concentrations currently observed in cities of Europe and North America. Due to the drastic measurements by the German government (Fig. 26) NO*x* emissions from automobiles have considerably decreased in recent years.

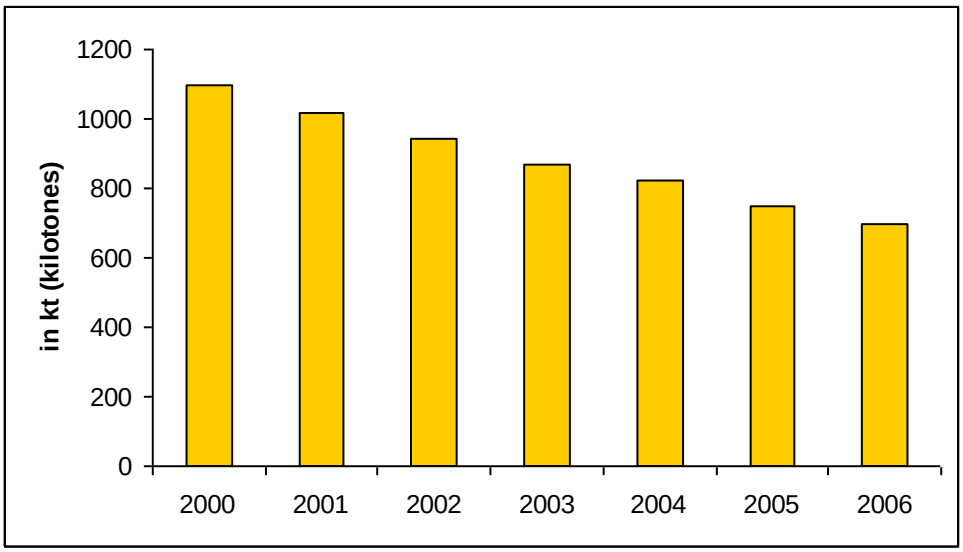

Fig. 26: NO*x* emissions from automobiles (related only to road traffic) in Germany from 2000-2006.[78]

Chapter 5: Regulations and pollution reduction

5.1: Recent developments in emission reduction

Even though advanced engine technology offers a substantial reduction in hazardous emissions, the improvement in engine combustion alone is not sufficient to reduce the emissions levels satisfying the current and future emission legislation. EU legislation [Regulation 715/2007][97] has finalized the regulations for Euro V and Euro VI light-duty engines which will be implemented for 2009 and 2014.[98] According to the legislation the emission standards for Euro V and VI light-duty vehicles are as follows (Table 3)

Diesel engines	**CO**	**HC**	**HC + NO*x***	**NO*x***	**PM**
Euro V	0.50		0.23	0.18	0.005 [2]
Euro VI	0.50		0.17	0.08	0.005 [2]
Petrol engines					
Euro V	1.0	0.10 [1]		0.06	0.005 [2, 3]
Euro VI	1.0	0.10 [1]		0.06	0.005 [2, 3]

Table 3: EU Emission Standards for Passenger Cars (light-duty engines), g/km [97]

1- And NMHC (non-methane hydrocarbons) = 0.068 g/km

2- Proposed to be changed to 0.003 g/km using the PMP measurement procedure

3- Applicable only to vehicles using DI engines

Due to the increased demand for low-emission vehicles, all automobile industries are now focusing on different strategies to reduce emissions; the most commonly used methods are mechanical modification (example: piezo inline injectors, exhaust gas recirculation etc.) and chemical modification (fuel additives and catalytic exhaust gas treatment etc.)

5.2: Catalytic exhaust gas treatment (for CO, HC and NO*x*)

In the past 30 years significant progress has been made in the field of catalytic converters to reduce exhaust gas emissions. The majority of light-duty vehicles are propelled by spark ignition engines which are largely responsible for the urban pollution. Spark ignition engines work efficiently under stoichiometric fuel to air ratio. As discussed above (Chapter 4.1.2) when an engine works under stoichiometric (λ=1) conditions the concentration of pollutants released is very low. The advanced catalytic converters work efficiently only under stoichiometric (λ=1) conditions. Under such operational conditions the thermodynamic

equilibria to convert exhaust gas pollutants to carbon dioxide and water is more towards the product side. Catalytic converters play an important role to attain the kinetic equilibria and higher conversion rates.

5.2.1: Catalytic converters

Basically, the catalytic converter completes the oxidation process of unburned hydrocarbons and partially oxidized carbon monoxide to carbon dioxide and water. These systems were first single bed oxidation catalysts (1975).[73] Later due to the stringent NO*x* control regulation, dual-bed catalysts were introduced which can reduce NO*x* and oxidize CO and HC separately. The present day three-way catalytic converts (TWC) (Fig. 27) can perform red-ox reactions on a single bed. Both the reduction of NO*x* and oxidation of CO and HC are performed on a single platform using different precious metal catalysts.[73]

5.2.2: Construction and working of a three-way catalyst (TWC)

5.2.2.1: The core (substrate or monolith)

The monolith is a porous solid support which is mostly made of ceramic or modern metal monoliths; the geometric surface area is in the range of 2-4 m^2 per liter of catalyst.[99] Some early vehicles used a palletized TWC packed tightly in a metal capsule. In modern vehicles TWC is most often an extruded ceramic honeycomb (cordierite: 2 Al_2O_3 x 2 SiO_2 x 5 MgO). Cordierite ceramic can withstand both the high temperatures of the exhaust gases, and the rapid temperature changes. Rolled stainless steel foil honeycombs are also used for high performance engines requiring large exhaust throughputs. The purpose of the core is to provide a support on which the catalyst is deposited. To increase the surface area of a monolith the channel walls are coated with a thin layer of inorganic oxides the so called washcoat. It provides a high internal surface area, holds the catalyst, and provides the catalyst with a higher surface area of exposure.[100, 101]

5.2.2.2: The washcoat

In an effort to make catalyst more efficient, a washcoat is incorporated. This provides a much greater surface area (app. 50-200 m^2/g), and therefore more places for active precious-metal catalytic sites. The washcoat (Fig. 27) with the catalyst is usually prepared as an aqueous slurry and applied to the monolith by dipping or spraying. Depending on manufacturer, different materials are used as washcoats. Alumina (Al_2O_3, boehmite), present in the gamma modification, is the most suitable and most often used high surface area support for noble

metals (Fig. 27). However, at high temperatures γ-alumina transforms into the α-phase and enables the diffusion of rhodium into alumina (diffusion barrier), a high surface change from 200-350 m^2/g (γ phase) to 5 m^2/g (α phase) is observed in phase transformation.[102] Besides alumina other washcoat constituents are cerium (ceria) and zirconium oxides. Ceria mostly acts as an oxygen storage component and as an oxygen buffer with the variation of A/F ratio. Mixed oxides like Ce_2O_2/ ZrO_2 are used in the washcoat due to their ability to catalyze water gas shift reactions. For improving the efficiency most of the materials are doped with lanthanides.

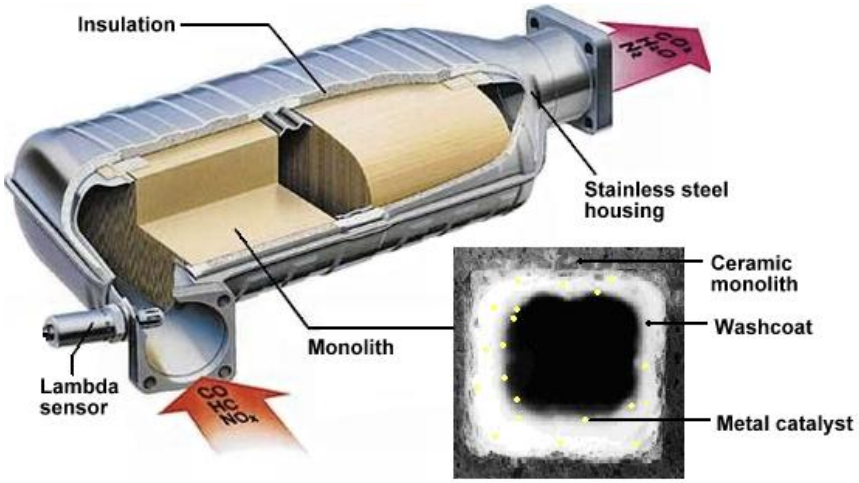

Fig. 27: TWC (Three Way Catalyst) and a closer look of monolith.[103, 73]

5.2.2.3: The catalyst

The catalyst is usually a platinum group metal. Most commonly used metals are platinum, palladium and rhodium.[73, 102] However, all three have their advantages and disadvantages. Pt shows higher resistance to poisoning but can cause sintering problems at high temperatures. Pd shows higher resistance to high temperature aging, but palladium has a narrow catalytic conversion window (λ range). Rhodium is the crucial ingredient of the three-way catalyst reduction process.[104] Rhodium displays sintering at high temperatures and NO*x* reduction on Rh is inhibited by high oxygen concentrations.[105, 106] This means that under lean exhaust conditions (diesel engine exhaust) NO reduction by the three-way catalyst is negligible.

5.2.2.4: Conclusion

Presently, the TWCs work excellently under stoichiometric conditions (λ=1) reducing the exhaust gas pollution up to 80 %. The application is, however, limited to the spark ignition

engine where a sigma sensor can control F/A ratio and throttle it accordingly. In the diesel and some gasoline engines which run on lean fuel to air ratio or release lean exhaust gas emissions, in other words higher oxygen content in the exhaust lead to poorer efficiency of TWCs.

5.2.3: Methods to reduce NO*x* emissions form lean exhaust

There are several methods discussed in the literature to reduce NO*x* emissions from lean exhausts. This includes SNCR (selective non-catalytic reduction) and SCR (selective catalytic reduction).

5.2.3.1: SNCR (selective non-catalytic reduction)

Among the physical or mechanical conditions with which NO*x* reduction can be achieved in SNCR, the following are the most important,

- Reduction of flame temperature by adjustment of injection timing and engine operation temperature.[107]
- EGR (*exhaust gas recirculation*) which is inert and used to reduce the adiabatic flame temperature.[108] EGR is the most cost-efficient method to control NO*x* emissions; it indirectly promotes rich fuel combustion and controls NO*x* emissions.
- FEW (*Fuel Water Emulsion*),[83] a low cost method to reduce NO*x* emissions, which can lead to lubrication problems and reduce the engine efficiency.[108, 109] It is mostly used to regulate engine temperature in stationary diesel engines (thermal NO*x* control).
- NO*x* additives are compounds that can be added to the fuel to reduce NO*x* emissions. This is a new concept and partially a goal of the present thesis (see below)

5.2.3.2: SCR (selective catalytic reduction)

SCR comes into action in the exhaust gas treatment downstream of the engine; it includes:

- DeNO*x* catalysts
- NO*x* absorber catalysts
- NH_3 SCR (selective catalytic reduction by ammonia)

5.2.3.2.1: DeNO*x* Catalysts

Lean De-NO*x* catalysts, also known as hydrocarbon-SCR systems use hydrocarbons from the exhaust to reduce the nitrogen oxides to nitrogen. Efficient conversion of NO*x* by DeNO*x* requires the presence of high concentrations of hydrocarbons in the exhaust, which can be achieved by adjustment of engine timing or by additional injection of fuel into the exhaust. Different types of catalytic systems such as Cu-ZSM-5, Cu-Fe-S-1, and Cu-S-1 catalysts,[111] and V_2O_5–WO_3/TiO_2,[112] among which the Cu-ZSM-5 DeNO*x* system has been intensively studied. The catalyst is activated at 500 ^oC using a thermostat where O_2 oxidizes the catalyst to form $[Cu\text{-}O\text{-}Cu]^{2+}$ oxocations, which can be readily reduced by NO and CO at room temperature. NO oxidizes Cu^+ ions and Cu_2O particles to form $[Cu\text{-}O\text{-}Cu]^{2+}$ cations and CuO clusters.[113] $[Cu\text{-}O\text{-}Cu]^{2+}$ oxocations act as catalytic sites for the disproportionation of NO into N_2O + NO_2, The catalyst is activated at very high temperatures; it shows a narrow temperature window of operation, one of the reasons why it is not widely used.

5.2.3.2.2: NO*x* absorber catalysts

NO*x* absorber or lean NO*x* trap catalyst (LNTC) adsorb and store NO*x* under lean conditions. Under lean exhaust condition NO is converted by platinum in the presence of oxygen to NO_3 which is stored in the zeolite based washcoat for a while.[73] Most frequently used washcoats in this case are alkali metal oxides (BaO and K_2O).[102] When the storage capacity of the oxide is saturated the engine is switched to rich operation conditions for few seconds, which is monitored by a sensor giving a signal to the on board computer. The stored NO*x* is released by temporarily inducing rich exhaust conditions and is reduced to N_2 by TWC mounted downstream.[98] The basic problem with NO*x* absorber catalysts are sulfur oxides from fuel sulfur, and the periodical shifting to rich fuel conditions leads to a fuel consumption penalty. NO*x* absorbers are experimental technology as of the early 2006. In recent vehicles a NO*x* trap is used on the VW Jetta Clean TDi and the VW Tiguan.[114]

5.2.3.2.3: NH_3 SCR (selective catalytic reduction by ammonia)

The Selective Catalytic Reduction (SCR) of NO*x* with ammonia as the reducing agent has been used for many years mostly in stationary diesel engine applications, as well as in some mobile applications. In the NH_3 SCR process, NO*x* reacts with ammonia,[115] which is injected into the exhaust gas stream just before a special SCR Catalyst (Fig. 28).[116] SCR is considered as the only technology capable of reducing diesel NO*x* emissions to the levels

required by future emission standards. Unfortunately, the NH_3 SCR system is presently permitted only for the heavy duty trucks and busses, and not yet for the diesel driven passenger cars. The NH_3-SCR system was introduced for commercial application in 2005 for HD diesel engines in Europe. Ammonia or any ammonia liberating source can be used in the catalyst. However, the most commonly used source is an aqueous solution of urea (commercialized as AdBlue)[117] which is a 32.5 % urea solution in water. A separate tank (75 L) is loaded in each truck which can serve up to 27000 km with a consumption rate of 1 %/km. For the automobile application NH_3 is generated onboard by the catalytic or thermal (above 250 ^oC) decomposition of urea.[98] Thus formed ammonia is injected into the reduction catalyst which is mounted downstream to the DOC.

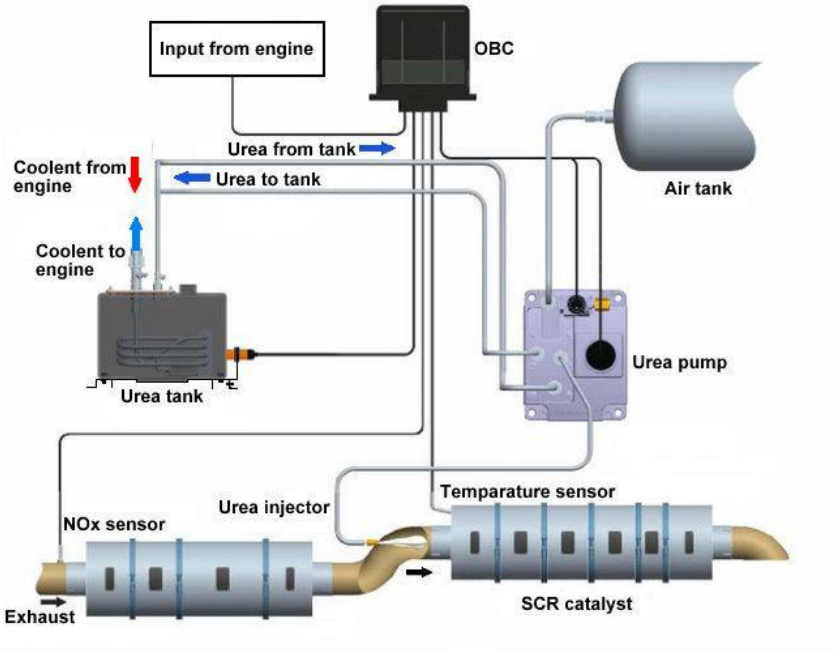

Fig. 28: SCR-NH_3 urea injection system.[116]

The amount of NO*x* in the exhaust is monitored by a sensor and sends a signal to OBC which regulates the NH_3 injection accordingly; the following reactions presumably take place in the conversion.

$$4\ NH_3 + 4\ NO + O_2 \longrightarrow 4\ N_2 + 6\ H_2O$$

$$2\ NH_3 + NO + NO_2 \longrightarrow 2\ N_2 + 3\ H_2O$$

$$8\ NH_3 + 6\ NO_2 \longrightarrow 7\ N_2 + 12\ H_2O$$

5.2.3.2.4: NH_3 SCR Catalysts

The catalyst is built in a traditional way (Fig 29). It contains a honeycomb support made of ceramic honeycomb (sillimanite, zirconia, petalite, spodumene, magnesium silicates, mullite, alumina, cordierite ($Mg_2Al_4Si_5Oi_8$), silicon carbide), or a metallic honeycomb. The washcoat is mostly made of carrier metal oxides or can comprise zeolites with oxygen storage material.

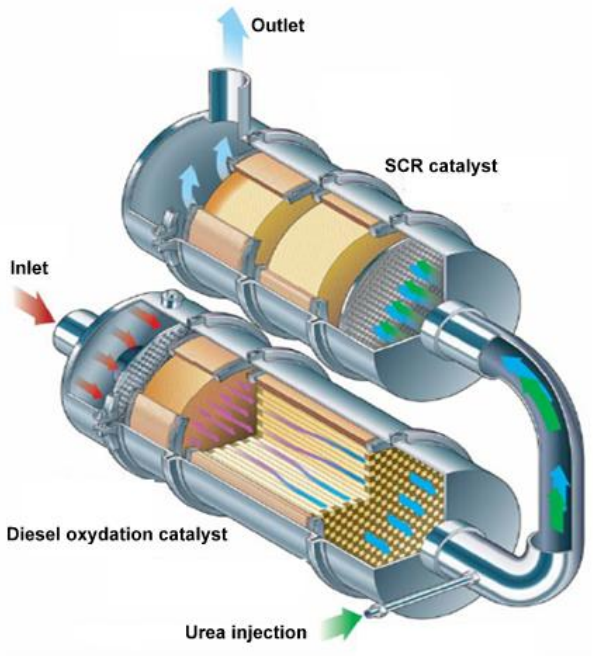

Fig 29: SCR-NH_3 urea catalyst system.[116]

The active catalytic material is traditionally based on vanadium/titanium (Ti_{6c}/V_{6c}),[115, 118] the temperature window for optimal operation of the catalyst is much higher (app. 250-370 ^oC) than the exhaust gas temperature of light duty vehicles (less than 200 ^oC).

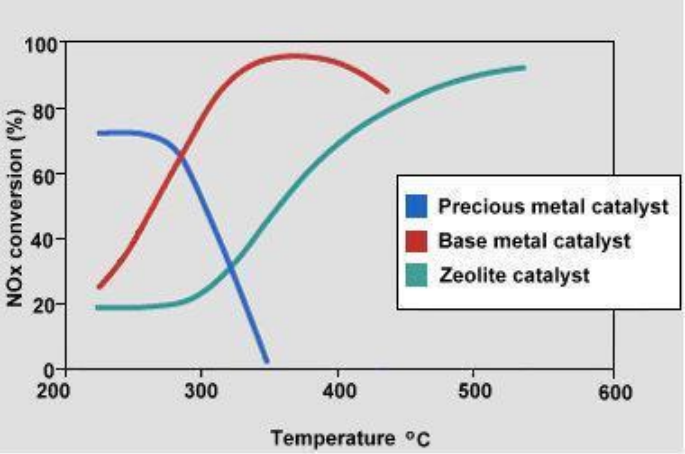

Fig.30: Temperature window in which different catalysts operate.[120]

Byrne *et al.*[119] proposed iron or copper-promoted zeolite catalysts. Copper-promoted catalysts possess good activity but lose it by aging; and there is a major concern of dioxin generation by the catalyst. Although the iron catalyst is far more stable than the copper catalyst it has maximum activity at about 350-500° C (Fig. 30). Stephen *et al.*[121] have proposed different types of zeolites (ZSM-5, zeolite beta, MCM-type zeolites etc.).

The composition of the catalyst varies with the manufacturer. However, presently, most commonly used catalysts are base metal catalyst, precious metals (platinum group metals, zeolites doped with lanthanides) and zeolites. The secondary products that are generated by the decomposition of urea (excess of ammonia, isocyanic acid, nitrous oxide and nitro hydrocarbons) are removed by a slip catalyst downstream.

5.2.3.2.5: Conclusion

None of the catalysts mentioned above is highly promising for reducing diesel NO*x* emissions (Table 4). Every catalyst has its strengths and limitations to attain the standards and requirements (for example ultra-low sulfur diesel is required for DeNO*x*) and the price is paid by the consumer. NH_3 SCR is the only catalyst system which shows some promising results. Presently, it is permitted only to heavy-duty diesel vehicles.

NO*x* control technologies	**NO*x* reduction (%)**
Low excess air (LEA)	0-15
Reduced air preheat (RAPH)	25-50
Water/Steam injection (WSI)	40-60
Exhaust gas recirculation (EGR)	50-80
Selective non-catalytic reduction (SNCR)	25-50
Selective catalytic reduction (SCR)	50-80

Table 4: Comparison of NO*x* control technologies[122a]

5.2.4: Control of PM emission

Removal of particulate matter from the exhaust is a physical separation process using particle filters. The exhaust gas is forced to flow through a monolith with fine pores and PM is deposited on the walls. The accumulated particulate matter on the walls is burnt from time to time at temperatures around 600 ^{o}C. Such higher temperatures are not possible to reach in

diesel engines. The continuously regenerating trap (CRT) system has been introduced in modern diesel vehicles, where NO_2 is used to oxidize the deposited particulate matter regenerating the monolith. In platinum based diesel particulate filters (DPFs) which are integrated with a diesel oxidation catalyst,[85] the system contains a flexible CRFI (common rail fuel injection system) which injects fuel into platinum based DOC and enables the regeneration of DPF upon burning the PM. Most recently aluminum titanate (AT) filters have been introduced which show higher efficiency and very low thermal expansions. The most advanced FBCs can reduce fuel NO*x* and PM emissions simultaneously.[122b]

Chapter 6: Aim of the thesis

The introduction of biodiesel into the market lead to an increase in glycerol reserves (Chapter 2), causing an increase in research interest on synthesis of value added products from it. The aim of this thesis was to look for the plausible synthetic routes towards the value added products of glycerol which included mainly the synthesis of fuel additives (Chapter 3) from glycerol, i. e. additives to reduce hydrocarbon, CO, and PM emissions as well as additives to reduce NO*x* emissions from the diesel engine

6.1: Fuel additives (fuel oxygenates)

Since glycerol is an oxygen rich compound, the most effective way to use it as fuel additive is to produce fuel oxygenates. Fuel oxygenates are the components (mostly alcohols, ethers and esters) which are added to the base fuel in less than 2 wt % to enhance the fuel properties and also reduces emissions. Diesel fuel is generally added with fuel oxygenates to reduce HC, PM and CO emissions. A new concept has been introduced in the field of fuel additives called "*green additives*",[123] compounds that are derived from renewable sources, for example from glycerol or glycerol derivatives which can hit both sides of the coin. Since, they reduce emissions and they are partially carbon neutral, it makes *green additives* more promising compared to the conventional diesel fuel additives. A part of this thesis focuses on the synthesis of fuel oxygenates from glycerol followed by engine tests performed with the oxygenated fuel.

6.2: Fuel additives to reduce NO*x* emissions from diesel engines

NO*x* emissions in diesel engine are the by-product of the combustion process. To reduce NO*x* emissions from diesel engines is the biggest challenge for many automobile industries. It is also a challenge for the fast growing biodiesel industry in present days. As shown above (Chapter-4) biodiesel has an advantage of effectively reducing HC, CO and PM emissions over petroleum diesel, but both the pure biodiesel (B100) as well as the blended biodiesel (B10 and B20) have the disadvantage of higher NO*x* emissions compared to petroleum diesel. Many approaches have been suggested in the literature to reduce NO*x* emissions from biodiesel, like fuel water emulsion (FWE), lowering the aromatic content of base fuel form 31.9 % to 7.5 %, blending B40 with kerosene.[96] The aromatic content of base fuel (diesel fuel), iodine value and cetane number of biodiesel play a key role in reducing NO*x* emissions.[124] However, most of the approaches mentioned above are based on the alteration

of the fuel. This thesis is focused on finding an alternative method by the addition of specifically designed compounds to the diesel and biodiesel fuels to reduce NO*x* emissions without altering the base fuel.

The reduction of NO*x* (especially NO) to N_2 by the addition of an external compound to the combustion process or to the stream of exhaust gases in the absence of a catalyst is termed as SNCR (Selective Non Catalytic Reduction). SNCR was primarily introduced in coal based furnaces to treat the combustion effluents. The efficiency of SNCR is basically influenced by the fuel composition, operational conditions, the reducing agent used (additive), and the type of system (coal based furnace or gas operated furnace or internal combustion engines).[125a] Accordingly, many variants of this technique have been patented, among which fuel rich process with ammonia,[125b] fuel lean process with ammonia[126] and the fuel rich process with urea[127a] are successfully used to reduce NO emissions in furnaces. However, to the present day any application of SNCR to the diesel engines has not proven to be successful. This has two basic reasons: primarily, the introduction of any reducing agent (NH_3, urea) into the exhaust gases of diesel engines (up to 600 ^oC) to reduce NO*x* concentration does not support the temperature gradient of the reaction at which the SNCR takes place (800-1200 ^oC) and secondly, in the furnaces, ammonia, urea or the combination of ammonia with hydrogen peroxide or with hydrogen are mainly used as reducing agents. Most of these reagents are insoluble in diesel fuel. Therefore, it is difficult to use them as additives other than there introduction as emulsions.[127i]

6.2.1: Application of SNCR to diesel engines

The combustion process in internal combustion engines is different to that of an open flame furnaces. To apply the theory of SNCR to the internal combustion engines, which is well established in open flame furnaces, requires some scrutiny. The important point that has to be considered is that in both the cases NO is primarily generated as a side product during the combustion of fuel (equation 1) from the oxidation of atmospheric nitrogen (except in the case of fuel NO*x*) above 1500 ^oC at atmospheric pressure; no evidence of NO production at elevated pressure has been reported. In an internal combustion engine the pressure variation during deflagration certainly affects the chemical kinetics of NO production. Thus, produced NO is further oxidized in the subsequent processes to produce higher oxides of nitrogen. If

the production of NO is reduced in the primary stages, it automatically decreases the overall NO*x* emissions.

$$N_{2\ (air)} + 1/2\ O_2 \xrightarrow[\text{app. 760 mm Hg}]{> 1500\ ^oC} 2\ NO \quad \text{equation (1)}$$

$$N_{2\ (air)} + 1/2\ O_2 \xrightarrow[\text{up to 60 bar}]{?} 2\ NO$$

Temperature plays a major role both in the production as well as in the reduction by SNCR of NO*x* emissions. The efficiency of NO*x* (especially NO) reduction by SNCR strongly dependdent on the temperature at which the reaction is carried out.[126] The effective reduction temperature is between 800-1200 ^oC. When carried out at this temperature the SNCR can provide a NO*x* reduction up to 90 % in a small well mixed system (which can be considered as an ideal system). However, in large furnaces the SNCR can provide a NO*x* reduction from 55-60 % only. This is due to the large temperature gradient and also the physical limitation to achieve uniform mixing and the shorter residence time. The NO*x* reduction by SNCR drops sharply above and below this temperature (800-1200 ^oC); at lower temperature unreacted ammonia is released and at higher temperatures NO*x* reduction efficiency drops sharply (15-30 %).[127a-127i]

The temperature gradient in any form of combustion is based on the type of combustion. An open flame combustion, which is generally used in furnaces, is a continuous form of combustion. The fuel is burned continually in the presence of air generating heat at a constant rate at atmospheric pressure. In an internal combustion engine the combustion is periodical. It is a controlled form of combustion; which is generally termed as deflagration. In the diesel engine a constant amount of fuel self-ignites in the presence of excess of air and deflagrates in a confined space to generate high temperature and pressure, and the thus produced gases are permitted to expand. The expanding gases are directly used to move a piston. The expansion leads to a constant decrease in the temperature and pressure of the gases inside the engine; this phenomenon is repeated periodically in the running engine. The periodical expansion and contraction generates a change in the thermal gradient inside the engine. The periodicity of this process is directly proportional to the speed of the engine. The speed of the engine influences the residence time of the reactants at a given temperature.

At a given speed of an engine, the residence time of ions formed during the combustion in a specific temperature zone is constant. In other words, the period of time the ions formed during the combustion that stay above 1500 ^{o}C (which leads to the formation of NO from atmospheric nitrogen, equation 1) is almost constant to the period of time they stay at a temperature of 800-1200 ^{o}C (effective reduction temperature of SNCR) due to the continuous movement of the piston. The amount of thermal NO that is formed at an elevated temperature (above 1500 ^{o}C) at a given speed is constant, and the amount of NO that can be reduced at lower temperature (800-1200 ^{o}C) at certain speed is also constant, provided, the reducing ions ($NH_{i=0,1,2,3}$) are readily available in the combustion chamber. The residence time of the reactants can be compensated by the rate of reactivity of an additive towards NO. If this assumption is valid, it provides an excellent opportunity to suppress the NO*x* emissions at a primary stage inside the combustion chamber.

The reduction of NO to N_2 by reducing ions ($NH_{i=0,1,2,3}$) during the combustion is well established in the literature at atmospheric pressure. Poole *et al*[128a] have shown that the reaction between NO and NH_3 follows a half order reaction rate with respect to NH_3 and 1.3 order dependence on NO at 700 ^{o}C at atmospheric pressure. They also showed that N_2O ions have an appreciable effect on the reaction properties of NO-NH_3 mixture.[128a] However, the extent of availability and the major pathways followed by the ions is basically decided by the environment in which the combustion takes place. It is well known that under fuel rich conditions there is a reduction of NO*x* emissions[128b] whereas an increase in NO*x* emissions are observed in fuel lean conditions. The major pathways followed under these conditions are comprehensively shown in Fig 31a and 31b. In an oxidized environment mainly in the diesel engines the $NH_{i=0,1,2,3}$ formed through different reaction pathways are converted back to NO. In other words, the equilibrium lies more towards NO rather than towards its reduction to N_2. The key strategy of SNCR is to shift the equilibrium by providing $NH_{i=0,1,2,3}$ ions externally as an additive or an external reagent and taking the advantage of difference in reactivity between NO and O_2 towards the reducing agent (NH_3 or R-$NH_{i=0,1,2}$). Leon[126] has proved that in open flame burners the reducing agent (NH_3) selectively reduces NO to N_2 in the presence of excess of oxygen at a temperature range of 900-1100 ^{o}C without being oxidized ($NH_3 + O_2 \rightarrow 2\ H_2O + 2/3\ N_2$). However, when the reducing agent is added directly into the combustion zone, one must consider the possibility of combustion or oxidation of the reducing agent (R-$NH_{i=0,1,2} \rightarrow \rightarrow$ R + NO) and the possibility of thermal decomposition of the reducing agent into corresponding ions (R-$NH_{i=0,1,2} \rightarrow$ R + $NH_{i=0,1,2}$). The processes are

assumed to depend on the structural, physical and chemical properties of the additive and on the combustion environment (oxidized or reduced environment) as well as on the residence time of an additive at a given temperature zone.[127a-127f] Eventually, the reduction ability of $NH_{i=0,1,2,3}$ ions is enhanced by different combination of additives like H_2O_2/NH_3, CH_3OH/NH_3, CO/NH_3, H_2/NH_3 and the hydrocarbons among which CO/NH_3 is effective in reducing the temperature at which NH_3 reduces NO in the presence of oxygen.

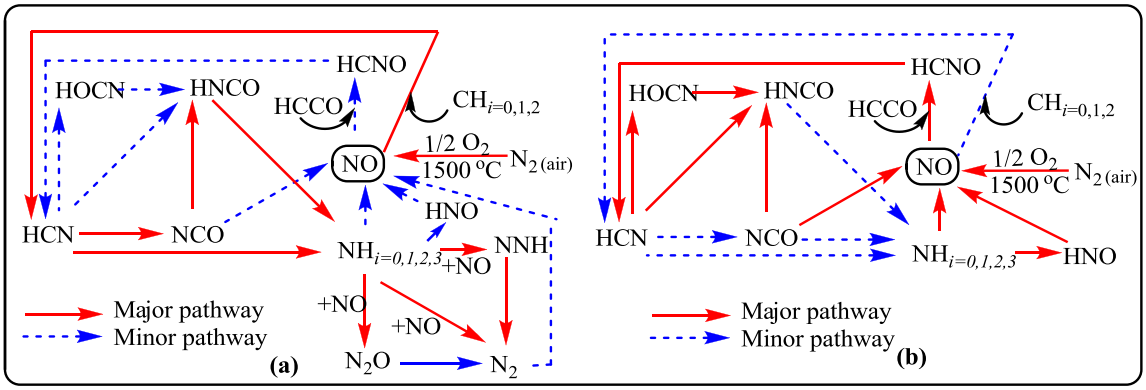

Fig 31: a) Schematic representation of all major reaction pathways involved in the combustion process under fuel rich conditions, b) Schematic representation of all major reaction pathways involved in the combustion process under fuel lean conditions. (The kinetics of the reactions mentioned above have been studied throughly)[129a-129e]

One of the major concerns about the addition of nitrogen containing compounds to the fuel is the production of fuel NO*x*. Especially, in diesel engines, when the fuel is deflagrated in the presence of excess of oxygen, it provides a high possibility of oxidation of nitrogen containing additive to produce increased NO*x* emissions. Leon[126] in his patent has shown that NO emissions can be successfully reduced from the stream of exhaust gases in the presence of excess oxygen using ammonia without oxidizing the reducing agent. However, the patent also provides evidence for the increase of NO emissions when the reducing agent (NH_3) is directly introduced into the combustion zones or when the reducing agent is introduced into the exhaust gases above 1100 ^oC. Eventually, this argument cannot be applied to the internal combustion engines due to the basic difference in the process of combustion between furnaces and internal combustion engines (as explained above). This was also proved by Reiter *et al.*[129a] by introducing ammonia–air mixture into a combustion chamber of a diesel engine. Both diesel and biodiesel fuels were used as base fuels. The idea was to use ammonia as alternative form of energy in combination with diesel or biodiesel fuel.

Introduction of ammonia showed a reduction in the NO*x* emissions. However, the reduction in NO*x* emissions were not due to the reducing effect of ammonia but due to a decrease in engine temperature caused by the low energy content of ammonia (18.6 MJ/kg fuel).

The process of combustion of ammonia in the presence of oxygen has been studied well in the literature. Edgar *et al*[129b] have shown that the stoichiometric ammonia-air mixture cannot be ignited at room temperature and pressure by a spark ignition. Only by increasing the concentration of oxygen in air and by exploding 1-2 mg of guncotton yarn can detonate the mixture. Similarly, Farber *et al*[129c] have studied the NH_3-O_2 diffusion flames and reported that the decomposition of NH_3 proceeds through a thermal stripping process with the removal of hydrogen and formation of NH_2 and NH radicals. The process of thermal stripping proceeds not by the direct reaction of ammonia with atmospheric oxygen ($NH_3 + O_2 \rightarrow 2\ H_2O + 2/3\ N_2$) but by the reaction of ammonia with OH radicals above 1500 ^oC ($NH_3 + OH \rightarrow NH_2 + H_2O$), these are abundantly present in a flame over the thermodynamic equilibrium as shown by Farkas *et al* using D_2 exchange with ammonia, or by the reaction of ammonia with O atoms as shown by Herman using atomic flames.[129d] This provides evidence that ammonia or amines resist oxidation by atmospheric air to NO under any temperature conditions. However, Finamore *et al*[129e] have shown that in a NH_3-O_2 flame almost 40 % of the ammonia fed may be converted into NO by the action of atomic oxygen which is irrespective of the temperature zone ($NH_3 + O \rightarrow \rightarrow NO + \ldots$) as it was estimated by the amount of nitrogen formed in the flame ($NH_2 + NO \rightarrow N_2 + \ldots$). However, Finamore[129e] also showed that in the presence of excess NH_2 radicals the consumption of NO is twice as fast as its formation. Eventually, the formation of NO from NH_3 in a post flame zone is not evident, due to the temperature dependence of formation of O atoms which propagate the reaction in post flame gases.

Based on the above discussion it is concluded that ammonia is resistant to oxidation in the presence of air and it requires O atoms to gradually convert it to NO. Unlike in a NH_3-O_2 flame as proposed by Finamore[129e] in the diesel engine environment the competition for O atoms by the carbon atoms of the fuel is much larger, reducing the availability of O and OH radicals to oxidize amines. However, the possibility of oxidation of amines cannot be neglected when an oxygen rich fuel is used. Apart from the thermal NO*x* produced from atmospheric nitrogen, 40 % of the added additive (amine) is converted to NO (in a NH_3-O_2 flame) which can be considered as an upper limit when compared to the diesel engine

environment. Such a condition promotes an increase in NO*x* emissions (fuel NO*x* from additive) only when a stoichiometric amount of additive is added with respect to the thermal NO*x* produced. Therefore, it can be presumed that by the addition of sufficient amounts of an additive, that survives the oxidation process, one could successfully reduce the NO formation (see discussion above). Above all the most important part that has to be addressed is the state of amine (1^o, 2^o or 3^o). As proven by Poole *et at*[128a] and Finamore *et al*[129e] in NH_3-NO flames that the NH_2 radical is an active reducing agent ($NH_2 + NO \rightarrow N_2 + OH + H$) which supports the presumption that primary amines are the best reducing agents that can be tested as additives. In case of secondary amines, Oshawa *et al*[129f] have shown that the reaction of secondary amines with nitric oxide (NO) to produce N_2O takes place only in the presence of oxygen ($RR^1NH + NO + ¼\ O_2 \rightarrow RR^1NNO + ½\ H_2O$) which presents an excellent condition for diesel engine combustion (fuel lean combustion). Moreover Miller *et al*[129g, 129h] and Popovic *et al*[129i] have shown that N_2O in fuel lean mixtures undergoes reduction in the presence of hydrogen atoms ($N_2O + H \rightarrow N_2 + OH$ or $NH + NO \rightarrow N_2 + OH$). However, the rate of formation of N_2O is faster than the direct N_2 formation from NH. Thus, the formation of N_2 via N_2O is predominant under fuel rich conditions whereas the latter is leading under fuel lean conditions. When tertiary amines are used as additives the fate of its reducing ability depends on the thermal-stripping process followed by the reduction as shown by Lindstedt *et al* ($N + NO \rightarrow N_2 + O$).[129j] Eventually, the thermal stripping process must be considered for all the primary, secondary and tertiary amines to produce NH_2, NH and N ions from their corresponding alkyl amines which could further promote the reduction of NO. Therefore, it is evident that upon addition of equal amounts of primary, secondary and tertiary amines to the fuel, their ability to reduce NO partially depends on their compatibility to thermal stripping, and partially on their rate of reactivity towards NO which is in the order of primary > secondary > tertiary.

Partial aim of this thesis is to produce nitrogen containing fuel additives from glycerol (R-$NH_{i=0,1,2}$), test there solubility both in diesel and biodiesel fuels, and to study their ability to provide $NH_{i=0,1,2}$ ions that could participate in NO reduction under diesel engine conditions. The idea is schematically presented in Fig. 32.

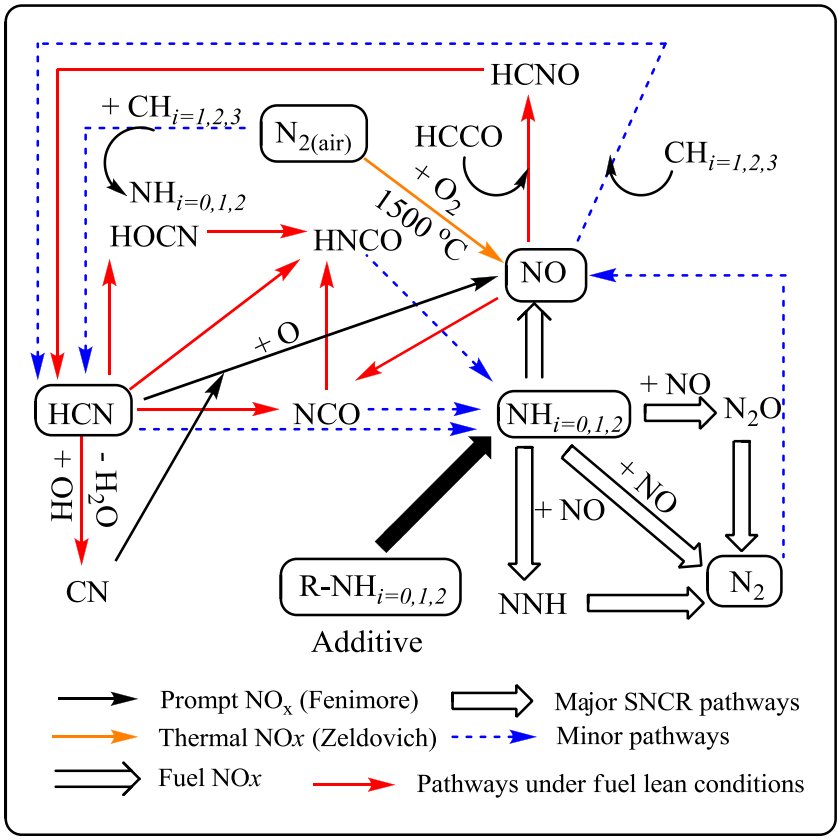

Fig. 32: Schematic representation of all major reaction pathways involved in the combustion process in a fuel lean combustion and the chemical pathways involved in the reduction of NO through SNCR by the nitrogen containing additive (R-NH$_{i=0,1,2}$). (The kinetics of the reactions mentioned above are well studied in the literature)[129a-129k]

Chapter 7: Engine Parameters

The fuel additives were tested separately by vTI (FAL) and ASG (Analytic-Service Gesellschaft) and the test engine parameters were as follows:

7.1: Fuel additive tests at FAL (vTI)

Some of the additives (mentioned in the experiments) were tested at the Institute of Agricultural Technology and Biosystems Engineering (vTI). The tests were conducted using a Mercedes-Benz truck engine (ATEGO). The test engine is coupled with an eddy current brake and the tests are performed according to the European Stationary Cycle (ESC). The engine parameters are mentioned in Table 5.

Engine model	OM 906 LA
Configuration	inline 6 cylinders
Bore (mm) x Stroke (mm)	102 x 130
Engine Displacement (L)	6.37
Maximum torque [Nm / speed (r/min)]	1100/1300
Rated power (kW)/speed (r/min)	205/2300
Emission standard	Euro III

Table 5: Engine parameters (Institute of Agricultural Technology and Biosystems Engineering, vTI)

The ESC test cycle (also known as OICA/ACEA cycle) has been introduced together with the ETC (European Transient Cycle) and the ELR (European Load Response) tests for emission certification of heavy duty diesel engines in Europe starting in the year 2000.[130] However, all experiments were performed according to ESC test cycle relevant to Euro III engines

7.2: Analytical methods

Individual analytical instruments were connected to the exhaust of the engine to measure different parameters separately (Fig. 33). The exhaust is taped into a gas analyzer (Multor 710) equipped with a non-dispersive infrared sensor (NDIR) to measure carbon monoxide. Similarly, hydrocarbons (HC) from the exhaust are measured using using an FID detector. The NO*x* emissions were measured by a chemiluminescence detector. The instrument is equipped with a catalytic converter which first converts the NO_2 from the exhaust to NO. The

attached ozoniser generates ozone for the oxidation of NO back to NO_2 which releases photons which are measured by the chemiluminescence detector.[131a]

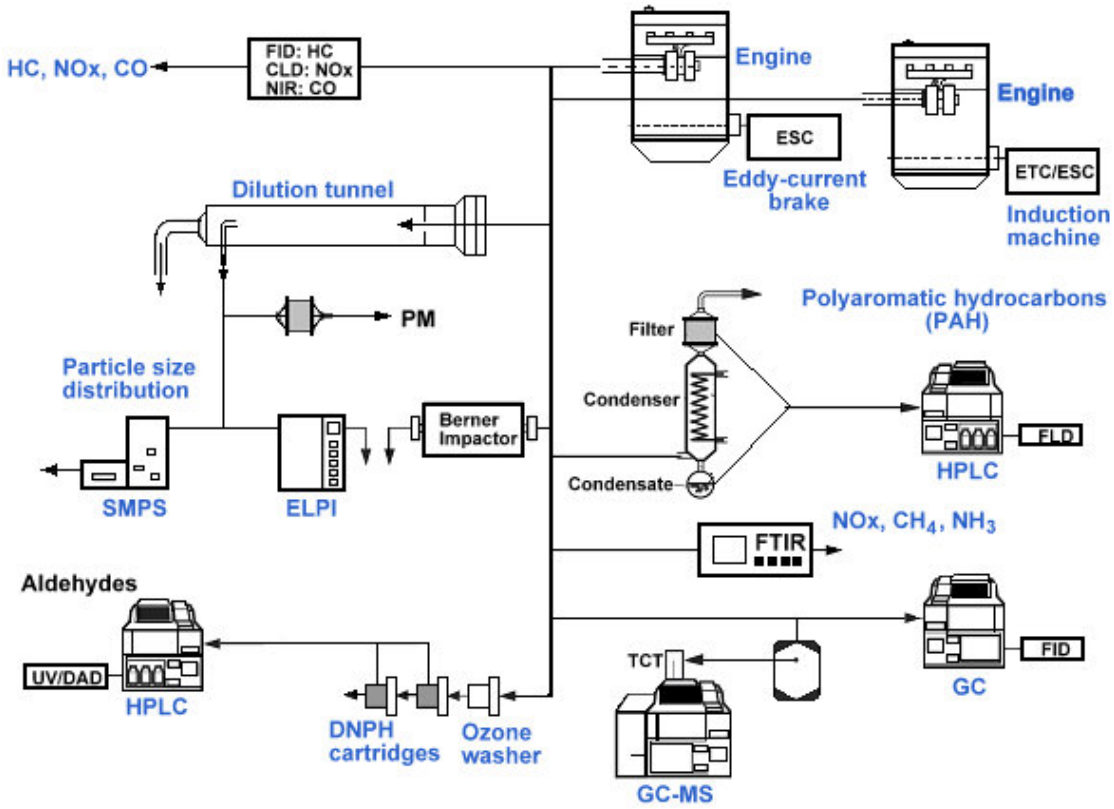

Fig. 33: Schematic representation of engine and analytical equipment at Institute of Agricultural Technology and Biosystems Engineering (vTI) (Engine: Mercedes OMD 906 LA, EURO III).

Particulate matter analysis was performed by the dilution of the exhaust and further cooling it to 51.7 °C, and the particles were collected on a filter paper. The total volume/time of the exhaust that was passed through the filter is measured according to the ESC-test standards. The filter paper was weighed on a balance and the amount of PM was calculated according to the following equation:

$$PT = \frac{M_{PF} \cdot \sum_i \left(V''_{EDF,i} \cdot WF_i \right)}{V_{SAM} \cdot \sum_i \left(P_i \cdot WF_i \right)}$$

PT: Specific particle emissions.

M_{PF}: Total weight of particle filters.

V_{SAM}: Total sample volume.

$V''_{EDF,i}$: Emission gas volume of the operating point- i.

WF_i: Weighting factor at the operating point-i.

P_i: Engine output at the operating point-i

7.3: Test parameters of AFIDA combustion chamber

The equipment used to test the emissions by ASG analytic was a combustion chamber (AFIDA). The combustion chamber is designed to measure the cetane number of the fuel accurately.[131b] It is attached with the equipment to measure all the major components of exhaust gases (Fig. 34).

7.4: AFIDA Combustion chamber

The AFIDA combustion chamber can be considered as equivalent to a stationary diesel engine. The combustion chamber contains a high-pressure cylinder with a ca. 0.6 L combustion chamber (as shown in Fig. 34). Sampling is done automatically using an auto-sampler and the sample is injected into the chamber using a Bosch piezo-injector. The combustion chamber is filled with pressurized air which can reach up to 400-2000 bar; the pressure inside the chamber is measured by a quartz pressure sensor.

Arbitrary injection volume	2-50 mL
Variable injection pressure	400–2000 bar
Combustion chamber temperature	400–730 °C
Combustion chamber pressure	20-100 bar
Fuel Thermostat	up to 120 °C
Fuel injection system	Bosch Piezo-Injector

Table 6: AFIDA combustion chamber parameters

The combustion chamber is covered with electrical thermostat and a cool water jacket for heating and cooling the chamber externally. After the combustion the exhaust gases are sampled for analysis.[131b]

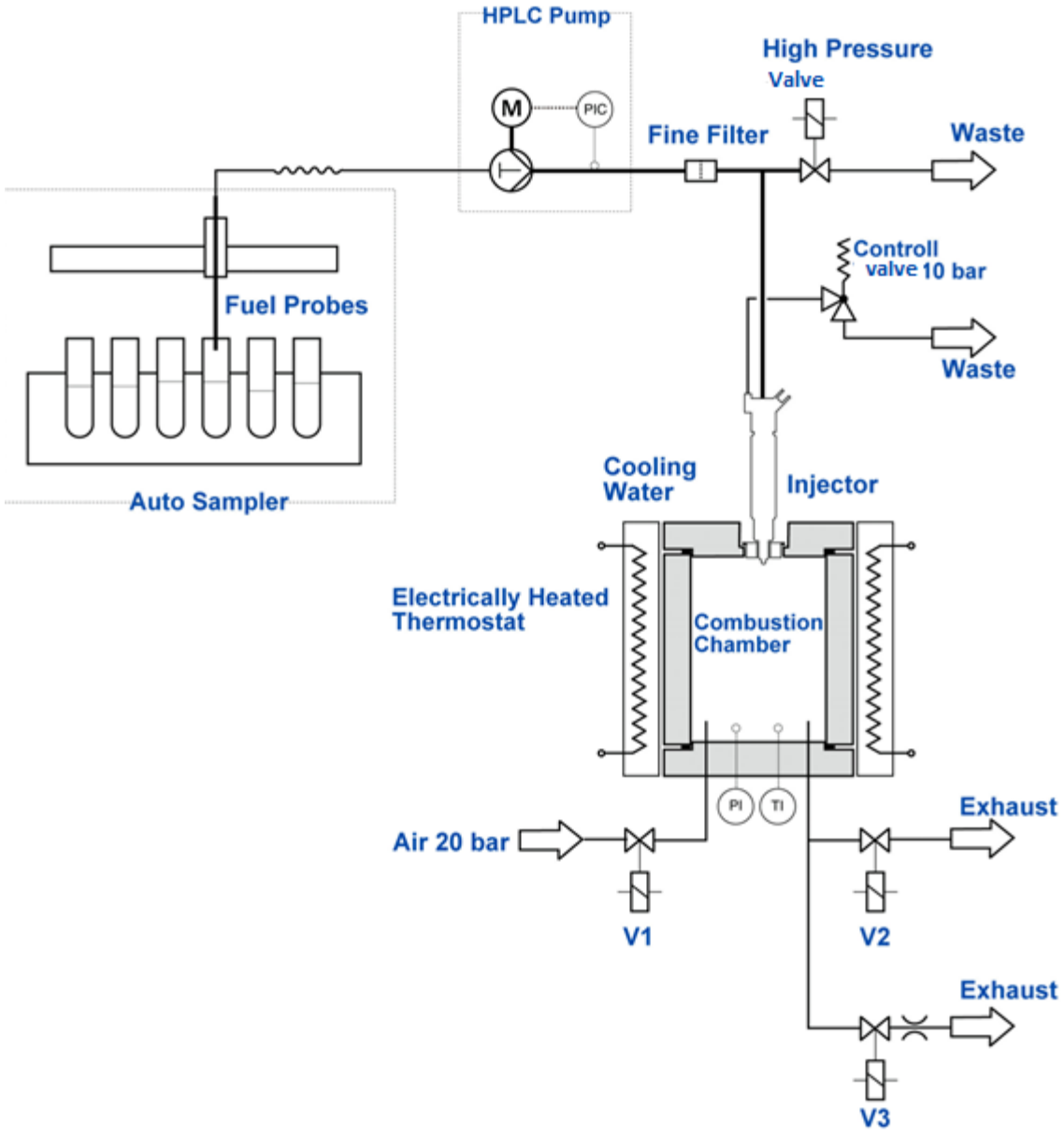

Fig. 34: Schematic representation of AFIDA combustion chamber.

Chapter 8: Tertiary alkyl ethers of glycerol (14, 16-19)

8.1: Introduction

The first known synthesis of 3-*tert*-butoxypropane-1,2-diol **(14)** by Malinavskii and Vvedenskii[132] dates back to 1953. According to their report 2,3-epoxy-1-propanol **(12)** was heated with five times excess *tert*-butyl alcohol **(13)** in the presence of 1% H_2SO_4 to yield **14** exclusively.

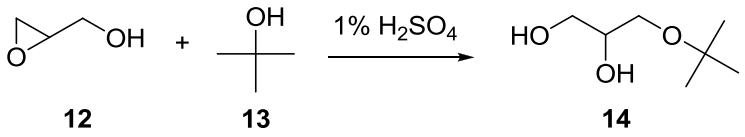

Scheme 7: Synthesis of 3-*tert*-butoxypropane-1,2-diol **(14)** from **12**.[132]

8.1.1: Synthesis using isobutene (15)

Synthesis of glycerol *tert*-butyl ethers **(14**, **16-19)** with isobutene **(15)** was first patented by Gupta[133] in 1995 and in the same year patented by Dewattines and Carine.[134, 135] This work was reinvestigated by Behr[136] in 2001 (Scheme 8) and was followed by many other researchers who examined a variety of catalysts. The synthesis using isobutene involves high pressure (3-70 bar) and moderate to high temperatures (50-200 ^{o}C). The reaction was performed using a wide range of acidic catalysts (Table 7) with isobutene **(15)** to glycerol **(2)** ratio of 1:1 to 6:1 and a gravimetric ratio of catalyst to **2** in the range of 0.01 % to 10 % for 3-6 h. The reaction has a high to moderate conversion rates of glycerol **(2)** and it mostly yielded a mixture of products, which includes 3-*tert*-butoxypropane-1,2-diol **(14)**, 2-*tert*-butoxypropane-1,3-diol **(16)**, 2,3-di-*tert*-butoxypropane-1-ol **(17)**, 1,3-di-*tert*-butoxypropane-2-ol **(18)** and 1,2,3-tris-*tert*-butoxypropane **(19)**, with dimers of isobutene 2,4,4-trimethylpentene **(20**, **21)** and *tert*-butanol **13** as side products.

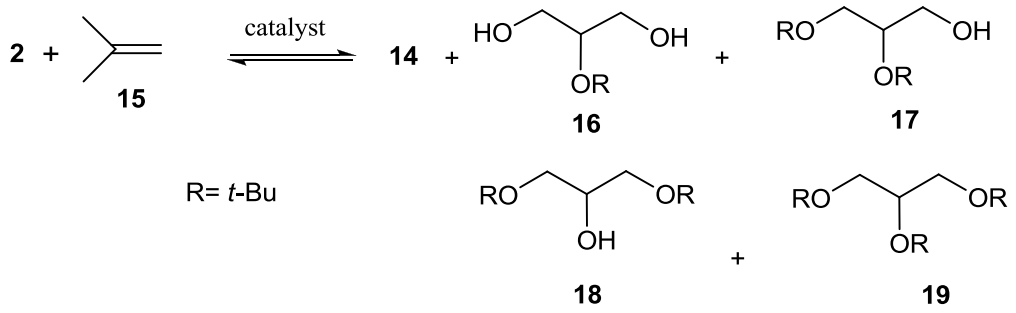

Side products

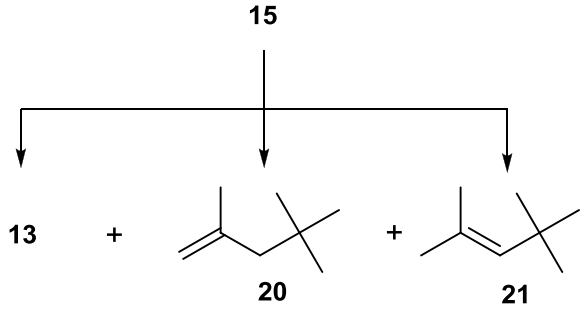

Scheme 8: Synthesis of glycerol *tert*-butyl ethers **14**, **16-19** with isobutene **(15)**.[136]

Catalyst	Cg (%)	**14, 16** (%)	**17, 18** (%)	**19** (%)	**13** (%)	**20, 21** (%)
p-TsOH	97.5	27.73	60.01	9.35	2.83	0
Heteropolyacid ($H_3PW_{12}O_{40}$)	98.9	25.71	54.07	8.02	0.87	11.2
$CS_2HPW_{12}O_{40}$	97.1	30.34	42.72	4.85	0.80	21.2
Amberlist-15	98.5	24.09	47.07	6.39	1.11	21.2
Mordenite-11	3.11	100	0	0	0	0
Mordenite-100	1.33	100	0	0	0	0
Zeolite β (12.5)	97.5	32.38	54.58	0.22	1.45	11.2
Zeolite Y (28)	98.9	24.62	60.36	6.42		7.35

Table 7: Results of etherification of glycerol with isobutene.[134] (Cg: Conversion of glycerol, *p*-TsOH: *para*-toluenesulfonic acid)

Catalysts like ZSM-5, SAPO-5, Zeolite-L, Zeolite Omega showed no conversion of glycerol **(2)**.

8.2: Synthesis using *tert*-butanol (13)

Due to the high costs of isobutene **(15)** (150 Euro/L) and a need to produce the ethers on a liter scale our emphasis was shifted towards *tert*-butanol **(13)** as the alkylating agent (6 Euro/1L). The reaction (Scheme 9) was first performed in 2004 in my master thesis where glycerol **(2)** was heated with *tert*-butanol **(13)** in the presence of the entrainment agent toluene in 1:3:3 ratios and *p*-toluenesulfonic acid as catalyst obtaining over 95 % conversion of glycerol **(2)** and a mixture of products, with diethers **17** and **18** as the major products in 72 % total yield. It was observed that with increased reaction times a large difference in product distribution occurred.

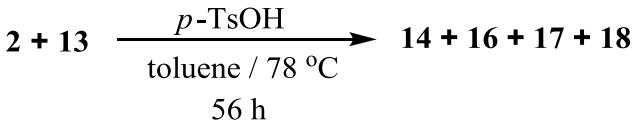

Scheme 9: Synthesis of **14**, **16**, **17**, **18** using *tert*-butanol **(13)**

An attempt was made in my master thesis to synthesize compound **19** from **18** using *tert*-butanol **(13)** in the presence of *p*-toluenelsulfonic acid and toluene as the entrainment agent. In the course of the reaction *tert*-butanol was completely consumed by liberating water and isobutene **(15)** whereas compound **18** was converted to **14** and glycerol **(2)** without any traces of **19**. However, synthesis of **19** from **18** was achieved by using isobutene **(15)** in the presence of *p*-toluenesulfonic acid at -78 °C in THF.

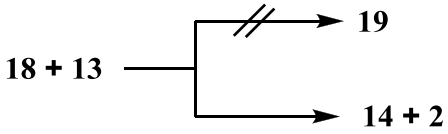

Later in my PhD work the reaction was optimized using *tert*-butanol **(13)** and a heterogeneous catalyst, amberlyst-15®. A selective synthesis of **14** and **18** was achieved. The results are summarized in Table 8 and Fig. 35. The optimization of the reaction was concentrated on obtaining the maximum possible yield of compound **14**. About 20 L of **14** was synthesized by this method with 87 % conversion of glycerol **(2)** and up to 92 % selectivity.

8.2.1: Product distribution and selectivity of 14, 16-19

Product distribution depends on reaction time, catalyst concentration and on the molar ratio of glycerol **(2)** to *tert*-butanol **(13)**. Table 8 represents the results of a series of experiments performed where the molar ratio of **2** to **13** was kept constant (1:4) and the catalyst percentage was varied to observe the product distribution in the reaction. The results indicate that the increased catalyst concentration decreases the reaction time; however, it also decreases the percentage of glycerol conversion and the yield of **14**. Eventually, a large difference in the product distribution of **14**:**16**:**17**:**18** was not observed. The change in catalyst percentage from 5 % to 5.4 % did bring a difference in the yield of compound **14**. However, it was not caused by the slight increase in the catalyst concentration but by the reduction in

reaction time to 140 min, which was irrespective of the amount of water collected in the Dean-Stark apparatus. However, it caused a decrease in glycerol conversion.

Catalyst (wt %)	Time (min.)	Cg (%)	Yield of compounds (%)			
			14	**16**	**17**	**18**
5 %	180	87	88	2	2	8
7 %	150	80	86	3	3	8
10 %	120	68	83	3	4	9
5.4 %	140	84	92	2	2	3

Table 8: Preparation of **14**, **16**, **17**, **18** using *tert*-butanol and amberlyst-15® as a catalyst. (Cg: Conversion of glycerol based on weight of the product) (% yield of compounds are based on GC analysis)

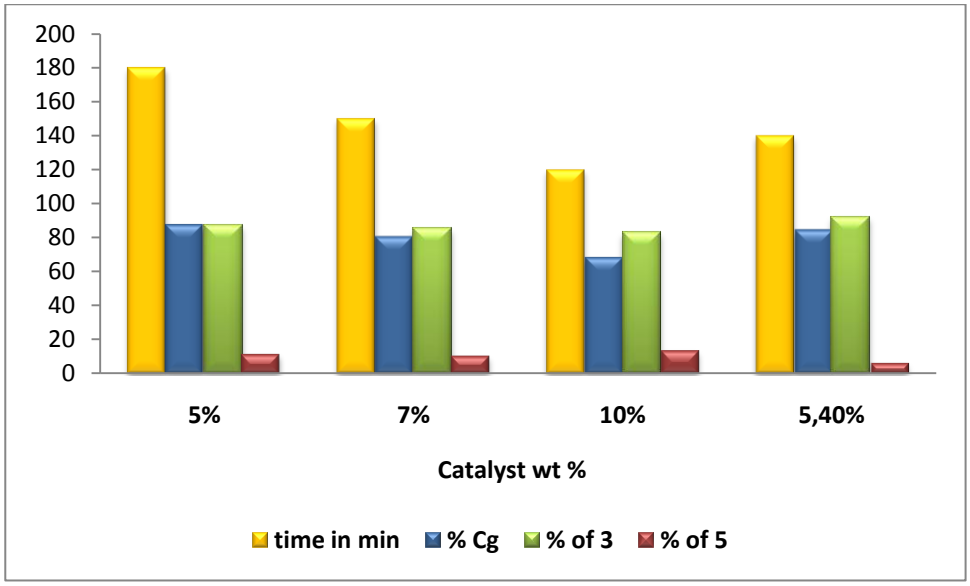

Fig. 35: Optimization of formation of **14** and **18** using the amberlyst-15® catalyst. (Cg: Conversion of glycerol based on weight of the product) (% yield of compounds are based on GC analysis)

The reason for the formation of compound **14** as a major product in this reaction and the type of product distribution observed is rationalized by the reaction mechanism.

8.2.2: Reaction mechanism of the formation of 14, 16-19

In the presence of excess *tert*-butanol **(13)** the acid catalyst reacts with **13** to form a stable *tert*-butyl carbocation **(22)** by loss of water. Formation of **22** is a reversible process. In the

absence of water or a suitable nucleophile **22** can lose a proton to produce isobutene **(15)** which is also a reversible process but the equilibrium lies more towards **15** due to the increase in enthalpy (Scheme 10).

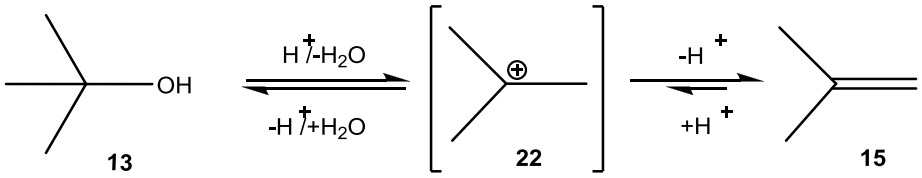

Scheme 10: Formation of *tert*-butyl carbocation **(22)**

In the presence of glycerol **(2)** as the nucleophile intermediate **22** reacts with either of the two primary alcohol or secondary alcohol functions leading to the formation of intermediates **23** and **24.**

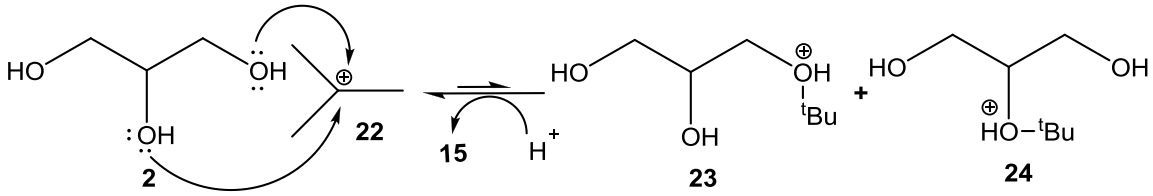

Scheme 11: Attack of glycerol **(2)** on **22** to form intermediates **23** and **24**

Intermediate **23** is obviously produced preferentially, both the statistics and the greater steric availability of the primary –OH group favors the attack of **22** at the terminal position. As the reaction is under equilibrium control by extension of the reaction time compound **14** can isomerise to compound **16** via intermediate **24**.

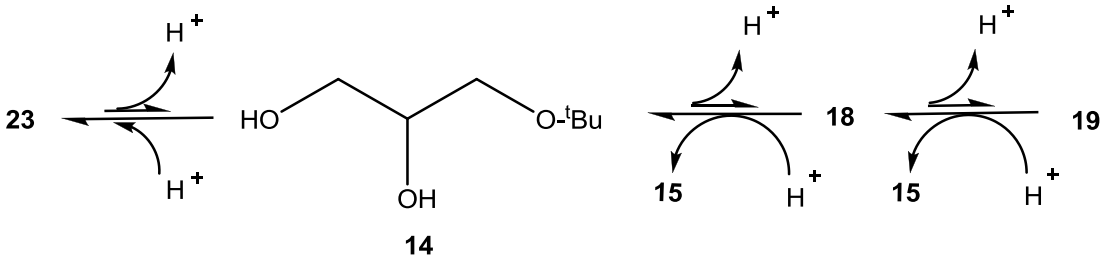

Scheme 12: Mechanism of formation of **14**, **18**, **19** from **23**

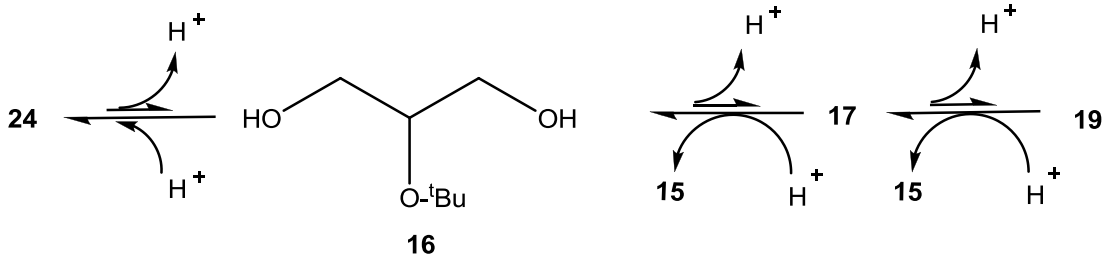

Scheme 13: Mechanism of formation of **16**, **17**, **19** from **24**

The isomerisation (Schemes 11-13) of *tert*-butyl ethers is a known process where the ether undergoes E1 elimination under acidic conditions by formation of alcohol and isobutene **(15)**. The reaction proceeds in three steps, in the first step ether is protonated to give intermediate **23** (oxonium ion) from compound **14**, followed by a rate determining step essentially irreversible, leading to the formation of *tert*-butyl cation **(22)**. The third step is a fast step in which a bimolecular deprotonation of the carbenium ion leads to the formation of isobutene **(15)** and releases the alcohol. The rate of elimination increases with increase in acid concentration, which explains the fact that a large excess of *tert*-butanol **(13)** is required in the reaction to compensate escaping isobutene **(15)** from the reaction mixture. This was clearly observed when an attempt was made to synthesize **19** from **18** using *tert*-butanol **(13)**. From the mechanism it can be rationalized that by increasing the acid concentration the reaction is shifted more towards glycerol. This also provides a clue that **17**, **18** and **19** can be produced either under low acidic conditions with longer reaction time or under high pressure conditions using isobutene **(15)**. The method involving *tert*-butyl alcohol **(13)** is suitable under laboratory conditions due to the low cost of the alcohol **13**. However, the synthesis using isobutene **(15)** is an industrially viable process.

8.3: Purification of crude mixture containing 14, 16-18

8.3.1: Distillation of 14, 16-18: A typical preparation

The crude mixture of 125 g containing 92 % of **14**, 2 % of **16**, 2 % of **17** and 3 % of **18** (based on GC analysis) was subjected to fractional distillation using a 40 cm Vigruex column. The first four fractions were collected at 76-78 ^{o}C at 0.4-0.5 mbar (110-115 ^{o}C at 15-20 mbar), from which the second fraction (8.31 g) contained maximum amount of compound **18** (69 %) and 7 % of **17** and 14 % of compound **14**. The next four fractions were collected at 85-90 ^{o}C at 0.4-0.5 mbar pressure (125-128 ^{o}C at 4-5 mbar pressure) from which the last

three fractions (109.4 g) had almost pure **14** (94-96 %). The second fraction of the first four fractions was subjected to a second distillation to obtain (6.4 g distributed in 2 fractions) of 86 % of compound **18** and 6 % of compound **17** and 2 % of compound **14** at 112-114 ^{o}C and 18-19 mbar pressure (it was not possible to separate compound **17** from **18** by distillation). Fractional distillation works well when the product distribution is not large i.e. when one of the products is dominating like compound **14** in the above case. An attempt to distill the crude mixture using a rectification column at atmospheric pressure failed. The distillation apparatus was calibrated using acetone which distilled at a constant boiling point of 56 ^{o}C. About 80 g of pre-distilled mixture was taken in a flask and was subjected to distillation using the rectification column at 220 ^{o}C. It took a long time to attain the temperature equilibrium (1.5 h) and the compound slowly started turning brown due to decomposition. The first fraction (5.63 g) was collected at 110-170 ^{o}C with a raise in temperature, the second fraction (7.35 g) was collected between 170 and 190 ^{o}C. A third fraction (12.87 g) at 200-202 ^{o}C, and a fourth fraction (17.24 g) at 205 ^{o}C and a fifth fraction (23.64 g) at 205 ^{o}C (constant boiling fractions). 3.25 g of charred material was left over in flask after distillation. All the fractions contained compounds **14**, **16** and **17**, **18**. Fraction 1 and 2 contained mixture of decomposition products, fractions 3, 4 and 5 contained pure mixture of ethers **14**, **16-18**.

8.3.2: Column chromatography of 14, 16-18

Column chromatography was performed using silica gel (see experimental section) and diethyl ether as solvent, where compound **14** and **16** has an R_f of 0.3 and compound **17** and **18** has a R_f of 0.8. It was possible to obtain the compound mixture in over 99 % purity of using this purification technique. But it was not possible to separate **14** from **16** and **17** from **18** by this approach.

8.3.3: Solvent separation of 14 from 18

Compound **14** is insoluble in pentane and compound **17** and **18** are well soluble in pentane. Using this advantage 500 mL of pentane was added to 300 g of crude mixture containing **14** (88 %), **16** (2 %), **17** (2 %) and **18** (8 %) till a cloudy solution was observed (amount of pentane added depends on the percentage of compound **14** in the crude). The solution was allowed to settle down with compound **14** precipitating. The solvent was decanted and the process was repeated twice. The decanted solvent was collected and evaporated to obtain 43.2 g of a mixture of compounds **17** and **18** (10 %, 22 %) which contains about 70 % of

compound **14** (based on GC analysis). The remaining solvent was evaporated from the precipitate to obtain compounds **14** (94 %), **16** (4 %), **17** (1 %) and **18** (1 %) respectively. The process works well when the concentration of compounds **17** and **18** are less than 20 % in the crude mixture. The advantage of this process is its ease to wash the crude with pentane to obtain ethers **14** and **16** high purity. The disadvantage is that unreacted glycerol is left over in the precipitated product which can be only separated by distillation. Mostly, such a separation was performed when the reactions were carried out on a liter scale where the loss of desired product **14** by distillation is much higher than by the method mentioned above.

It must be mentioned that the GC concentration of compounds given in percent in all above cases is a relative percentage which varies with the number of compounds in the mixture. And it is only relative to the compounds that pass through the column to the FID detector without any loss. For example glycerol does not show a peak in the chromatogram in any of the GC methods used above and is not considered in the relative concentration of the products.

8.3.4: Structural analysis of compound 14

The ^{1}H NMR spectrum of the compounds **14** is difficult to explain by using first order principles. In glycerol **(2)** which is the precursor of compounds **14** and **16** is a typical example for diastereotopism where both the *H* atoms of the methylene group H_a and H_b cannot be brought in to a chemically identical position by the rotation or by any element of symmetry.[137, 138]

Theoretically **2** must displays a $(AB)_2C$ type of spectrum. However, due to the free rotation about the C-C bonds the terminal CH_2OH rotates to attain three stable conformations. They are best shown as Newman projections **(2a-2c)** and the chemical environment of methylene protons H_a and H_b are examined in particular reference to geminal and synclinal (gauche) neighbours. The methylene protons show *six* possible near-neighbour relationships which are all different.[139] The population of conformers in a given solution depends on the rate of free rotation of the conformers at room temperature. Therefore, the spectrum of **2** shows a complex multiplet at δ=3.48-3.67 ppm for H_a and H_b (CH_aH_bOH) protons and a second complex multiplet at δ=3.70-3.79 ppm for H_c protons (CH_cOH).

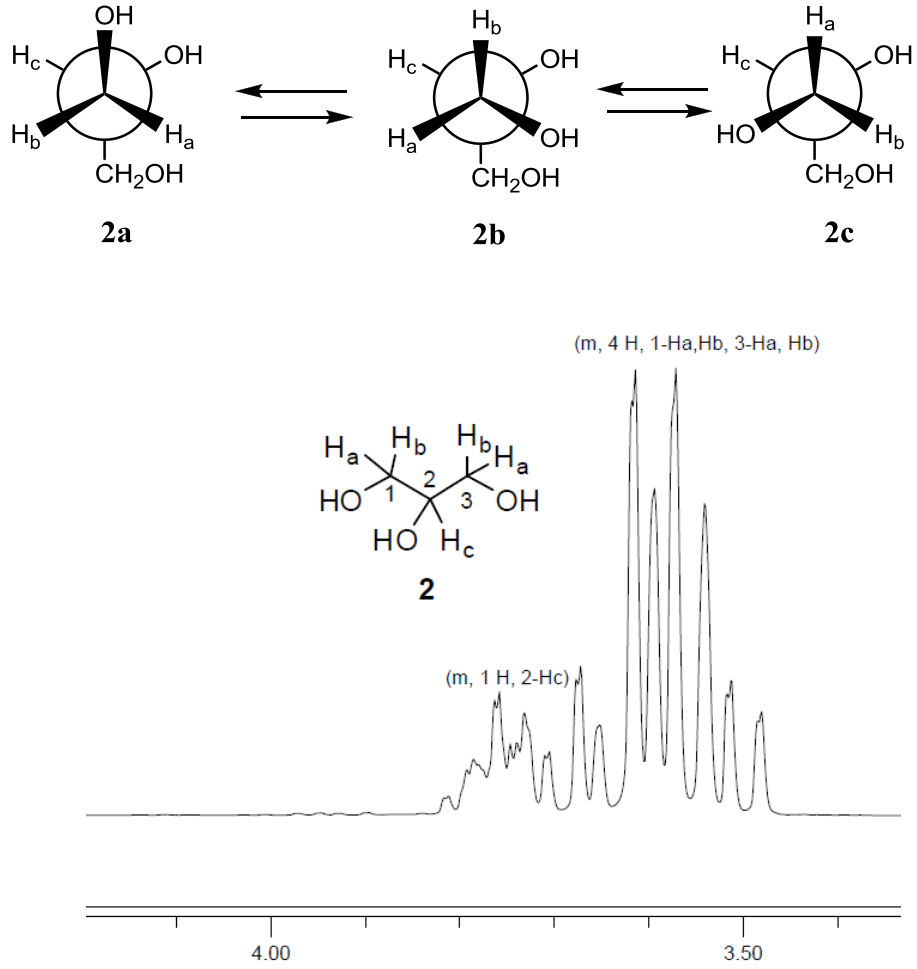

Fig 36: ^{1}H NMR spectrum of glycerol **(2)** (δ (ppm), D_2O, 12 % (w/w), 25 ^{o}C, 200 MHz)
(Sample: Sigma-Aldrich-99 % pure)

In compound **14** a stereocenter is created at C-2 by the introduction of *tert*-butyl group at one of the terminal –OH, due to which the two methylene groups in the glycerol are differentiated and it leads to a condition where *H* atoms on both methylene groups are chemically and magnetically different. Theoretically **14** must display a (AXBY)C type of spectrum. However, a much more complex spectrum is displayed by **14** due to the free rotation of CH_aH_xOH and CH_bH_yO-^{t}Bu around the chiral carbon (C-2) to attain 6 different conformations. They are best shown as Newman projections **(14a-14f)** and the chemical environment of methylene protons H_a, H_x and H_b, H_y are examined in particular reference to geminal and synclinal neighbours. The methylene protons show about 12 possible near-neighbour relationships, which are all different.[137] If the rotations would be frozen, then three different chemical shifts would be measured for H_a, H_x and H_b, H_y in each of the conformations **14a-14f** (δ_1, δ_2, δ_3 for H_a, δ_4, δ_5, δ_6 for H_x, δ_7, δ_8, δ_9 for H_b and δ_{10}, δ_{11}, δ_{12} for H_y) with reference to geminal and synclinal neighbours. If there is a free rotation at room

temperature and if *Xa*, *Xb*.….*Xf* are the population of conformers **14a-14f**, then different average chemical shifts ($\delta H_a = \delta_1 Xa + \delta_2 Xb + \delta_3 Xc$….. $\delta H_y \delta_{10} Xd + \delta_{11} Xe + \delta_{12} Xf$) are recorded which remain different ($\delta H_a \neq \delta H_x \neq \delta H_b \neq \delta H_y$) when all the conformations **14a-14f** occur with equal population ($Xa = Xb = \ldots Xf = 1/6$), then the chemical equivalence of such protons would be purely coincidental.

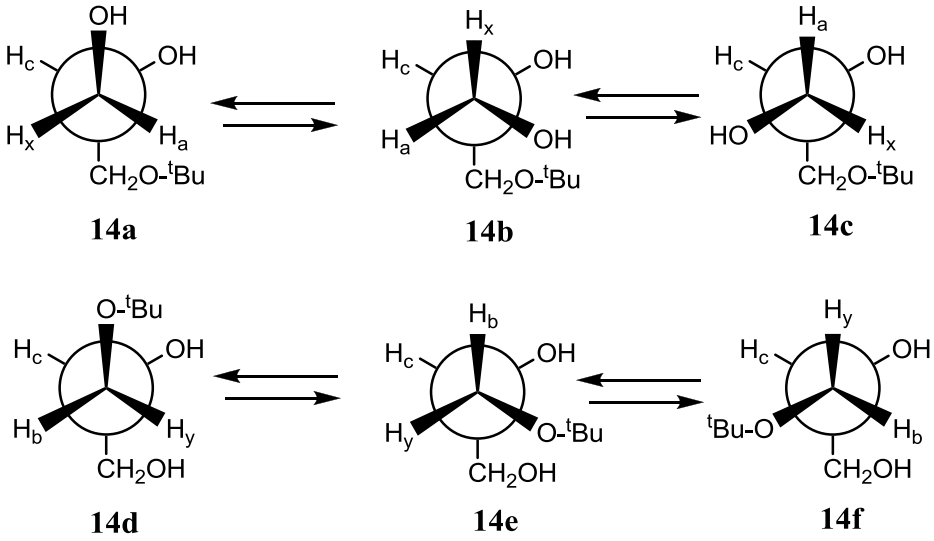

Therefore the ^{1}H NMR spectrum of **14** show a singlet at δ=1.25 ppm for the *tert*-butyl group (CCH_3) and a complex multiplet at δ=3.39-3.68 ppm for the H_a, H_x (CH_aH_xOH), H_b, H_y (CH_bH_yO-^{t}Bu) protons and a multiplet (9 peaks) at δ=3.70-3.83 ppm for H_c protons (CH_cOH).

The ^{13}C NMR spectrum of **14** recorded at 50 MHz in $CDCl_3$ show *five* different peaks as expected, corresponding to *five* different carbons atoms. The *tert*-butyl group (C-5) appears at δ= 27.3 ppm and the methylene carbon C-3 appears upfield at 63.4 ppm due to the ether linkage and the C-1 is shifted slightly downfield to δ=64.2 ppm. The secondary C-2 carbon atom appears at 70.8 and the C-4 tertiary carbon atom at 73.3 ppm. However, when the ^{13}C NMR spectrum of **14** was recorded at 50 MHz in D_2O it was surprising to see only *four* different peaks. The methyl carbons from the *tert*-butyl group (C-5) appear at δ=29.4 ppm, apparently the chemical shifts of C-1 and C-3 overlap with each other and appear at δ=65.7 ppm (δ= C-1= C-3), which could be mislead with compound **16** in which C-1 and C-3 are chemically equivalent carbon atoms. The secondary C-2 carbon atom appears at δ=73.9 and the C-4 tertiary carbon atom at δ= 77.6 ppm.

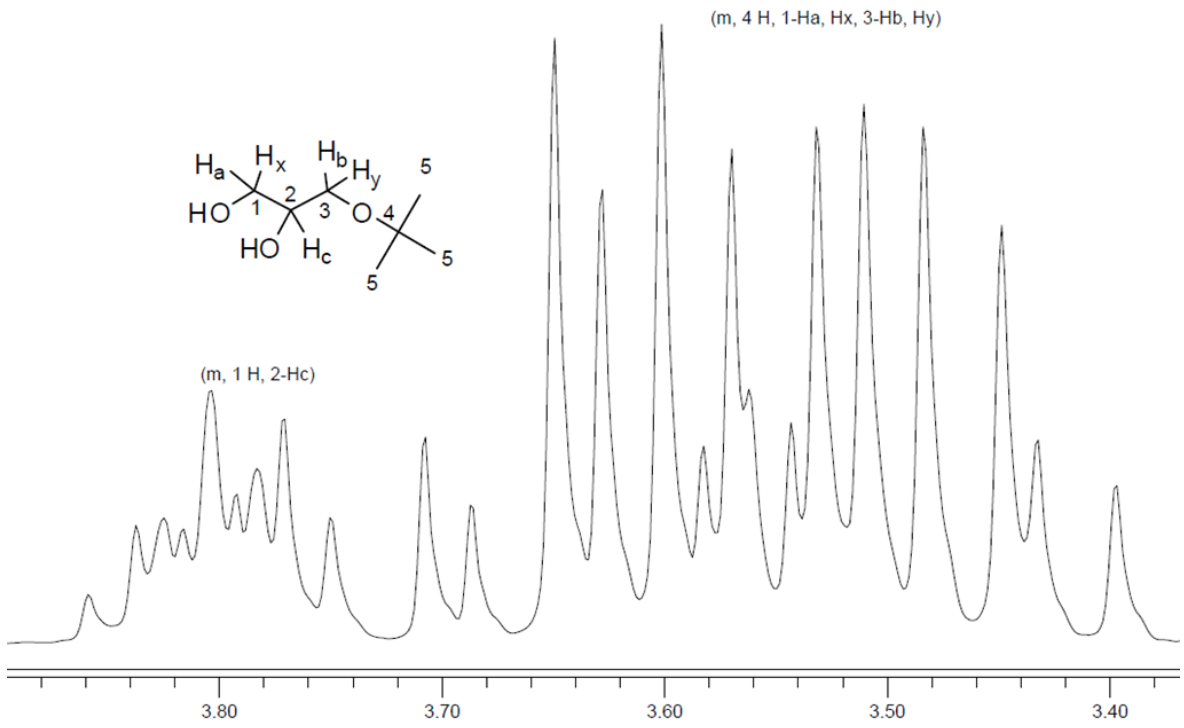

Fig 37: ^{1}H NMR spectrum of C-1, C-2 and C-3 protons in compound **14** (δ= (ppm), D_2O, 14 % (w/w), 25 ^{o}C, 200 MHz)

Mass spectrometry of the compound **14** shows a 5 % peak at *m/z*=133 corresponding to the loss of CH_3 radical from molecular ion $[M]^+$ and a 5 % peak at *m/z*=117 corresponding to the loss of CH_2OH radical from $[M]^+$. The base peak is observed at *m/z*=57 from the *tert*-butyl carbocation (analysis is attached in the end of the thesis). The IR spectrum shows a broad absorption band at 3449 cm^{-1} corresponding to the O-H stretching vibration and two bands at 2931 and 2878 cm^{-1} corresponding to the C-H stretching vibrations and a strong absorption band at 1079 due to O-H bending vibrations.

As mentioned above the introduction or the displacement of any atom on one of the primary carbinol groups of **2** generates a stereocenter at C-2 and thus a racemic product mixture.[140] A similar case is observed in compound **14** which is a racemic mixture of (*2S)*-3-*tert*-butoxypropane-1,2-diol and (*2R)*-3-*tert*-butoxypropane-1,2-diol (**14g** and **14h**, respectively). However, as the purpose of this thesis was not focused on enantioselective synthesis, no attempts were made to separate the enantiomers. Wherever compound **14** is mentioned or used in this thesis it is a racemic mixture of **14g** and **14h** (the unequivocal rules proposed by Hirschmann *et al.*[140] and Chan *et al.* [141] are used in this thesis to describe the stereochemistry of glycerol derivatives).

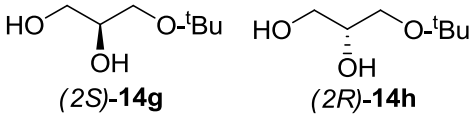

(2S)-**14g** *(2R)*-**14h**

8.4: Conclusion

The interest in glycerol *tert*-butyl ethers has grown in recent years due to their potential use as fuel additive (fuel oxygenates) in gasoline engines. As compound **19** is protected three times with a *tert*-butyl group it was expected that it could have three times the effect of the presently used octane enhancer methyl *tert*-butyl ether **(4)** with its single *tert*-butyl moiety. However, the slight variation in the "ξ" values of compound **19** (10.9) and methyl *tert*-butyl ether (11.1) calculated from equation-6 (chapter 4.2.4.4) disproves the above assumption.

Unfortunately, none of the reactions mentioned above could deliver **19** on an industrial scale. 1,3-di-*tert*-butoxypropane-2-ol **(18)** which could be synthesized in significant amounts has a higher boiling point and density as a gasoline additive and as a diesel additive it is not useful since its *tert*-butyl groups are octane enhancers or flame inhibitor, whereas diesel fuel requires cetane enhancers to improve diesel quality. Even though 3-*tert*-butoxypropane-1,2-diol **(14)** can be synthesized easily compared to the other ethers, all derivatives show a poor solubility in diesel fuel. Possibly a mixture of **18** and **14** could be used as fuel additive in gasoline.

As it was possible to produce **14** selectively in good amounts (about 20 L) following the above method, it was decided to use the compound in further transformations. To solve the problem of solubility and density, it was decided to protect the diol **14** as an acetal or acetate. Acetals were selected as a proper choice because of a known problem with acetates involves an increases in NO*x* emissions due to the increase of fuel oxygen content and lower ξ values compared to ethers or acetals.

Chapter 9: Synthesis of acetals 26-31

9.1: Introduction

Acetals are widely used to protect alcohols with an aldehyde/ ketone or vice versa, as shown by Fischer[142] in 1894 as protecting groups for sugars. The method was slightly improved by Newman *et al*.[143] in 1945, who synthesized isopropylidene glycerol or solketal **(26)** from glycerol **(2)** using acetone in the presence of *p*-toluenesulfonic acid as a catalyst. The reaction took 48 h due to the low solubility of glycerol in the acetone and petroleum ether mixture.

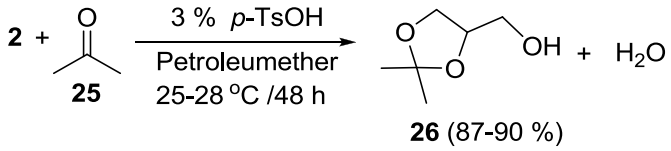

Scheme 14: Preparation of solketal **(26)** from glycerol **(2)**[143]

About 6-8 liters of solketal **(26)** were prepared using the above mentioned method. The reaction produces a recemic mixture of (*2S*)-2,2-dimethyl-4-hydroxymethyl-1,3-dioxolane and (*2R*)-2,2-dimethyl-4-hydroxymethyl-1,3-dioxolane (**26a** and **26b)**. Whernever compound **26** is mentioned or used in this thesis it is a racemic mixture of **26a** and **26b**.

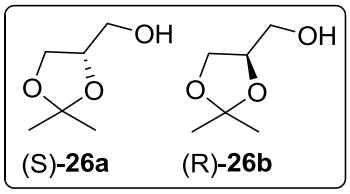

9.2: Synthesis of 2,2-dimethyl-4-*tert*-butoxymethyl-1,3-dioxolane (27)

Compound **27** was synthesized for the first time by Kaumaker and Thiele[144] (Scheme 15). According to the patent, compound **26** was synthesized by the reaction of **2** with acetone followed by the introduction of the *tert*-butyl group using isobutene **(15)**. After repeated reactions **27** was obtained in 70 % yield.

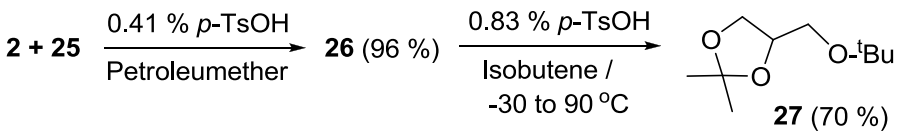

Scheme 15: Synthesis of **27** by Kaumaker *et al*.[144]

However, a different synthetic route was followed by us to attain **27**. In our case compound **14** was reacted with acetone in the presence of *p*-toluenesulfonic acid following Newman's method[143] to obtain 2,2-dimethyl-4-*tert*-butoxymethyl-1,3-dioxolane **(27)** in 96 % yield.

About 2 % of **26** was formed as a trace side product, probably due to the decomposition of starting material **14**. Around 10-12 L of **27** was successfully synthesized using this method (Scheme 16).

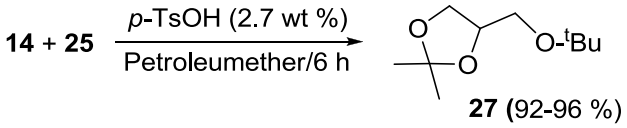

Scheme 16: Preparation of **27** from **14**

When large scale reactions were performed, the crude mixture of **14** obtained by the solvent separation method (Chapter 8.3.3) was used. The reaction produced up to 16 % of **26** depending on the amount of glycerol present in the mixture. The formation of **26** was reduced to 2-5 % due to a large difference in the reactivity between **14** and **2** towards acetone (compound **2** takes 48 h and **14** takes 6 h for completion of reaction). The diethers **17** and **18** present in the mixture did not participate in the reaction. Unfortunately, in this case, it was difficult to separate the product mixture by distillation due to a very similar boiling range of **26** and **27**. However, when the reaction was performed with pure starting material **14** (98 %) the product mixture was purified by distillation either at 184-185 ^{o}C at atmospheric pressure or at 42-43 ^{o}C at 0.3-0.4 mbar pressure to obtain analytically pure product. As mentioned above **27** was produced from a racemic mixture of **14g** and **14h**.

9.2.1: Structural and conformational analysis of 27

Literature evidence[145-147] indicates that the 1,3-dioxolane ring like numerous other cyclopentane ring systems exists in puckered conformation related to the envelop or half chair (twist) conformations. The energy difference between the conformers is very low (0.05-0.3 kcal/mol) and the molecule is thus in a rapid state of conformational flux known as *pseudorotation*. However, substituents on the five-membered ring have been shown to interrupt the *pseudorotational* circuit preventing a complete *pseudorotation*. Lemieux *et al.*[147] have shown that the introduction of substituents on C-2 and C-4 carbon increases the puckering of the ring. The conformation of **27** is best shown in **27a** where the methylene carbon C-2 is displaced out of the plane of the other four atoms of the ring.

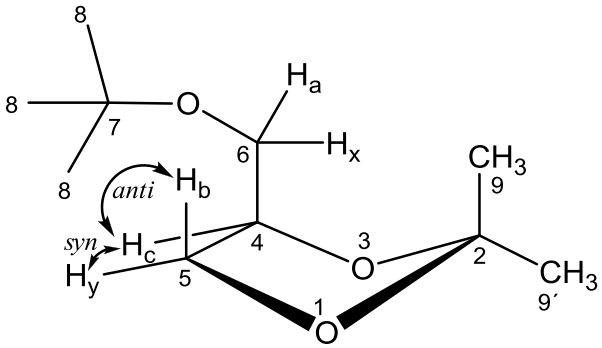

27a

Theoretically the ^{1}H NMR spectrum of **27** must display a (AXBY)C type of spectrum for the C-4, C-5 and C-6 protons (Fig. 38). However, the ^{1}H NMR spectra of **27** recorded at 400 MHz in $CDCl_3$ slightly deviates from the theory. The two methyl groups on C-2 carbon which are chemically and magnetically different, due to their *pseudo-equatorial* and *pseudo-axial* arrangement as expected show two different signals at δ=1.35 and 1.41 ppm, respectively. The *tert*-butyl group appears at δ= 1.18 ppm as a singlet. The methylene proton H_a from C-6 displays a (AB)C pattern of a doublet of doublet at δ= 3.2-3.3 ppm with a geminal coupling constant $^{2}J_{Ha,Hx}$ of 9.1 Hz, and a vicinal coupling constant $^{3}J_{Ha,Hc}$ of 6.68 Hz. The H_x proton from C-6 displays a multiplet (*six peaks*) at δ= 3.46-3.49 ppm. The ring proton H_b displays a doublet of doublet pattern at δ= 3.71-3.75 ppm and H_y at δ= 4.02-4.06 ppm with a geminal coupling constant of $^{2}J_{Hb,Hy}$ of 8.23 Hz, respectively.

The vicinal coupling constants in substituted 1,3-dioxolanes have been previously investigated by many researchers[148, 160] especially by Anteunis *et al.*[147, 149] and have given a typical vicinal coupling constant for H(4)-H(5) in the range $^{3}J_{4\text{-syn-}5}$ of 5.4-7.5 Hz and $^{3}J_{4\text{-anti-}5}$ of 5.9-8.5 Hz corresponding to torsion angles ϕ of 35-50 ^{o} for *syn* and 125-140 ^{o} for *anti* H atoms (values taken from Karplus curve modified for 1,3-dioxolanes) as represented in **27a**. Anteunis *et al*.[148] have recorded several NMR spectra of substituted dioxolanes and showed that the *pseudo-axial* hydrogen appears at a higher field shift than the *pseudo-equatorial* hydrogen atom. In compound **27** the vicinal coupling constants for H_y proton $^{3}J_{Hc,\ Hy}$ is 5.9 Hz and for H_b proton $^{3}J_{Hc,\ Hb}$ is 6.34 Hz. The $J_{4\text{-}5}$ couplings are in a normal range and are in general agreement with the literature values. The H_c proton displays a quintet at δ= 4.14-4.20 ppm.

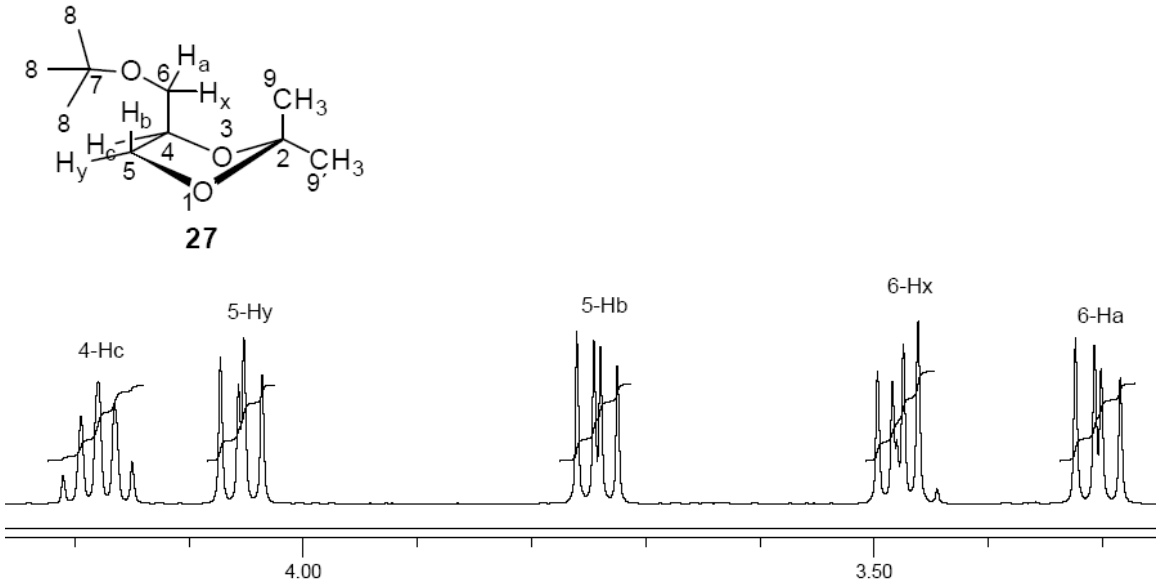

Fig. 38: ^{1}H NMR spectrum of C-4, C-5 and C-6 protons of compound **27** (δ (ppm), $CDCl_3$-TMS, 16 % (w/w), 25 ^{o}C, 400 MHz)

The ^{13}C NMR spectrum of **27** was recorded at 100 MHz in $CDCl_3$ and was solved by using H-C correlation via $^{1}J_{(C\text{-}H)}$ and DEPT experiments, in correlation with the ^{1}H NMR spectrum explained above. The methyl groups from C-9 and C-9´ carbons display two different signals at δ=25.2 and 26.6 ppm, respectively. The C-8 carbon atoms of the *tert*-butyl group appear at δ=27.3 ppm. The C-6 carbon atom is shifted upfield compared to the other ring carbons at δ=63.1 ppm.

The ^{13}C chemical shifts of the ring carbon atoms in substituted 1,3-dioxolanes have been previously investigated by Eliel *et al.*[147] and by Espinosa *et al.*[150, 151] who have shown that C-4 in substituted 1,3-dioxolanes appears mostly downfield from C-5, and C-2 appears at 95 ppm in unsubstituted 1,3-dioxolanes and shifts downfield to δ= 109 ppm in substituted dioxolanes. In **27** C-5 appears at δ=67.3 ppm whereas C-4 is registered at δ=75.1 ppm which is slightly outside the normal range, and C-2 appears at δ=109 ppm.

Mass spectrometry (GC-MS) of the compound **27** shows a 25 % peak at *m/z*=173 corresponding to the loss of CH_3 radical from molecular ion $[M]^+$, and a 15 % peak at *m/z*= 117 caused by the loss of isobutene from *m/z*= 173, and a 75 % peak at *m/z*= 101 by the loss of *tert*-butoxy methyl radical from $[M]^+$. The base peak observed at *m/z*= 57 originates from the *tert*-butyl carbocation.

The IR spectra of compound **27** recorded neat shows absorption bands at $\tilde{\nu}$ =2976 and 2936 cm^{-1} attributed to CH_3 asymmetrical and symmetrical stretch and at $\tilde{\nu}$ =2873 cm^{-1} corresponding to CH_2 symmetrical stretching vibrations, and a strong absorption bands at $\tilde{\nu}$ =1083 and 1055 cm^{-1} corresponding to the ring breathing vibrations in 1,3-dioxolanes.

9.2.2: Preparation of acetals 28a-31b

Using Newman's method[143] compound **14** was reacted with different prochiral carbonyl compounds to obtain various acetals (Scheme 17) including *cis*-2-methyl-4-*tert*-butoxymethyl-1,3-dioxolane **(28a)**, *trans*-2-methyl-4-*tert*-butoxymethyl-1,3-dioxolane **(28b)**, *cis*-2-ethyl-4-*tert*-butoxymethyl-1,3-dioxolane **(29a)**, *trans*-2-ethyl-4-*tert*-butoxy methyl-1,3-dioxolane **(29b)**, *cis*-2-ethyl-2-methyl-4-*tert*-butoxymethyl-1,3-dioxolane **(30a)**, *trans*-2-ethyl-2-methyl-4-*tert*-butoxymethyl-1,3-dioxolane **(30b)**, *cis*-2-isopropyl-4-*tert*-butoxymethyl-1,3-dioxolane **(31a)**, and *trans*-2-isopropyl-4-*tert*-butoxymethyl-1,3-dioxolane **(31b)**. The parameters used in the preparation are described in Table 9. It was observed that the *cis* isomer was predominantly formed in the reaction.

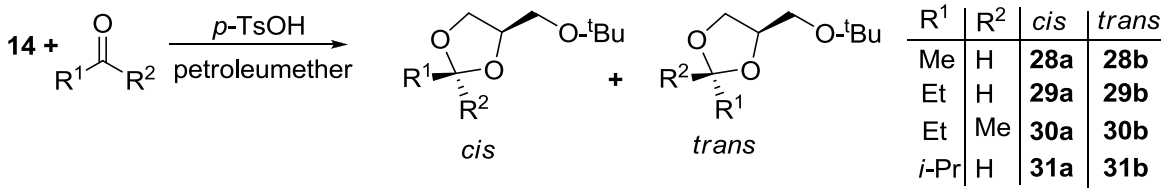

R^1	R^2	*cis*	*trans*
Me	H	**28a**	**28b**
Et	H	**29a**	**29b**
Et	Me	**30a**	**30b**
i-Pr	H	**31a**	**31b**

Scheme 17: General reaction for preparation of acetals from **14**

Reaction of glycerol **(2)** with any prochiral aldehyde or ketone produces stereoisomers. The diastereoselectivity of the reaction is well documented in the literature with numerous examples,[152] and such a behavior was also observed in our case (Table 9). Some of the interesting examples from the literature are 2,4-dimethyl-1,3-dioxolane, for which Baker *et al.*[153] have demonstrated the greater selectivity of *cis*-2,4-dimethyl-1,3-dioxolane over its *trans* isomer due to its higher stability. Hibbert *et al.*[154] have demonstrated the same in 2,4-bromomethyl-substituted 1,3-dioxolanes and shown that the *cis* isomer is formed preferentially in the reaction (62 %), it is thermodynamically more stable than the *trans* isomer.

Product	**14**+reactant	mole ratio	time, (h)	yield (%)	*cis* (%)	*trans* (%)
28a, 28b	acetaldehyde	1:10	4.5 h	50-54	50	45
29a, 29b	propanaldehyde	1:10	2.5 h	50	52	48
30a, 30b	2-butanone	1:7.5	1.5 h	92-94	74	26
31a, 31b	isopropanaldehyde	1:10	2 h	75	81	19

Table 9: Reaction parameters used in the synthesis of acetals (% yield is isolated yield; the *cis* / *trans*-ratio was determined by GC analysis).

Clode *et al.*[152] have shown that in 2,4-*cis*-5-tri-substituted 1,3-dioxolanes, the *cis* isomers are configurationally more stable than their *trans* counterpart at room temperature (80 % *cis* and 20 % *trans* at 25 ^{o}C). By analogy, the examples mentioned above are similar in the 1,3-dioxolane ring substitution to our compounds **(28a-31b)**. The predominant formation of the *cis* isomer in the reaction (Scheme 17) can be rationalized according to the reaction mechanism presented below.

9.2.3: Reaction mechanism and stereoselectivity in acetal formation

The addition of alcohols to a carbonyl double bond is a reversible process; therefore, the extent of product formation is subjected to thermodynamic control. Adkins *et al.*[155] have shown that acetal formation proceeded through hemiacetal intermediates **(32)** as represented in Scheme 18. To consider the rate-controlling transition state in the mechanism it is essential to know the rate limiting step. Logically, it could be the either step **33** → **34** or step **34** → **35**. However, it has been shown by Adkins[155] that the formation of the hemiacetal and the proton exchange is a faster step.

In general, the hydrolysis of most cyclic and acyclic acetals and ketals proceeds by an A-1 mechanism[156] involving the hydrolysis of a protonated intermediate as the rate determining step. Thus if the ring opening step is considered as rate determining for hydrolysis, because of the principle of microscopic reversibility, step **34** → **35** must be the rate determining step for the ring closure, leading to the formation of the acetal. However, the preferential formation of one of the stereoisomers during the kinetic phase of the reaction cannot be explained by the assumption that the transition state resembles the oxocarbonium ion **34a**, since both diastereomers must be formed from the same intermediate **(34a)**, which cannot be rationalized due to the free rotation around C-O bond. Therefore, it is reasonable to assume

that the transition state resembles the oxocarbonium ion **34b**. Provided that the intermediate ion **34b** has considerable oxonium ion character, then it may exist in two different conformational states, which may be designated as *transoid* and *cisoid*, respectively.

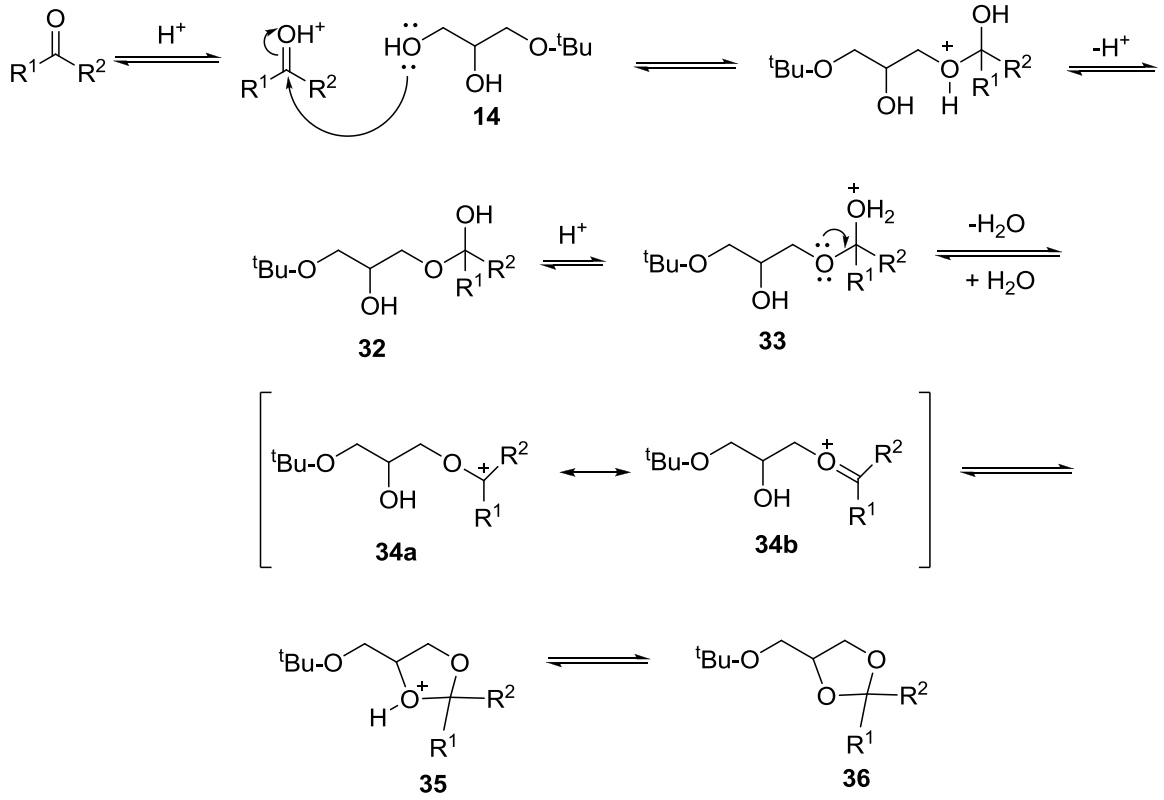

Scheme 18: Mechanism of acetal formation from **14** (R^1 and R^2 are the respective alkyl groups as shown in Scheme 17)

Tuner *et al.*[157] have shown that the *transoid* arrangement is assumed to be more stable than the *cisoid* form. It may be best explained by consideration of the reaction between isopropanal and **14**. Thus for the intermediate **34b** four different conformers (two *cisoid* **37**, **38** and two *transoid* **39**, **40)** may be drawn, such that the hydroxyl group is well placed for the cyclisation reaction which may be assumed to resemble the rate limiting transition state for the formation of one of the isomer predominantly.

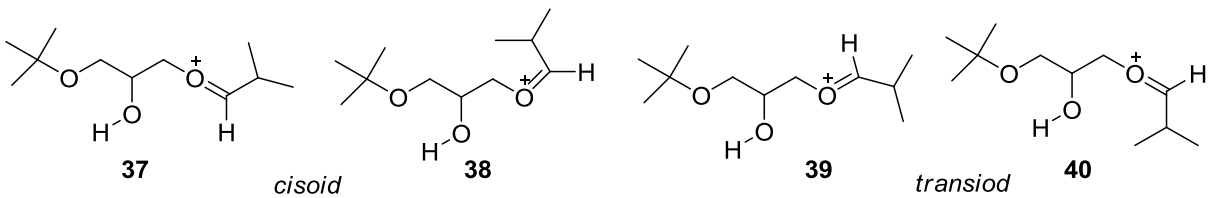

From the conformers **37-40** it may be concluded that the *anti-transoid* conformer **37** must be the most stable one with the least steric hindrance and the hydroxyl group placed in near proximity to the acetal carbon atom compared to the other conformers. Thus, it may further lead to the rapid formation of an acetal with a *cis* orientation of isopropyl group. This is in agreement with the experimental observation the *cis* isomer **31a** being formed in 81 % yield compared to 19 % yield of the *trans* isomer **31b** (GC analysis). It can be concluded that the isomer with an *endo*-alkyl group will be the kinetically stable product in acetal formation; this is in good agreement with the experimental results from other acetals **(28a-30b)** (Table 9).

9.2.4: Structural and conformational analysis of compounds 28a-31b

When the 1,3-dioxolane ring carries substituents at C-2 and C-4, one of the major tasks is the separation and correct characterization of the resulting diastereomers by assignment of the proton signals and also the configuration. For the compounds **28a-31b** all spectral analyses were carried out with the mixture of diastereomers. Except compound **30a** which was separated in 96 % purity from a mixture of **30a** and **30b**.

The configurational assignments for the 1,3-dioxolane are extrapolated from the known configuration of *cis* and *trans*-2,4-dimethyl-1,3-dioxolanes which are more definitely established through the synthesis of the *cis*-isomer by degradation of 1,6-anhydrogalactose.[147, 158] Thus the knowledge of 2,4-dimethyl-1,3-dioxolanes combined with the fact that the *cis*-isomer is thermodynamically more stable and displays an upfield chemical shift for the C-2 protons (compared to the C-2´ *trans* protons) permits the configurational assignment of the substituted 1,3-dioxolanes **(28a-31b)**.

The ^{1}H NMR spectrum of the mixture of **28a** and *trans*-2-methyl-4-*tert*-butoxymethyl-1,3-dioxolane **(28b)** recorded at 400 MHz in $CDCl_3$ is in agreement with the literature evidence (Fig. 39). The C-2 proton for **28a** appears as a quartet at δ= 4.92-4.95 ppm with $^{3}J_{2,9}$ = 4.8 Hz upfield with higher intensity compared to C-2´ proton from **28b** as a quartet at δ= 5.01-5.04 ppm with a coupling constant $^{3}J_{2',9'}$ of 4.8 Hz. The protons are correlated with the methyl group protons C-9 and C-9´ as shown by using H-H COSY 2D experiments, and the *cis*-methyl group protons (9-H) are shifted downfield to δ=1.29-1.3 ppm (*four peaks*) compared to the *trans*-methyl protons (9´-H) appearing at δ=1.26-1.28 ppm (*four peaks*). The C-8 and C-8´ protons from the *tert*-butyl group resonate at δ=1.11 ppm and δ=1.12 ppm, respectively.

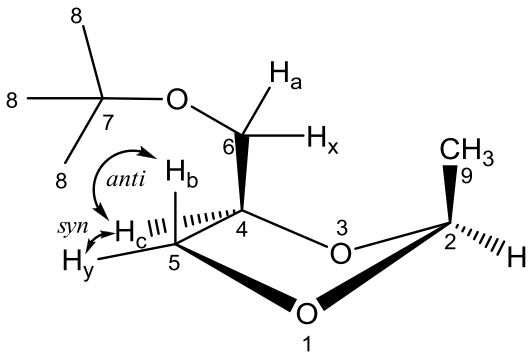

cis-**28a**

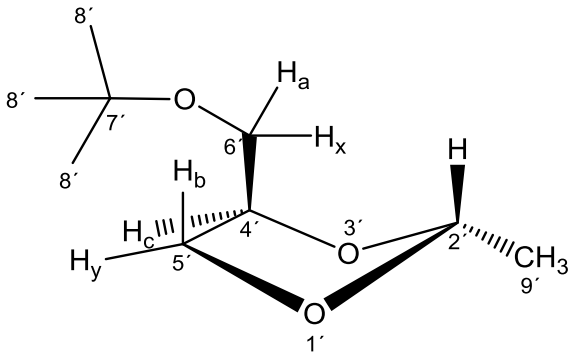

trans-**28b**

The configurational assignments of the C-4, C-5 and C-6 protons for **28a** and **28b** rest on the basis of examples from the literature;[147-156] furthermore, the protons were correlated using H-H-COSY 2D experiments. Mucci *et al.*[159] have shown that in 4-trimethylammoniummethyl-1,3-dioxolane iodide the vicinal coupling constants ($^3J_{4H,6H}$) of 6 and 6´-H_a (*anti* to H_c) are smaller that 6 and 6´-H_x (*syn* to H_c) and he also showed that the 6 and 6´-H_x protons appear downfield from the 6 and 6´-H_a protons. In **28a** the methylene proton H_a from C-6 display a pattern of doublet of doublets at δ=3.18-3.22 ppm with a geminal coupling constant $^2J_{Ha,Hx}$ of 8.78 Hz, and a vicinal coupling constant $^3J_{Ha\text{-}anti\text{-}Hc}$ of 7.04 Hz. Similarly, in compound **28b** the methylene proton H_a at C-6´ displays doublet of doublets pattern at δ=3.27-3.30 ppm with a geminal coupling constant $^2J_{Ha,Hx}$ of 9.39 Hz, and a vicinal coupling constant $^3J_{Ha\text{-}anti\text{-}Hc}$ of 5.72 Hz. In both cases the values are in the range of general values assigned to the *syn* protons (To avoid confusion the neighboring protons are represented as *syn* and *anti* and the isomers as *cis* and *trans* as shown in *cis*-**28a**, see also Chapter 9.2.1). The H_x protons from C-6 and C-6´ display a multiplet (*eight peaks*) at δ=3.38-3.43 ppm. In compound **28b** the ring proton 5´-H_b appears as a doublet of doublet at δ=3.54-3.58 ppm with $^2J_{Hb,Hy}$ of 8.10 Hz, and $^3J_{Hb\text{-}anti\text{-}Hc}$ of 6.66 Hz upfield to the 6´-H_y proton which resonates as a multiplet at δ=4.01-4.07 ppm. The C-4 proton (H_c) shows a similar chemical shift range and appears as multiplet together with the 6´-H_y proton.

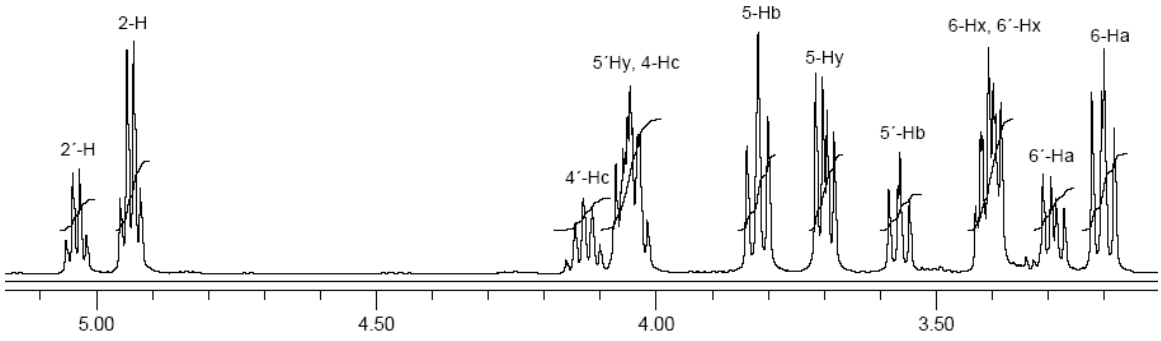

Fig. 39: ^{1}H NMR spectrum of the *cis* and *trans*-C-2, C-4, C-5 and C-6 protons of the **28a** and **28b** mixture. (δ (ppm), $CDCl_3$-TMS, 22 % (w/w), 25 ^{o}C, 400 MHz)

In compound **28a** the ring proton H_y from C-5 display a doublet of doublets at δ=3.68-3.71 ppm with $^{2}J_{Hb,Hy}$ of 8.16, and $^{3}J_{Hy\text{-}syn\text{-}Hc}$ of 4.96 Hz. The latter value is smaller compared to the general values assigned to the *syn* protons. The *anti*-proton H_b from *cis*-C-5 displays a *pseudo*-triplet at δ= 3.8-3.83 ppm with a geminal coupling constant $^{2}J_{Hb,Hy}$ of 7.5 and a vicinal coupling constant $^{3}J_{Hb\text{-}anti\text{-}Hc}$ of 7.5 Hz. Inspection of the coupling constants indicates that H_y could be accounted for the *syn* proton and H_b for the *anti* proton with respect to H_c. The *trans*-4´-H_c proton from **28b** shows a multiplet at δ=4.11-4.14 ppm.

The ^{13}C NMR spectrum of **28a** and **28b** was recorded at 100 MHz in $CDCl_3$. The spectrum was solved using H-C correlation via ^{1}J (C-H) and DEPT experiments in accordance with the ^{1}H NMR spectrum explained above. The methyl groups C-9´ and C-9 display two different signals at δ=19.74 and 19.79 ppm, respectively. The C-8 carbon atoms of *tert*-butyl group appear at δ=27.2 ppm. The C-6´ carbon from **28b** appears upfield at δ=62.45 ppm compared to 63.2 ppm for C-6 in **28a**. The ring carbon atoms C-5´ of **28b** appears at δ=67.8 ppm whereas C-5 of **28a** appears downfield at δ=67.9 ppm. The C-7 and C-7´ carbons appear at δ=72.94 and 72.97 ppm, respectively. The C-4´ carbon of the *trans*-isomer appears upfield at δ=74.87 ppm compared to δ=75.34 ppm of the C-4 carbon of the *cis*-isomer. The C-2´ carbon atom of the *trans*-isomer is registered at δ=101.32 ppm upfield to the *cis*-C-2 carbon which appears at δ=101.71 ppm.

The data are in good agreement with the literature data of analogous compounds like *cis* and *trans*-2,4-dimethyl-1,3-dioxolane provided by A. Espinosa *et al.*[150] The authors have shown that the C-2 and C-4 carbon atoms from the *cis*-isomer appears downfield from C-2´ and C-4´ for the *trans*-isomer, with the exception of C-5 and C-5´ which are reversed in our case.

Mass spectrometry of both diastereomers **(28a, 28b)** shows similar peaks in the GC-MS analysis. The compounds show a 15 % peak at *m/z*=173 corresponding to the loss of a hydrogen radical from the molecular ion $[M]^{+}$, and a 80 % peak at *m/z*=159 corresponding to the loss of a methyl radical from $[M]^{+}$, and a 70 % peak at *m/z*=117 by loss of isobutene from *m/z*=173. A 40 % peak at *m/z*=103 is attributed to the loss of isobutene from *m/z*=159 and a 75 % peak at 101 by the loss of *tert*-butoxy methyl radical from $[M]^{+}$. The base peak is observed at *m/z*=57.

Similarly, the ^{1}H NMR spectra of **29a**, and *trans*-2-ethyl-4-*tert*-butoxymethyl-1,3-dioxolane **(29b) (**mixture), recorded at 400 MHz in $CDCl_3$ show similar signal patterns as **28a** and **b**. However, there are some differences which are explained as follows. The C-10 and C-10´ protons display a multiplet (*six peaks*) at δ=1.13-1.17 ppm. The C-2 (*cis*-isomer) proton appears as a triplet at δ=4.84-4.86 ppm with a coupling constant $^{3}J_{2,9}$ of 4.68 Hz upfield to C-2´ (*trans* isomer) protons which appear as a triplet at δ=4.93-4.95 ppm a with $^{3}J_{2,9}$ of 4.68 Hz. The H_m and H_n protons from C-9 and C-9´ carbons atoms appear as multiplet at δ= 1.61-1.71 ppm. Thus it was impossible to differentiate the C-9 (*cis*) protons form the C-9´ (*trans*) protons by correlation with the C-2 and C-2´ protons using H-H COSY 2D experiments. In compound **29a**, the methylene proton H_a of C-6 display a doublet of doublets at δ=3.24-3.28 ppm with $^{2}J_{Ha,Hx}$=8.96, and $^{3}J_{Ha\text{-}anti\text{-}Hc}$ of 7.08 Hz. Similarly, in compound **29b** the methylene proton H_a from C-6´ displays a doublet of doublets at δ=3.27-3.30 ppm with $^{2}J_{Ha,Hx}$=9.36 Hz, and $^{3}J_{Ha\text{-}anti\text{-}Hc}$ of 6.04 Hz. The H_x proton from C-6 and C-6´ displays a multiplet at δ=3.42-3.52 ppm.

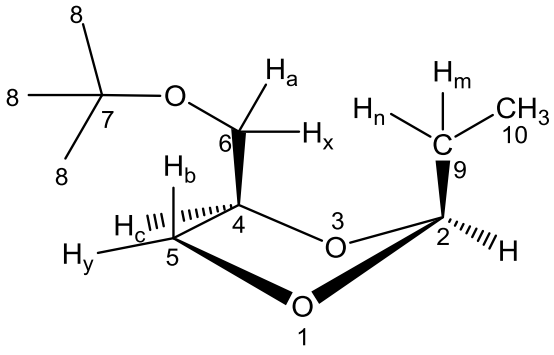

cis-**29a**

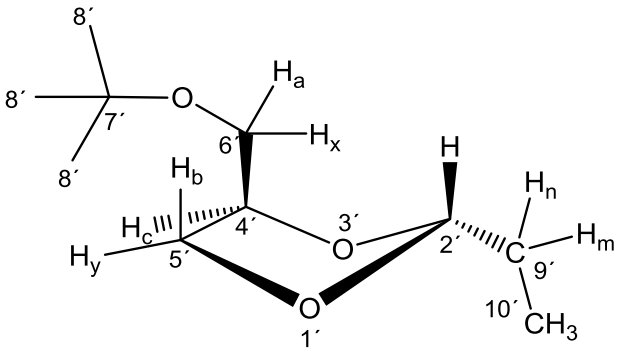

trans-**29b**

In compound **29b** the ring proton 5´-H_b appears as a doublet of doublets at δ= 3.63-3.66 ppm with $^{2}J_{Hb,Hy}$=8.06, and $^{3}J_{Hb\text{-}anti\text{-}Hc}$ of 6.40 Hz upfield from the 6´-H_y proton which appears as a multiplet at δ=4.09-4.19 ppm. Chemical shifts of 6´-H_y and of C-4 and C-4´ protons are similar (4-H_c, 4´-H_c) and the peaks overlap with each other in the same range (δ=4.09-4.19 ppm).

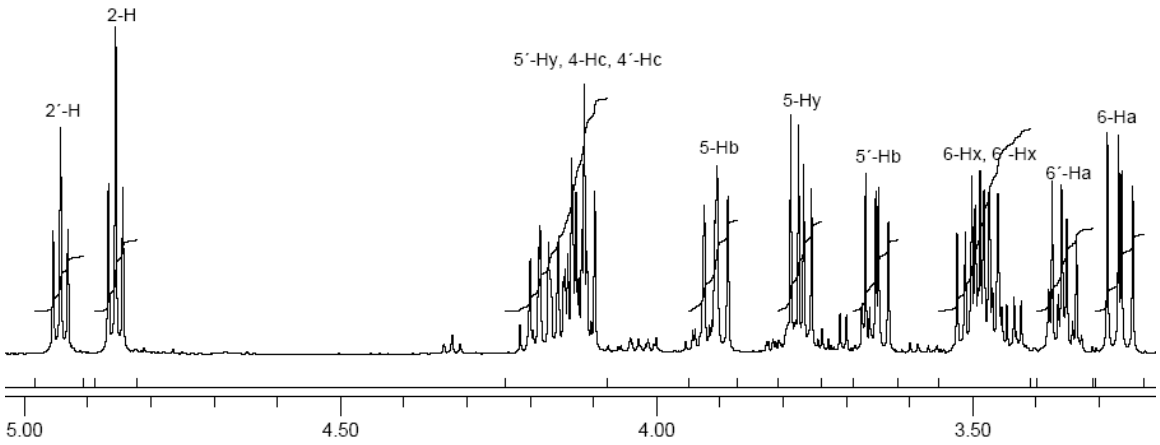

Fig. 40: ^{1}H NMR spectrum of the *cis*-and *trans*-C-2, C-4, C-5 and C-6 protons of the **29a** and **29b** mixture. (δ (ppm), $CDCl_3$-TMS, 16 % (w/w), 25 ^{o}C, 400 MHz)

In **29a** the ring proton H_y at C-5 display a doublet of doublets at δ=3.75-3.78 ppm with $^{2}J_{Hb,Hy}$ of 8.18, and $^{3}J_{Hy\text{-}syn\text{-}Hc}$=4.93 Hz. The value is smaller than the general values assigned to the *syn*-protons (see Chapter 9.2.1). The *anti*-proton H_b from C-5 displays a doublet of a doublets at δ=3.88-3.90 ppm with $^{2}J_{Hb,Hy}$=8.10 and $^{3}J_{Hy\text{-}anti\text{-}Hc}$=6.8 Hz.

The ^{13}C NMR spectrum of **29a** and **29b** was recorded at 100 MHz in $CDCl_3$ and has been examined by H-C correlation via $^{1}J_{(C\text{-}H)}$ [HSQC/HMBC] and by DEPT experiments in correlation with the ^{1}H NMR spectrum explained above. The methyl groups C-10 and C-10´ display two different signals at δ=8.18 and 8.20 ppm. The C-9´ and C-9 carbon atoms display two different signals at δ=27.33 and 27.40 ppm, respectively. The C-8 carbons from the *tert*-butyl group appears at δ=27.73 and 27.75 ppm, respectively. The C-6´ carbon atom from **29b** appears upfield at δ=62.93 ppm compared to 63.57 ppm for C-6 carbon from **29a**. From the ring carbon atoms C-5´ of **29b** appears at δ=68.44 ppm downfield to the C-5 carbon atom at δ= 68.37 ppm. Both C-7 and C-7´ carbons appear at δ=73.45 ppm. The C-4´ carbon atom of the *trans*-isomer is shifted upfield at δ=75.36 ppm compared to δ=75.61 ppm for C-4 of **29a**. The C-2´ carbon atom of the *trans*-isomer appears at δ=105.7 ppm upfield with respect to C-2 appearing at δ=106.0 ppm, respectively.

Mass spectrometry of both the diastereomers **(29a**, **29b)** show similar peaks, and the fragmentation pattern is similar to the compounds above **(28a**, **28b)**, some of the major peaks are assigned as follows. The compounds showed a 5 % peak at *m/z*=187 corresponding to the loss of a hydrogen radical from $[M]^{+}$, and a 50 % peak at *m/z*=159 attributed to the loss of an ethyl radical from $[M]^{+}$, and a 40 % peak at 103 by the loss of isobutene from *m/z*=159. A 40

% peak at *m/z*=101 is attributed to the loss of a *tert*-butoxymethyl radical from $[M]^+$. The base peak is observed at *m/z*=57.

As mentioned above, it was possible to obtain compound **31a** in 98 % (GC purity) by column chromatography and the ^{1}H NMR spectrum of *cis*-2-ethyl-2-methyl-4-*tert*-butoxymethyl-1,3-dioxolane **(30a)**, and the mixture of **30a** and *trans*-2-ethyl-2-methyl-4-*tert*-butoxymethyl-1,3-dioxolane **(30b)** recorded at 200 MHz in $CDCl_3$ show a complex second order spectrum compared to the compounds mentioned above **(28a-29b)**. It is especially difficult to recognize the multiplicities of the peaks, and therefore the coupling constants. The effect of substituents at the C-2 and C-4 carbon atoms in 1,3-dioxolanes has been studied carefully by Eliel *et al.*[147] who reported that the change of a C-2 or C-4 substituent has no or palpable effect on the free-energy difference of the diastereomers. However, the compounds **30a-31b** display shoulders in each set of ^{1}H NMR signals of the C-2, C-4, C-5 and C-6 protons which could probably be caused either by the restriction in the *pseudo-rotation* and *pseudo-liberation* of the 1,3-dioxolane ring system due to the bulky substituents (undoubtedly not all but a few rotational conformations are sterically disfavored), or by the increased *syn*-axial interactions as the molecule is forced to a less favored conformation. The most favored conformations in the *cis*-conformers **30a** and **31a** are best shown in **41a-c**. The ^{1}H NMR spectra of **30a-31b** could be partly rationalized due to the hindrance of free rotation around C_6-C_4 and C_9-C_2 at room temperature caused by the bulky substituents.

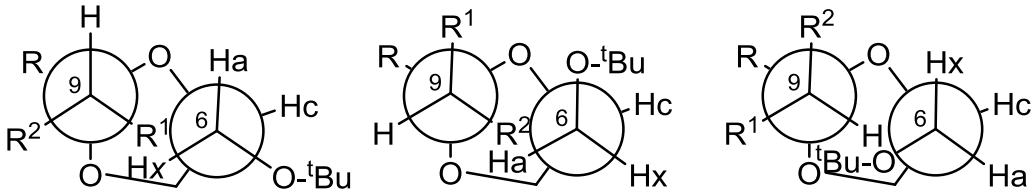

41a **41b** **41c**

30a: R=R^1=H, R^2=Me
31a: R=H, R^1=R^2=Me

The chemical shifts corresponding to each set of multiplets are interpreted as follows. The ^{1}H NMR spectrum of **30a** isolated as a pure diastereomer, shows an ABX_3 spectrum for the C-10 protons, which shows a doublet of a triplet at δ=0.81-0.90 ppm with $^3J_{9,10}$=2.8 and 7.48 Hz.

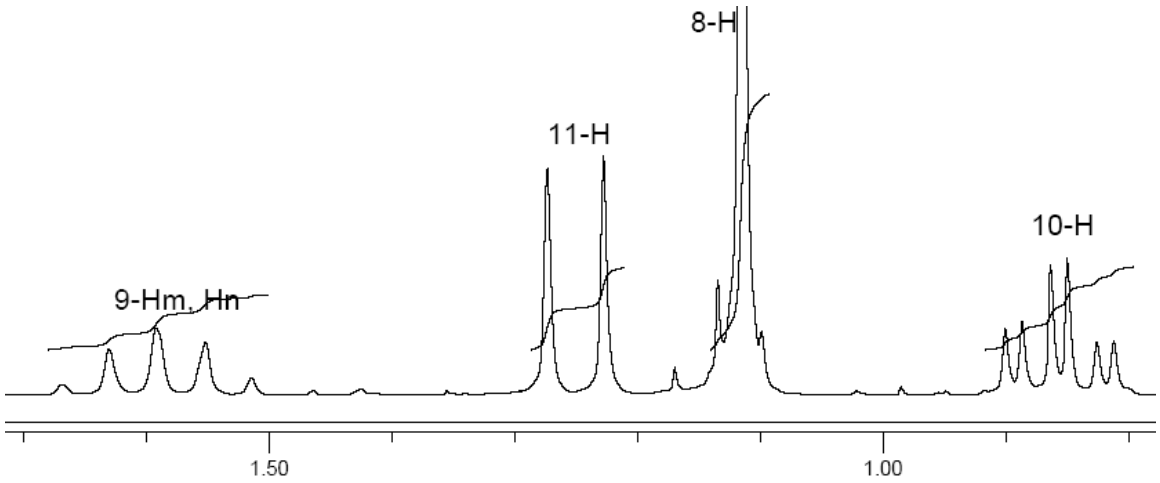

Fig. 41: ^{1}H NMR spectrum of the *cis*-C-8, C-9, C-10 and C-11 protons of **30a** (δ (ppm), $CDCl_3$-TMS, 22 % (w/w), 25 ^{o}C, 200 MHz)

The *tert*-butyl group protons of C-8 appears at δ=1.11 ppm with a shoulder at 1.13 ppm and the methyl group protons C-11 and C-11´ appear as two singlets at δ=1.22 and 1.27 ppm, respectively. The H_m, H_n protons at C-9 appear as multiplets at δ=1.51-1.66 ppm.

The *Ha* protons at C-6 appear at δ=3.18-3.28 ppm as a multiplet. The H_x protons at C-6 display a multiplet at δ=3.35-3.47 ppm. The H_b proton displays a multiplet at δ=3.58-3.71 ppm. The H_y proton shows a multiplet at δ=3.95-4.03 ppm. The H_c proton at C-4 is registered as a multiplet at δ=4.04-4.16 ppm.

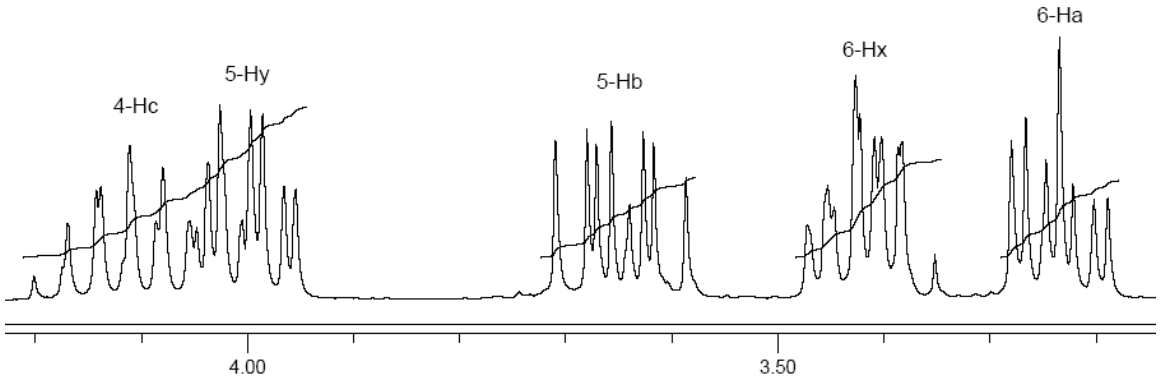

Fig. 42: ^{1}H NMR spectrum of the *cis*-C-2, C-4, C-5 and C-6 protons of **30a** (δ (ppm), $CDCl_3$-TMS, 22 % (w/w), 25 ^{o}C, 200 MHz)

The ^{13}C NMR spectrum of **30a** was recorded at 50 MHz in $CDCl_3$ at room temperature and has been examined by DEPT experiments. The compound displays two signals for the C-10 carbon atom at δ=9.5 and 9.8 ppm, respectively, and two signals for C-9 at δ=24.6 and 25.7

ppm, respectively. The C-11 carbon atom appears downfield at δ=33.1 and 33.9 ppm whereas C-8 appears at δ=28.8 ppm. The C-6 carbon atom appears at δ=64.6 and 64.7 ppm and C-5 at 69.0 and 69.1 ppm. The C-7 carbon atom appears at δ=74.4 ppm and *cis*-C-4 is recorded at 76.90 ppm. The C-2 carbon atoms appear at 112.4 and 112.6 ppm downfield from the normal range (δ= 100- 109 ppm).

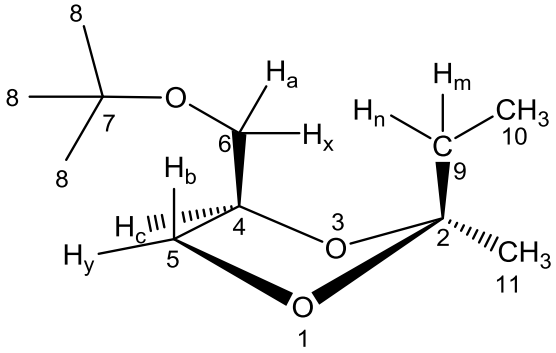

cis-**30a**

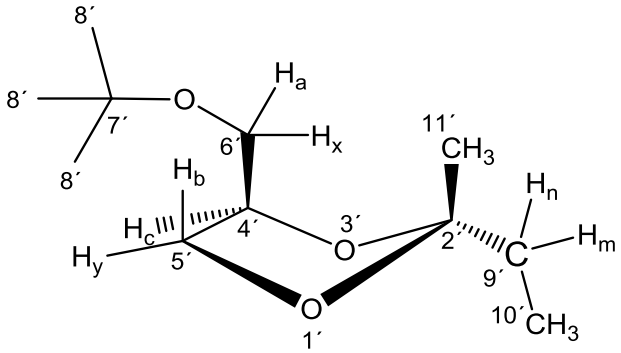

trans-**30b**

Unfortunately, it was not possible to obtain the *trans*-isomer in pure form. However, an attempt was made to differentiate the peaks corresponding to **30b** from the ^{1}H NMR spectrum recorded of a mixture of *cis*-**30a** (72 %) and *trans*-2-ethyl-2-methyl-4-*tert*-butoxymethyl-1,3-dioxolane **(30b)** (23 %) at 200 MHz in $CDCl_3$. The spectrum of this mixture displayed similar chemical shifts for the C-10´ and C-10 protons at δ=0.81-0.90 ppm. The *tert*-butyl group protons appear at δ=1.12 ppm and the methyl group C-11´ protons appear as two singlets at δ=1.22 and 1.27 ppm, respectively, overlapped by the signals of the C-11 protons. The H_m, H_n protons from C-9´ appear as a multiplet at δ=1.46-1.67 ppm overlapping with the signals of the C-9 protons.

The chemical shift assignments for the C-4, C-5 and C-6 protons are extrapolated from the known chemical shifts of compounds **30a** which are more precisely established. The chemical shifts of the ring protons differ widely in **30a** and **30b**. The *Ha* protons of C-6´ appear at δ=3.30-3.34 ppm as a doublet of a doublets with $^2J_{Ha,Hx}$=5.48, and $^3J_{Ha,Hc}$=3.39 Hz. The coupling constant range is very small in comparison to the general range (Chapter 9.2.1). The H_x protons at C-6´ display a multiplet at δ=3.36-3.47 ppm, overlapping with the signals of 6-H_x from **30a**. The H_b from the *trans* isomer displays a multiplet at δ=3.58-3.74 ppm, overlapping with the signals of 5-H_b from **30a**. The H_y proton from C-5´ display a multiplet at δ=3.95-4.05 ppm, overlapping with the signals of 5-H_y. The H_c proton at C-4´ displays multiplets at δ= 4.08-4.17 ppm, overlapping with the signals of 4-H_c.

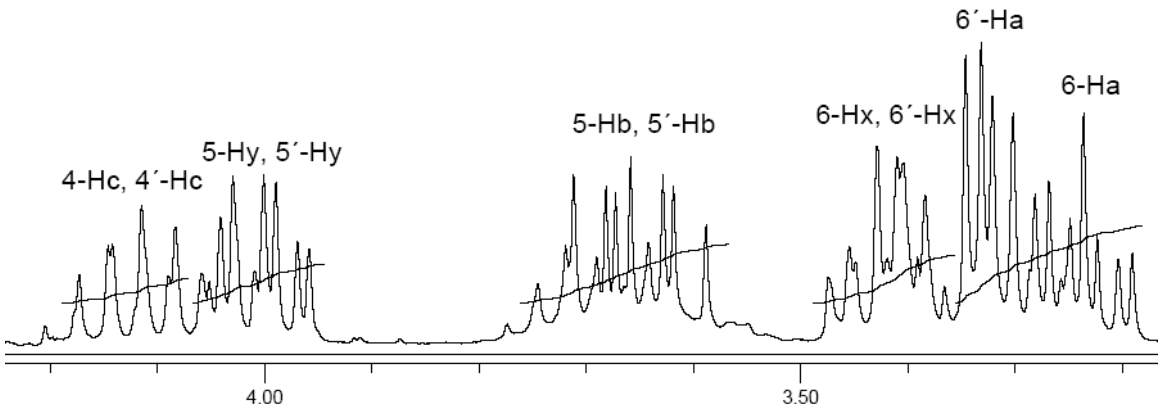

Fig. 43: ^{1}H NMR spectrum of the *cis*-and *trans*-C-2, C-4, C-5 and C-6 protons of a mixture of **30a** and **30b**. (δ (ppm), $CDCl_3$-TMS, 16 % (w/w), 25 ^{o}C, 400 MHz)

The ^{13}C NMR spectrum of the **30a** and **30b** mixture was recorded at 50 MHz in $CDCl_3$ at room temperature and has been examined by DEPT experiments. The peaks corresponding to the *trans*-isomer **30b** were differentiated from the ^{13}C NMR spectrum recorded with a mixture of *cis*-**30a** (72 %) and *trans*-**30b** (23 %). In the ^{13}C NMR spectrum of the **30a** and **30b** mixture all peaks corresponding to C-9´, C-10´ and C-11´ show no difference in chemical shifts compared to analogous carbon atoms in *cis*-**30a**. Whereas C-8´ appear at δ=28.74 ppm. The C-6´ carbon displays a single peak at δ=64.21 ppm upfield from C-6. The C-5´ carbon atoms appears at δ=69.0 and 69.1 ppm and shows a similar chemical shift as C-5. The C-7´ tertiary carbon atoms appear at δ=74.3 ppm upfield from C-7. The *trans*-C-4´ carbon atom appears at δ=76.90 ppm downfield to *cis*-C-4. The C-2 and C-2´ carbon atoms appear at δ=112.3 and 112.5 ppm downfield to the normal range (δ=100-109 ppm).

It can be clearly seen from the above NMR spectra that the most strongly affected carbon atoms and protons are related to C-8, C-6 and C-4 and also C-7 due to the rotational barrier of the compounds. Examination of the NMR spectra of **30a** and **30b** opens a new door for further investigations in-to the conformational analysis of this class of compounds.

Mass spectrometry of **30a** and **30b** shows similar peaks from which some of the major peaks are assigned as follows. The compounds show a 20 % peak at *m/z*=187 corresponding to the loss of methyl radical from $[M]^+$, a 50 % peak at *m/z*=173 attributed to the loss of ethyl radical from $[M]^+$, and a 40 % peak at *m/z*= 131 by loss of isobutene from *m/z*=187. A 90 % peak at *m/z*=115 is generated by the loss of *tert*-butoxymethyl radical from $[M]^+$. The base peak is observed at *m/z*=57.

The ^{1}H NMR spectrum of **31a** and *trans*-2-isopropyl-4-*tert*-butoxymethyl-1,3-dioxolane **(31b)** are complex. Regarding the isopropyl substituent at C-2, Eliel *et al*.[147] have shown that the coupling constants between the 2-H and the 9-H protons in the *cis*-isomer increase with increasing bulkiness of the substituents on the C-4 carbon atom from 4.4 Hz to 7.5 Hz (Me to ^{t}Bu), suggesting that in the *cis*-stereoisomer, the isopropyl group is increasingly forced into the rotational conformation in which the methyl groups point away from the ring and the protons (2-H and 9-H) are *anti* to each other. In **31a** and **31b**, the methyl protons of *cis* and *trans*-C-10, C-11 display a multiplet at δ=0.87-0.92 ppm. The *cis*-and *trans*-C-8 protons appear as singlets at δ=1.14 ppm and the C-9 and C-9´ protons appear as multiplets at δ=1.70-1.83 ppm. The H_a protons at C-6 appear at δ=3.17-3.23 ppm as a multiplet and the H_a from the C-6´ at δ=3.26-3.32 ppm as a multiplet. The H_x protons from C-6 and C-6´ carbons atoms display a multiplet at δ=3.37-3.50 ppm.

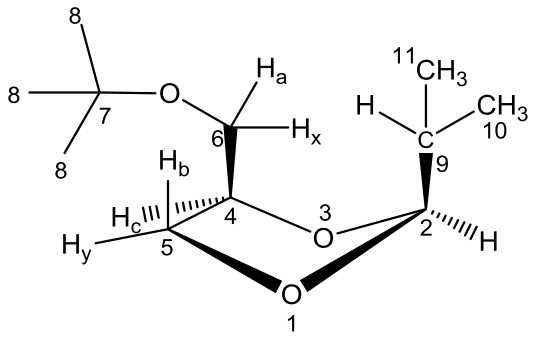

cis-**31a**

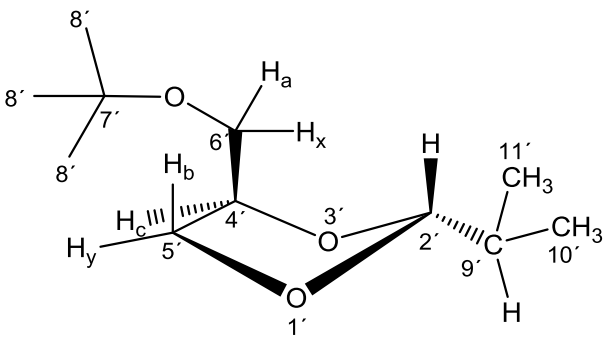

trans-**31b**

The H_b of the *trans*-isomer **(31b)** is registered at δ=3.58-3.63 ppm and H_y shows a multiplet at δ=4.02-4.15 ppm. The H_c proton at C-4 and C-4´ displays a multiplet at δ=4.02-4.15 ppm which overlaps with the signal of 6´-H_y proton. The H_y from the *cis*-isomer displays a doublet of doublets with shoulders in every peak at δ=3.69-3.73 ppm and H_b at *cis*-C-6 displays a multiplet at 3.83-3.88 ppm. The protons at *cis*-C-2 display a doublet with shoulders at δ= 4.59-4.61 ppm and *trans*-C-2´ displays a doublet with shoulders at δ=4.67-4.69 ppm, respectively.

The ^{13}C NMR spectra of **31a** and **31b** were recorded at 100 MHz in $CDCl_3$ at room temperature and have been examined by H-C correlation via ^{1}J (C-H) [HSQC/HMBC] and by DEPT experiments in accordance with the ^{1}H NMR spectrum explained above. The compounds **31a**, **31b** displays three signals for the C-10 and C-10´, C11, C-11´ carbon atoms at δ=16.49 and 16.56 and 16.84 ppm, respectively, and two signals for C-9 and C-9´ at 31.7 and 32.0 ppm. The C-8 carbon atom appears at δ=27.3 ppm. The C-6 and C-6´ carbon atoms

absorb at δ=62.5 and 63.0 ppm and the *trans*-C-5´ carbon appears at δ=68.3 downfield from *cis*-C-5 carbon peak at 68.0 ppm. The C-7 and C-7´ tertiary carbons appear at δ=73.0 ppm, and the *cis*-C-4 and *trans* C-4´ at 75.0 ppm. The *cis*-C-2 carbon atom resonates downfield at δ=108.4 ppm and *trans*-C-2´ at 108.1 ppm, respectively.

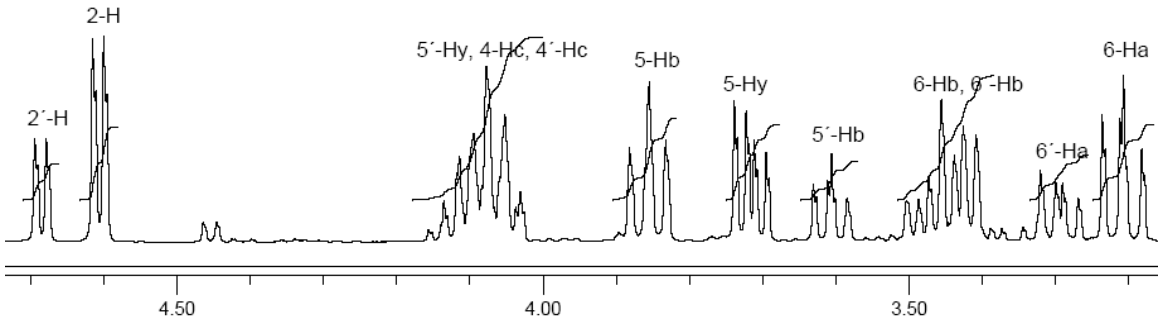

Fig. 44: ^{1}H NMR spectrum of the *cis*-and *trans*-C-2, C-4, C-5 and C-6 protons of a mixture of **31a** and **31b** (δ (ppm), $CDCl_3$-TMS, 17 % (w/w), 25 ^{o}C, 400 MHz)

Mass spectrometry of **31a**, and **31b** shows similar peaks. Some of the major peaks are assigned as follows. The compounds show a 5 % peak at *m/z*=187 which is attributed to the loss of methyl radical from $[M]^+$, and a 98 % peak at *m/z*=159 corresponding to the loss of the isopropyl radical from $[M]^+$, and a 20 % peak at *m/z*=115 corresponding to the loss of *tert*-butoxymethyl radical from $[M]^+$. The base peak is observed at *m/z*=57 from the *tert*-butyl carbocation.

The IR spectra of compounds **28a**-**31b** show the absence of O-H stretching vibrations and display the typical ring breathing motions associated to the 1,3-dioxolane ring system.[161] Some of the major peaks in the IR spectrum of compounds **28a**-**31b** are summarized in the Table 10.

Compound	CH_3 *asym.*	CH_3 *sym.*	CH_2 *sym.*	*vib* (rb)
28a, 28b	2975	2936	2874	1116, 1085
29a, 29b	2974	2936	2874	1195, 1084
30a, 30b	2975	2937	2877	1136, 1084
31a, 31b	2973	2933	2874	1194, 1086

Table 10: IR spectral data of compounds **28a**-**31b** (*vib* (rb): ring breathing vibrations, frequencies (ῦ) are given in cm^{-1})

9.3 Preparation of 4-*tert*-butoxymethyl-2-oxo-1,3,2-dioxathiolane (43a, 43b)

Following the method of Garner and Lucas,[162] compound **14** was reacted with thionylchloride **42** at 0 °C in 1:1.5 molar ratio to obtain *cis*-and *trans*-4-*tert*-butoxymethyl-2-oxo-1,3,2-dioxathiolane as diastereomers **43a** and **43b** (Scheme 19), with a diastereomeric ratio of 67:32; **43a** and **43b** were separated by column chromatography using a mixture of pentane and diethyl ether (3:7 v/v) as eluent.

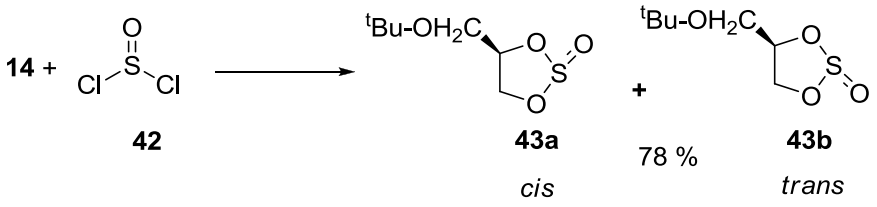

Scheme 19: Preparation of 4-*tert*-butoxymethyl-2-oxo-1,3,2-dioxathiolane **(43a, 43b)**

9.3.1: Structural and conformational analysis of 43a and 43b

It is well known that the configuration at the sulfur atom in molecules of the type OSX_2 (X=Cl or O) is pyramidal with C_{3v} symmetry in both crystalline state and in aqueous solution.[163] If the alkyl sulfites have a pyramidal structure at the sulfur atom, then the compounds **43a** and **43b** must be diastereomeric. The chemistry of the S=O bond and the conformational analysis of 1,3,2-dioxatholane-2-oxide ring systems have been thoroughly investigated and explained in the literature.[163-165] Compounds of this class have been successfully studied for many years by the use of practically all physical methods including CD, IR and NMR spectroscopy.[166, 167]

By utilizing electronic circular dichroism (CD) spectroscopy Chochrek *et al.*[167] have shown that in cyclic sulfites the diastereomers differ from each other by the configuration at the S=O bond which is *pseudo-axial* in the *cis* and *pseudo-equitorial* in *trans* isomer. The ^{1}H NMR spectrum of the compounds is mainly explained by using the $^{\delta+}S{=}O^{\delta-}$ electric field effect on the chemical shift. Pritchard *et al.*[163] have shown that the sulfur–oxygen bond in sulfites is a p^2-*pd* hybrid double bond. The presence of a *d* orbital makes the electron density distribution in the S=O π-bond somewhat asymmetric about the *xy* plane. However, the symmetry about the *zx* and *zy* planes is retained.[168] Compared to a pure *p*-orbital π-bond, the electrons in the S=O π-bond are more diffused and therefore show higher negative values of magnetic

susceptibility. Snatzke *et al*.[168] also rationalized that the major contribution to the difference in chemical shifts is caused by the magnetic anisotropy of $^{\delta+}S=O^{\delta-}$ bond.

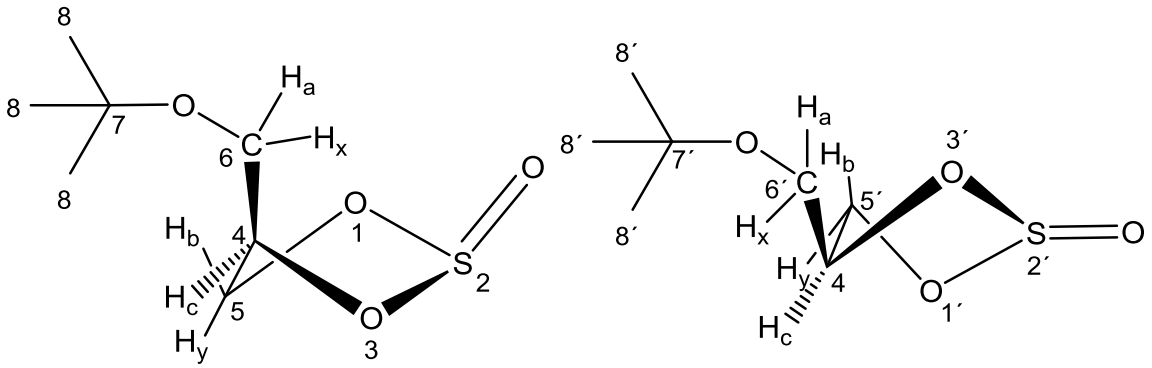

43a **43b**

However, Green *et al*.[164, 165] have shown that a methyl group *cis* to a S=O bond appears at lower field than a *trans* methyl group in 1,1-dimethylethylene sulfite. Anteunis *et al*.[169] have shown that in propylene sulfite the *syn-axial* protons (when sulfur is in *pseudo-synaxial* position, similar to **43a**) apparently shifts to lower field, and the proton *syn* to the methyl group are always found at the highest field. This has also been shown by Green *et al*.[164, 165] for 1,2-diphenylehtylene sulfite.

Similarly, Buchanan *et al*.[170] have studied the trans-annular γ-methyl effect in trimethylene sulfites and shown that the protons *syn-axial* to the exocyclic oxygen show an upfield shift. By analogy the ^{1}H NMR spectra of **43a** and **43b** are explained as follows.

The ^{1}H NMR spectra of compounds *cis*-**(43a)** and *trans*-4-*tert*-butoxymethyl-2-oxo-1,3,2-dioxathiolane **(43b)** were individually recorded at 400 MHz in $CDCl_3$ and are in agreement with literature (Fig 45, Fig. 46). In compound **43a**, the H_x proton at C-6 appears as a doublet of doublets at δ=3.37-3.41 ppm with $^2J_{Ha,Hx}$ of 9.76, and $^3J_{Hx\text{-}anti\text{-}Hc}$ of 6.46 Hz upfield from the H_a proton. This appears as doublet of doublets at δ=3.51-3.55 ppm with $^2J_{Ha,Hx}$ of 9.74, and $^3J_{Ha\text{-}syn\text{-}Hc}$ of 4.73 Hz. In compound **43b** the C-6´ methylene protons appear as multiplet at 3.60-3.67 ppm and 3.78-3.81 ppm, lower than the C-6 protons from the *cis*-isomer which is in agreement with the literature evidence by Green *et al.*[165] Moreover the ring proton H_y at C-5 of **43a** is registered as doublet of doublets at δ=4.29-4.32 ppm with $^2J_{Hb,Hy}$ of 8.42 Hz, and $^3J_{Hy\text{-}syn\text{-}Hc}$ of 4.93 Hz upfield from H_b. The latter resonates as a doublet of doublet at δ=4.66-4.70 ppm with $^2J_{Hb,Hx}$ of 8.45, and $^3J_{Hb\text{-}anti\text{-}Hc}$ of 6.40 Hz whereas the C-5´ protons (H_y, H_b) from the *trans*-isomer are measured as a multiplet at δ=4.48-4.62 ppm.

Pritchard *et al.*[163] calculated the effect of the electronic field of the $^{\delta+}S{=}O^{\delta-}$ dipole on the chemical shift of C-5 *pseudo-axial* (in above case H_b) and *pseudo-equatorial* (in above case H_y) protons in cyclic sulfites (Δ_{Ei}). The authors[163] stated, that the positive charge associated with the sulfur atom effects both hydrogens (H_b, H_y) equally. However, by calculating the Δ_{Ei} values of the negative charged oxygen atom (considered to be in *pseudo-synaxial* position) in ethylene sulfite shows that the *cis*-protons are shifted to downfield by approximately 0.05 ppm. Almost a 30 % shift was observed in butylene sulfites compared to the corresponding *trans*-protons. In compound **43a** an almost 0.3 ppm downfield shift of H_b proton was observed compared to H_y. Green *et al.*[165] have shown that the protons *cis* to the S=O bond in ethylene sulfite resonates at lower field than the *trans*-protons. In our case H_b which is in *cis*-arrangement to the S=O bond (*anti* to H_c) resonates at lower field by 0.34 ppm than H_y in the *trans*-position.

Unfortunately, Abraham *et al.*[171] and Tabacik *et al.*[172] have shown that the values of $^3J_{vic}$ in five-membered rings (see Chapter 9.2.1) cannot be accounted by the Karplus equation. The uncertainty in the calculation by this method originates from the determination of the constant *R* involved.

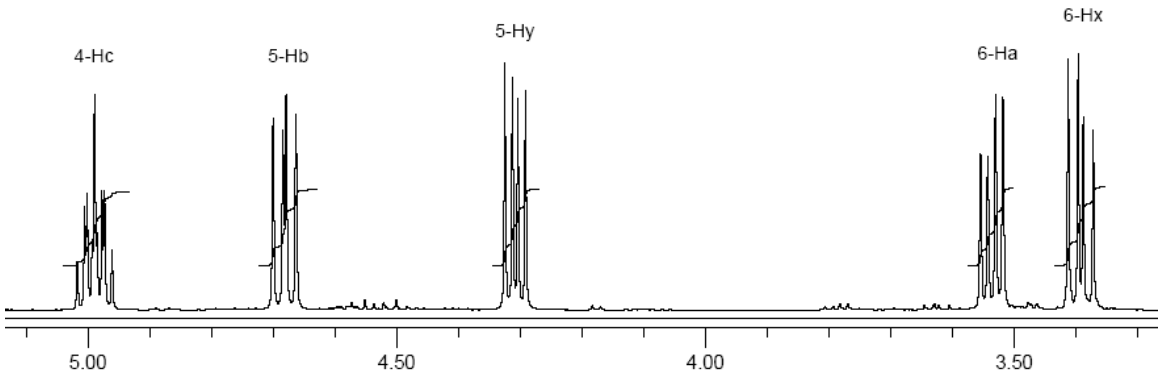

Fig. 45: ^{1}H NMR spectrum of the *cis*-C-2, C-4, C-5 and C-6 protons of **43a** (δ=(ppm), $CDCl_3$-TMS, 18 % (w/w), 25 ^oC, 400 MHz)

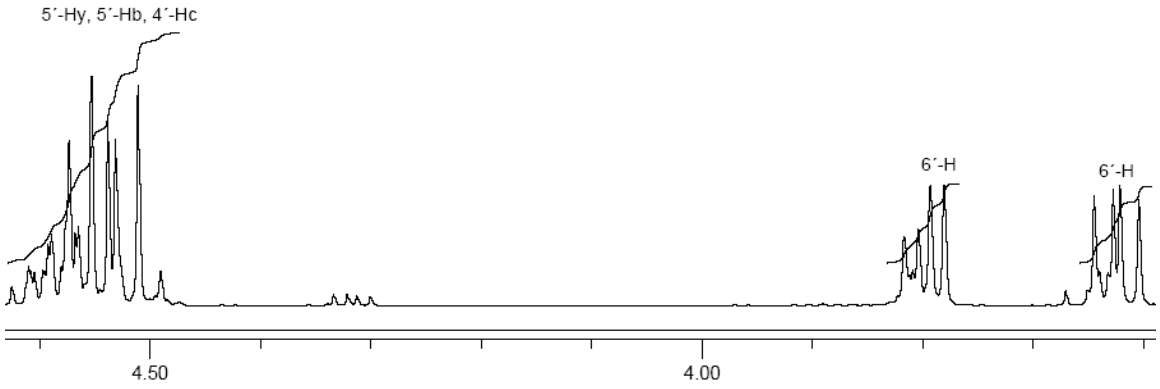

Fig. 46: ^{1}H NMR spectrum of the *trans*-C-2, C-4, C-5 and C-6 protons of **43b** (δ= (ppm), $CDCl_3$-TMS, 18 % (w/w), 25 ^{o}C, 400 MHz,)

The *R* parameter introduced by Lambert[173] in the relationship cos *ø* = $[3/(2+4R)]^{1/2}$ where *R* = $^{3}J_{vic}$ (*anti*) / $^{3}J_{vic}$ (*syn*) provides an expression for the torsion angle *ø* which is not adequate to the Karplus constants. Generally, *R* values can be obtained by the interconversion of conformers which is best shown in **44a**, **44b** for the *cis* isomer and **45a**, **45b** for the *trans*-isomer.

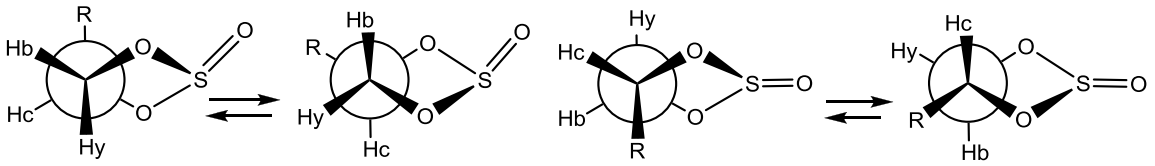

44a **44b** **45a** **45b**

R= CH_2O-^{t}Bu

However, it has been acknowledged by Hiller *et al.*[166] that the *R* values for mono-substituted ethylene sulfites cannot be calculated (and hence the torsion angles), because in general in substituted five-membered rings, the coupling constants must be properly integrated over the whole rotational circuit of conformational mobility, where the energy wells are not so deep. However, it has been shown by the Hiller[166] that the $^{3}J_{anti}$-coupling constants are greater than the $^{3}J_{syn}$-coupling constants in ethylene sulfites and substituted ethylene sulfites; this is in agreement with the spectral data of **43a**. The H_c proton in **43a** displays a typical multiplet at δ=4.96-5.01 ppm. The C-4´ proton (H_c) in **43b** has a similar chemical shift as the C-5´ protons (H_y, H_b) and appears as a multiplet at δ=4.48-4.62 ppm. The C-8 protons of the *cis*-isomer appear at δ=1.18 ppm upfield from the C-8´ protons from the *trans*-isomer at δ=1.20 ppm.

The ^{13}C NMR spectrums of **43a** and **43b** were recorded individually at 100 MHz in $CDCl_3$ at room temperature and have been examined by DEPT experiments. All carbon atoms of the *cis*-isomer were observed upfield compared to analogous carbon atoms in the *trans*-isomer. The C-8 carbon appears downfield at δ=27.1 ppm compared to δ=27.2 ppm in the *trans*-isomer. The C-6 and C-5 carbon atoms from the *cis*-isomer appears at δ=60.62 ppm and 68.64 ppm, respectively, whereas C-6´ and C-5´ of the *trans*-isomer appear at δ=62.98 ppm and δ=70.09 ppm respectively. The C-7 carbon atom appears at δ= 73.6 ppm and C-7´ at δ=73.8 ppm. The *cis*-C-4 carbon atom appears at δ=78.9 ppm upfield from the *trans*-C-4´ at δ= 81.3 ppm.

On the basis of above analysis it can be rationalized that the ^{1}H NMR spectrum shown in Fig. 45 represents the *cis* diastereomer which is also the major product of the reaction (67 %) and the ^{1}H NMR spectrum shown is Fig. 46 represents the *trans* diastereomer obtained as a minor product (32 %). Apart from all the evidence provided above, Limaire *et al*.[174] synthesized enantimerically pure *cis-trans*-4-hydroxymethyl-2-oxo-1,3,2-dioxodiolane by enzymatic resolution. The analytical data reported are in good agreement with the conclusions discussed above.

Mass spectrometry of **43a** and **43b** show similar peaks and some of the major peaks are assigned as follows. The compounds show a 10 % peak at *m/z*=179 corresponding to the loss of methyl radical from $[M]^+$, and a 25 % peak at *m/z*= 121 corresponding to the loss of isopropoxy cation from *m/z*= 179, a 20 % peak at *m/z*= 59 is attributed to the isopropoxy cation and as usual the base peak is observed at *m/z*= 57.

It is known that organic sulfites give rise to intense bands near 1200 cm^{-1} attributed to S=O stretching vibrations. In particular, the $\lambda_{S=O}$ in ethylene sulphite and its derivatives gives value in a range of 1199-1201 cm^{-1}. Green *et al*.[164] have attempted to differentiate the diastereomers using the S=O stretching vibrations in different substituted ethylene sulfites and failed due to very similar bands in both the isomers. Similarly **43a** and **43b** show almost similar S=O stretching vibrations at 1195 cm^{-1} and 1192 cm^{-1} attributed to the *cis*-and *trans*-isomers, respectively.

9.4: Fuel additive experiments with compound 27

The above compounds were specially designed to reduce the hydrophilicity, to reduce the boiling point of glycerol in order to be used in the boiling range of diesel fuel, and to attain a reduction in density. Compound **27** was synthesized on a large scale up to 12 L and was tested as an additive to monitor the NO*x*, CO, HC and PM emissions from the diesel fuel (Fig. 47a-e).

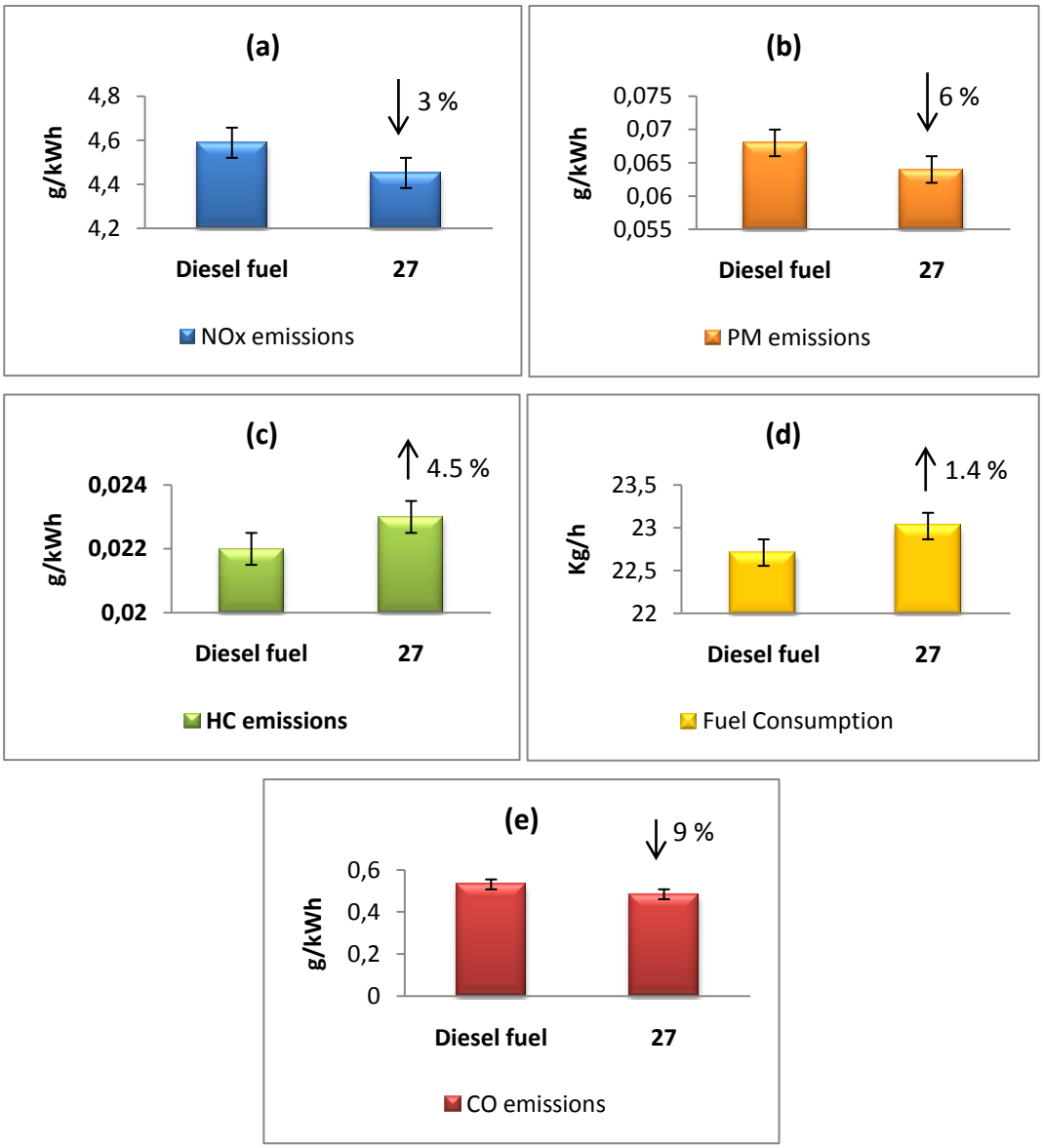

Fig. 47: (a) NO*x* emissions, **(b)** Particulate matter emissions (PM), **(c)** Hydrocarbon emissions (HC), **(d)** Fuel consumption, **(e)** Carbon monoxide (CO) emissions from a diesel engine with 5 % of **27** blended into the diesel fuel. Measurements performed at Institute of Agricultural Technology and Biosystems Engineering (vTI) (Engine type: Mercedes OMD 906, EURO III).

From the above data (Fig. 47a-e), with **27** as 5 % blend in diesel fuel there was a 3 % reduction in NO*x* emissions, 4.5 % increase in hydrocarbon (HC) emissions, 9 % decrease in carbon monoxide (CO) emissions and 6 % decrease in particulate matter emissions, with a fuel penalty of 1.4 % which, however, is a negligible amount.

To introduce glycerol derivatives as fuel additives compound **27** was synthetically and economically the most viable compound with ξ value of 9.59 (equation-6, Chapter 4.2.4.4). The lower percentage of reduction in CO and PM emissions compared to the other additives is compensated by the 3 % reduction in NO*x* emissions which shows a typical PM-NO*x* tradeoff behavior (Chapter 4.2.4.4). The reason for the increase in HC emissions is not yet known, but it can be associated with the acetal function due to its degradation to carbonyl compounds or to the *tert*-butyl group which could interrupt the burning process and cause the release of excess HC. Compared to the other acetals derived from glycerol, compound **27** is the most promising additive for diesel fuel in terms of synthesis, boiling range and solubility. The 4.5 % increase in HC emissions show the reductive environment during the combustion which may be the cause or 3 % reduction in NO*x* emissions (see Fig. 31a, Chapter 6.2.1).

The major problem dealing with diesel engines is to reduce NO*x* emissions (see Chapter 4.2.4), especially from blended and pure biodiesel fuel. After a successful synthesis of fuel oxygenates from glycerol it was decided to deal with the problems associated with NO*x* emissions from diesel engines. It was assumed that amine containing additives (Chapter 5.2.5.2.3) could reduce NO*x* emissions from the diesel exhaust shall follow.

Chapter 10: Synthesis of amines from glycerol (48) and (58)

10.1: Introduction

To perform in a single step the chemical transformation of the hydroxy functional groups in glycerol **(2)** to the amino moiety is difficult; it should theoretically yield 1,2,3-trisaminopropane **(46)**. Industrial alcohols like methanol are converted to methyl amines (1^o, 2^o, 3^o) in one step by the reaction of methanol with ammonia in the presence of dehydration catalysts like alumina or silica at 350-400 ^oC. In the case of **2** such a process may lead to dehydration products.

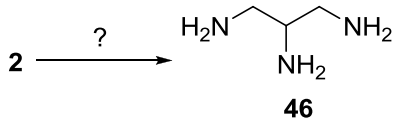

Instead, compound **46** was successfully synthesized by Pope *et al*.[175] from citric acid (citric acid → acetonedicarboxylic acid → diisonitrosoacetone → diaminoacetone → diacetyldiaminoacetoxime → 1,2,3-trisaminopropane). Unfortunately no further literature evidence was found to allow a one-step synthesis of **46**. However, Green *et al*.[176] have achieved a single step preparation of 2,2-dimethyl-1,3-dioxolane-4-methylamine **(48)** from [2,2-dimethyl-1,3-dioxolan)-4-yl] methyl-4-methylbenzenesulfonate **(47)** in an autoclave with ammonia at 50 ^oC under a pressure of 250 psi (17 atm) for 4 days, resulting in 81 % of **48** (Scheme 20).

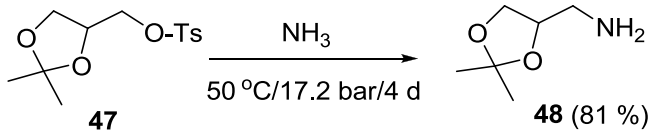

Scheme 20: Synthesis of solketal amine **(48)** from **47.**[176]

10.2: Preparation of 1,2,3-trisaminopropane (46)

The introduction of a leaving group like tosylate into glycerol to produce glycerol 1,2,3-tristosylate **(49)** and further reaction with ammonia according to Green's method[176] could yield **46**. Though **49** is a commercially available product, it was easily synthesized using Baer's[177] procedure (Scheme 21) according to which glycerol was reacted with 3.5 equivalents of purified tosylchloride (recrystalised from $CHCl_3$ and petroleum ether)[178] in the presence of pyridine at 0 ^oC to yield mixture of glycerol tosylates. The product mixture

was purified according to the given procedure to isolate 27 % of tristosylate **(49)** (m.p. 100-102 ^{o}C).

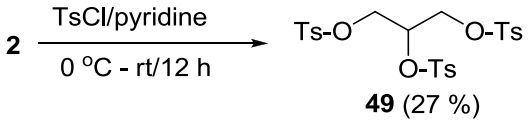

Scheme 21: Preparation of glycerol 1,2,3-tristosylate **(49)**

Even though there was a risk of forming elimination rather than substitution products, an attempt was made to synthesize **46** following the conditions reported by Green *et al*.[176] using 200 mg of **49** and approximately 10 mL of dry ammonia sealed in an ampoule, which was heated at 50 ^{o}C in a hot air oven for 26 h. The resulting product mixture was washed with diethyl ether to precipitate the unreacted **49**, which was filtered off; workup yielded a small amount of viscous oil, GC-MS analysis of which showed a mixture of unidentified products.

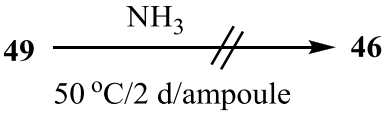

10.3: Preparation of l-amino-2,3-propandol isopropylidene ketal (48)

Solketal amine **(48)** was synthesized following the protocol reported by Rapoport *et al*.[179] according to which **26** was converted first to 2,2-dimethyl-1,3-dioxolan-4-methoxy methanesulfonate **(50)** in 74 % yield (lit. [179] 96 %) followed by the reaction with sodium azide to produce 1-azido-2,3-propanediol isopropylidene ketal **(51)** in 81 % yield (lit.[179] 96 %). Compound **51** was then reduced to **48** using Na_2S in 68 % yield (lit.[158] 93 %) (Scheme 22).

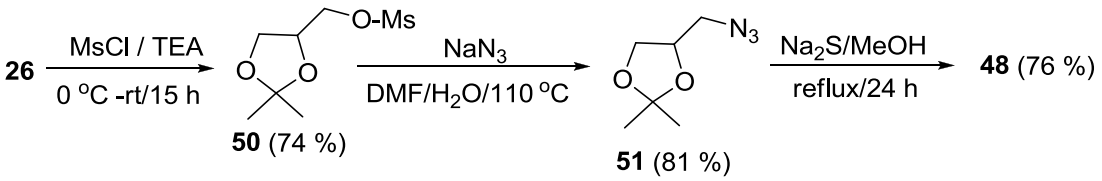

Scheme 22: Preparation of **48** from **26**.[179]

Further, a similar synthetic approach was attempted by using **47**. Solketal **26** was converted to **47** in 71 % yield (lit.[177] 80 %) according to the procedure of Bear[177] followed by the introduction of azide as above to yield 92 % of **51**, which was further reduced using hydrogen with Pd/C as catalyst to yield 68 % of **48** (Scheme 23). Reduction of the reaction time in this case resulted in lower yields.

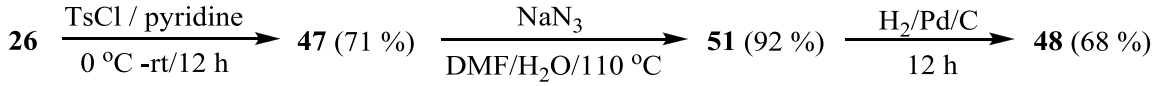

Scheme 23: Preparation of **48** from **26**.

The compounds **47**, **48**, **50** and **51** are well known and have been characterized in the literature.[177, 179] The analytical data (^{1}H NMR, mass and IR spectra, see also the experimental section) were compared and are in good agreement with those reported in the literature.

10.4: Synthesis of 3-*tert*-butoxy-1,2-diamino propane (58)

Similarly, following the linear synthetic approach of Rapoport *et al*.[179] **14** was converted to **58**, for which compound **14** was mesylated in the presence of pyridine to obtain a mixture of 3-*tert*-butoxypropane-1,2-bis(dimethylsulfonate) **(52)** and 3-*tert*-butoxy-2- hydroxypropane-1- methylsulfonate **(53)** in 92 % yield (Scheme 24).

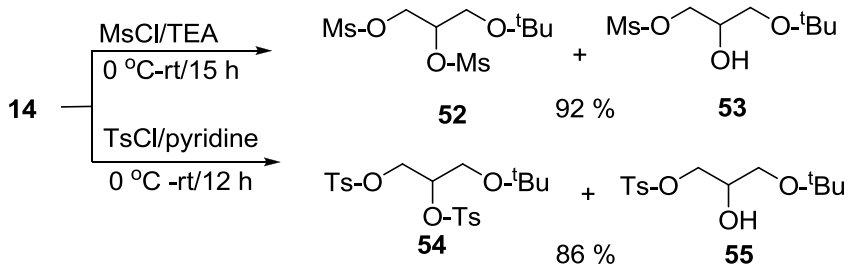

Scheme 24: Synthesis of mesylates **52**, **53**, and of tosylates **54**, **55** from **14**

Unfortunately, compounds **52** and **53** could not be separated due to the difficulty in staining the compounds during TLC analysis. However, it was observed by GC and TLC analysis that **14** was completely consumed during the reaction. To overcome the problem of staining, **14** was converted to tosylates **54** and **55** in an yield of 86 % according to the procedure reported by Bear.[177] As expected, it was possible to identify the spots on TLC plates by UV irradiation (R_f=0.62). An attempt to separate **54** and **55** using column chromatography failed though.

However, the above mixture was further converted to azides without separation. The mixture of **52** and **53** yielded 73 %, whereas **54** and **55** yielded 10 % of 1,2-diazido-3-*tert*-butoxypropane **(56)** and 1-azido-3-*tert*-butoxypropane-2-ol **(57)** as yellow oils, respectively (Scheme 25). The compounds **56** and **57** were separated by column chromatography using diethylether as solvent (R_f=0.75 and 0.86, respectively) to obtain 47 % of **56** and 26 % of **57** (from **52** and **53**) as pure colorless oils. The product mixture from tosylates **(54** and **55)** was not further separated due to poor yield.

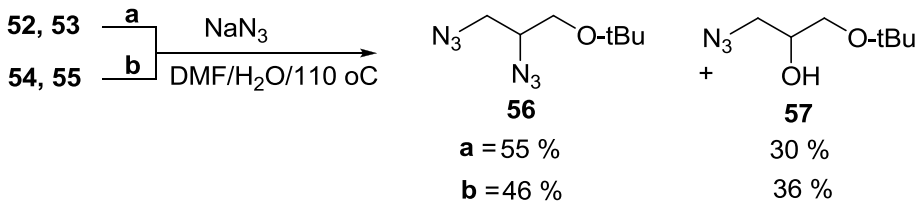

Scheme 25: Preparation of **56** and **57** (a) from a mixture of **52** and **53**, (b) from a mixture of **54** and **55** (yields based on GC analysis).

Compound **56** was reduced with Na_2S to obtain 1,2-diamino-3-*tert*-butoxypropane **(58)** as an analytically pure yellow oil in 92 % yield. (Scheme 26).

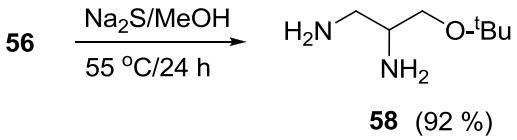

Scheme 26: Preparation of 1,2-diamino-3-*tert*-butoxypropane **(58)**

The reduction with sodium sulfide provides milder conditions and produces better yields compared to the reduction with zinc/acetic acid or H_2S in dichloromethane. The mechanism of the reaction (Scheme 27) has not been established in detail. However, a reasonable pathway has been proposed by Hassner *et al.*[180] according to which the sulfur in Na_2S acts as an electron donor similar to H_2S reduction and is oxidized to Na_2S_2 by reducing the azide **(56)** to the amine **(58)**.

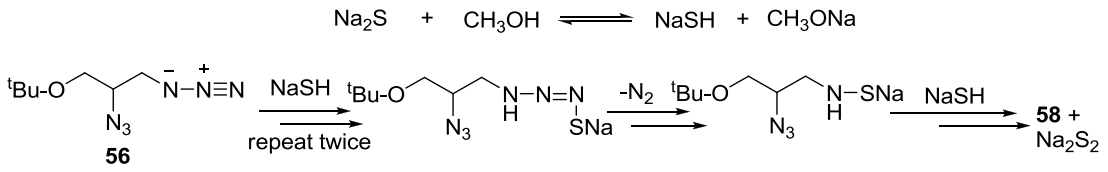

Scheme 27: Mechanism of azide reduction by Na_2S

10.5: Structural and conformational analysis of compounds 56-58

As mentioned above (Chapter 8.3.4), compounds **56** and **57** are produced from a racemic mixture of **14**. Thus, the products **56** and **57** are mixtures of the enantiomers **56a**, **56b** and **57a**, **57b**.

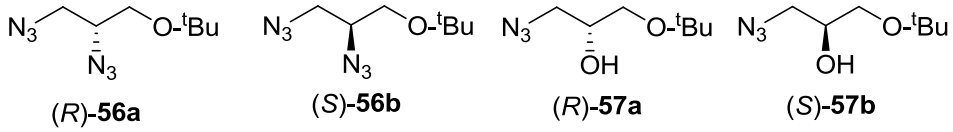

For conformational analysis compounds **56** and **57** may be considered as structural analogues of 1,2-disubstituted ethanes. As such they must exhibit a *gauche*-effect which is well known for e.g. 1,2-difluoroethane and many other 1,2-disubstituted ethane derivatives with a general structure of P-C-C-Q where at least P or Q is an electron withdrawing substituent or electronegative atoms (e.g. Cl, F, OH).[181, 182] The term *gauche* effect is given to the phenomena that in 1,2-disubstituted ethanes the *gauche*-conformer (in our case **56c)** is populated to larger extent than the *anti*-conformer **56d**. Similarly, in compound **57** the *gauche* conformer **57c** predominates over the *anti*-conformer **57d**.

The *gauche* effect has been well established by both theoretical calculations and by experimental methods predominantly in substituted fluoroethanes and in a variety of 1-substituted propanes.[182] Sonntag *et al*.[183] have recently shown by molecular mechanics calculations of azidoethane derivatives that the *gauche* effect exerted by the azido group is either comparable or slightly stronger than the fluorine *gauche* effect. The most frequently used methods to study *gauche* effect are microwave spectroscopy, IR, gas-phase NMR spectroscopy especially by ^{13}C NMR chemical shift measurements.[184] However, there is often no evidence in the literature regarding the conformation attained by these compounds in solution and we assume that all conformers exist in solution. This can be observed particularly well in the ^{13}C spectrum of compound **57**.

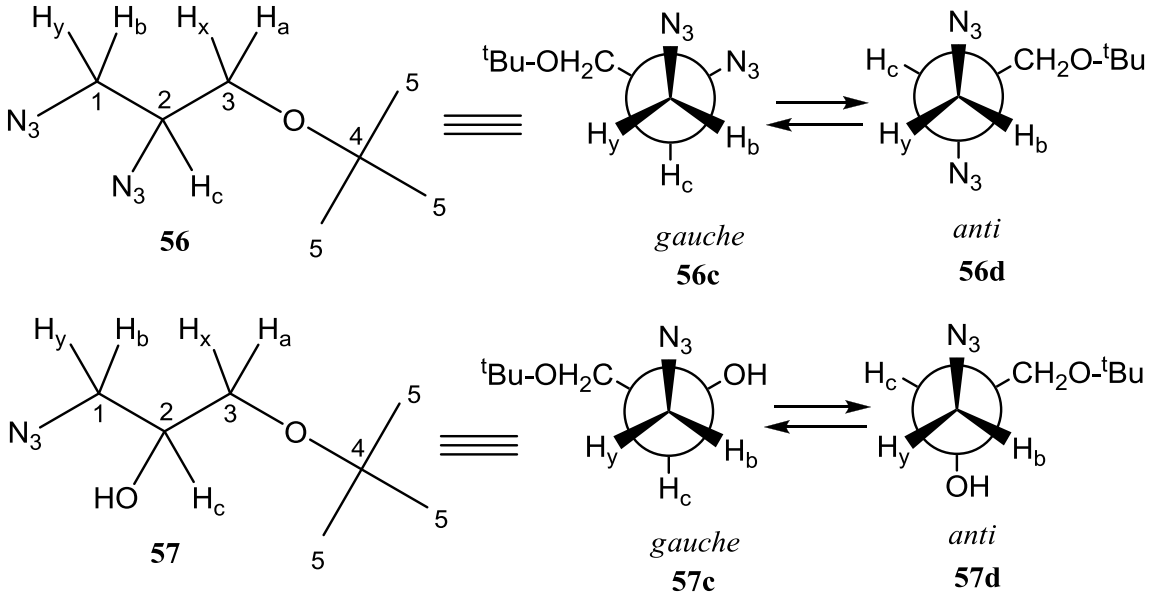

The ^{1}H NMR spectrum of the azides **(56**, **57)** is difficult to explain by using first order principles. In compound **56** the C-5 protons from the *tert*-butyl group appears at δ=1.21 ppm. The C-1, C-2 and C-3 protons in theory should display a (AXBY)C type of spectrum. However, they show a complex series of multiplets for H_a, H_x, H_b, H_y and H_c at δ=3.27-3.61 ppm similar to compound **14** (Chapter 8.3.4).

In compound **57** a varied pattern of multiplets was observed in the ^{1}H NMR spectrum, where the H_a, H_x, H_b and H_y protons display multiplets at δ=3.31-3.68 ppm upfield from H_c which appears at δ=3.85-3.99 ppm as a multiplet. The hydroxyl (O-H) proton appears as a broad doublet at δ=2.9 ppm and the C-5 protons from the *tert*-butyl group at δ=1.18 ppm. The broad doublet of the hydroxyl proton is caused by the coupling with H_c and a paramagnetic shift of H_c suffices to rationalize that the hydroxyl group belongs to the C-2 secondary carbon atom and not to the C-1 primary carbon atom.

The ^{13}C NMR spectrum of **56** recorded at 50 MHz in $CDCl_3$ shows *five* different peaks corresponding to *five* different carbon atoms. The *tert*-butyl group (C-5) appears at δ=27.8 ppm and the methylene carbon C-1 is extremely shielded due to the anisotropic effect of the azide group. It shows strong diamagnetic shift to δ=52.2 ppm compared to C-3 carbon appearing at δ=62.4 ppm. The secondary C-2 carbon atom also shows a diamagnetic shift compared to C-3 due to similar reasons and appears at δ=61.3 ppm; the C-4 tertiary carbon atom is registered at δ=74.4 ppm. In compound **57** the *tert*-butyl group (C-5) appears at δ=27.2 ppm, and C-1 displays two peaks at δ=53.4 and 53.8 ppm, respectively. The C-2 carbon atoms display two different peaks at δ=69.4 and 69.8 ppm, probably corresponding to

two different conformations **57a** and **57b**, it can be assumed that both conformers are populated almost equally at room temperature. The C-3 carbon atom resonates at δ=65.7 ppm and the C-4 tertiary carbon atom appears at δ=73.4 ppm.

IR spectroscopy plays a major role in the identification of the azido group.[185] The IR spectrum of compound **56** recorded neat displayed medium absorption bands at $\tilde{\nu}$ =2976 and 2935 cm^{-1} attributed to CH_3 asymmetrical and symmetrical stretching vibrations and at $\tilde{\nu}$ =2873 cm^{-1} corresponding to CH_2 symmetrical stretching vibrations. A very strong absorption band at $\tilde{\nu}$ =2092 cm^{-1} is attributed to N≡N stretching vibrations and a medium broad band at 1267 cm^{-1} attributed to N=N stretching vibrations. A weak broad absorption band at $\tilde{\nu}$ =667 cm^{-1} corresponds to N_3 in-plane bending at 555 cm^{-1} corresponds to N_3 out of plane bending vibrations.

Similarly, in compound **57** a broad absorption band is observed at $\tilde{\nu}$ =3412 cm^{-1} attributed to the O-H stretching vibration. A medium absorption bands at $\tilde{\nu}$ =2976 and 2932 cm^{-1} are attributed to CH_3 asymmetrical and symmetrical stretching vibrations and at $\tilde{\nu}$ =2874 cm^{-1} corresponding to CH_2 symmetrical stretching vibrations. The azide group absorbs at $\tilde{\nu}$ =2093 cm^{-1} and a medium broad band at $\tilde{\nu}$ =1268 cm^{-1} attributed to the N=N stretch vibrations.

Mass spectrometry (GC-MS) analysis of the compound **56** shows a pronounced peak with a 2 % intensity at *m/z*=198 corresponding to the $[M]^+$ ion (even nitrogen rule) followed by a 20 % peak at *m/z*=142 attributed to the loss of *tert*-butyl carbocation and a base peak at *m/z*=57 attributed to *tert*-butyl carbocation. Similarly compound **57** shows a $[M]^+$ peak with a 2 % intensity at *m/z*=173 (odd nitrogen rule) followed by a 20 % peak at *m/z*=117 attributed to the loss of *tert*-butyl carbocation. The 2 % peak at *m/z*=173 is attributed to the loss of a *tert*-butoxymethyl radical and the base peak as usual is seen at *m/z*=57.

As mentioned above (Chapter 8.3.4), compound **58** was produced from a racemic mixture of **14**. Thus, the product **58** is a mixture of enantiomers as shown in **58a** and **58b**.

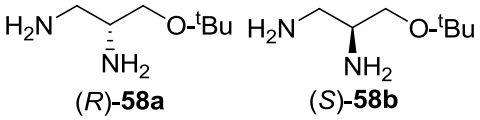

(*R*)-**58a** (*S*)-**58b**

Conformational analysis of 1,2-diamino-3-*tert*-butoxypropane **(58)** is assumed to reveal a *gauche*-effect similar to ethylene-1,2-diamine. It shows a strong preference for one

conformer (gauche) with a N-C-C-N dihedral angle measured for the *cis*-position of 64 ± 4 ^{o}C. The fraction of any other isomers if present was estimated to be less than 5 %.[186-189] However, Buslaeva *et al*.[190] have concluded from the analysis of various temperature dependent physicochemical properties that all conformers exist in solution.

Therefore, by analogy **58** is assumed to exist in the possible conformations (**58c** and **58d**) in solution at room temperature. Thus, the ^{1}H NMR spectrum of the amine **58** (Fig. 48) recorded at 200 MHz in D_2O displays a complex multiplet for the H_a, H_x, H_b, H_y and H_c protons at δ= 2.80-3.81 ppm analogous to compound **56** and **14** and it can thus be rationalized by similar explanations (Chapter 8.3.4). Apart from the above protons the C-5 protons of the *tert*-butyl group appears at δ=1.19 ppm.

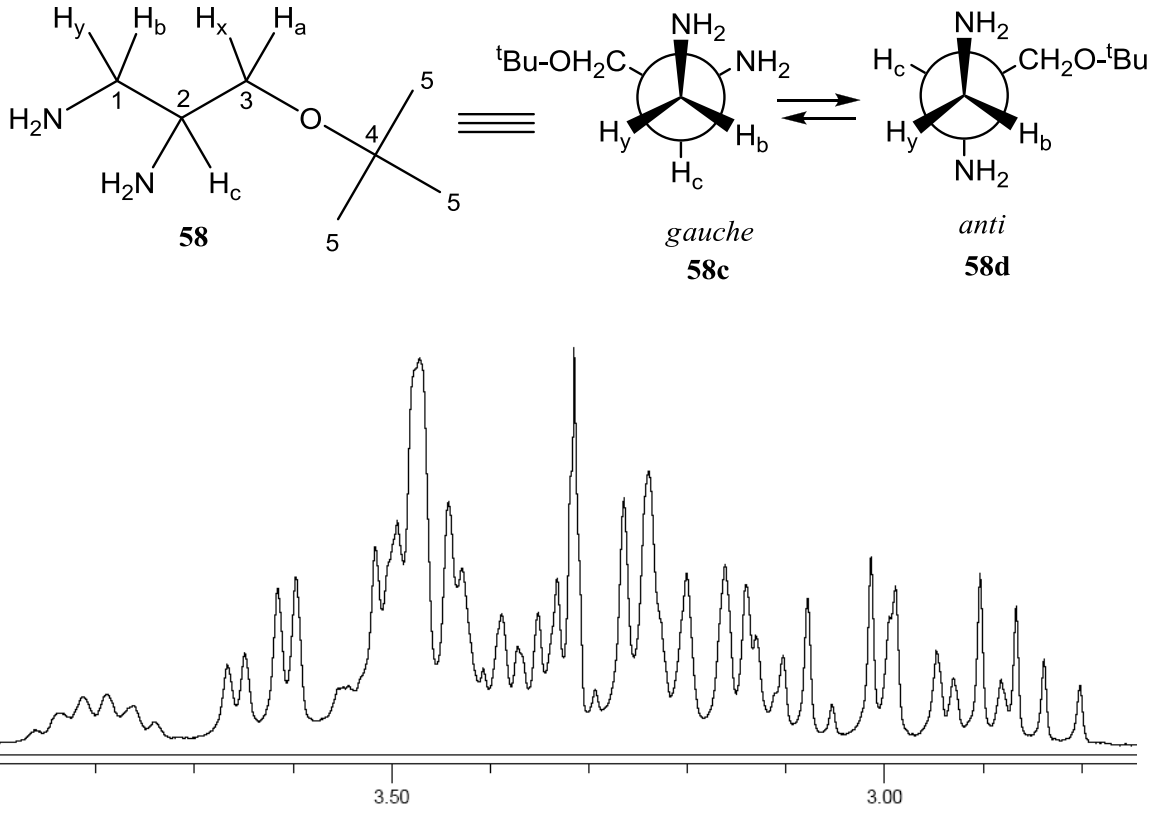

Fig. 48: ^{1}H NMR spectrum of the C-1, C-2 and C-3 protons of **58**. (δ=(ppm), D_2O, 22 % (w/w), 25 ^{o}C, 200 MHz)

In ^{13}C NMR spectrum of **58** the *tert*-butyl group (C-5) appears at δ=27.6 ppm and the methylene carbon atom C-3 appears upfield at δ=49.4 ppm, C-1 is shifted slightly downfield to δ=64.9 ppm. The secondary carbon atom C-2 appears at δ=76.4 ppm and the C-4 tertiary carbon atom at δ=72.9 ppm.

The IR spectrum of **58** displays medium absorption bands at $\tilde{\nu}$ =3356 and 3275 cm^{-1} attributed to a primary amine, symmetrical and asymmetrical stretching vibrations, strong to medium absorption bands at $\tilde{\nu}$ =2976 and 2935 cm^{-1} attributed to CH_3 asymmetrical and symmetrical stretch and at $\tilde{\nu}$ =2873 cm^{-1} corresponding to the CH_2 symmetrical stretching motions. A broad medium absorption band is observed at $\tilde{\nu}$ =1633 cm^{-1} attributed to N-H bending vibrations of primary amines and a strong band is observed at $\tilde{\nu}$ =1236 cm^{-1} corresponding to C-N stretching vibrations. A medium signal at $\tilde{\nu}$ =836 cm^{-1} is caused by N-H wagging motions.

Mass spectrometry (GC-MS) analysis of the compound **58** shows a pronounced peak with a 50 % intensity at *m/z*=116 corresponding to the loss of $[CH_2\text{-}NH_2]^+$ from $[M]^+$ (even nitrogen rule) and a 96 % peak at *m/z*=60 corresponding to $[C_2H_8N_2]^+$ and a base peak at *m/z*=57.

The amines **48** and **58** were insoluble in both diesel and biodiesel. Hence, they were not subjected to fuel additive experiments. Unfortunately, the preparation of 1,2,3-trisaminopropane **(46)** could not be undertaken by the above procedure due to the well-known reason that aliphatic (saturated and unsaturated) azides are explosive by nature. This has been clearly acknowledged by Nielsen *et al.*[182] from their personal experience who have shown that the unsaturated azides and diazides are highly reactive compounds which can, and do explode violently and must be handled in small quantities at low temperatures. However, we were fortunate in this regard that **56** was not explosive but decomposed slowly in the condensed state to **57** and further to an unknown polymeric material by slow liberation of nitrogen (bench life 3-5 days). This phenomenon was not observed when the compound was stored as a $CHCl_3$ solution.

10.6: Synthesis of triazoles (60 and 61)

10.6.1: Introduction

The copper (I) catalyzed Huisgen [3+2]cycloaddition reaction of terminal alkynes and organic azides to obtain 1,4-disubstituted-1,2,3-triazoles is the best click reaction to date. It has a wide range of applications[191] and supports an unlimited array of triazole containing architectures. Many different procedures have been reported in the literature to carry out the process. In most of the reactions a copper (II) salt is used in combination with a salt of ascorbic acid. The reaction proceeds well in a variety of solvents. Water with *tert*-butanol is the most commonly used combination; other solvent systems like DMS, THF, acetone, DMF and acetonitrile have also been employed successfully.

10.6.2: Preparation of 60 and 61

The preparation of 1-(9,9-dimethyl-8,10-dioxolan-6-methyl)-4-phenyl-1*H*-1,2,3-triazole **(60)** was carried out using classical reaction conditions[191] according to which solketal azide **(51)** was reacted with phenyl acetylene (**59)** in the presence of copper sulfate and sodium ascorbate as the catalyst in a solvent mixture of water and *tert*-butanol. After 12 h of stirring the product mixture was purified using column chromatography to isolate 26 % of **60**.

The well known disadvantage[192] of this method is the copper contamination in the product. In our case the solketal azide **(51)** was additionally deprotected under the reaction conditions by the *in situ* formation of ascorbic acid. To overcome this disadvantage a slightly modified method of Sharpless *et al*.[192] was adopted (Scheme 28), according to which the copper-sodium ascorbate catalyst was replaced by simple metallic copper powder (45 μ) on activated charcoal and the reaction was carried out in a 1,4-dioxane and triethylamine solvent mixture. After 12 h of stirring at room temperature the product mixture was filtered through a silica gel pad and evaporation of the solvents provided 72 % yield of amorphous solid as pure product **60** without any copper contamination.

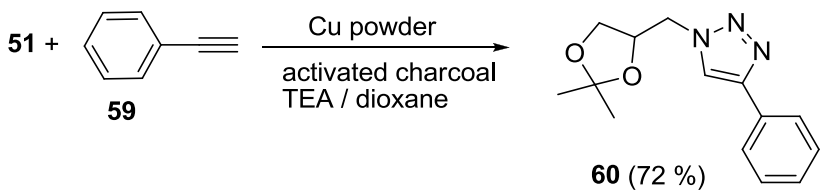

Scheme 28: Preparation of solketal triazole **60**

Preparation of 1,1'-(8-*tert*-butoxypropane-6,7-diyl)-bis-(4-phenyl-1*H*-1,2,3-triazole) **(61)** was carried out using the second procedure mentioned above (Scheme 29), by which **56** was reacted with **59** to obtain a 88 % yield of pure white solid **61** melting at 165 ^{o}C.

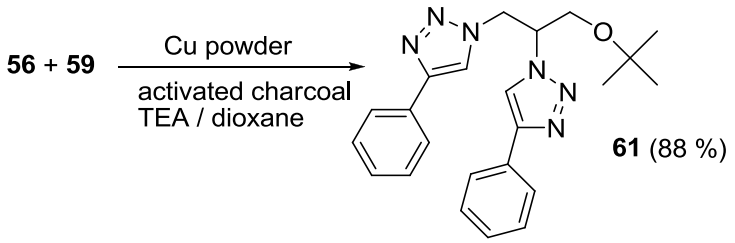

Scheme 29: Preparation of 1,1'-(8-*tert*-butoxypropane-6,7-diyl)-bis-(4-phenyl-1*H*-1,2,3-triazole) **(61)**

10.7: General mechanism of the triazole synthesis

In the first procedure mentioned above where copper (II) and sodium ascorbate were used as the catalyst, the active catalyst is generated from Cu (II) salt by reduction with sodium ascorbate or ascorbic acid. A slight excess of ascorbate is added in order to prevent oxidative couplings which is often observed when a Cu (I) source is used as a catalyst[192] (Scheme 30).

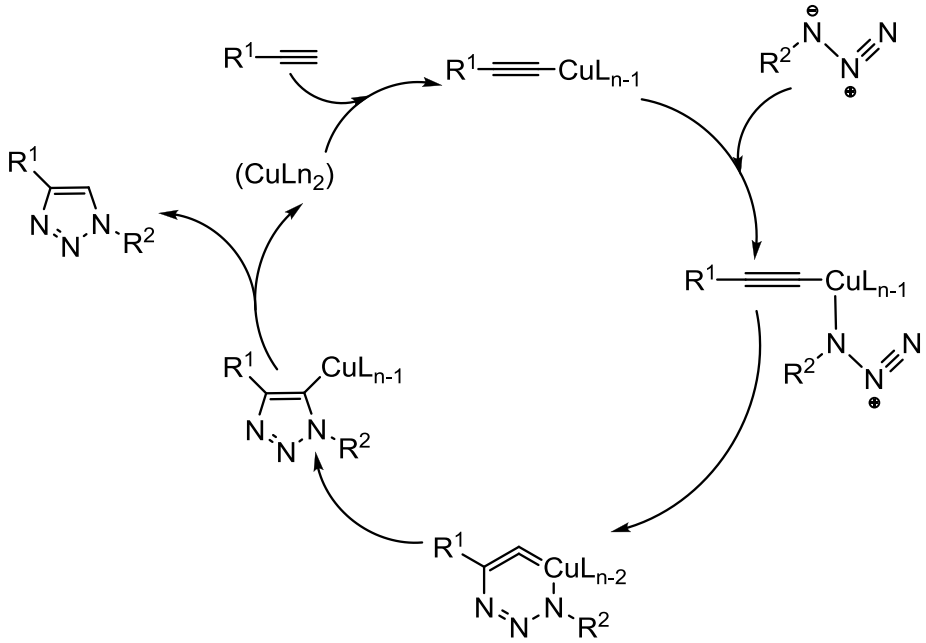

Scheme 30: Proposed reaction mechanism involved in triazole formation.[191]

In the second procedure in which copper powder was used, the catalyst was in oxidized form and would have contained oxides of copper (Cu_2O and CuO). Ciavatta *et al.*[193] have shown the possibility of comproportionation of copper salts in solution ($Cu^{+2}+Cu^{0} \rightleftharpoons 2Cu^{+1}$), by analogy we assume that in our case the comproportionation of copper oxide (Cu^{+2}) with copper metal (Cu^{0}) could have provided an active Cu^{+1} catalyst for the reaction.

A similar type of catalytic approach has been reported by Lipshutz *et al.*[194] in which copper was incorporated on activated charcoal (Scheme 31) using $Cu(NO_3)_2$ in water. The thus formed catalyst was further used for the reaction, which was performed without exclusion of moisture or air to provide the adduct in over 98 % yield. Lipshutz *et al.*[194] have also studied the effect of different basic solvents on the process and here reported that triethylamine showed better results than compared to other basic solvents (DBU or pyridine).

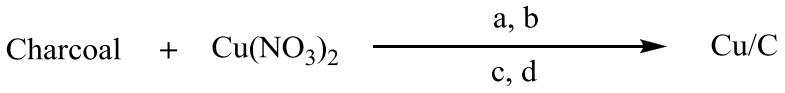

(a) dissolved in H_2O; (b) ultrasound bath; (c) filter/wash; (d) dry

Scheme 31: Preparation of Cu/C catalyst according to Lipshutz *et al.*[194]

When the [3+2]cycloaddition of an azide and an alkyne is performed with a Cu^{+1} catalyst under classical "click" conditions, excess sodium ascorbate is used to avoid homocoupling of the alkyne. However, when a copper metal is used as the catalyst, as mentioned above[192, 194] the formation of oxidative coupling products from acetylene were not reported, although the reaction is carried out in the presence of air, moisture and strong bases, which are the general conditions applied in homocoupling coupling reactions. It could be argued that in the presence of copper metal [192] or a Cu/C [194] catalyst the [3+2]cycloaddition is preferred over the dimerisation of terminal acetylenes. To test this argument we tried the homocoupling of phenyl acetylene **(59)** in the presence of copper powder on activated charcoal under atmospheric conditions using triethylamine as a solvent. It was not surprising to notice the absence of any traces of **62** even after 18 h of stirring at room temperature. In the case of copper it is well known[190-194] that it forms copper acetylide (as show in Scheme 30) and it is assumed that the complex precipitates without further participation in the reaction.

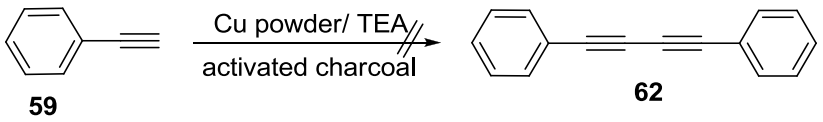

Scheme 32: Attempted coupling of **59** to **62** using Cu powder catalyst

Further, an experiment was conducted to investigate the oxidative homocoupling in the presence of palladium catalyst [$PdCl_2(PPh_3)_2$] and copper powder catalyst. The reaction was performed under atmospheric conditions with 2 mmol of **59**, 10 wt % of Cu powder and 7 wt % of palladium (II) in triethylamine and the mixture was stirred for 8 h. After workup compound **62** was isolated in 12 % yield, besides unreacted substrate **59**.

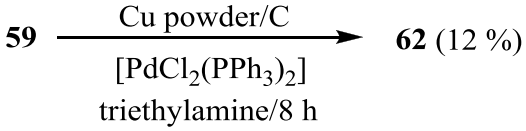

Scheme 33: Oxidative homo-coupling with Pd (II) and copper powder as catalyst

Chapter 11: *N,O*-acetals 65, 67 and 68

11.1: Introduction

O,O-, *N,N*- and *S,S*-acetals are well known and have thoroughly been described in the literature. However, *N,O*-acetals are relatively unusual compounds. In *N,O*-acetals the oxygen and a nitrogen atom are attached to the same carbon atom, which leads to an increased ease of hydrolysis. *N,O*-acetals are prone to rapid hydrolysis with dilute acids to the corresponding starting materials. In particular, the acetals derived from alcohols of smaller molecular weight like diethylaminomethoxyethane are readily hydrolyzed by shaking them with cold water. Furthermore, the derivatives of dialkyl amine are less stable than the derivatives of cyclic amines like piperidine.

N,O-acetals were first investigated by Robinson *et al*.[201] under the heading of *pseudo-bases*. The authors synthesized various *N,O*-acetals from formaldehyde **(63)** and diethyl amine **(64)**. A general method was used for their synthesis in which formalin (35 % solution of formaldehyde) was added to **64** in the cold followed by the addition of the desired alcohol and an equimolar amount of K_2CO_3. The reaction mixture was stirred overnight to obtain 60-90 % of product yields, respectively. In the case of glycerol **(2)** the above general procedure failed to deliver 1,2,3-tris-(diethylaminomethoxy) propane **(65)**. Instead, tetraethyldiaminomethane **(66)** was obtained quantitatively. Eventually, the authors have successfully synthesized **65** in 11 % yield by changing the order of addition from **64**+**63** plus **2** to **64**+**2** plus **63** (Scheme 34).

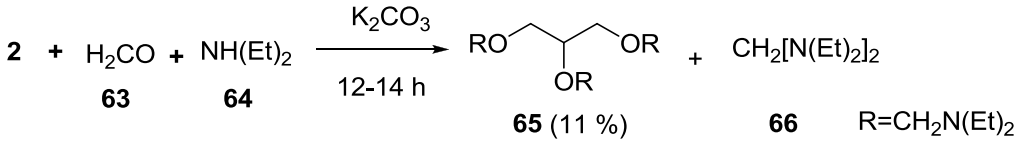

Scheme 34 Preparation of **65** according to Robinson *et al*.[201] using formalin.

According to Robinson *et al*.[201] the compounds are readily soluble in most organic solvents and are immiscible with water, and in most of the cases the products were purified by distillation under atmospheric pressure without decomposition. However, any attempts to replace formaldehyde by an aromatic aldehyde failed.

11.2: Preparation of *N,O*-acetals 65, 67 and 68

In a view of the low yields for **65** reported by the Robinson *et al*.[201] we adopted a slight modification in the procedure. Instead of formalin, paraformaldehyde was used as a substitute. The reaction was performed in the presence of equimolar dry K_2CO_3 which was added periodically to a cold solution of glycerol **(2)** and 10 % excess of diethyl amine **(64)** and a 10 % excess of paraformaldehyde **(63)** was slowly introduced (Scheme 35) into the reaction mixture during a period of 30 min. It is well known that the condensation of **64** with **63** is a highly exothermic process; hence care was taken to maintain the temperature below 30 ^{o}C.

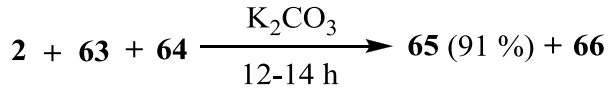

Scheme 35: Preparation of **65** from glycerol **(2)** using paraformaldehyde

The reaction mixture was stirred overnight and the product mixture was filtered and washed with excess diethyl ether to obtain almost 91-95 % of 1,2,3-tris-(diethylaminomethoxy) propane **(65)** as a colourless oil. The only side product **66** was removed by vacuum distillation at 0.2 mbar and 30 ^{o}C. It was observed that upon cooling below 15 ^{o}C glycerol **(2)** was precipitated which formed a thick mass with K_2CO_3. The unavailability of glycerol in the solution promoted the formation of **66** as the major product.

The fundamental disadvantage of the above procedure is the use of more than stoichiometric amounts of potassium carbonate which furthermore could not be reused. As mentioned above the addition of **63** to the mixture of glycerol **(2)** and diethyl amine **(64)** is an exothermic reaction. When the reaction was up scaled from 0.1 M to 6 M of glycerol, the presence of stoichiometric amounts of K_2CO_3 caused difficulties in stirring and thus in thermal exchange. It was observed that at higher temperatures the formation of **66** was favored and the yield of **65** diminished dramatically (50-52 % based on GC analysis).

1,2-Bis-(diethylaminomethoxy)-3-*tert*-butoxy propane **(67)** was synthesized from **14** following the similar procedure as above. The yields were poorer (79-94 %, based on GC analysis), and an attempt to separate **14** from the product mixture by distillation was not successful (Scheme 36).

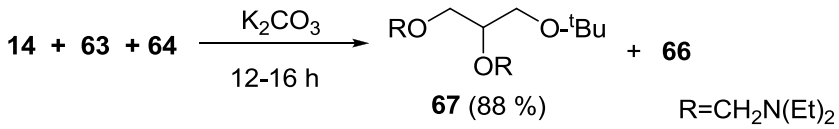

Scheme 36: Preparation of **67** from **14**.

Similarly, following the above procedure 2,2-dimethyl-(4-diethylaminomethoxymethy)-1,3-dioxolane **(68)** was prepared in almost quantative yield with respect to **26** (Scheme 37). The reaction was up scaled and about 8 L of **68** was prepared with 90-94 % purity (GC analysis).

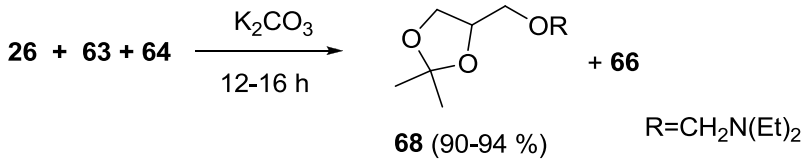

Scheme 37: Preparation of **68** from **26** using paraformaldehyde

11.3: Purification of *N,O*-acetals 65, 67 and 68

Attempts to purify the compounds **65, 67** and **68** by distillation under vacuum and under atmospheric pressure or by column chromatography were not successful. In one of the attempts when a 96 % pure (GC purity) **65** was subjected to distillation under vacuum, four different constant boiling fractions were collected including a major fraction boiling at 160 ^{o}C/2 mbar. The GC analysis of the fraction showed 65 % of **65** and 27 % of **66**. Unfortunately, the distillation under atmospheric conditions decomposed the product **65** to a charred material and **66** was largely collected as a distillate. The situation was similar with **68**, it was hydrolyzed upon distillation under vacuum and also under atmospheric pressure leaving charred material. In one of the cases, when a 5 g scale fractional distillation was performed in a kugelrohr distillation apparatus with **68** (87 %), **26** (10 %) and **66 (**3 %). The distillation provided **66** as the first fraction at 30 ^{o}C and 0.2 mbar pressure, as a second fraction (1.25 g) a mixture of **68** (33 %) and **66** at 68-72 ^{o}C 0.4 mbar, and a third fraction (2.46 g) with 22 % of **26** and 71 % of **68** at 78-85 ^{o}C 0.4 mbar pressure, and a fourth fraction (1.02 g) with 20 % of starting material **26** and 74 % of **68** at 87- 93 ^{o}C and 0.4 mbar pressure. In a distillation under atmospheric pressure from 145-205 ^{o}C, all fractions collected at different constant temperatures showed the presence of **66**, **26** and product **68**, while the major part of **68** had decomposed to a charred material. Proper understanding of the decomposition of **68** has not been achieved. Presently, however, it was not possible for **68** to

decompose into starting material **26** without the presence of equimolar amounts of water in the product.

However, to overcome the difficulty of purification the respective alcohol was allowed to react completely by the addition of excess **63** and **64** periodically. The confirmation of the complete consumption of the respective alcohol was obtained by GC analysis and further by IR spectroscopy (especially in the case of glycerol). The thus formed product mixture was separated from the side product **66** by vacuum distillation (30 ^{0}C/ 0.2 mbar) to obtain analytically pure product. Unfortunately, a complete conversion of compound **14** to **67** could not be achieved according to the above process.

11.4: Structural and conformational analysis of 65, 67 and 68

Even though **65** looks like a highly symmetrical molecule, the conformation adopted by the compound in solution state is not clear. However, Robinson *et at.*[201, 202] have proposed the existence of *N,O*-acetals in a partially ionized state ($RO^{\delta-}$-CH_2-$N^{\delta+}R^1R^2$) based on their reactivity towards Grignard reagent in which alkoxy group (OR) is rapidly replaced by alkyl group (R), and also based on their reactivity towards ethyl cyanoacetate. The assumption was further rectified by Stewart *et al.*[203] by the calculation of the basic strength of acetals during hydrolysis. Thus, by analogy, we assume that a part of **65** could exist in partially ionic state creating a partial double bond between CH_2 and nitrogen as proposed by Stewart *et al.*[203] (CH_2-$N^{\delta+}R^1R^2$).

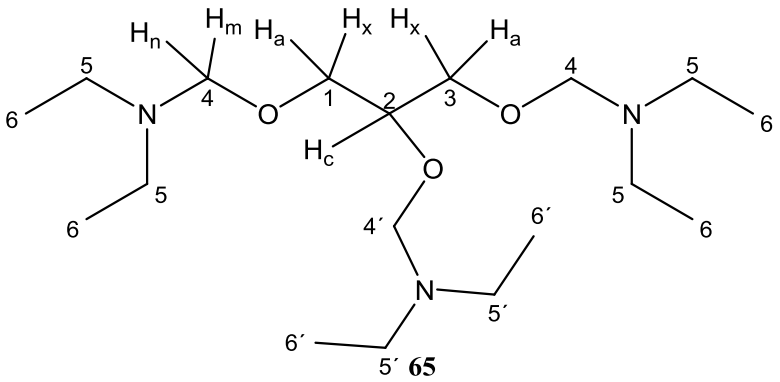

65

The ^{1}H NMR spectrum of **65** recorded at 400 MHz in $CDCl_3$ display a complex second order spectrum. The H_a, H_x, and H_c protons appear as multiplet at δ=3.41-3.61 ppm and the ethyl protons from (NEt_2) display a triplet with shoulders attributed to the C-6 and C-6´ protons at

δ 1.05-1.09 ppm. A quartet with shoulders is attributed to the C-5 and C-5´ protons at δ=2.56-2.62 ppm, respectively. The CH_2 bridged protons C-4 and C-4´ (*Hm*, *Hn*) display a paramagnetic shift and show four singlets at δ=4.155,4.158, 4.22 and 4.38 ppm, respectively.

The ^{13}C NMR spectrum of **65** was recorded at 100 MHz in $CDCl_3$ and was solved by using H-C correlation spectra via $^1J_{(C\text{-}H)}$ and DEPT experiments in correlation to the ^1H NMR explained above. The ^{13}C spectrum shows two different peaks for the C-6´ and C-6 carbon atoms at δ=12.3 and 13.0 ppm, respectively. Similarly, three peaks were observed for C-5´ and C-5 at δ=44.7, 45.0 and 45.2 ppm, respectively. The C-1 and C-3 carbon atoms display two different peaks at δ=68.2 and 71.7 ppm, respectively. Carbon atom C-2 appears at δ=75.8 ppm and C-4 and C-4´ display three signals at δ=83.9, 84.6 and 85.8 ppm.

Compound **65** is highly stable in the gas chromatograph and its mass spectrum shows a 2 % peak at *m/z*=275 corresponding to the loss of the NEt_2 radical cation from molecular ion, and a 5 % peak at *m/z*=261 caused by the loss of CH_2NEt_2 radical from $[M]^+$. A 2 % peak at *m/z*=231 is attributed to the loss of CH_2-O-CH_2NEt_2 from $[M]^+$, and a 40 % peak at *m/z*=160 to the loss of second NEt_2 moiety from *m/z*=231. A 50 % peak at *m/z*=102 is attributed to diethylaminomethoxy cation, and the base peak is observed at *m/z*=86.

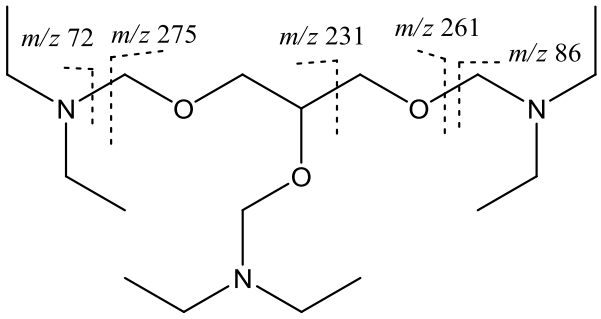

Not much information can be gathered from the IR spectrum of **65**. However, it can be observed that the O-H, N-H and C=O stretching vibrations are absent, conforming the complete consumption of starting materials in the reaction. Medium absorption bands are observed at $\tilde{\nu}$ =2969 and 2931 cm^{-1} attributed to CH_3 asymmetrical and symmetrical stretching vibrations and at $\tilde{\nu}$ =2871 cm^{-1} corresponding to CH_2 symmetrical stretching vibrations. The C-N stretching vibrations are observed as a strong maximum at $\tilde{\nu}$ =1065 cm^{-1}.

Similarly, the ^1H NMR spectrum of **67** recorded at 200 MHz in $CDCl_3$ displays a complex second order spectrum. The H_a, H_x, H_b, H_y and H_c protons are recorded as multiplets at

δ=2.95-3.8 ppm and the ethyl protons from (NEt_2) display a triplet with shoulders attributed to the C-6 and C-6´ protons at δ=0.72-0.79 ppm. The methyl protons from the *tert*-butyl group appear as two singlets at δ=0.86 and 0.87 ppm. The protons at C-5 and C-5´display a multiplet at δ=2.35-2.42 ppm, respectively. The protons at C-4 and C-4´ (*Hm*, *Hn*) show a paramagnetic shift and are registered as four singlets at δ=4.071, 4.076, 4.09 and 4.10 ppm, respectively.

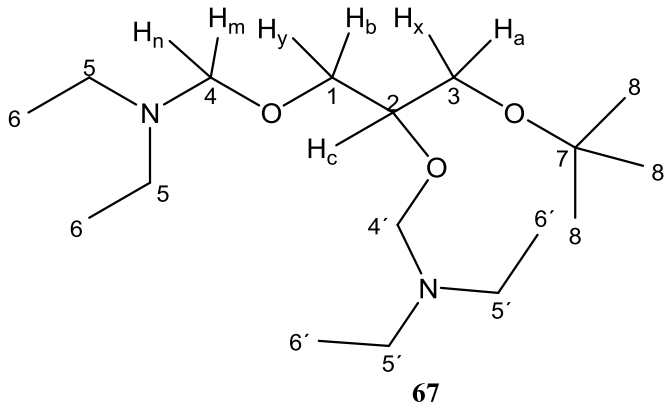

67

The ^{13}C spectrum of **67** shows two different peaks for the C-6´ and C-6 carbon atoms at δ=11.4 and 12.3 ppm, respectively. The C-8 carbon atoms show a single peak at δ=26.6 ppm. Similar to compound **65**, three different peaks were observed for C-5´ and C-5 at δ=43.9, 44.3 and 44.4 ppm, respectively. The C-1 and C-3 carbon atoms display two different signals at δ=66.2 and 69.2 ppm, respectively. The C-2 atom appears at δ=75.4 ppm and C-7 at δ=76.3 ppm. The C-4 and C-4´ carbon atoms display three peaks at δ=83.2, 83.8 and 85.3 ppm, respectively.

Compound **67** is highly stable during GC analysis the mass spectrum shows a 2 % peak at *m/z*=173 corresponding to the loss of two NEt_2 radicals from the molecular ion, and a 5 % peak at *m/z*=147 caused by the loss of two CH_2NEt_2 radical. A 5 % peak at *m/z*=117 is attributed to the loss of two CH_2-O-CH_2NEt_2 radical cation from $[M]^+$. A 5 % peak at *m/z*=100 is attributed to the loss of methyl radical from *m/z*=117. The base peak is observed at *m/z*=57.

In the IR spectrum of **67**, it is observed that the O-H, N-H, and C=O stretching vibrations are absent indicating the complete consumption of starting materials in the reaction. Medium intensity absorption bands are observed at $\tilde{\nu}$ =2971 and 2931 cm^{-1} attributed to CH_3 asymmetrical and symmetrical stretching vibrations and at $\tilde{\nu}$ =2871 cm^{-1} corresponding to

the CH_2 symmetrical stretching vibrations, and the C-N stretching vibrations are observed as a strong absorption band at $\tilde{\nu}$ =1076 cm^{-1}.

As mentioned in the previous Chapter compound **68** is derived from a racemic mixture of **26** and thus, the product **68** is a racemic mixture as well as mentioned in Chapter 9.2.1. The 1,3-dioxolane ring systems exists in a puckered conformation related to envelope or half chair (twist) conformations and the puckering depends on the substituents at C-2 and C-4 carbon atoms. An increase in the bulk of substituents may interrupt the *pseudorotational* circuit. Thus compound **68** may attain two different conformations: *pseudoaxial* and *pseudoequatorial* as shown in **68a** and **68b.** Conformations of this type have been described by Mucci *et al*.[159] for 4-trimethylaminomethyl-1,3-dioxolanes.

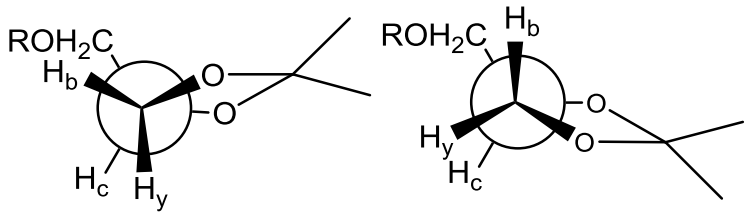

Psudoaxial **68a** R=CH_2-NEt_2 *Psudoeqatorial* **68b**

However, in our case we assume that the substituent (*CH_2O-CH_2NEt_2*) is bulky enough to interrupt the *psudorotational* circuit at room temperature. The ^{1}H NMR spectrum of **68** displays a complex spectrum which is difficult to explain using first order principles. The protons from the methyl groups at C-2 which are chemically and magnetically different show two singlets with shoulders at δ=1.35 and δ=1.36 and at δ=1.41 and 1.43 ppm (intensity of the signals are in the ratio of 6:1). The C-12 methyl groups display a triplet with shoulders at δ=1.04-1.08 ppm and the protons at C-11 shows a quartet with shoulders at δ=2.69-2.74 ppm. The methylene proton H_a at C-6 display a (AB)C pattern of a doublet of doublets at δ=3.40-3.44 ppm with a geminal coupling constant $^2J_{Ha,Hx}$ of 10.09 Hz, and a vicinal coupling constant $^3J_{Ha\text{-}anti\text{-}Hc}$ of 5.91 Hz. The H_x proton displays a doublet of doublets at δ=3.47-3.51 ppm with a vicinal coupling constant $^3J_{Hx\text{-}syn\text{-}Hc}$ of 5.17 Hz.

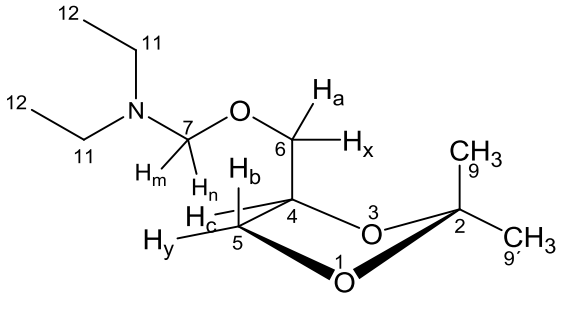

70

The ring proton H_b produce a multiplet at δ=3.74-3.77 ppm and H_y a multiplet at δ=4.02-4.06 ppm. The H_c proton is recorded as multiplet at δ=4.20-4.27 ppm. The protons *Hm* and *Hn* display a doublet at δ=4.240-4.247 ppm overlapping with the chemical shift of H_c.

In the ^{13}C NMR spectrum of **68** the C-12 carbon atoms appear at δ=13.04 ppm, and C-9 and C-9´ display two different signals at δ=25.3 and 26.6 ppm, respectively. The C-11 carbon atoms from the ethyl group appear at δ=45.16 ppm. Unlike in **27**, the C-6 carbon is deshielded and shows a paramagnetic shift at δ=66.7 ppm compared to C-5 appearing at δ=66.8 ppm. The C-4 carbon atom appears at δ=74.8 ppm and C-7 is highly deshielded and is registered at δ=85 ppm. The quaternary carbon C-2 appears at δ=109 ppm in a normal range similar to compound **27**.

The mass spectrum of **68** shows a 2 % peak at *m/z*=216 corresponding to the loss of hydrogen radical from the molecular ion $[M]^+$ and a 5 % peak at *m/z*=202 by the loss of methyl radical from $[M]^+$ ion. A 2 % peak at *m/z*=188 is attributed to the loss of ethyl radical. A 5 % peak at *m/z*=145 attributed to the loss of second NEt_2 radical from $[M]^+$ ion and a 10 % peak at *m/z*=102 is attributed to diethylaminomethoxy cation. The base peak is observed at *m/z*=86 for the diethylaminomethyl carbocation. The IR spectrum is similar to those of compounds **65** and **67** (see Experimental Section also)

11.5: Fuel aadditive experiments with compounds 65, 67 and 68

It is known from the literature that compounds like 2-ethylhexyl nitrate (EHN) which contain polarized bonds are used as cetane enhancers.[70] Certainly it is not possible to use glycerol nitrates as cetane enhancers. Instead, alkoxy methyl amine derivatives of glycerol were chosen to be used as fuel additives, due to the well known reason that these compounds exist in a polarized state ($RO^{\delta-}$-CH_2-$N^{\delta+}R^1R^2$).[201, 202] It is also known[70] that a higher cetane number correlates with lower NO*x* emissions (Chapter 3.6.1-3.6.3). This makes *psudo-bases* interesting as additives. Since alkoxy methyl amines contain both oxygen and nitrogen atoms in one molecule it was expected to use them as oxygenates and nitrogenates. It also provides an opportunity to study the effect of protected amines (secondary amines in this case) in the reduction of NO*x* emissions.

11.5.1: Tests conducted in diesel engines

When compound **65** was tested as an additive in the diesel engine as a 1:1 mixture of **65** and **66** blended to the diesel fuel, an unusual bumping sound of the engine was observed and the experiments were terminated. We assume that the peculiar engine behavior could be due to the presence of low boiling **66** in the mixture. The tests were however, successfully performed with a small amount of **65** added in pure state to both diesel and biodiesel fuels (Chapter 11.5.1, 11.5.2). Compound **68** was successfully tested as a 5 % blend in the diesel fuel, and the results are disclosed below (Fig. 49a-d).

It is interesting to observe a 3.3 % increase in NO*x* emissions by the addition of 5 wt % of the nitrogen containing additive. It shows that the presumption of nitrogen containing additives increases fuel NO*x* emissions may not be true in case of compound **68**, due to a very small difference (0.106 g/Kwh) between NO*x* emissions from pure diesel fuel and 5 wt % additive **(68)** containing diesel fuel, which must be theoretically very high if all the additive participates in NO formation (fuel NO*x*) instead of reduction. It can be presumed that not all of the additive could have undergone thermal-stripping. However, a part of the additive that had undergone thermal stripping would have been oxidized to NO (in ideal conditions up to 40 %)[129e] and a part of it has participated in NO reduction. The total increase in NO*x* shows the difference in excess NO formed from the additive and the amount that was reduced by the additive. Eventually, the reducing ability of a tertiary amine is much lower compared to primary or secondary amines and also its resistance to form NO.

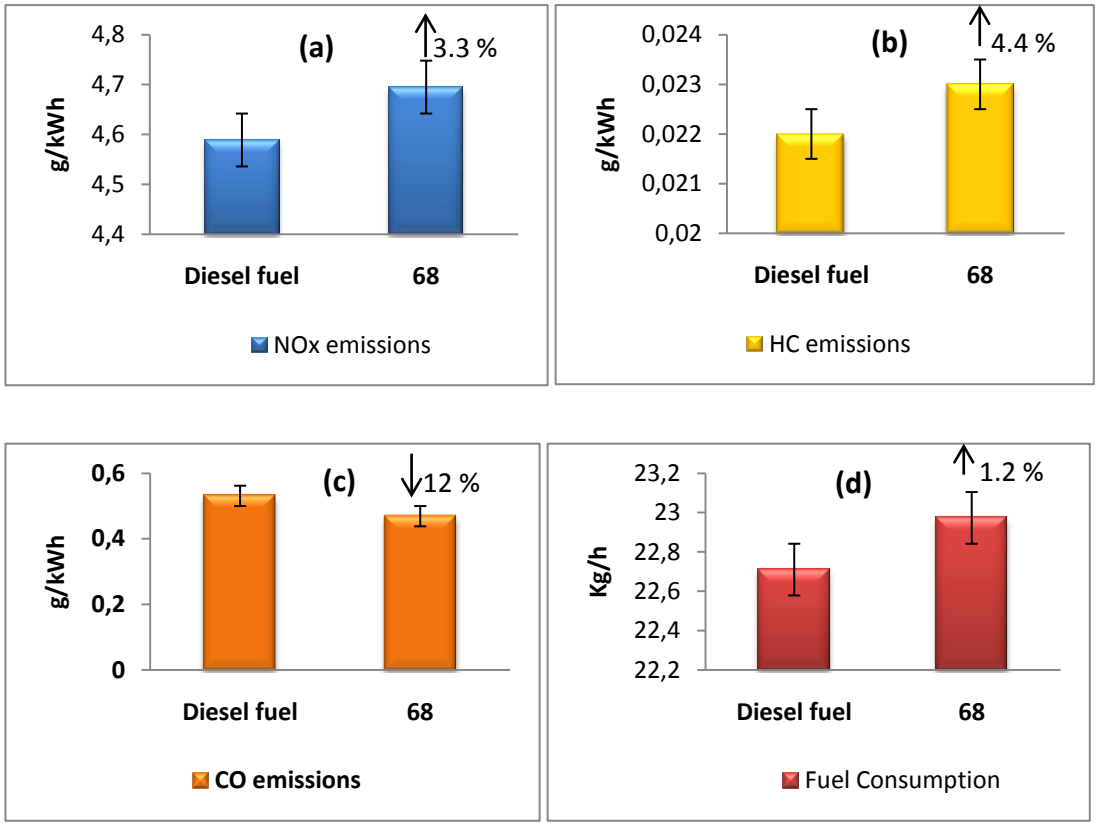

Fig. 49: a) NO*x* emissions, **b)** Hydrocarbon (HC) emissions, **c)** Carbon monoxide (CO) emissions from the diesel engine with 5 wt % of **68** blended in the diesel fuel. **d)** Fuel consumption of the diesel engine. Measurements performed at Institute of Agricultural Technology and Biosystems Engineering (vTI) (Engine type: Mercedes OMD 906, EURO III).

As expected, compound **68** showed a good performance as oxygenate with a 12 % reduction in CO emissions. Unfortunately, a 4.4 % increase in the HC emissions and a 1.2 % fuel penalty were observed. The cause for the increase in HC emissions is not known. However, the increase is also an advantage since it promotes an efficient use as additive in vehicles mounted with DeNO*x* catalyst; it could thus indirectly reduce the fuel penalty (Chapter 5.2.5.2.1).

11.5.2: Tests conducted in AFIDA combustion chamber (additive in diesel fuel)

The AFIDA combustion chamber theoretically represents a stationary diesel engine without a piston. Thus, it provides a much simple combustion process without turbulences caused by the moving piston. The idea of using a combustion chamber was that the tests could be conducted with smaller amounts of the additive (up to 2-6 g) compared to 2-6 L in a diesel

engine. It provides an almost equivalent environment as the diesel engine or any experiments conducted in a quartz tube or a steel cylinder in the literature.[126, 129e] Finally we wanted to test whether the nitrogen containing additives undergo thermal stripping processes and participate in the reduction of NO. Secondly the laboratory synthesis of some of the compounds on a liter scale was not practical. All three compounds **65**, **67**, and **68** were tested for NO*x* emissions (Chapter 7.3) with 2 % (2 g) additive in 100 mL diesel fuel (w/v). The results are described in Fig. 50 and Table 11.

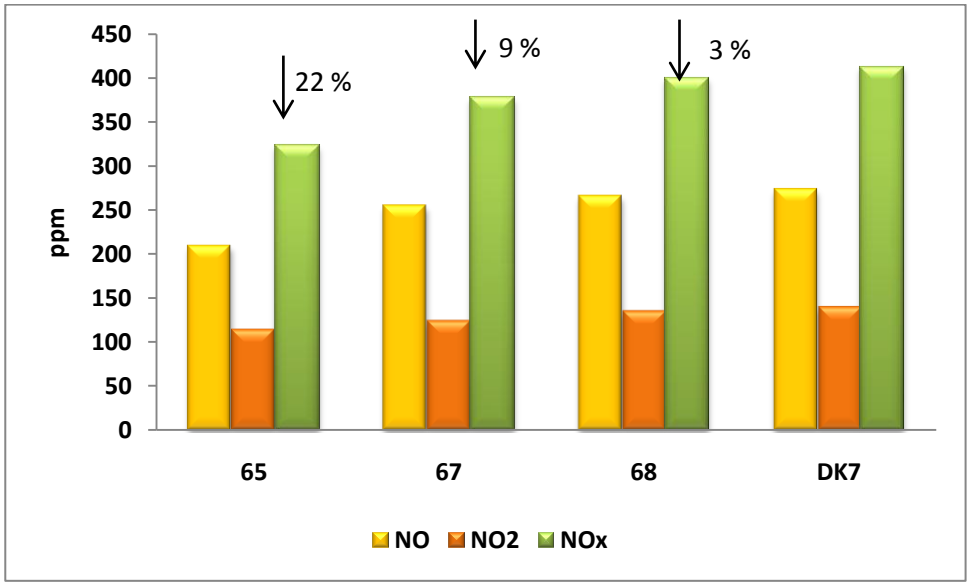

Fig. 50: NO, NO_2 and NO*x* emissions with 2 % of **65**, **67** and **68** as additives in diesel fuel (tests conducted in an AFIDA combustion chamber at ASG Analytic GmbH).

The assumption that nitrogen containing additives would reduce NO*x* emissions from diesel engines is clearly proven from the raising staircase of the graph starting from **65** to **68** in which DK-7 was used as a reference fuel.

2 % of additive in diesel fuel (DK 7)	% reduction in NO*x* emissions
65	22
67	9
68	3

Table 11: NO*x* reduction from diesel fuel compared with the reference fuel DK-7 (neat) (test results from AFIDA combustion chamber (ASG Analytic GmbH).

As expected, **65** which is a tris-substituted nitrogen containing compound shows almost 22 % reduction in NO*x* emissions in diesel fuel whereas **67** with its di-substitution and **68** with a

mono-substitution pattern show a lower reduction of 8.5 % and 3.2 %, respectively. The above results allow us to conclude that a substantial reduction in NO*x* emission from diesel fuel can be achieved by the nitrogen containing additives using SNCR.

11.5.3: Tests conducted in AFIDA combustion chamber (additive in biodiesel fuel)

Compound **65** and **68** were tested as additives in biodiesel fuel (RME) for the effect of NO*x* reduction; results are given in Fig 51

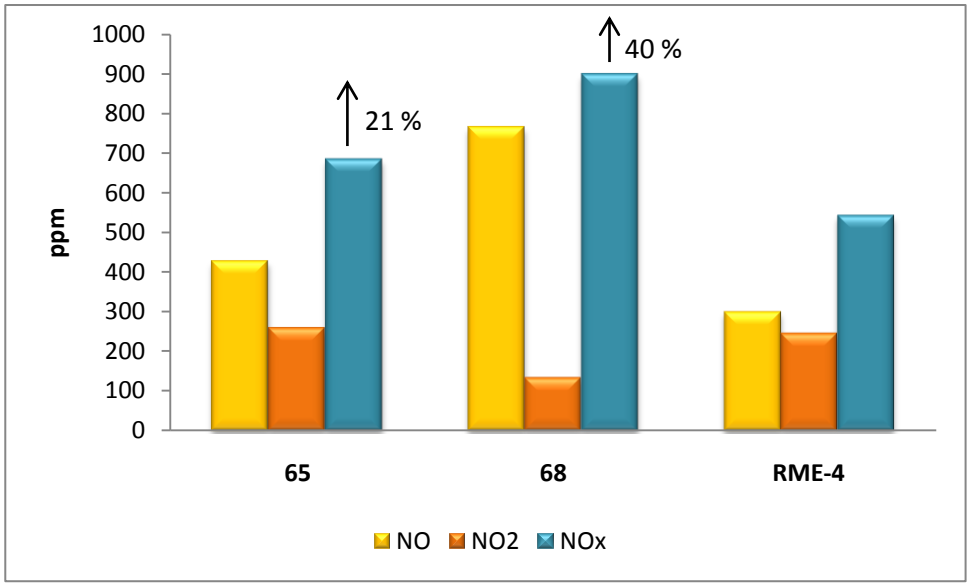

Fig. 51: NO, NO_2 and NO*x* emissions from diesel engine with 2 % of **65** and **68** as additive in biodiesel (tests conducted in an AFIDA combustion chamber at ASG Analytic GmbH).

When added as an additive to RME the compounds **65** and **68** showed about 21 % and 40 % *increase* in the NO*x* emissions. It is presently not clear to provide a concrete explanation for this increase whereas the same compounds show a decrease in NO*x* emissions from diesel fuel (see above). It could be postulated that the biodiesel might be involved in the increase in concentration of oxygen atoms in the combustion zone. It is clearly shown by Feber *et al*[129c] and Finamore *et al*[129e] that the presence of OH radicals or oxygen atoms in excess above the thermodynamic equilibrium in the combustion zone may cause the oxidation of nitrogen containing additive leading to an increase in NO*x* emissions. Possibly, such an environment is created by biodiesel due to its oxygen content (see also Chapter 6.2.1). However, the difference in the NO*x* emissions by compound **65** (22 %) and compound **68** (40 %) could be explained as the limitation of OH radicals and O atoms towards the oxidation of additive, certainly due to the competition between the additive and the carbon content of the fuel

towards the oxygen atoms. It provides a clue, which was also observed by Johnson *et al*[127g] that when ammonia is added as an additive in to the combustion zone. It was also observed by Finamore *et al*[129e] in NH_3/O_2 flames that the addition of NH_3 in near stoichiometric amounts causes an increase in NO*x* emissions. This might be because, as explained by Finamore[129e] almost half of the ammonia (in our case $NH_{i=0,1,2}$ ions from additive after thermal stripping) decomposes forming intermediate NO (in NH_3/O_2 flames) and only 82 % of the injected ammonia was consumed. In other words we assume that only 82 % of compound **65** or **68** participated in the thermal stripping process from which about 50 % was converted to NO. Thus, when injected in near stoichiometric amounts (generally referred to the amount of NO formed in the absence of an additive), there would be no left over ammonia to reduce the additional NO formed from the amine. In our case compound **65** has more amine packed in it than compound **68**, thus more $NH_{i=0,1,2}$ ions are produced. Therefore, there is a greater chance that a sufficient number of $NH_{i=0,1,2}$ ions survive the oxidation process in case of **65** than **68**. A similar phenomenon was observed when the additive was added to diesel fuel. Compound **65** with a higher nitrogen content showed more reduction compared to **67** and **68**, assuming that all three compounds participated equally in thermal stripping and produced $NH_{i=0}$ ions accordingly in 1:2:3 ratio. However, when added in 2 wt % the ratio of nitrogen content differs in **65**, **67** and **68** 1:1.5:2; hence, the ratio of their participation is different in reduction or oxidation.

11.5: Conclusion

The assumption that amines when used as additives reduce NO*x* emissions was shown to be correct for diesel fuel and thus SNCR. However, added to biodiesel they show a reversed effect. This raises the question of the effect of the oxygen content of the fuel and the way it affects the reducing nature of the additive. To study this effect the nitrogen is introduced in a reduced state *i.e.* instead of tertiary amine a secondary amine is introduced as a replacement. To answer this question it was decided to synthesize *N,O*-aminals which are very similar to the above compounds. They, however, possess a more strongly reduced nitrogen atom.

Chapter 12: Synthesis of *N,O*-aminals 76 and 79

12.1: Introduction

The synthesis of *N,O*-acetals using primary amines is more difficult than using secondary amines, because the product that is formed initially in the condensation of formaldehyde and the primary amine can undergo a series of transformations under participation of the remaining N-H bonds leading to a complex product mixture. The nature of it mainly depends on reaction conditions such as the amine/formaldehyde ratio, temperature and pH of the reaction mixture. In order to overcome these difficulties many synthetic equivalents have been proposed (Fig. 52) in the literature[204, 205] which can undergo elimination of the group B to afford the reactive methyl amines or their protonated forms in situ. These are capable of being used in a formal Mannich reaction.

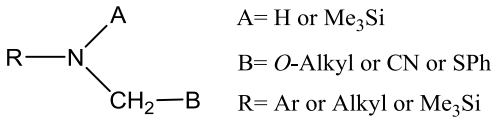

Fig. 52: General representation of synthetic equivalents for methylenamines

The synthesis of *N,O*-acetals starting from an alcohol and a primary amine using any alkyl or aryl aldehyde is seldom reported in the literature. The basic difficulty is in the reproducibility of the reaction, stability, and also the difficulty in purification of the products. Campos *et al*.[206] have reported the synthesis of *N*-alkoxymethylarylamines **(70)** using an arylamine, paraformaldehyde **(63)** and sodiummethoxide in methanol (Scheme 38) to obtain product **70** almost quantatively.

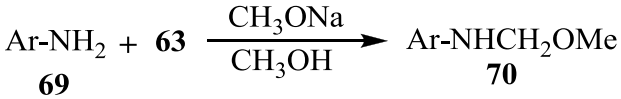

Scheme 38: General synthesis of *N*-alkoxymethylarylamines **(70)** according to Campos *et al*.[206]

In general the condensation of primary amines with formaldehyde must be performed under carefully controlled reaction conditions in order to avoid side and secondary reactions. According to Campos *et al*.[206] *N*-alkoxymethylarylamines **(70)** are highly instable compounds which are prone to decomposition at room temperature in a short period of time. They also acknowledged the impossibility of purifying the compounds by column

chromatography using acidic, basic or neutral absorbents. Attempts to synthesize *N*-alkoxymethylalkylamines using the above procedure were not successful,[206] which in all instances lead to the formation of the corresponding alkylperhydrotriazines. This was also observed by us in an attempt to synthesize *N*-(2,2-dimethyl-1,3-dioxylane-4-methoxymethyl) butylamine **(72)** using *n*-butylamine **(71)**, paraformaldehyde **(63)** and **26**, in the presence of K_2CO_3. In all instances butylperhydrotriazine **(73)** was obtained exclusively (Scheme 39), and it was observed that the nature of the alcohol **(2**, **14** or **26)** does not play a role in the trimerisation of primary amines.

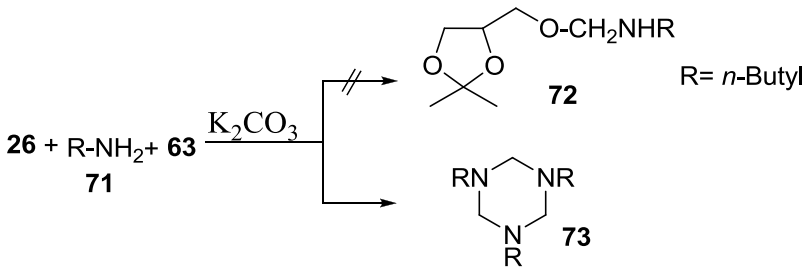

Scheme 39: Attempted synthesis of *N*-(2,2-dimethyl-1,3-dioxylane-4-methoxymethyl) butylamine **(72)**

12.2: Preparation of *N*-(2,2-dimethyl-1,3-dioxylane-4-methoxymethyl) aniline (76)

An attempt was made to prepare **76** under the conditions reported by Campos *et al*.[206] The sodium salt of solketal **(74)** was prepared using **26** and an equimolar amount of metallic sodium. Once the evolution of hydrogen has ceased, aniline **(75)** and **63** were added and the mixture stirred for 4 h at room temperature. The resulting product mixture was poured onto ice and extracted with diethylether. The solvent was evaporated under reduced pressure taking care that the temperature remained below 20 ^{o}C to obtain a quantative amount of a thick orange colored oil (Scheme 40). An immediate NMR spectroscopic analysis of the oil displayed a plausible spectrum that could be assigned to compound **76**. However, due to the very sensitive nature of the compound which within an hour decomposed into a white solid at room temperature, further structural conformation could not be acquired.

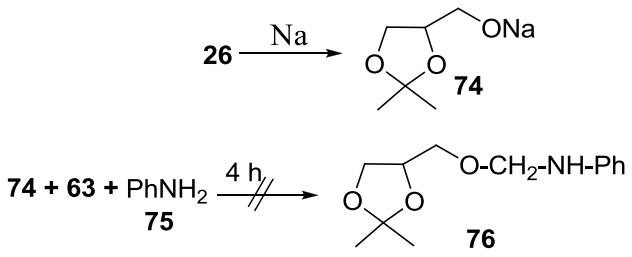

Scheme 40: Attempted preparation of **76**

Eventually, a similar reaction was performed using **26**, **63** and **75** in the presence of K_2CO_3, resulted in 1,3,5-trisphenylperhydro-1,3,5-triazine **(77)** quantitatively, the starting material **26** was extracted unchanged after the reaction (Scheme 41).

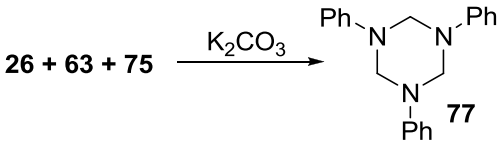

Scheme 41: Preparation of 1,3,5-trisphenylperhydro-1,3,5-triazine **(77)**

Compounds **73**, and **77** are well known and have been characterized in the literature.[204-206] The analytical data (^{1}H NMR, mass and IR spectrum) were compared and are in good agreement with those reported in the literature (see Experimental Section).

12.3: Synthesis of 1,2,3-tris-(*N*-butyl-*N*-methoxy) propane (79)

It is known from the literature that *N*-alkoxymethylalkylamines are less stable than *N*-alkoxymethylarylamines. This could be due to the enhanced nitrogen basicity of the alkyl amines compared to aromatic amines. Any method that was used to produce *N*-alkoxymethylalkylamines in the literature[170] using any alkyl amine and **63** in the presence of variety of alcohols and their sodium or lithium salts afforded 1,3,5-trisalkylperhydro-1,3,5-triazine. Therefore, it was decided to approach this problem by adopting a linear synthesis, for which the corresponding alcohol was chloromethylated using formaldehyde and dry HCl prior to the reaction with alkyl amine.

Glycerol **(2)** was chloromethylated using the Wedekind method by passing dry HCl into a solution of glycerol **(2)** and **63** in dichloromethane (Scheme 42). After 2 h of stirring the product mixture was distilled twice at 160 ^{o}C, 34-40 mbar to obtain 14 % of **78**.

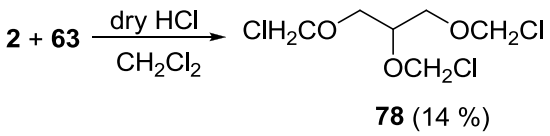

Scheme 42: Preparation of 1,2,3-tris-(chloromethoxy)propane **(78)**

Compound **78** has often been mentioned in the literature[207, 208] but was never completely characterized due to its highly hygroscopic nature. The only known parameter from the literature to characterize **78** is its boiling point which agrees with the boiling point mentioned above. Extreme care was taken to keep **78** away from moisture and it was used immediately after distillation.

When **78** was reacted with butylamine **(71)** a mixture of unidentified products was obtained (Scheme 43). Similar results were observed by Shono *et al.*[207] in an attempt to obtain α-methoxy-*N*,*N* dimethyl aniline **(81)** using *N*-methylaniline **(80)** and chloromethylmethyl ether in the presence of sodium hydride which resulted in the formation of 1,1-bis-(*N*-methylanaline) methane **(82)** (Scheme 44).

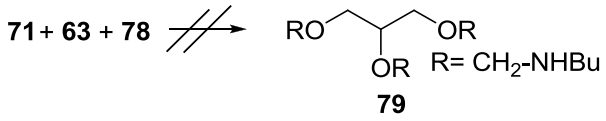

Scheme 43: Attempted preparation of 1,2,3-tris-(*N*-butyl-*N*-methoxy)propane **(79)**

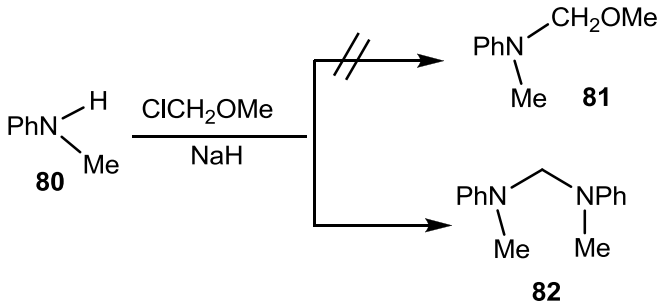

Scheme 44: Attempted preparation of α-methoxy-*N*,*N* dimethyl aniline **(81)** according to Shono[207]

However, to overcome the above problem it was decided to prepare the sodium salt of butylamine **(71)** and react it further with **78**. The sodium salt **83** was prepared by stirring sodamide ($NaNH_2$) with excess of butyl amine **(71)** in THF (Scheme 45). Once the evolution of gas had ceased the solvent and excess butylamine **(71)** were evaporated to obtain **83** as a white amorphous powder in quantitative yield.

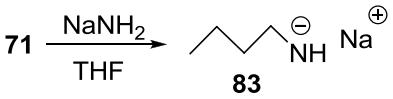

Scheme 45: Preparation of the sodium salt of butylamine **(83)**

The thus obtained **83** was suspended in THF. The suspention was cooled in an ice bath and freshly distilled **78** was added dropwise during a period of 30 min. After 4 h of stirring the product mixture was filtered and the THF was evaporated under vacuum taking care that the temperature remained below 20 ^{o}C to obtain a viscous yellowish oil in quantative yield (Scheme 46). Unfortunately, upon spectral analysis it was found that the obtained yellow oil was not the desired product **79**.

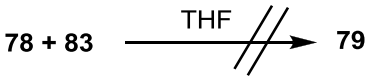

Scheme 46: Attempted preparation of 1,2,3-tris(*N*-butyl-*N*-methoxy) propane **(79)**

Chapter 13: Carbamates (85-88)

13.1: Introduction

There are numerous routes to organic carbamates. Some of the commonly used methods are a) alcoholysis of carbamoyl chlorides,[209, 210] b) aminolysis of chloroformates,[211] c) transamidation,[212] d) oxidative amination of carbon monoxide,[213] e) reductive carbonylation of organic nitro compounds,[214] f) reaction of urea with alcohol in the presence of heavy metals,[215, 216] g) reaction of carbondioxide with ammonia,[217, 218] and h) reaction of alcohols with isocyanates.

Reaction of isocynates with alcohols is the most widely used reaction in polymer industry to synthesize polyurethanes. The reaction of alcohols with alkyl or aryl isocyanates to produce carbamates is generally catalysed either by basic catalysts like triethylamine[219] and pyridine[220] or by Lewis acid catalysts[221] such as zinc chloride and stannous chloride.

13.2: Preparation of (2,2-dimethyl-1,3-dioxolane)-4-methoxy-*N*-ethylcarbamate (85)

Surprisingly compound **85** is seldom found in the literature. It was first synthesised by Len *et al*.[222] in 1998 using ethyl isocyanate **(84)** and **26** in the presence of triethylamine as a catalyst to obtain **85** in 54 % yield (Scheme 49).

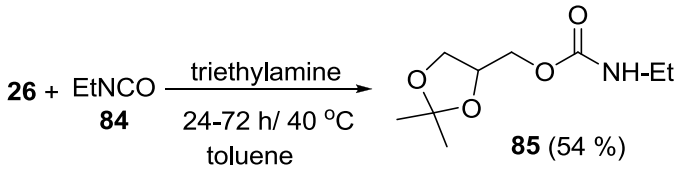

Scheme 49: Synthesis of (2,2-dimethyl-1,3-dioxolane)-4-methoxy-*N*-ethylcarbamate **(85)** by Len.[222]

A similar reaction was performed by us using **84** and **26** in the presence of triethylamine as a catalyst in dichloromethane. After 20 h of stirring at room temperature and upon purification by column chromatography using diethyl ether, compound **85** was obtained as analytically pure viscous colorless oil in 50 % yield (for characterisation see Chapter 13.5).

13.3: Preparation of 3-*tert*-butoxy-propyl-2-ol-1-*N*-ethylcarbamate (86) and 3-*tert*-butoxy-propyl-1,2-bis-(*N*-ethylcarbamate) (87)

The reaction of **14** with **84** produced a product mixture of **86** and **87**. In order to optimize the ratio of **86** and **87**, different catalysts were tested (Table 12). It was observed that basic

catalysts like trimethyl amine and pyridine favor the formation of **86.** When trimethyl amine was used as catalyst it was observed by careful monitoring of the reaction that compound **14** had completely reacted in 18 h to **86**. Even after continuation of the reaction for 72 h, no traces of **87** were observed. Variation of temperature and molar ratio of the reactants showed no effect on the product distribution. In the presence of Lewis acid catalysts like $ZnCl_2$ the product distribution was shifted more towards **87**. It was observed that under both acidic and basic catalytic conditions, **86** was formed first which upon continuation of the reaction produced **87** depending on the strength of the catalyst.

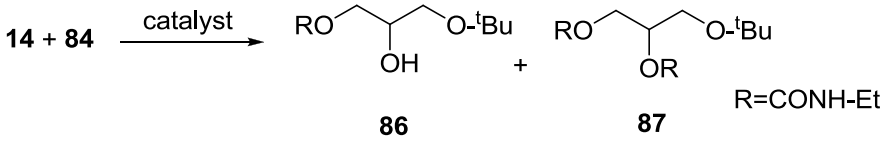

Scheme 50: Preparation of **86** and **87**

Compound **86** and **87** were separated by column chromatography using diethyl ether as eluent (R_f=0.48 and 0.56). Compound **86** was a viscous colorless oil, and **87** was a solid melting at 92 ^oC (for characterisation see Chapter 13.5).

However, it was observed that none of the catalysts provided a complete conversion of **14** into **87**. This could be due to the difference in order of reactivity of primary, secondary and tertiary alcohols towards alkyl isocyanates. Davis *et al*.[223] have shown that the reactivity of primary, secondary and tertiary alcohols towards phenyl isocyanate is in the order of 1, 0.3 and 0.003, respectively. Usually, alkyl isocyanates are less reactive than aryl isocyanates which supports the above observation.

Catalyst (wt %)	temperature (^oC)	time, h	**86** (%)	**87** (%)
Triethylamine (2)	20	12-18	96	0
Pyridine (6.7)	20	120	47	35
$ZnCl_2$ (6.7)	20	12-18	33 %	52 %
$ZnCl_2$ (26.8)	50	48	20 %	64 %

Table 12: Product distribution of **86** and **87** in the presence of different catalysts

Secondly, the steric hindrance caused by the *tert*-butyl group could also be a reason for the lower yields of **87**. This conclusion was drawn from the reaction of glycerol **(2)** with **84** (see below).

13.4: Preparation of propane-1,2,3-tris-(*N*-ethylcarbamate) (88)

Compound **88** was synthesised using glycerol **(2)** and **84** in the presence of triethylamine in benzene. After 72 h of stirring at room temperature the reaction mixture turned cloudy; it was filtered to collect **88** as a white solid (37 %) melting at 102 ^{o}C. Evaporation of the solvent from the filtrate provided a viscous liquid (44 %) which by NMR analysis was found to be a mixture of different glycerol carbamates. Eventually, compound **88** was produced quantatively, when a similar reaction was performed in the presence of 20 wt % $ZnCl_2$ (Scheme 51) as the catalyst.

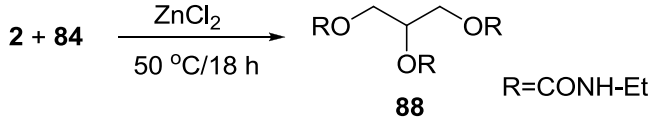

Scheme 51: Preparation of propane-1,2,3-tris-(*N*-ethylcarbamate) **(88)**

13.5: Characterisation of compounds 85 to 88

The barrier of rotation around C-N bond in amides has been studied by many researchers. By analogy, carbamates also exhibit a similar N-C=O planar framework. However, the additional oxygen atom of the carbamate functionality exerts a unique steric and electronic perturbation; one of the oxygen lone pair is able to donate electrons into the carbonyl π system and thereby partially compensates for the loss of π-interaction with the nitrogen lone pair, during the C-N bond rotation. One of the consequences of this difference is that the barrier of rotation in carbamates is usually 3-4 kcal/mol lower than those in the corresponding amides.[224, 225, 226] Cox *et al*.[224] have recently shown that the free energy barrier $\Delta G^{\ddagger}$ in a number of carbamates is almost independent of the solvent, showing a slight increase of 0.3 kcal/mol on going from the least to the most polar environment. Thus, by analogy the above literature evidence hints that compounds **85-88** should exhibit free rotation around the C-N bond at room temperature.

The ^{1}H NMR spectrum of the (2,2-dimethyl-1,3-dioxolane)-4-methoxy-*N*-ethylcarbamate **(85)** recorded at 200 MHz in $CDCl_3$ at room temperature is in agreement with the spectra of similar compounds reported in the literature.[227]

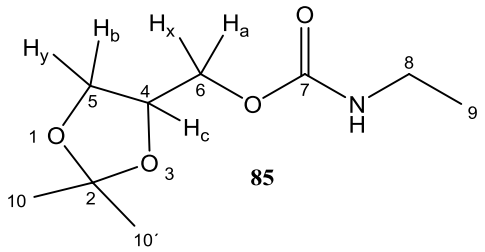

85

The C-9 methyl group protons display a clear triplet at δ=1.10-1.17 ppm with $^{3}J_{8,9}$ of 7.25 Hz. This multiplet is followed by the C-10 and C-10´ protons which shows two signals at δ=1.37 and 1.44 ppm in a general range observed in most of the 2,2-dimethyl-1,3-dioxolane ring systems. The C-8 protons appear as a broad multiplet at δ=3.15-3.28 ppm since these peaks are sharpened upon deuterium exchange of the N-H proton. The methylene proton H_a and H_x at C-6 display multiplets at δ=3.54-3.83 ppm. The ring proton H_b and H_y and *Hc* display a pattern of multiplets at δ=4.01-4.34 ppm. The N-H proton appears as a broad singlet at 4.9 ppm which disappears upon deuterium exchange.

In the ^{13}C NMR spectrum of **85** C-9 appears at δ=14.8 ppm followed by C-10 and C-10´ at δ=25.0 and 26.4 ppm, respectively. The C-8 carbon atom from the ethyl group appears at δ=35.6 ppm. The C-6 carbon appears upfield compared to the other ring carbons at δ=64.8 ppm. The C-5 carbon atom appears at δ=66.0 ppm and C-4 is seen at δ=73.8 ppm followed by the C-2 at 109.4 ppm. The carbonyl carbon atom C-7 resonates at δ=155.8 ppm.

The mass spectral analysis of carbamates were investigated by Lewis[231] who also generalized the fragmentation pattern in aliphatic and aromatic *N*-substituted carbamates. Mass spectral analysis of **85** is based on the fragmentation patterns described by Lewis *et al*.[231] Compound **85** shows a base peak at *m/z*=188 corresponding to the loss of CH_3 from $[M]^+$ followed by a 10 % peak at *m/z*=144 attributed to the loss of $[CH_2NH]^{+\cdot}$ from the base peak. A 80 % peak at *m/z*= 101 is attributed to the loss of methoxy radical. A 50 % peak at *m/z*=72 corresponds to the $[EtNHCO]^+$ ion, followed by a 57 % peak at *m/z*=57 attributed to the loss of CH_3 from *m/z*=72, finally 40 % peak at *m/z*=44 is attributed to the $[EtNH]^+$ ion.

The ^{1}H NMR spectrum of 3-*tert*-butoxy-propyl-2-ol-1-*N*-ethylcarbamate **(86)** displays a complex spectrum with broadened signals. The C-6 methyl group protons display a clear triplet at δ=1.10-1.18 ppm with a coupling constant of 7.24 Hz, followed by the protons of the C-8 *tert*-butyl group which appear as a singlet at δ=1.10 ppm. The C-5 protons display a

broad multiplet at δ=3.16 to 3.27 ppm (the peaks are sharpened upon deuterium exchange of N-H and O-H protons).

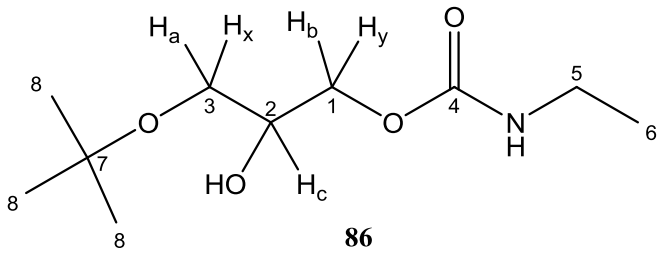

86

We assume that the H_b ad H_y protons show an upfield shift and appear as the multiplet at δ=3.32 to 3.46 ppm due to the anisotropic effect of the carbamate group, followed by H_c which appears as a multiplet at δ=3.85 to 3.95 ppm. The H_a ad H_x protons display a downfield shift and appear at δ=4.04 to 4.22 ppm as a broad multiplet. The N-H proton is observed as a broad singlet at δ=4.79 ppm and the O-H proton at δ=2.39 ppm.

In the ^{13}C NMR spectrum of **86** the carbon atom C-6 appears at δ=15.7 ppm followed by the C-8 carbon atoms at δ=27.9 ppm; C-5 appears at δ=36.4 ppm. The C-1 carbon atom shows an upfield shift and resonates at δ=63.0 ppm, and C-2 at δ=66.8 ppm. The C-3 carbon is seen at δ=70.1 ppm followed by C-7 at 73.9 ppm; the carbonyl carbon C-4 appears at δ=156.6 ppm.

The mass spectrum of **86** is explained on the basis of the fragmentation pattern suggested by Lewis.[231] It shows a 50 % peak at *m/z*=146 caused by the loss of $[CONH\text{-}Et]^+$ from $[M]^+$, and a 70 % peak at *m/z*=132 loss of isobutene and a methoxy radical. The base peak is observed at *m/z*=90 by the loss of isobutene fragment from *m/z*=146.

The ^{1}H NMR spectrum of the 3-*tert*-butoxy-propyl-1,2-bis(*N*-ethylcarbamate) **(87)** displays a complex spectrum with broad signals. The methyl group protons of C-6 and C-6´ display a multiplet at δ=1.14-1.27 ppm overlapping with the C-8 *tert*-butyl group protons appearing at a similar chemical shift. The protons at C-5 and C-5´ show a broad multiplet at δ=3.2 to 3.33 ppm.

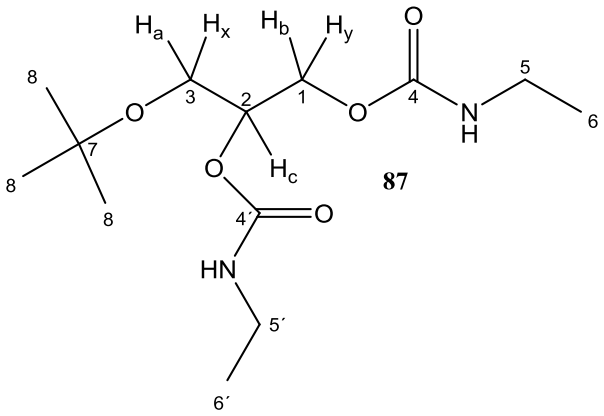

87

Similar to compound **86**, the H_b and H_y protons show an upfield shift and appear as multiplets at δ=3.51 to 3.55 ppm due to the anisotropic effect of the carbamate group. These signals are followed by the H_c protons which appear as multiplet at δ=4.08 to 4.13 ppm. The H_a and H_x protons display a downfield shift and appear at δ=4.26 to 4.31 ppm as broad multiplets. The N-H proton appear as a broad singlet at δ=4.78 ppm. Other than the N-H protons all protons in **87** show a downfield shift compared to the analogous protons in compound **86**.

In the ^{13}C NMR spectrum of **87** the C-6 and C-6´ appears at δ=15.17 ppm followed by the C-8 carbons at δ=27.2 ppm. The C-5 and C-5´ carbon atoms appears at δ=35.7 ppm. The C-1 carbon atom is characterized by an upfield shift and appears at δ=60.5 ppm. The C-2 carbon atom appears at δ=63.8 ppm an shifted upfield compared to the similar carbon atom in **86**. The C-3 carbon is seen at δ=67.4 ppm followed by C-7 at 73.2 ppm; the carbonyl carbons C-4 and C-4´ appear at δ=155.7 and δ=156.1 ppm, respectively.

The mass spectrum of **87** is explained on the basis of the fragmentation patterns proposed by Lewis.[231] It shows a 20 % peak at *m/z*=217 caused by the loss of $[CONH\text{-}Et]^+$ from $[M]^+$, the base peak is observed at *m/z*=132. A 50 % peak at *m/z*=72 corresponds to the $[EtNHCO]^+$ ion, followed by a 57 % peak at *m/z*=57 attributed to the loss of CH_3 from *m/z*=72, and a 40 % peak at *m/z*=44 attributed to $[EtNH]^+$.

The ^{1}H NMR spectrum of the propane-1,2,3-tris-(*N*-ethylcarbamate) **(88)** is complex with broad signals. The C-6 protons display a triplet at δ=1.10 to 1.13 ppm with a coupling constant of 7.25 Hz overlapping with the C-6´ methyl group protons appearing as shoulders at δ=1.11 to 1.14 ppm with a coupling constant of 7.24 Hz. The C-5 and C-5´ protons display a broad multiplet at δ=3.15 to 3.23 ppm. The H_b, H_y and H_a, H_x protons appear as a broad singlets at δ=4.18 ppm, followed by the H_c and N-H protons registered as broad singlets at δ=5.124 ppm.

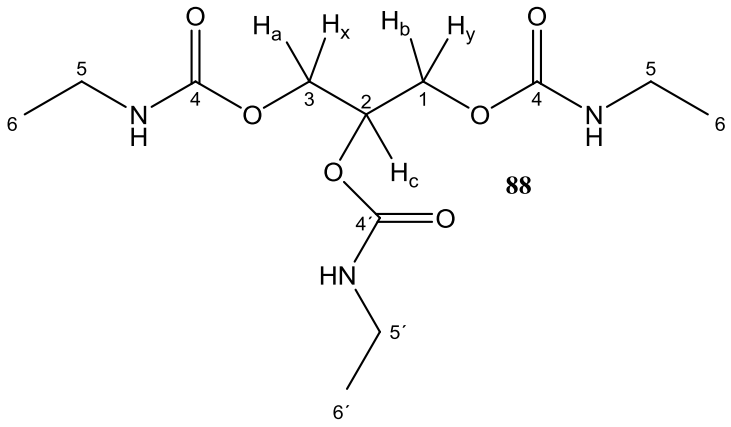

In the ^{13}C NMR spectrum of **88** C-6 appears at δ=14.92 ppm and C-6´ at δ=14.95 ppm. The C-5 carbon atom appears at δ=35.8 ppm. The C-1 and the C-3 carbon atoms appear at δ=62.9 ppm. The C-2 carbon resonates at δ=70.1 ppm, and the carbonyl carbon atoms C-4 and C-4´ appear at δ=155.4 and δ=155.9 ppm, respectively.

The mass spectrum (EI) of **88** shows a base peak at *m/z*=328 ($[M]^+$+Na) followed by a 50 % peak at *m/z*=217 by the loss of $[EtNHCOO]^+$ from the $[M]^+$ ion. A 10 % peak at *m/z*=146 corresponds to the loss of $[EtNHCOO]^+$ ion from *m/z*=217.

The IR spectra[228-230] of compounds **85-88** recorded neat displayed the following major peaks (Table 13)

	85 ($\tilde{\nu}$, cm^{-1})	**86** ($\tilde{\nu}$, cm^{-1})	**87** ($\tilde{\nu}$, cm^{-1})	**88** ($\tilde{\nu}$, cm^{-1})
N-H *str. vib*	3345	3332	3332	3331
CH_3 (*asym*)	2984	2974	2975	2975
CH_3 (*sym*)	2938	2936	2936	2939
CH_2 (*sym*)	2883	2877	2879	2878
amide-I	1710	1695	1691	1691
amide–II	1530	1535	1532	1534
amide-III	1241	1251	1247	1250
C-O *str. vib.*	1215	1194	1192	---
C-N *str. vib.*	1155	1148	1150	1148
O-H *str. vib.*	---	3332	---	---
O-H *bend. vib.*	---	1081	---	---

Table 13: IR specral data of compounds **85-88**

13.6: Fuel additive experiments with compounds 85-87

It was decided to synthesize glycerol carbamates as additives since carbamates show a chemical resemblance to urea or urea derivatives. The assumption that carbamates can reduce NO*x* emissions was based on the experiments performed by Perry *et al*.[232] who have shown the cyanuric acid reduces NO*x* emissions in the exhaust of a single cylinder diesel engine by 99 % at about 300 ^{o}C. The method was called RAPRENO*x* (rapid reduction of NO*x*). By analogy, it was assumed that carbamates which resemble urea or cyanuric acid should be able to reduce NO*x* emissions at lower temperatures when used as additives. Similarly, a 83 % reduction in NO was reported by Leon *et al*[126] upon the addition of NH_3 in presence of CO and O_2 at 800 ^{o}C.

13.6.1: Tests conducted in AFIDA combustion chamber (additive in biodiesel fuel)

The compounds **85-87** were not soluble in diesel fuel whereas compound **88** was insoluble in both diesel and biodiesel fuels. Therefore, **85** and **86** were tested as additives in biodiesel fuel and compound **87** was dissolved at 60 ^{o}C in biodiesel. All three compounds were tested as additives to reduce NO*x* emissions in biodiesel fuel. The results are presented in Fig. 53.

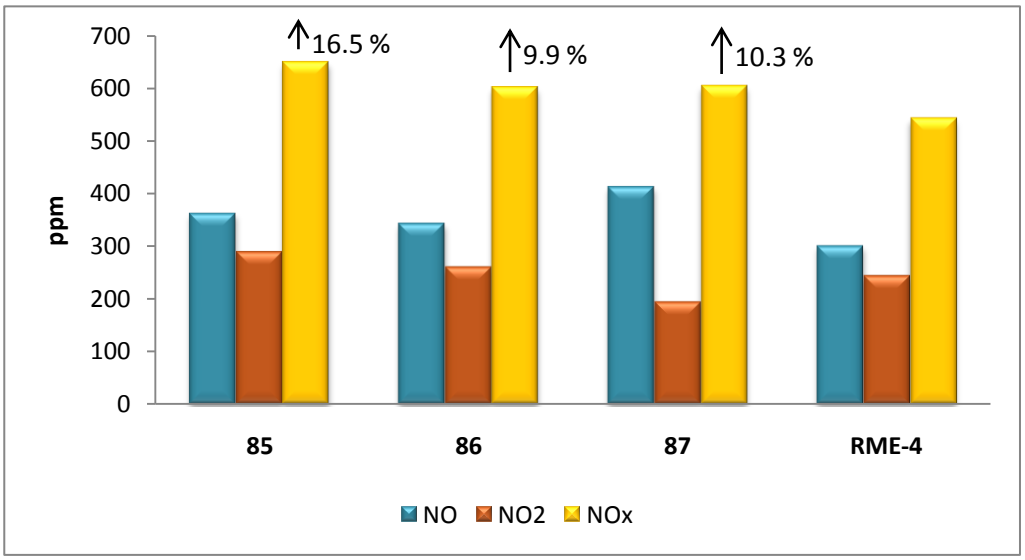

Fig. 53: NO, NO_2 and NO*x* emissions from diesel engine with 2 % (w/v) of **85**, **86** and **87** as additives in biodiesel, respectively (tests conducted in an AFIDA combustion chamber at ASG Analytic GmbH).

13.7: Conclusion

The compounds **85**, **86** and **87** cause an *increase* in NO*x* emissions by 16.5 %, 10.3 % and 9.9 %, respectively. The results illustrated above do not agree with the work of Perry *et al*.[232] who showed that NO is rapidly reduced by cyanuric acid in a steel tube at 700 ^{o}C to nitrogen and carbondioxide (Scheme 52).

$$2\ (HNCO)_3 + 9\ NO \xrightarrow{700\ ^{o}C} 7.5\ N_2 + 6\ CO_2 + 3\ H_2O$$

Scheme 52: Reaction of cyanuric acid with nitrous oxide

However, according to Wicke[233a] the reaction shown in Scheme 52 is possible only under inert conditions (argon). When similar tests were performed in the presence of oxygen, cyanuric acid reacted with oxygen to produce increased amounts of NO as shown in Scheme 53. It was concluded that at higher temperatures the reactivity of cyanuric acid towards oxygen is greater than its reactivity towards NO.

$$2\ (HNCO)_3 + 6.5\ O_2 \xrightarrow{700\ ^{o}C} 6\ CO_2 + 4\ NO + N_2 + 3\ H_2O$$

Scheme 53: Reaction of cyanuric acid with oxygen

Cyanuric aid is one of the thermal decomposition products of urea; it is formed preferentially at 275 ^{o}C. Perry *et al*[232] have shown that cyanuric acid undergoes thermal stripping above 330 ^{o}C to produce HNCO which further participates in NO reduction when introduced into the exhaust stream of jet engine following the reaction scheme HNCO + OH → NCO + H_2O, NCO + NO → N_2 + CO_2 or NCO + NO → N_2O + CO. The reaction sequence explained by the author is partially true in this particular case. We assume that because the cyanuric acid was introduced as an aqueous slurry into the exhaust at 600-700 ^{o}C, the isocynate might have decomposed to ammonia and CO_2 (NCO + H_2O → NH_2 + CO_2) as shown by Dorofeeva *et al*.[233b] Therefore, it can be concluded that cyanuric acid undergoes oxidation in presence of oxygen or oxygenated fuel and liberates excess NO as shown by Wicke.[233a]

However, the thermal decomposition of carbamates follows two different paths as shown by Dorofeeva *et al*.[233b] and Orzesko *et al*[233c]. A reversible thermal decomposition path where alkyl carbamate decomposes to the corresponding alcohol and isocyanate (equation-1), and an irreversible reaction of thermal decomposition which leads to the liberation of CO_2, amine

and olefin which generally takes place at a temperature above 390 ^{o}C (equation 2). The thermal decomposition follows equation (1) predominantly in carbamates containing primary alcohols by N-H bond cleavage and equation (2) in secondary and tertiary alcohols by β-C-H bond cleavage. However, the thermal decomposition in case of primary alcohols liberates CO_2 as observed by many researchers.[233c] This is explained in equation-3 to 5

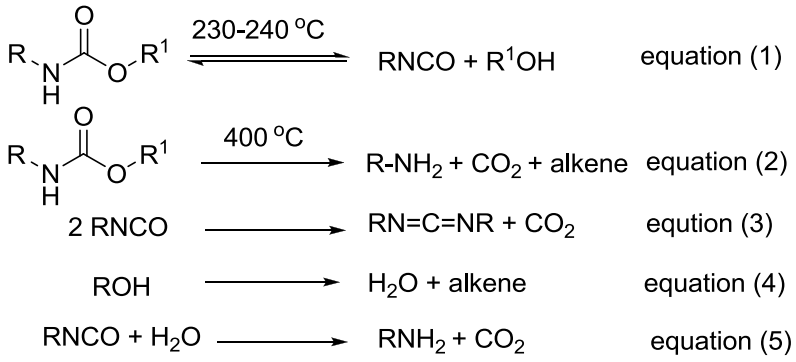

A similar conclusion can be drawn in our cause when compounds **85**, **86** and **87** are used as additives. The compounds are derivatives of primary alcohols and as expected they follow equation 1, 3, 4 and 5 where RNCO is mainly formed. Therefore, the combustion of the above compounds in the presence of oxygen or oxygenated fuels could facilitate the increase of NO*x* emissions with respect to the base fuel as shown by Wicke *et al*.[233a]

An overall comparison of compounds tested as additives in biodiesel is shown in Table 14 and Fig. 54.

2 % additive in biodiesel fuel (RME 4)	Increase in NO*x* compared with RME 4. (%)
65	39.6
68	20.8
85	16.5
86	9.9
87	10.1

Table 14: Overall view of percentage increase of NO*x* emissions caused by the additives to biodiesel compared to neat RME-4 (test results from AFIDA combustion chamber at ASG Analytic GmbH).

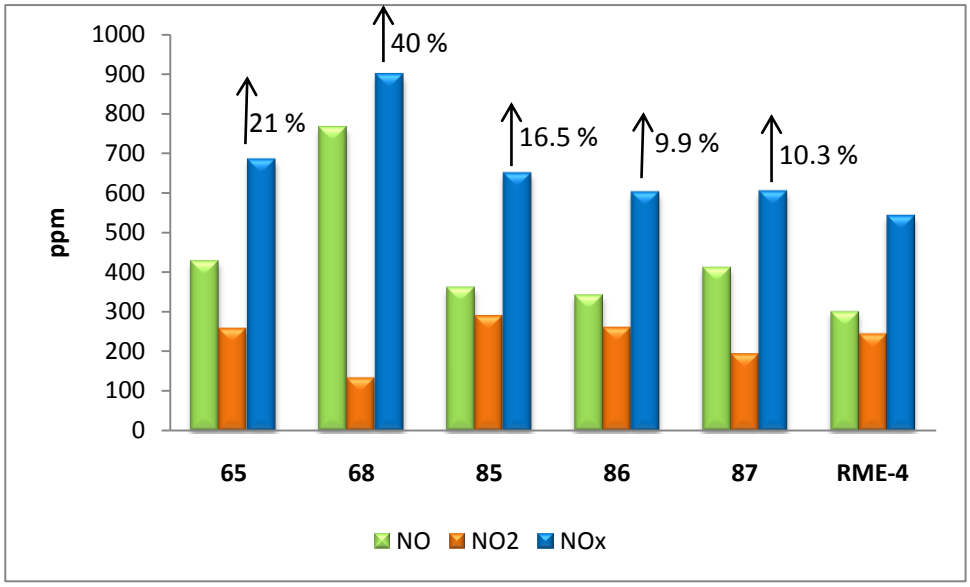

Fig. 54: Overall comparison of NO, NO_2 and NO*x* emissions from biodiesel fuel (tests conducted in an AFIDA combustion chamber at ASG Analytic GmbH).

It is interesting to analyse the overall test results of the increase in NO*x* emissions when our *N*-derivatives are added to biodiesel. The comparative analysis of increase in NO*x* between **65** and **68** is presented in Chapter 11.5.3. However, unlike compounds **65** and **68** the thermal stripping process in carbamates occurs completely. As explained above the carbamates **85-87** are derived from primary alcohols; they thus follow equation (1) and produce mainly RNCO, The amount of RNCO produced directly depends on the number of carbamate groups present in the compound. Theoretically, in this case compound **87** would have produced the highest amount of NO*x* compared to **86** and **85** according to equation (1) and Scheme 53. However, a part of the isocyanate that is formed also follows equations (3-5) where RNH_2 is produced. That is, the additive with more carbamate groups produces greater amount of isocyanate upon thermal decomposition and thus higher RNH_2 concentration which reduces NO efficiently. In this case compound **87** should show higher reducing ability. However, to produce RNH_2 the isocyanate must be hydrolysed according to equation (5) which needs H_2O, the amount of H_2O formed depends on the number of alcoholic groups formed during thermal decomposition (equation (4). The thermal decomposition of **85** produces one alcohol group, **87** produces two alcohol groups whereas **86** has one free alcohol group and produces one upon thermal decomposition, as shown in equation 6, 7 and 8. Therefore, even though **85** and **86** have an equal number of carbamate groups (one each), due to the presence of more free alcohols in **86** it has the advantage to produce more RNH_2 following the equation-5. Thus,

the difference in production and reduction of NO in compound **86** is almost 8 % lower compared to **85** in an oxygen rich environment.

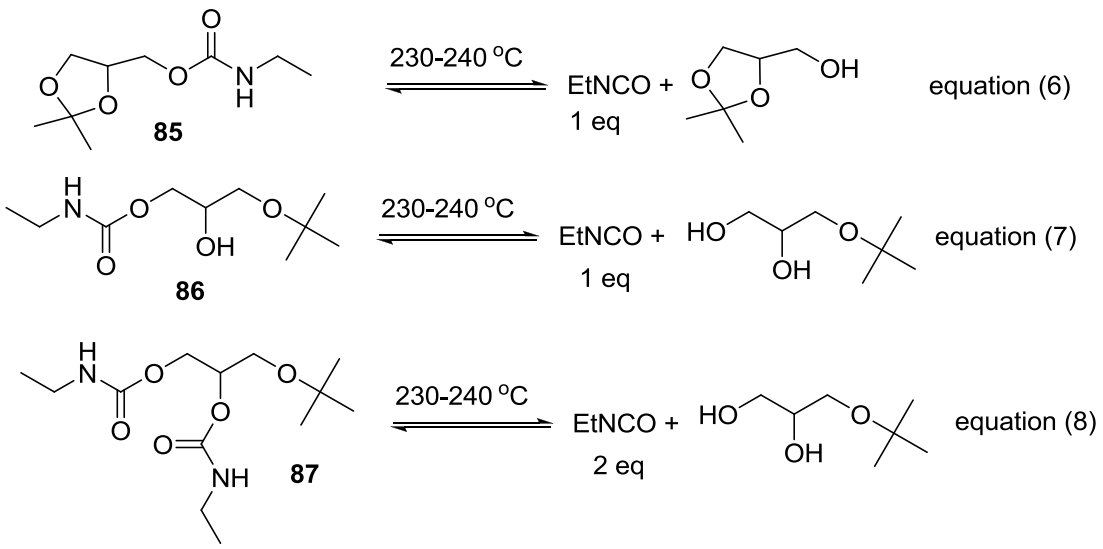

When compounds **86** and **87** are compared, both have similar number of free alcohols upon decomposition (two each). However, **87** produces higher amount of EtNCO compared to **86**, thus more NO is produced following Scheme-53. Therefore, the difference between the production and reduction of NO in compound **87** is slightly higher than in compound **86** leading to an overall increase in NO*x* emissions. However, the above explanation is confined to a small number of known reactions. We know that the hydrolysis of RNCO in a combustion zone is not confined to the number of free alcohols present in an additive. However, we assume that there is a relation between the free alcohol present in the compound and the amount of NO formation from isocyanate according to Scheme-53. Therefore, it can be concluded that the increase in NO*x* emissions shown by carbamates is mainly due to the environment created by the oxygenated fuel (biodiesel) during the deflagration. It can be assumed that when the carbamates dissolved in diesel fuel in the presence of ethanol would show a substantial reduction in NO*x* emissions based on above explanation. Eventually, many more similar compounds have to be synthesized and tested to allow a more systematic comparison. Derivatives of glycerol could be of high importance to reach these goals; this has been made very likely by this study.

Chapter 14: Preparation of *cis*-9-octadecanoic acid hydrazide (105) and *n*-octadecanoic acid hydrazide (106)

14.1: Introduction

Synthesis of hydrazides is a well-known process.[234, 235] Among the many synthetic routes to hydrazides[234, 236, 237] the most commonly known methods are acylation of hydrazines and its aryl or alkyl derivatives with acylating agents like acyl chlorides or esters.[234, 235] The synthesis of hydrazides using acyl chlorides **(89)**[236] known as the Schotten-Baumann reaction, provides mono hydrazides **(91)** and symmetrical hydrazides **(92)** (*sym*-hydrazides) under controlled conditions (Scheme 54).

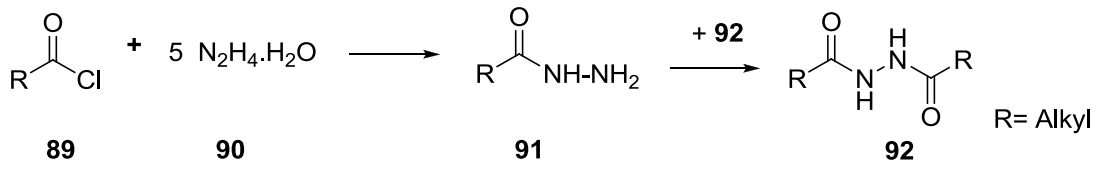

Scheme 54: Synthesis of alkyl hydrazides using acid chlorides

One of the well-known methods to prepare hydrazides is the reaction of esters **93** with hydrazine monohydrate **(90)** (Scheme 55). The reaction can be performed in the presence or absence of solvent.[238] The most commonly used solvent is ethanol apart from dimethylformamide and benzene.[239, 240]

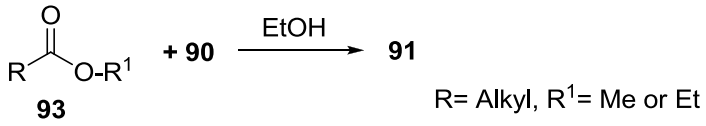

Scheme 55: Synthesis of alkyl hydrazides using esters

The reaction is exothermic and most often the esters need not have to be purified to obtain a desired hydrazide in sufficiently pure state. The formation of **91** depends on the reactivity of the ester, when a less reactive ester is used the reaction mixture has to be refluxed for a few hours to several days. In this case the formation of *sym*-hydrazides **(92)** can be avoided by the use of excess **102**.

14.2: Synthesis of RME hydrazides (105 and 106)

Rapeseed oil methyl ester (RME) is a mixture of fatty acid methyl esters. The sample that has been used for the reactions in this thesis was analyzed by GC-MS analysis which showed that methyl oleate **(94)** (56 %), methyl linoleate **(95)** (37 %) were present as the major components and linolenic acid methyl ester **(96)** (1.4 %), methyl palmatate **(97)** (4 %) and methyl stearate **(98)** (1.6 %) were present in trace amounts (Fig. 55).

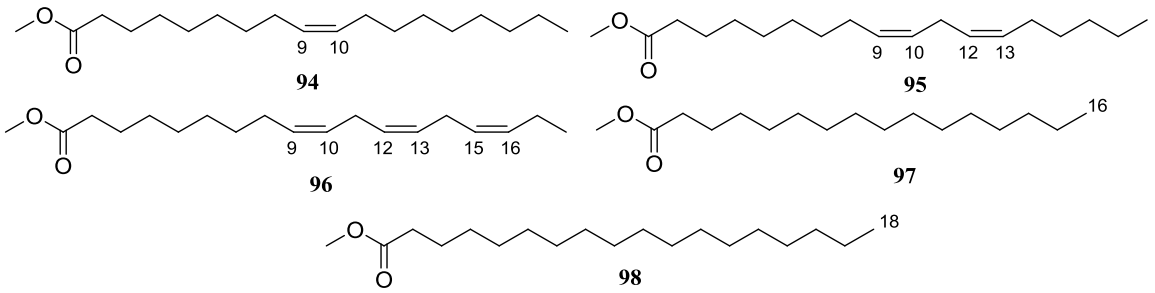

Fig. 55: Composition of RME (biodiesel).

The mixture of **94-98** was reacted with a six fold excess of hydrazine monohydrate **(90)** at 140 ^{o}C to obtain a mixture of hydrazides.

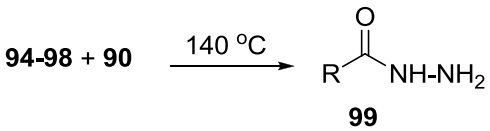

R= alkyl or alkenyl groups from compounds **94-98**, respectively.

Scheme 56: Synthesis of RME hydrazides

However, the reaction did not proceed as shown in Scheme 56. Under ideal conditions in the presence of excess of **90** a mono hydrazide **(99)** must have been obtained from RME **(94-98)**. However, Rao *et al*.[241, 246] have shown that oleic acid can be hydrogenated by **90** in ethanol solution at 50 ^{o}C to obtain more than 90% hydrogenation of the C=C bond in 8 hours, provided an excess of hydrazine (5 fold excess) is used. The actual reducing agent in this case was diimide (NH=NH) which was *in situ* generated by the oxidation of hydrazine in the presence of oxygen. Similarly, in our case, the reaction was expected to yield a complex product mixture (Fig. 56).

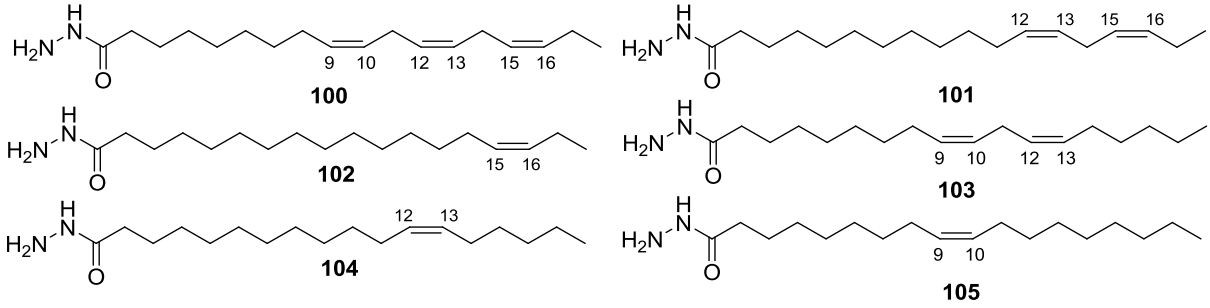

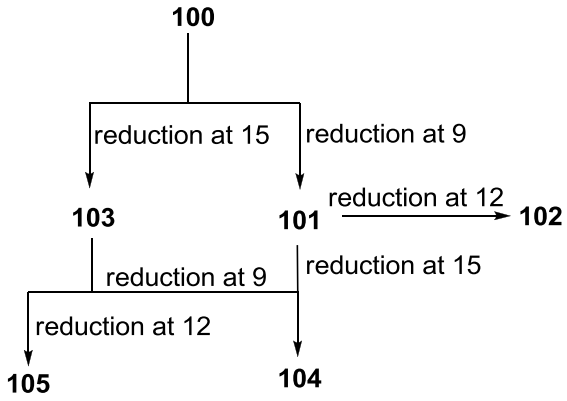

Fig. 56: Possible compounds formed by the partial reduction of RME by **90**.

The chance of formation of **102** is very low in the reaction due to the low concentration of **96** (1.4 %) in RME. The isomers that are expected to be present in higher amounts are **104** and oleic hydrazide **(105)**. If the reduction process was continued further, all the three isomers **102**, **104** and **105** may be reduced to **106**. The other possibility is the formation of *sym*-hydrazides **(92)** in the reaction (Scheme 54), which further complicates the process.

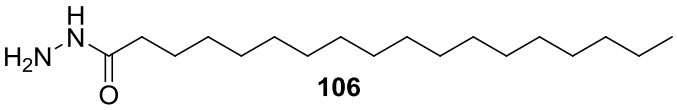

In the reaction (Scheme 56) the mixture of hydrazides contained a waxy solid melting at 50-55 ^{o}C and a soapy white solid melting at 110 ^{o}C. The product mixture was separated by heating it in a separating funnel at 60 ^{o}C and tapping out the low melting solid. TLC analysis of solid confirmed a single component (R_f=0.56) furthermore the ^{1}H NMR analysis displayed broad peaks for NH and NH_2 protons at δ=4.8 and 6.9 ppm, respectively. A multiplet δ=5.31-5.37 ppm is attributed to the alkenyl protons; the corresponding carbon atoms C-9 and C-10 appeared at δ=130.3 and 130.6 ppm in the ^{13}C NMR spectrum. The spectral data were compared and are in good agreement with those of **105** reported in the literature.[241-246]

Eventually, hydrazides of RME **(100-105)** were prepared by stirring RME **(94-98)** with a sixfold excess of hydrazine monohydrate **(90)** for 18 h at room temperature under nitrogen, under these conditions no reduction was noted.

The ^{1}H-NMR spectrum of the high melting solid shows a broad singlet for the NH and NH_2 protons at δ=3.8-4.0 and 6.68-6.76 ppm, respectively. The absence of a multiplet at *δ*=5.31-5.37 ppm demonstrates the absence of alkenyl protons. The spectral analysis were compared and are in good agreement with those of **106** reported in the literature.[241-246]

The compound **106** was also obtained by hydrogenation of RME using a Pd/C catalyst. RME was reduced to *n*-octadecanoic acid methyl ester **(107)** in quantitative yield, which was obtained as a white amorphous solid melting at 30-35 ^{o}C. Compound **107** was further reacted with **102** to obtain **106** quantitatively, as an analytically pure white solid melting at 110 ^{o}C (Scheme 57).

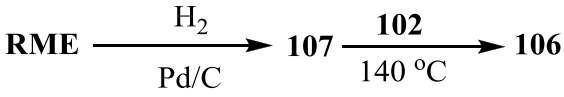

Scheme 57: Preparation of methyl stearate **(107)** and **106**

14.3: Fuel Additive experiments with compound 106

Hydrazides are interesting compounds to be used as additives. The very purpose to choose hydrazide to reduce NO*x* emissions was due to the practical role of hydrazine in rocket propellant combustion. As a matter of fact the reaction between dinitrogen tetroxide and hydrazine is so vigorous that it is difficult to monitor the reaction between the two liquid propellants. At the moment of contact between the reactants the reaction at the interface of the droplet is so fast and vigorous that the droplets are driven apart, thus preventing further reaction. Therefore, to prevent the uncontrolled exothermic reaction a 1:1 mixture of hydrazine and unsymmetrical dimethylhydrazine (UDMH-**110)** (the mixture is commercially known as Aerozine-50) or monomethylhydrazine (MMH-**111)** has been used as rocket propellant. The mixture is hypergolic and the reaction is exothermic, where nitrogen and water are produced as end products.[247a]

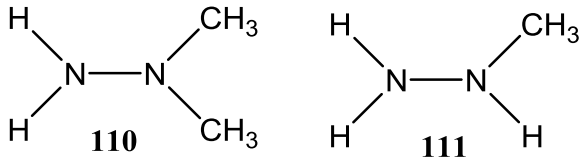

$$0.5\ N_2H_4 + NO \longrightarrow H_2O + N_2$$

Similarly, carboxylic acid hydrazides undergo thermal decomposes to hydrazine and their respective alkyl chain as shown by Govindarajan *et al*.[247b, 247c] Thus, from the above discussion hydrazides were a proper choice to be used as additives to reduce NO*x* emissions. It has been described in Chapter 10.4 that primary amines are poorly soluble in diesel and biodiesel. Hence, it was decided to use compounds with longer chain length to increase the solubility. Even though compound **106** was sparingly soluble in RME it was chosen as an additive because it is known (Chapter 4.2.4.5) that NO*x* emissions are directly proportional to the iodine number of the fuel. Since compound **106** is a saturated compound it was the best suitable choice as additive to reduce NO*x* emissions. To enhance the solubility of **106** in biodiesel compound **68** was chosen as a co-solvent. From all the compounds that were tested for NO*x* emissions by us (Chapter 11.4.2) previously, **68** was the only compound that could enhance the solubility of **106** in biodiesel. It was important to use a known compound so that the decrease or increase of NO*x* emissions by **106** could later be compared. A solution of 2 % of **106** with 2 % of **68** as co-solvent was dissolved in 100 mL RME and was used to perform additive tests.

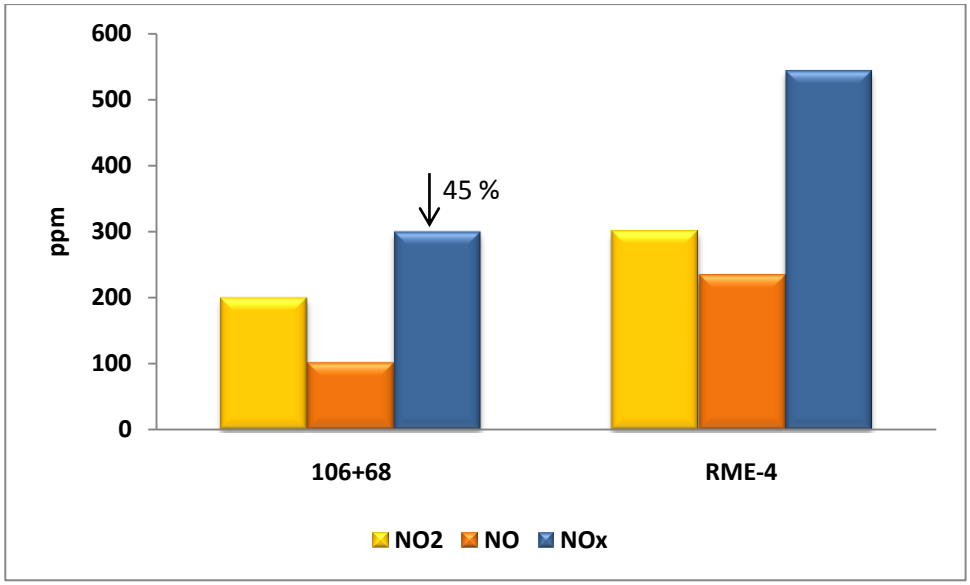

Fig. 57: NO, NO_2 and NO*x* emissions from diesel engine with 2 % of **106** and 2 % of **68** as additives in biodiesel fuel (tests conducted in an AFIDA combustion chamber at ASG Analytic GmbH).

It is known that the hydrazides undergo thermal decomposition processes and release hydrazine. Miller *et al*[129g] have performed an extensive study on the NO reduction by hydrazine and shown that hydrazine acts very similar to ammonia in the reduction and formation of NO, some of the local reactions are represented in equation (1-3) (see also Chapter 6.2).

$$N_2H_2 + O \rightarrow NO + NH_2 \qquad \text{equation (1)}$$

$$N_2H_2 + NO \rightarrow NH_2 + N_2O \qquad \text{equation (2)}$$

$$NH_2 + NO \rightarrow N_2 + H_2O \qquad \text{equation (3)}$$

However, in the thermal stripping, hydrazine produces two molecules of NH_2 and as shown by Finamore *et al*[129e] in NH_3-NO flames that the NH_2 radicle is an active reducing agent ($NH_2 + NO \rightarrow N_2 + OH + H$) during the combustion. Thus, addition of hydrazides to the fuel provides NH_2 radicles in flame which are in the highest priority of NO reduction. It is assumed that 40 % *reduction* in NO*x* emissions that is observed in our case is due to the high reducing ability of hydrazine. The interesting thing that has to be noted is the addition of hydrazide provided NH_2 ions in a sufficient amount in the combustion zone to overcome the oxidation caused by the oxygenated fuel and provided $NH_{i=0,1,2}$ ions to reduce NO. In other words, as shown by Fenimore *et al*[129e] in a NH_3-O_2 (which can be compared to oxygenated fuel in our case) flame that almost 40 % of the ammonia fed may be converted into NO by

the action of atomic oxygen irrespective of the temperature zone ($NH_3 + O \rightarrow \rightarrow NO + \ldots$), and in the presence of excess NH_2 radicals the consumption of NO is twice as fast as its formation. Thus, it may be concluded that addition of hydrazides to the biodiesel may significantly reduce NO*x* emissions. However, it may be assumed that any significant decrease in the amount of reducing agent may show an increase in NO*x* emissions (see Chapter 6.2.1) due to an imbalance created in the formation and reduction of NO by the additive. An alternative solution for the insoluble hydrazides would be to add compound **106** into the fuel by using a mechanically controlled fuel injection system which can heat **106** to its melting point and inject it in to the preheated fuel in a controlled fashion.

14.4: Conclusion

It can be concluded from the above tests that nitrogen in its primary and secondary state when used as additive clearly show a reduction of NO*x* emissions. However, it is difficult to dissolve the compound in the fuel in its pure state. It can be also concluded that lower oxygen and higher nitrogen content in a higher reduced state can efficiently reduce NO*x* emissions. The above results are clearly promising but the tests were conducted in an AFIDA combustion chamber (Chapter 7.3). In the future the compounds must be tested in a "real" diesel engine with respect to load and speed to allow a clear determination of the NO*x* reduction.

The above results are the primary steps of a new concept of SNCR by using amines as additives to reduce NO*x* emission from diesel engines. Further research has to be performed to completely establish this concept. There is a need for a new class of compounds that can be easily synthesized and could be easily soluble in fuel. Compounds like **110** and **111** could be tested and probably may show better results. It was not in the context of this thesis to synthesize compounds from a wide variety of sources as we were restricted here to prepare compounds from glycerol. However, most of the amines, carbamates and hydrazides can be successfully used in the future due to their solubility in ethanol which is being widely blended with petroleum fuels presently and with diesel fuel in future.

Chapter 15: Experimental section

15.1: Instrumentation and general experimental considerations

Thin Layer Chromatography (TLC) was carried out using 0.2 mm silica gel (SiO_2) pre-coated plastic sheets Polygram® Sil G/UV_{254} purchased from Macherey-Nagel GmbH & Co. KG (Düren). Visualization was effected by staining the plate with a staining reagent prepared by the addition of 21 g of ammonium molybdate, 4 g of cesium [IV] sulfate, 31 mL of conc. H_2SO_4 (exothermic) and diluted to 500 mL with dist. H_2O, or by iodine vapors. Basic $KMnO_4$ solution or exposure to UV light (254 nm) was also used.

Column Chromatography was carried out on Silica gel 60 M (70-230 mesh ASTM) purchased from Macherey-Nagel GmbH & Co. KG (Düren).

Melting Points were determined on a MEL-TEMP II apparatus from Büchi and are uncorrected.

NMR Spectroscopy:

^{1}H and ^{13}C -NMR spectra: NMR spectra were obtained on a Bruker Avance II 600 or a Bruker DRX-400 spectrometer at 400 MHz (^{1}H) and at 101 MHz (^{13}C). The solvent was $CDCl_3$ in all the cases unless specified otherwise, ^{1}H NMR chemical shifts are expressed in ppm (δ) downfield to internal TMS as reference. Coupling constants in the ^{1}H NMR spectra are in Hz. The following abbreviations are used to designate the multiplicities: s (singlet), s_b (broad singlet), d (doublet), t (triplet), t_b (broad triplet), q (quartet), qi (quintet), m (multiplet), six (sextet), dd (doublet of doublet). The chemical shifts in the ^{13}C spectra are expressed in ppm (δ) and in the DEPT spectrum q stands for (quartet, CH_3), t for (triplet, CH_2), d for (doublet, CH) s for (singlet, C). Two-dimensional H,H-COSY, H,H-NOESY, H,C-HSQC and H,C-HMBC spectra were recorded using standard Bruker pulse programs. Sweep widths and pulse delays were optimized for the samples under investigation.

IR-Spectroscopy: IR spectra were recorded on a Bruker Tensor 27 spectrometer using the diamond ATR technique. Notations are specified as: vs (strong), s (strong), m (medium), w (weak), br (broad)

UV/Vis Spectroscopy: UV/Vis spectra were obtained using a Hewlett-Packard 8452 A Diode Array or a Varian Cary 100 Bio spectrometer.

Mass Spectrometry: Mass spectra were recorded on a Finnigan MAT 95 mass spectrometer using electron ionisation (EI, 70 eV).

GC Analysis: GC analyses were carried out using the best suited method. Unless mentioned, all GC measurements were performed using a standard method abbreviated as nr.m.

NR.M method for GC analysis: The measurement was recorded on an Agilent gas chromatograph equipped with a 30 m analytical column. Conditions were as follows: injection temperature 250 °C; injection volume 1 µL; temperature program was 60 °C (2 min), increasing at 10 °C min^{-1} to 300 °C in 30 min, operated in split (ratio 1:10) mode; the carrier gas was H_2 (1.6 $mL.min^{-1}$) and pressurized air as auxiliary gas.

GC-MS analysis was carried out using different methods, based on the configuration and file type.

Method 1: The **FUGU-files** were recorded on an Agilent 6890 gas chromatograph equipped with a 30 m analytical column (J&W HP-5, 30 m x 0.32 mm ID, t_f = 0.25 µm). A split injection port at 250 °C was used for sample introduction and the split ratio was set to 1:10. The temperature program was 70 °C (3 min), increasing at 10 °Cmin^{-1} to 320 °C (5 min). The carrier gas He was set to 1.5 $mLmin^{-1}$ flow rate (constant flow mode). The transfer line was kept at 250 °C. The corresponding Jeol GCMate II bench top double-focusing magnetic sector mass spectrometer was operating in the EI mode at 70 eV with an ion source temperature at 180 °C. Low-resolution mass spectra were acquired at a resolving power of 650 (20 % height definition) and scanning from *m/z* 39 to *m/z* 650 at 1 seconds per scan with a 0.2 second inter-scan delay.

Method 2: The **TOF-files** were recorded on an Agilent 6890 gas chromatograph equipped with a 30 m analytical column (J&W HP-5, 30 m x 0.32 mm ID, t_f = 0.25 µm). A split injection port at 250 °C was used for sample introduction with a split ratio of 10:1. Flow rate (constant flow mode) of the carrier gas He was set to 1.0 $mLmin^{-1}$. The transfer line was set at 250 °C. A JMS-T100GC (GCAccuTOF, JOEL, Japan) time of flight mass spectrometer in EI mode at 70 eV and a JOEL MassCenter.M workstation software was used. The source temperature was set at 200 °C and the detector voltage was 2000 V. The acquisition range

was from m/z 41 to m/z 700 with spectrum recording interval of 0.4 s. The system was tuned with PFK to achieve a resolution of 5,000 (FWHM) at *m/z* 292.9824.

Elemental Analysis: Analyses were carried out at the Institut für Pharmazeutische Chemie and the Institut für Anorganische und Analytische Chemie, Technische Universität Braunschweig.

General Remarks: All reactions were conducted by using oven-dried glassware. All commercially available reagents were purchased and used without further purification. Solvents Et_2O, CH_2Cl_2, THF, and toluene were dried and distilled according to usual protocols.

15.2: Experiments from Chapter 8

15.2.1: 3-*tert*-Butoxypropan-1,2-diol (14)

In a round bottomed flask fitted with a Dean-Stark trap 92.1 g (1 mol) of glycerol **(2)** and 296 g (4 mol) of *tert*-butanol **(13)** were placed and the mixture was stirred well to dissolve. To the solution 5 grams (5.4 wt %) of amberlyst-15® and 520 mL (4 mol) of toluene were added and the mixture heated under reflux for 140 min. The reaction was allowed to cool down and filtered to separate the catalyst. Excess *tert*-butanol and toluene were evaporated under reduced pressure and the product mixture was twice washed with *n*-pentane and diethyl ether (7:3 v/v). The 3-*tert*-butoxypropane-1,2-diol **(14)** precipitated out as a colourless oil with an yield of 85 % (125 g, 0.85 mol). Further purification was achieved by distillation at 85- 90 ^{o}C at 0.4-0.5 mbar or 125-130 ^{o}C at 4-5 mbar (95-96 % based on GC purity). A column chromatography was performed to establish 99 % purity using diethyl ether as solvent (R_f. 0.3).[132-141]

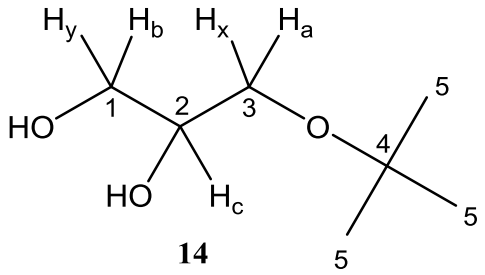

14

Refractive Index: n_D^{20}=1.43580

^{1}H-NMR (400.1 MHz, $CDCl_3$): δ = 1.21 (s, 9 H, 5-H), 3.1 (s_b, 2 H, 1, 2-OH), 3.4 (m, 2 H, 3-H_a, H_x), 3.6 (m, 2 H, 1-H_b, H_y), 3.7 ppm (m, 1 H, 2-H_c)

^{13}C-NMR (100.1 MHz, $CDCl_3$): δ = 27.35 (q, C-5), 63.4 (t, C-3), 64.2 (t, C-1), 70.8 (d, C-2), 73.3 ppm (s, C-4).

^{1}H-NMR (200.1 MHz, D_2O): δ = 1.25 (s, 9 H, 5-H), 3.39-3.68 (m, 4 H, 3-H_a, H_x, 1-H_b, H_y), 3.7-3.83 ppm (m, 1 H, 2-H_c)

^{13}C-NMR (50.1 MHz, D_2O): δ = 29.4 (q, C-5), 65.7 (t, C-3, C-1), 73.9 (d, C-2), 77.6 ppm (s, C-4).

MS (GC/MS: Method 2) (EI, 70 eV): *m/z* (%) = 133 (4, $[M^+-CH_3]$), 117 (2, $[C_6H_{13}O_2]^+$), 87 (4, $[C_5H_{11}O]^+$), 75 (10, $[C_4H_{11}O]^+$), 57.1 (100, $[C_4H_9]^+$).

IR (diamond-ATR): $\tilde{\nu}$ = 3449 (br), 2973 (s), 2931 (w), 2873 (w), 1474 (m), 1193 (s), 1079 (s) cm^{-1}.

Elemental analysis:

Calculated: C 56.73, H 10.88; found: C 56.61, H 10.85

These analytical data are in agreement with those reported in the literature.[248, 249]

15.3: Experiments from Chapter 9

15.3.1: 2,2-Dimethyl-4-hydroxymethyl-1,3-dioxolane (26)

Procedure 1

460 g of glycerol **(2)** (362.2 mL, 5 mol) and 790 g of acetone **(25)** (1000 mL, 13.4 mol) were placed in a flask and 2 g of *p*-toluenesulfonic acid monohydrate and 1200 mL of petroleum ether (low boiling fraction: 35-50 ^oC) were added. An azeotropic distillation was performed until no more water collected in the trap of the separating head (24-26 h). The reaction mixture was neutralized with saturated Na_2CO_3 solution and dried over Na_2SO_4 and petroleum ether and excess acetone were evaporated under reduced pressure. The product mixture was purified by distillation at 115 ^oC, 57 mbar to obtain 586 g (4.43 mol, 89 %, lit. [143] 87-90 %) of **26** as a colourless oil.

Procedure 2

9.2 g of glycerol **(2)** (7.3 mL/ 0.1 mol) and 57.9 g of acetone **(25)** (73.4 mL/ 1 mol) were placed in a flask to which 1.05 g (8 mmol) of $AlCl_3$ and 125 mL of pentane were added. An azeotropic distillation was performed until no more water was collected in the trap of the separating head (3 h). The reaction mixture was neutralized with saturated Na_2CO_3 solution and dried over Na_2SO_4. Pentane and excess acetone **(25)** were evaporated under reduced pressure. The residue was dissolved in dichloromethane, filtered and the solvent was evaporated. The product mixture was purified by distillation at 80-81 ^oC, 11 mbar to obtain 9.39 g (0.071 mol, 71 %) of **26** as colourless oil. (R_f in diethylether 0.62)

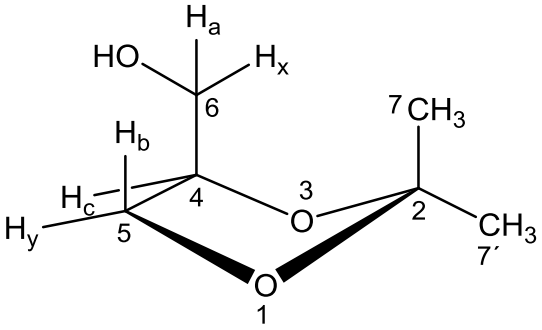

Refractive Index: n_D^{20}=1.4321

^{1}H-NMR (200.1 MHz, $CDCl_3$): δ = 1.3 (s, 3 H, 7-H), 1.4 (s, 3 H, 7´-H) 3.2 (s_b, 1 H, 6-OH), 3.58-3.62 (m, 2 H, 6-H_a, H_x), 3.72-3.79 (dd, 1 H, 5-H_b, $^2J_{Hb, Hy}$ = 8.16 Hz, $^3J_{Hb, Hc}$ = 6.48 Hz), 4.0-4.07 (dd, 1 H, 5-H_y, $^2J_{Hy, Hc}$ = 8.11 Hz, $^3J_{Hy, Hc}$ = 6.38 Hz), 4.18-4.24 ppm (m, 1 H, 4-H_c)

^{13}C-NMR (50.3 MHz, $CDCl_3$): δ = 25.9 (q, C-7), 27.3 (q, C-7´), 63.6 (t, C-6), 66.6 (t, C-5), 77.0 (d, C-4), 110 ppm (s, C-2)

MS (GC/MS: Method 2) (EI, 70 eV): *m/z* (%) = 133 (4, $[M^+ +1]$), 117 (40, $[M^+ - CH_3]$), 101 (20, $[C_5H_{11}O]^+$), 72 (10, $[C_4H_{11}O]^+$), 43 (100, $[C_4H_9]^+$). (GC NR.M: 1.904)

IR (diamond-ATR): $\tilde{\nu}$ = 3417 (br), 2987 (s), 2937 (w), 2883 (w), 1457 (m), 1045 (s) cm^{-1}. These data are in good agreement with those reported in reference.[143]

15.3.2: 2,2-Dimethyl-4-*tert*-butoxymethyl-1,3-dioxolane (27)

615.7 g of **14** (580 mL, 4.1 mol) and 1186 g of acetone **(25)** (1500 mL/ 20.4 mol) were placed in a flask and 20 g of *p*-toluenesulfonic acid monohydrate (2.7 %) and 1650 mL petroleum ether (low boiling fraction: 35-50 ^oC) was added. An azeotropic distillation was performed until no more water was collected in the trap of the separating head (6-8 h). The reaction mixture was neutralized with saturated Na_2CO_3 solution and dried over Na_2SO_4 or K_2CO_3. Petroleum ether and excess acetone were evaporated under reduced pressure. The product mixture was purified by distillation at 184-185 ^oC at atmospheric pressure or 42-43 ^oC at 0.3-0.4 mbar pressure to obtain 719.1 g (3.82 mol, 93%) of **27** as a colourless oil.

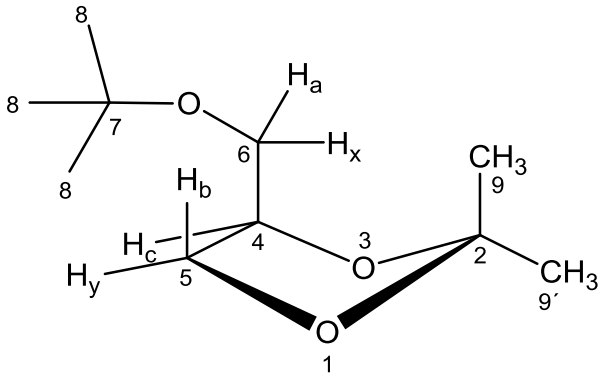

27

Refractive Index: n_D^{20} =1.41574

^{1}H-NMR (400.1 MHz, $CDCl_3$): δ = 1.18 (s, 9 H, 8-H), 1.35 (s, 3 H, 9-H), 1.41 (s, 3 H, 9´-H), 3.2-3.3 (dd, 1 H, 6-Ha, $^2J_{Ha,Hx}$ = 9.1 Hz, $^3J_{Ha,Hc}$ = 7.04 Hz), 3.46-3.49 (m, 1 H, 6-H_x), 3.72-3.76 (dd, 1 H, 5-H_b, $^2J_{Hb,Hy}$ = 8.26 Hz, $^3J_{Hb\text{-}syn\text{-}Hc}$ = 5.9 Hz), 4.03-4.07 (dd, 1 H, 5-H_y, $^2J_{Hy,Hc}$ = 8.22 Hz, $^3J_{Hy\text{-}anti\text{-}Hc}$ = 6.34 Hz), 4.14-4.21 ppm (qi, 1 H, 4-H_c).

^{13}C-NMR (101 MHz, $CDCl_3$): δ = 25.2 (q, C-9), 26.6 (q, C-9´), 27.3 (q, C-8), 63.1 (t, C-6), 67.3 (t, C-5), 72.9 (s, C-7), 75.1 (d, C-4), 109 ppm (s, C-2).

MS (GC/MS: Method 2) (EI, 70 eV): *m/z* (%) = 173 (25, $[M^+\text{-}CH_3]$), 117 (15, $[C_5H_9O_3]^+$), 115 (15, $[C_6H_{11}O_2]^+$), 101 (60, $[C_5H_9O_2]^+$), 57 (100, $[C_4H_9]^+$).

IR (diamond-ATR): $\tilde{\nu}$ = 2976 (s), 2935 (w), 2874 (w), 1458 (m), 1193 (s), 1083 (s) cm^{-1}.

Elemental analysis:

Calculated: C 63.80, H 10.71; found: C 63.54, H 11.1

15.3.3: 2-Methyl-4-*tert*-butoxymethyl-1,3-dioxolane (28a, 28b)

9.78 g of **14** (11 mL, 0.06 mol) was placed in a round bottomed flask with 29 g (36.8 mL, 0.65 mol) of freshly distilled acetaldehyde. *p*-toluenesulfonic acid monohydrate (1 g) and 1650 mL of petroleum ether (low boiling fraction: 35-50 ^oC) were added. An azeotropic distillation was performed until no more water was collected in the trap of the separating head. The reaction mixture was neutralized with saturated Na_2CO_3 solution and dried over Na_2SO_4. Petroleum ether and excess of acetaldehyde were evaporated under reduced pressure. The product mixture was purified by distillation at 42 ^oC at 0.4-0.5 mbar pressure to obtain **28a** and **28b** in a yield of 7.19 g (0.041 mol, 54 %) as a colourless oil with a

diastereomeric ratio of 50:45 % (based on GC analysis). Further purification was performed by column chromatography using diethylether (R_f=0.9, 0.86) to obtain 98 % (GC purity) of the diastereomeric mixture.

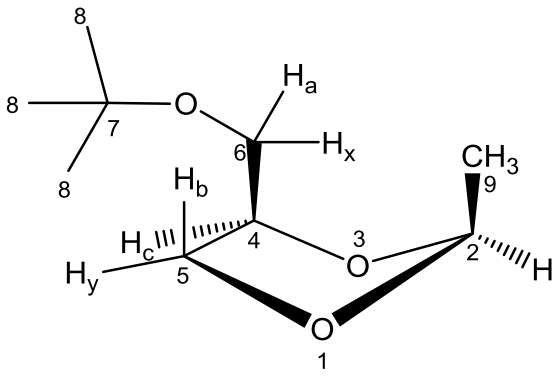

cis-**28a**

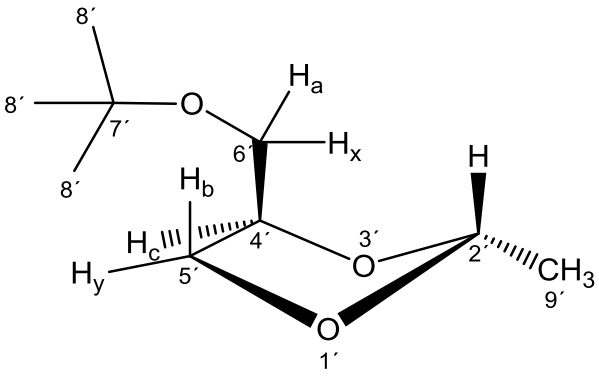

trans-**28b**

^{1}H-NMR (400.1 MHz, $CDCl_3$) (*cis*-**28a** and *trans*-**28b**): δ = 1.11 (s, 9 H, 8-H), 1.12 (s, 9 H, 8´-H), 1.26-1.28 (m, 3 H, 9´-H), 1.29-1.3 (m, 3 H, 9-H), 3.18-3.22 (dd, 1 H, 6-H_a, $^2J_{Ha,Hx}$ = 8.78 Hz, $^3J_{Ha\text{-}anti\text{-}Hc}$ = 7.04 Hz), 3.27-3.3 (dd, 1 H, 6´-H_a, $^2J_{Ha,Hx}$ = 9.39 Hz, $^3J_{Ha\text{-}anti\text{-}Hc}$ = 5.72 Hz), 3.38-3.43 (m, 2 H, 6-H_x, 6´-H_x), 3.68-3.71 (dd, 1 H, 5-H_y, $^2J_{Hb,Hy}$ = 8.16 Hz, $^3J_{Hy\text{-}syn\text{-}Hc}$ = 4.96 Hz), 3.54-3.58 (dd, 1 H, 5´-H_b, $^2J_{Hb,Hy}$ = 8.10 Hz, $^3J_{Hb\text{-}anti\text{-}Hc}$ = 6.66 Hz), 3.8-3.83 (pt, 1 H, 5-H_b, $^2J_{Hb,Hy}$ = 7.5 Hz, $^3J_{Hb\text{-}anti\text{-}Hc}$ = 7.5 Hz), 4.01-4.07 (m, 2 H, 4-H_c, 5´-H_y), 4.11-4.14 (m, 1 H, 4´-H_c), 4.93-4.95 (q, 1 H, 2-H, $^3J_{2,9}$ = 4.8 Hz), 5.01-5.04 ppm (q, 1 H, 2´-H, $^3J_{2´,9´}$ = 4.8 Hz).

^{13}C-NMR (101 MHz, $CDCl_3$) (*cis*-**28a** and *trans*-**28b**): δ = 19.79 (q, C-9), 19.74 (q, C-9´), 27.25 (q, C-8´), 27.27 (q, C-8), 63.2 (t, C-6), 63.45 (t, C-6´), 67.8 (t, C-5´), 67.9 (t, C-5), 72.94 (s, C-7), 72.97 (s, C-7´), 74.87 (d, C-4´), 75.34 (d, C-4), 101.32 (s, C-2´), 101.71 ppm (s, C-2).

MS (GC/MS: Method 2) (EI, 70 eV): *m/z* (%) = 173 (5, $[M^+-1]$), 159 (40, $[C_8H_{15}O_3]^+$), 117 (85, $[C_5H_9O_3]^+$), 87 (90, $[C_4H_7O_2]^+$), 57 (100, $[C_4H_9]^+$).

IR (diamond-ATR): $\tilde{\nu}$ = 2975 (m), 2936 (w), 2874(w), 1476 (w), 1364 (m), 1196 (s), 1085 (s) cm^{-1}.

Elemental analysis:

Calculated: C 62.04, H 10.41; found: C 61.51, H 10.39

15.3.4: 2-Ethyl-4-*tert*-butoxymethyl-1,3-dioxolane (29a, 29b)

14.8 g of **14** (0.1 mol) was placed in a round bottomed flask with 55.8 g (0.96 mol) of freshly distilled propanal. The mixture was stirred well and 0.78 g of *p*-toluenesulfonic acid monohydrate (4.8 mmol, 5 %) and 100 mL of pentane were added. An azeotropic distillation was performed until no more water was collected in the trap of the separating head (150 min). The reaction mixture was neutralized with saturated Na_2CO_3 solution and dried over Na_2SO_4. Pentane and excess propanal were evaporated under reduced pressure. The product mixture (15.4 g) was purified by fractional distillation at 90-94 ^{o}C/10-11 mbar to obtain 9.2 g (0.49 mol, 49 %) of **29a** and **29b** with a diastereomeric ratio of 0.8:1 (based on GC analysis). Further purification was performed by column chromatography using diethylether as eluent (Rf=0.87, 0.80) to obtain 98 % (GC purity) of the diastereomeric mixture.

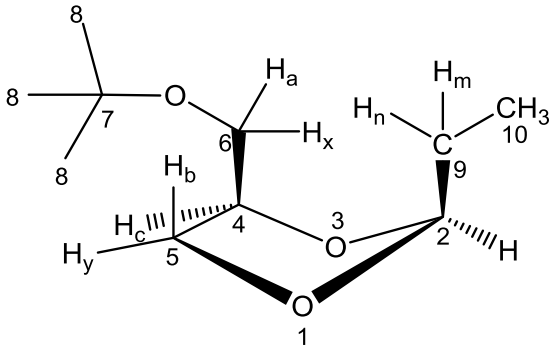

cis-**29a**

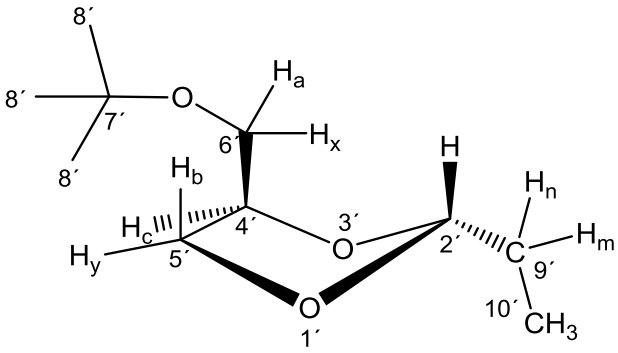

trans-**29b**

^{1}H-NMR (400.1 MHz, $CDCl_3$) (*cis*-**29a** and *trans*-**29b**): δ = 0.93-0.97 (m, 6 H, 10-H, 10´-H), 1.18 (s, 18 H, 8-H, 8´-H), 1.61-1.72 (m, 4 H, 9-H_m, H_n, 9´- H_m, H_n), 3.24-3.28 (dd, 1 H, 6-H, $^{2}J_{Ha,Hx}$ = 8.96 Hz, $^{3}J_{Ha\text{-}anti\text{-}Hc}$ of 7.08 Hz), 3.27-3.30 (dd, 1 H, 6´-H_a, $^{2}J_{Ha,Hx}$ = 9.36 Hz, $^{3}J_{Ha\text{-}anti\text{-}Hc}$ of 6.04 Hz), 3.42-3.52 (m, 1 H, 6-H_x, 6´-H_x), 3.63-3.66 (dd, 1 H, 5´-H_b, $^{2}J_{Hb,Hy}$ = 8.06 Hz, $^{3}J_{Hb\text{-}anti\text{-}Hc}$ = 6.40 Hz), δ 3.75-3.78 (dd, 1 H, 5-H_y, $^{2}J_{Hb,Hy}$ = 8.18 Hz, $^{3}J_{Hy\text{-}syn\text{-}Hc}$ of 4.93 Hz), 3.88-3.90 (dd, 1 H, 5-H_b, $^{2}J_{Hb,Hy}$ of 8.10 Hz, $^{3}J_{Hy\text{-}anti\text{-}Hc}$ of 6.8 Hz), 4.09-4.19 (m, 3 H, 4-H_c, 4´-H_c, 5´-H_y), 4.84-4.86 (t, 1 H, 2-H, $^{3}J_{2,9}$ = 4.68), 4.93-4.95 ppm (t, 1 H, 2-H, $^{3}J_{2,9}$ = 4.68).

^{13}C-NMR (101 MHz, $CDCl_3$) (*cis*-**29a** and *trans*-**29b**): δ = 8.18 (q, C-10), 8.20 (q, C-10´), 27.33 (t, C-9), 27.40 (t, C-9´), 27.73 (q, C-8), 27.77 (q, C-8´), 62.93 (t, C-6´), 63.57 (t, C-6),

68.37 (t, C-5), 68.44 (t, C-5´), 73.4 (s, C-7, C-7´), 75.36 (d, C-4´), 75.6 (d, C-4), 105.7 ppm (s, C-2´), 106.0 ppm (s, C-2).

MS (GC/MS: Method 2) (EI, 70 eV): *m/z* (%) = 187 (2, $[M^+-1]$), 159 (55, $[C_8H_{15}O_3]^+$), 131 (10, $[C_6H_{11}O_3]^+$), 103 (40, $[C_4H_7O_3]^+$), 101 (60, $[C_5H_9O_2]^+$), 57 (100, $[C_4H_9]^+$).

IR (diamond-ATR): $\tilde{\nu}$ = 2974 (m), 2936 (w), 2877 (w), 1467 (m), 1195 (m), 1084 (s) cm^{-1}.

Elemental analysis:
Calculated: C-63.85, H-10.73; found: C 63.24, H 10.85

15.3.5: 2-Ethyl-2-methyl-4-*tert*-butoxymethyl-1,3-dioxolane (30a, 30b)

100 g of **14** (0.67 mol) and 362.2 g of 2-butanone (450 mL/ 5.05 mol) were placed in a flask to which 3.02 g *p*-toluenesulfonic acid monohydrate (3 wt%) and 1000 mL petroleum ether (low boiling fraction: 35-50 ^oC) were added. An azeotropic distillation was performed until no more was water collected in the trap of the separating head (90 min). The reaction mixture was neutralized with saturated Na_2CO_3 solution and dried over Na_2SO_4. Petroleum ether and excess 2-butanone were evaporated under reduced pressure to obtain a product mixture of 130 g (0.64 mol, 96 %). Further purification was performed by fractional distillation at 206-208 ^oC and atmospheric pressure or 100 ^oC at 20-24 mbar pressure to obtain 116 g (0.57 mol, 85 %) of **30a** and **30b** as a colourless oil in a diastereomeric ratio of 74:26 (based on GC analysis). However, *cis*-**30a** was successfully separated as a pure diastereomer (98 % GC purity) by column chromatography using diethylether (Rf=0.85, 0.8). By using the same technique an attempt to obtain pure *trans*-**30b** form failed.

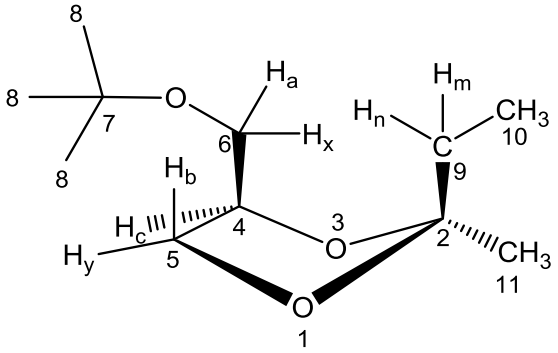

cis-**30a**

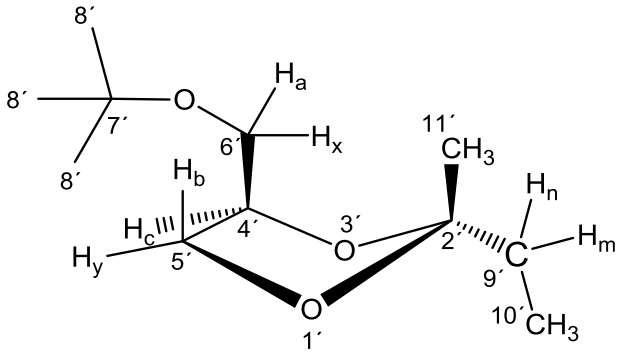

trans-**30b**

^{1}H-NMR (200.1 MHz, $CDCl_3$) (*cis*-**30a**): δ = 0.81-0.90 (dt, 3 H, 10-H, $^{3}J_{9,10}$ = 2.8, 7.48 Hz), 1.11 (s, 9 H, 8-H), 1.22 and 1.27 (s, 3 H, 11-H), 1.51-1.66 (m, 2 H, 9-H_m, H_n), 3.18-3.28 (m, 1 H, 6-H_a), 3.35-3.47 (m, 1 H, 6-H_x), 3.58-3.71 (m, 1 H, 5-H_b), 3.95-4.03 (m, 1 H, 5-H_y), 4.04-4.16 ppm (m, 1 H, 4-H_c)

^{13}C-NMR (50 MHz, $CDCl_3$) (*cis*-**30a**): δ = 9.5, 9.8 (q, C-10), 24.5, 25.7 (t, C-9), 28.8 (q, C-8), 33.1, 33.9 (q, C-11), 64.6, 64.7 (t, C-6), 69.0, 69.1 (t, C-5), 74.4 (s, C-7), 76.3 (d, C-4), 112.4, 112.6 ppm (s, C-2).

^{1}H-NMR (200 MHz, $CDCl_3$) (*cis*-**30a** ,*trans*-**30b**): 0.81-0.90 (dt, 6 H, 10, 10´-H, $^{3}J_{9,10}$ = 2.8, 7.48 Hz), 1.12 (s, 9 H, 8´-H), 1.22 and 1.27 (s, 6 H, 11, 11´-H), 1.46-1.67 (m, 2 H, 9, 9´-H_m, H_n), 3.30-3.34 (dd, 1 H, 6´-H_a, $^{2}J_{Ha,Hx}$ = 5.48 Hz, $^{3}J_{Ha,Hc}$ = 3.39 Hz), 3.36-3.47 (m, 2 H, 6, 6´-H_x), 3.58-3.74 (m, 1 H, 5, 5´-H_b), 3.95-4.05 (m, 1 H, 5, 5´-H_y), 4.08-4.17 ppm (m, 1 H, 4, 4´-H_c).

^{13}C-NMR (50 MHz, $CDCl_3$) (*trans*-**30b**): 9.5, 9.8 (q, C-10, 10´), 24.5, 25.7 (t, C-9, 9´), 28.7 (q, C-8´), 33.1, 33.9 (q, C-11,11´), 64.21, 64. 6, 64. 7 (t, C-6, 6´), 69.0, 69.1 (t, C-5, 5´), 74.3, 74.4 (s, C-7, 7´), 76.3, 76.90 (d, C-4, 4´), 112.3, 112.5 ppm (s, C-2, 2´).

MS (GC/MS: Method 2) (EI, 70 eV): *m/z* (%) = 187 (20, $[M^+-CH_3]$), 173.2 (60, $[C_9H_{17}O_3]^+$), 131 (20, $[C_6H_{11}O_3]^+$), 117 (35, $[C_5H_9O_3]^+$), 115 (80, $[C_6H_{11}O_2]^+$), 57 (100, $[C_4H_9]^+$).

IR (diamond-ATR): $\tilde{\nu}$ = 2975 (m), 2937 (w), 2878 (w), 1466 (w), 1365 (m), 1236 (s), 1081 (s) cm^{-1}.

15.3.6: 2-Isopropyl-4-(*tert*-butoxymethyl)-1,3-dioxolane (31a, 31b)

14.8 g of **14** (0.1 mol) was placed in a round bottomed flask with freshly distilled 73.4 g (1 mol) isobutyraldehyde and the mixture was stirred well until homogenous. 0.7 g (4.1 mmol) of *p*-toluenesulfonic acid monohydrate and 75 mL of pentane were added to the mixture. An azeotropic distillation was performed until no more water was collected in the trap of the separating head (90 min). The reaction mixture was neutralized with saturated Na_2CO_3 solution and extracted with diethylether twice and dried over Na_2SO_4. Pentane and diethylether and excess of isobutyraldehyde were evaporated under reduced pressure. The product mixture (42.6 g) was purified by fractional distillation at 60-61 ^{o}C/ 27 mbar to obtain 17.3 g (0.085 mol, 86 %) of a mixture **31a** and **31b** as a colourless oil in a diastereomeric

ratio of 81:19 (based on GC analysis). Further purification was performed by column chromatography using diethylether (Rf=0.83) to obtain 98 % (GC purity) of diastereomeric mixture.

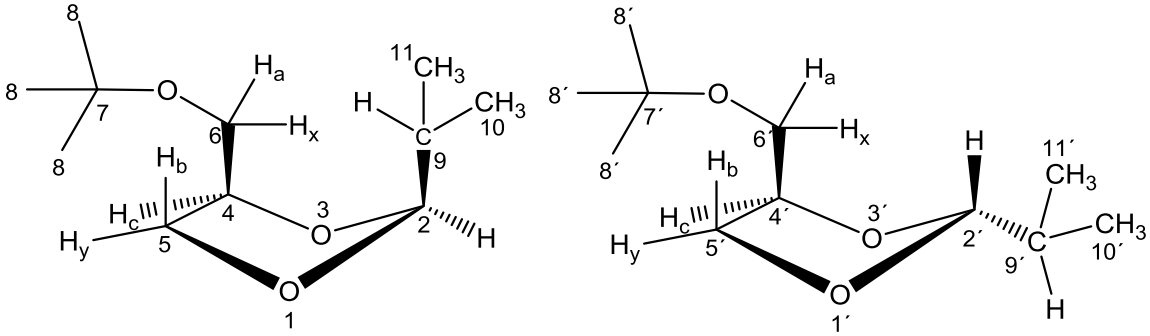

cis-**31a** *trans*-**31b**

^{1}H-NMR (400.1 MHz, $CDCl_3$) (*cis*-**31a** and *trans*-**31b**): δ = 0.87-0.92 (m, 12 H, 10-H, 10´-H, 11-H, 11´-H), 1.14 (s, 9 H, 8-H, 8´-H), 1.70-1.83 (m, 1 H, 9-H, 9´-H), 3.17-3.23 (m, 1 H, 6-H_a), 33.26-3.32 (m, 1 H, 6´-H_a), 3.37-3.50 (m, 2 H, 6-H_x, 6´-H_x), 3.58-3.63 (m, 1 H, 5´-H_b), 3.69-3.73 (m, 1 H, 5-H_y), 3.83-3.88 (m, 1 H, 5-H_b), 4.02-4.15 (m, 3 H, 5´-H_y, 4-H_c, 4´-H_c), 4.59-4.61 (d, 1 H, 2-H, $^3J_{2,9}$ = 4.56 Hz), 4.67-4.69 ppm (d, 1H, 2´-H, $^3J_{2´,9´}$= 4.56 Hz).

^{13}C-NMR (101 MHz, $CDCl_3$) (*cis*-**31a** and *trans*-**31b**): δ = 16.49, 16.56 (q, C-10), 16.8 (q, C-10´), 27.3 (q, C-8), 31.7 (d, C-9), 32.0 (d, C-9´), 62.5 (t, C-6), 63.0 (t, C-6´), 68.0 (t, C-5), 68.3 (t, C-5´), 75.0 (s, C-7), 76.3 (d, C-4), 108.2 (s, C-2), 108.4 ppm (s, C-2´)

MS (GC/MS: Method 2) (EI, 70 eV): *m/z* (%) = 201.1 (5, $[M^+-1]$), 187.1 (10, $[C_{10}H_{17}O_3]^+$), 159.1 (100, $[C_8H_{15}O_3]^+$), 103 (90, $[C_4H_7O_3]^+$), 57.1 (100, $[C_4H_9]^+$).

IR (Diamond-ATR): $\tilde{\nu}$ = 2973 (m), 2933 (w), 2874 (w), 1473 (w), 1365 (m), 1194 (s), 1086 (s) cm^{-1}.

Elemental analysis:

Calculated: C 63.84, H 10.96; found: C 63.19, H 10.75

15.3.7: 2-Oxo-4-*tert*-butoxymethyl-1,3,2-dioxathiolane (43a, 43b)

In a three-necked flask fitted with a condenser and a dropping funnel 4.4 g (0.3 mol) of 1-*tert*-butoxy propane-1,2-diol **(14)** dissolved in 150 mL of dichloromethane was placed and

56.2 g (0.45 mol) thionylchloride **(42)** was added dropwise at 0 °C with vigorous stirring. When the addition was complete (120 min), the reaction mixture was refluxed for 1 h. After cooling the reaction mixture was poured into 100 mL of ice cold water, the organic layer was separated and washed twice with 50 mL saturated Na_2CO_3 solution and once with 50 mL dist. water. Drying ($MgSO_4$) and evaporation of the solvent yielded 45.5 g (0.23 mol, 78 %) of crude product containing a isomeric mixture of **43a** and **43b (**67:32 %) (based on GC analysis 99 % of **14** was consumed in the reaction). 5 g of the crude mixture was separated by column chromatography using diethyl ether and petroleum ether (7:3, v/v) to obtain 3.62 g (0.018 mol, 57 %) (R_f=0.7) of analytically pure **43a** and 1.13 g (0.005 mol, 17 %) (R_f=0.8) of analytically pure **43b**.

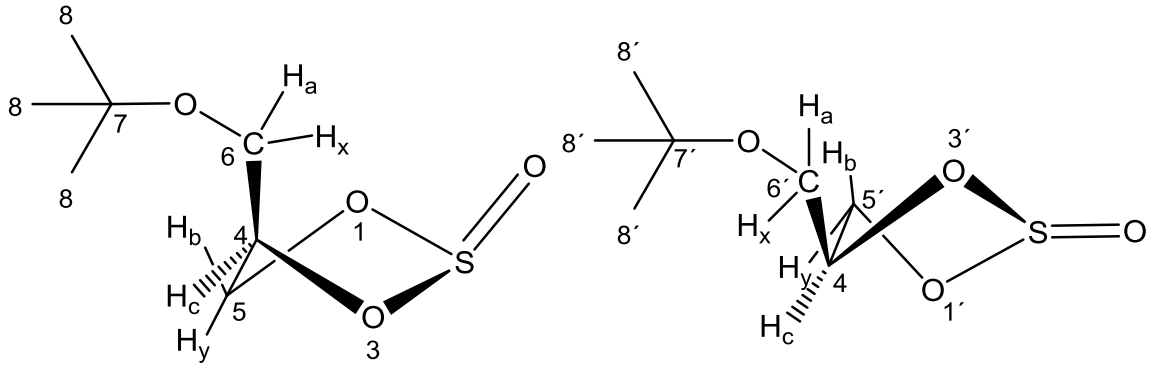

43a **43b**

^{1}H-NMR (300.1 MHz, $CDCl_3$) (*cis*-**43a**): δ = 1.18 (s, 9 H, 8-H), 3.7-3.41 (dd, 1 H, 6-H_x, $^2J_{Ha,Hx}$ = 9.76 Hz, $^3J_{Hx\text{-}anti\text{-}Hc}$ = 6.46 Hz), 3.51-3.55 (dd, 1 H, 6-H_a, $^2J_{Ha,Hx}$ of 9.74 Hz, $^3J_{Ha\text{-}syn\text{-}Hc}$ = 4.73 Hz), 4.29-4.32 (dd, 1 H, 5-H_y, $^2J_{Hb,Hy}$ = 8.42 Hz, $^3J_{Hy\text{-}syn\text{-}Hc}$ = 4.93 Hz), 4.66-4.70 (dd, 1 H, 5-H_b, $^2J_{Hb,Hx}$ = 8.45 Hz, $^3J_{Hb\text{-}anti\text{-}Hc}$ = 6.40 Hz), 4.96-5.01 ppm (m, 1 H, 4-H_c).

^{13}C-NMR (75 MHz, $CDCl_3$) (*cis*-**43a**): δ = 27.1 (q, C-8), 60.6 (t, C-6), 68.8 (t, C-5), 72.9 (s, C-7), 78.9 ppm (d, C-4).

^{1}H-NMR (300.1 MHz, $CDCl_3$) (*trans*-**43b**): δ = 1.20 (s, 9 H, 8´-H), 3.60-3.67 (m, 2 H, 6´-H_a), 3.78-3.81 (m, 1 H, 6´-H_x), 4.48-4.62 ppm (m, 3 H, 5´-H_b, H_y, H_c).

^{13}C-NMR (75 MHz, $CDCl_3$) (*trans*-**43b**): δ = 27.2 (q, C-8´), 62.9 (t, C-6´), 70 (t, C-5´), 73.8 (s, C-7´), 81.3 ppm (d, C-4´).

MS (GC/MS: Method 2) (EI, 70 eV): *m/z* (%) = 179 (25, $[M^+\text{-}CH_3]$), 121 (40, $[C_3H_5O_3S]^+$), 115 (5, $[C_6H_{11}O_2]^+$), 57.1 (100, $[C_4H_9]^+$).

IR (diamond-ATR): $\tilde{\nu}$ = 2975 (m), 2937 (w), 2911 (w), 2875 (w), 1471 (w), 1192 (s), 954 (s) cm^{-1}.

Elemental analysis:

Calculated: C 43.28, H 7.26, S 16.51; found: C 43.61, H 7.28, S 16.23

15.4: Experiments from Chapter 10

15.4.1: [(2,2-Dimethyl-1,3-dioxolan)-4yl]-methyl-4-methylbenzenesulfonate (47)

In a three-necked round bottomed flask fitted with a condenser and a mechanical stirrer 26.4 g (0.2 mol) of **26** dissolved in 50 mL of chloroform was placed. To the solution 32.4 mL (0.4 mol) of freshly distilled pyridine was added and the mixture was cooled in an ice bath. To the cooled mixture 38.5 g (0.2 mol) of freshly purified *p*-toluene sulfonyl chloride was added in 5 g portions during 30 min. The reaction was stirred for 1 h at 0 ^{o}C and allowed to stir overnight at room temperature. The resulting mixture was poured onto ice and the organic layer was thrice extracted with 50 mL of diethyl ether and dried over Na_2SO_4. Upon evaporation of the solvent 50.2 g of crude compound **47** was obtained. The crude was dissolved in 100 mL solvent mixture of diethyl ether and petroleum ether (1:2 v/v) and the solution cooled to -70 ^{o}C; the precipitated impurities were filtered off and the solvents evaporated to obtain 42 g (73 %, lit.[177] 80 %) of product **47** which was further purified by column chromatography using diethylether and petroleum ether (0.5:9.5 v/v) (R_f=1.6) to obtain **47** as a colorless viscous oil.

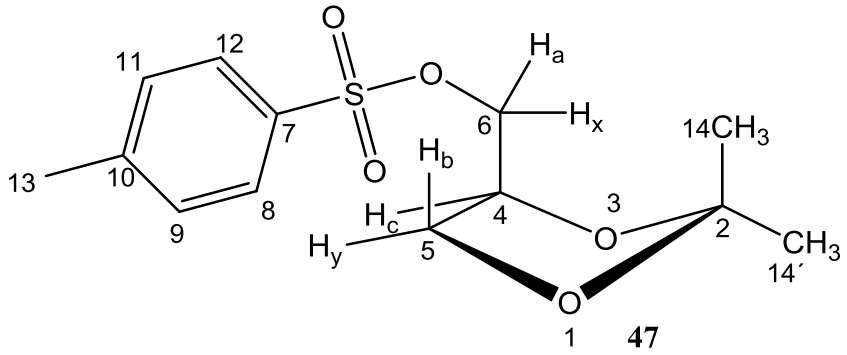

^{1}H-NMR (200 MHz, $CDCl_3$): δ = 1.16 (s, 3 H, 14-H), 1.19 (s, 3 H, 14´-H), 2.30 (s, 3 H, 13-H), 3.81-3.84 (dd, 1 H, 6-Ha, $^{2}J_{Ha,Hx}$ = 8.6 Hz, $^{3}J_{Ha\text{-}syn\text{-}Hc}$ = 4.9 Hz), 4.08-4.12 (dd, 1 H, 6-H_b, $^{2}J_{Ha,Hx}$ = 8.8 Hz, $^{3}J_{Hx\text{-}anti\text{-}Hc}$ = 6.2 Hz), 4.22-4.23 (m, 1 H, 5-H_b), 4.35-4.41 (m, 1 H, 5-H_y),

4.64-4.51 (m, 1 H, 4-H_c), 7.20-7.24 (d, 2 H, 9-H, 11-H, $^3J_{8\text{-}9}$ = 8.2 Hz), 7.63-7.65 ppm (d, 2 H, 8-H, 12-H, $^3J_{8\text{-}9}$ = 8.2 Hz).

^{13}C-NMR (101 MHz, $CDCl_3$): δ = 21.5 (q, C-14), 25.0 (q, C-14´), 26.5 (q, C-13), 66.3 (t, C-6), 69.5 (t, C-5), 72.2 (d, C-4), 110.2 (s, C-2), 127.6 (s, C-10), 129.2 (d, C-9, C-11), 132.3 (d, C-8, C-12), 145.0 ppm (s, C-7).

MS (GC/MS: Method 2) (EI, 70 eV): *m/z* (%) = 271.1 (10, $[M]^+$-CH_3]), 171 (5, $[C_7H_7O_3S]^+$), 115 (45, $[C_6H_{11}O_2]^+$), 91.0 (30, $[C_7H_7]^+$), 43.1 (100, $[C_2H_3O]^+$).

IR (diamond-ATR): $\tilde{\nu}$ = 3091 (w), 3038 (w), 2989 (m), 2941 (w), 2894 (w), 1350 (s), 1172 (s), 958 (s), 823 (s) cm^{-1}.
These analytical data are in good agreement with those reported in the literature.[177]

15.4.2: [(2,2-Dimethyl-1,3-dioxolan)-4yl]-4-methoxymethanesulfonate (50)

In a round bottomed flask fitted with a dropping funnel 13.89 g (12.9 mL, 0.1 mol) of **26** and 12 g (16.6 mL, 0.12 mol) of triethylamine were dissolved in 50 mL of dichloromethane. The reaction mixture was cooled in an ice bath and 6.3 mL (11.45 g, 0.1 mol) of methylsulfonylchoride was added dropwise during 90 min. The reaction mixture was allowed to stand for 15 h at room temperature. The resulting slurry was washed thrice with 70 mL of saturated Na_2CO_3 solution and twice with 70 mL of dist. water. The organic layer was separated and dried over Na_2SO_4 and evaporated to yield 19.6 g of orange oil. The crude was further purified by column chromatography using a 4:1(v/v) mixture of diethylether: methanol (R_f 0.73) to yield 16.48 g (0.078 mol, 74 %, lit.[179] 96 %) of **50** as an analytically pure yellowish orange colored oil.

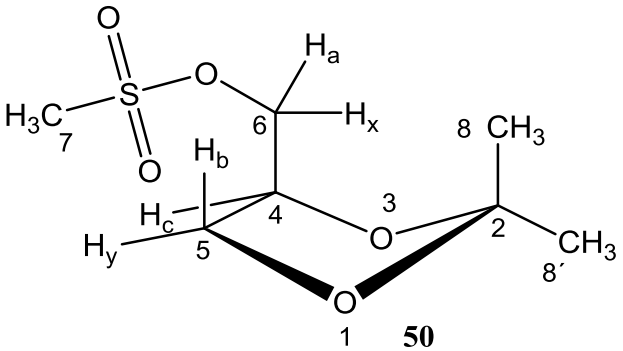

50

^{1}H-NMR (400.1 MHz, $CDCl_3$): δ = 1.37 (s, 3 H, 8-H), 1.44 (s, 3 H, 8´-H), 3.07 (s, 3 H, 7-H), 3.81-3.84 (dd, 1 H, 6-Ha, $^{2}J_{Ha,Hx}$ = 8.8 Hz, $^{3}J_{Ha\text{-}syn\text{-}Hc}$ = 5.5 Hz), 4.08-4.12 (dd, 1 H, 6-H_b, $^{2}J_{Ha,Hx}$ = 8.8 Hz, $^{3}J_{Hx\text{-}anti\text{-}Hc}$ = 6.5 Hz), 4.22-4.23 (d, 1 H, 5-H_b, $^{3}J_{Hb\text{-}syn\text{-}Hc}$ = 5.3 Hz), 4.35-4.41 (m, 1 H, 5-H_y), 4.64-4.51 ppm (m, 1 H, 4-H_c)

^{13}C-NMR (101 MHz, $CDCl_3$): δ = 25.1 (q, C-8), 26.6 (q, C-8´), 37.6 (q, C-7), 65.8 (t, C-6), 69.1 (t, C-5), 73.2 (d, C-4), 110.2 ppm (s, C-2)

MS (GC/MS: Method 2) (EI, 70 eV): *m/z* (%) = 195.1 (60, $[M]^+$-CH_3]), 115.1 (5, $[C_5H_{11}O_2]^+$), 101 (45, $[C_5H_9O_2]^+$), 79.0 (30, $[CH_3SO_2]^+$), 43.1 (100, $[C_2H_3O]^+$).

IR (diamond-ATR): $\tilde{\nu}$ = 2989 (m), 2941 (w), 2894 (w), 1350 (s), 1172 (s), 958 (s), 823 (s) cm^{-1}.
These data agree with those reported in the literature.[179]

15.4.3: 1-Azido-2,3-propanediol isopropylidene ketal (51)

Synthesis 1

14 g (0.06 mol) of 2,2-dimethyl-1,3-dioxolan-4-methoxymethanesulfonate **(50)** was dissolved in 25 mL of dimethylformamide and a solution of 5.1 g (0.078 mol) of sodium azide in 20 mL of water was added and the mixture refluxed at 110 ^{o}C for 6 h. The product mixture was allowed to cool and washed twice with 15 mL of saturated sodium chloride solution and extracted five times with 20 mL diethyl ether. The organic layer was evaporated to half its volume and washed twice with 10 mL water, dried over Na_2SO_4 and evaporated to obtain 8.85 g (94 %) of a yellow oil. The crude mixture was subjected to further purification by column chromatography using pentane and diethylether (1:1, v/v) (R_f=0.62) to obtain 8.55 g (92 %, 0.054 mol, lit.[179] 96 %) of **51** as a colorless oil.

Synthesis 2

4.87 g (0.017 mol) of [2,2-dimethyl-1,3-dioxolan)-4-yl]-methyl-4-methylbenzene sulfonate **(47)** was dissolved in 28 mL of dimethylformamide, a solution of 5.1 g (0.078 mol) of sodium azide in 21 mL of water was added, and the mixture was refluxed at 110 ^{o}C for 6 h. The reaction mixture was allowed to cool and washed twice with 15 mL of a saturated sodiumchloride solution and extracted five times with 20 mL of diethyl ether. The organic layer was evaporated to half of its volume and washed twice with 10 mL of water, dried

($MgSO_4$) and evaporated to obtain 4.1 g (due to DMF in the product) of yellow oil. The crude mixture was subjected to further purification by column chromatography using a 8:2 (v/v) pentane: diethylether mixture (R_f=0.41) to obtain 2.16 g (80.9 %, 0.013 mol) of **51** as a colourless oil.

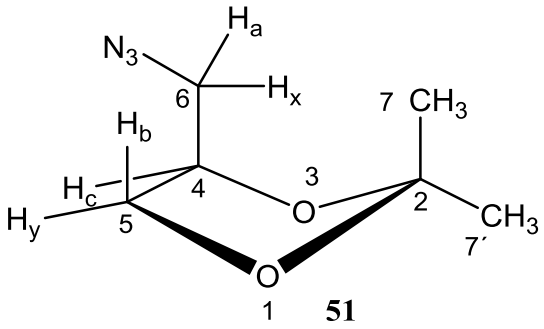

51

^{1}H-NMR (400.1 MHz, $CDCl_3$): δ = 1.36 (s, 3 H, 8-H), 1.46 (s, 3 H, 8´-H), 3.27-3.33 (dd, 1 H, 6-Ha, $^2J_{Ha,Hx}$ = 12.8 Hz, $^3J_{Ha\text{-}anti\text{-}Hc}$ = 5.47 Hz), 3.37-3.43 (dd, 1 H, 6-H_x, $^2J_{Ha,Hx}$ = 12.8 Hz, $^3J_{Hx\text{-}syn\text{-}Hc}$ = 4.7 Hz), 3.75-3.8 (dd, 1 H, 5-H_y, $^2J_{Hb,Hy}$ = 8.41 Hz, $^3J_{Hy\text{-}syn\text{-}Hc}$ = 5.93 Hz), 4.03-4.08 (dd, 1 H, 5-H_b, $^2J_{Hb,Hy}$ = 8.41 Hz, $^3J_{Hb\text{-}anti\text{-}Hc}$ = 6.41 Hz), 4.2-4.3 ppm (m, 1 H, 4-H_c)

^{13}C-NMR (101 MHz, $CDCl_3$): δ = 24.7 (q, C-8), 26.1 (q, C-8´), 52.3 (t, C-6), 66.1 (t, C-5), 74.0 (d, C-4), 109.4 ppm (s, C-2)

MS (GC/MS: Method 2) (EI, 70 eV): *m/z* (%) = 157 (5, $[M]^+$), 142 (70, $[C_4H_8O_2N_3]^+$), 127 (15, $[C_4H_7O_2N_3]^+$), 72 (35, $[C_3H_4O_2]^+$), 56 (65, $[C_3H_4O]^+$), 43 (100, $[C_2H_3O]^+$).

IR (diamond-ATR): $\tilde{\nu}$ = 2988 (m), 2937 (w), 2885 (w), 2097 (s), 1373 (m), 1260 (s), 1212 (s), 1075 (s), 1052 (s), 835 (s) cm^{-1}.

These analytical data are in good agreement with those reported in the literature.[179]

15.4.4: 1-Amino-2,3-propanediol isopropylidene ketal (48)

Procedure 1

3 g (0.019 mol) of **51** was dissolved in 5 mL of methanol and the solution was added to a solution of 5.73 g (0.023 mol) $Na_2S(H_2O)_9$ in 10 mL of H_2O. The reaction mixture was heated at 55 ^oC for 24 h, 10 mL of saturated NaCl solution was added to the resulting homogenous yellow-orange reaction mixture, and it was extracted 5 times with 20 mL diethyl ether. The organic layer was dried ($MgSO_4$) and the solvent was evaporated to obtain 2.26 g

of a thick orange oil. The crude was subjected to column chromatography using a 4:1 (v/v) pentane: methanol mixture (R_f=0.1) to yield **48** (1.91 g, 0.014 mol, 76 %, lit.[179] 93 %) as an analytically pure yellow oil.

Procedure 2

3 g (0.019 mol) of **58** was dissolved in 5 mL of methanol and hydrogenated with hydrogen gas using 150 mg (5 mol %) of Pt/C as catalyst for 12 h. To the reaction mixture 10 mL of saturated NaCl solution was added and extracted 5 times with 20 mL of diethylether. The organic layer was dried over $MgSO_4$ and evaporated to yield an yellow oil. The crude mixture was purified by column chromatography using pentane and methanol mixture (4:1 v/v) (R_f=0.1) to yield 1.7 g (0.013 mol, 68 %) of an analytically pure yellow oil.

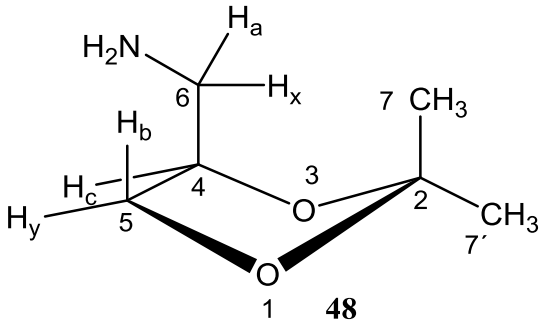

48

^{1}H-NMR (200.1 MHz, $CDCl_3$): δ = 1.35 (s, 3 H, 7-H), 1.42 (s, 3 H, 7´-H),1.44-1.45(s_b, 2 H, N-H), 2.75-2.80 (m, 2 H, 6-H_a, H_x), 3.68-3.72 (dd, 1 H, 5-H_y, $^2J_{Hb,Hx}$ = 8.02 Hz, $^3J_{Hy\text{-}syn\text{-}Hc}$ = 6.47 Hz), 4.03-4.05 (dd, 1 H, 5-H_b, $^2J_{Hb,Hx}$ = 8.01 Hz, $^3J_{Hb\text{-}anti\text{-}Hc}$ = 6.82 Hz), 4.11-4.19 ppm (m, 1 H, 4-H_c).

^{13}C-NMR (50.1 MHz, $CDCl_3$): δ = 26.7 (q, C-8), 28.1 (q C-8´), 44. (t, C-6), 67.1 (t, C-5), 78.0 (d, C-4), 114.2 ppm (q, C-2)

MS (GC/MS: Method 2) (EI, 70 eV): *m/z* (%) = 131.0 (5, $[M]^+$), 116.0 (40, $[C_5H_{11}O_2N]^+$), 101 (65, $[C_5H_9O_2N]^+$), 73 (70, $[C_3H_5O_2]^+$), 56 (70, $[C_3H_4O]^+$), 43.1 (100, $[C_2H_3O]^+$).

IR (diamond-ATR): $\tilde{\nu}$ = 3374-3306 (w_b), 2986 (m), 2936 (w), 2875 (w), 1672 (w), 1371 (m), 1211 (s), 1057 (s) cm^{-1}.

15.4.5: 3-*tert*-Butoxypropane-1,2-bis-(dimethylsulfonate) (52, 53)

A solution of 25 g of **14** (0.16 mol) in 100 mL of dichloromethane was placed in a round bottomed flask fitted with a dropping funnel; the flask was cooled with an ice bath and 40.87 g (0.40 mol) of freshly distilled triethylamine was added. To the mixture 42.5 g (0.372 mol) of dimethylsulfonylchloride was introduced dropwise during a period of 90 min. The reaction mixture was allowed to warm to room temperature and stirred overnight. The product mixture was poured onto ice and was twice extracted with 50 mL of dichloromethane. The organic layer was separated and washed with saturated Na_2CO_3 solution and washed twice with dist. water. After drying over $MgSO_4$, dichloromethane was evaporated to obtain 37.6 g (0.138 mol, 81 %) of **52** and **53** as a yellow oil. The compound was used without further separation (see Chapter 10.4 for explanation).

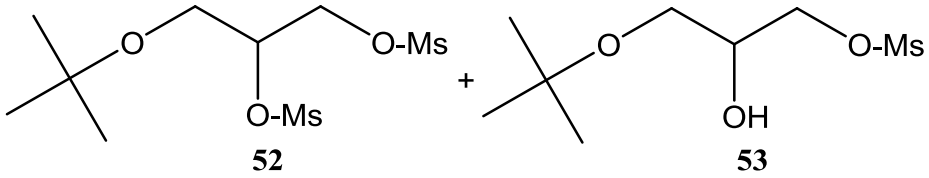

52 **53**

15.4.6: 1,2-Diazo-3-*tert*-butoxypropane (56), 1-Azido-3-*tert*-butoxypropane-2-ol (57)

35 g (0.129 mol) of a mixture of **52** and **53** was dissolved in 50 mL of dimethylformamide and a solution of 20.15 g (0.31 mol) of sodium azide in 80 mL water was added, and the mixture refluxed at 110 ^{o}C for 6 h. The reaction mixture was allowed to cool down and washed twice with 40 mL of saturated sodium chloride solution and extracted five times with 50 mL of diethyl ether. The organic layer was evaporated to half its volume and washed twice with 30 mL of water, dried over Na_2SO_4 and the solvent was evaporated to obtain 18.55 g (73 %) of a yellow oil. 5 g of the crude mixture was subjected to further purification by column chromatography with diethylether and pentane (7:3, v/v) to yield 3.24 g (47 %, 0.06 mol) of 1,2-diazo-3-*tert*-butoxypropane **(56)** as a colourless oil (R_f=0.86) and 1.58 g (27 %, 0.034 mol) of 1-azo-3-*tert*-butoxypropane-2-ol **(57)** as a colourless oil (R_f=0.75).

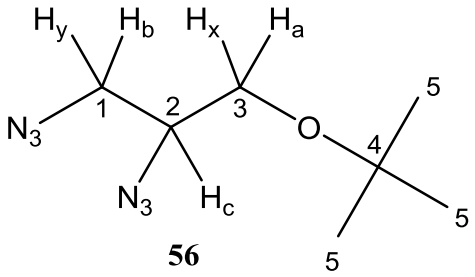

56

^{1}H-NMR (200.1 MHz, $CDCl_3$) **(63)**: δ = 1.21 (s, 9 H, 5-H), 3.27-3.61 ppm (m, 5 H, 1-H_b, H_y, 3- H_a, H_x, 2-H_c).

^{13}C-NMR (50 MHz, $CDCl_3$) **(63)**: δ = 27.8 (q, C-5), 52.2 (t, C-1), 61.3 (d, C-2), 62.4 (t, C-3), 74.4 ppm (s, C-4)

MS (GC/MS: Method 2) (63) (EI, 70 eV): *m/z* (%) = 198 (2, $[M]^+$), 171.0 (2, $[C_5H_{10}ON_6]^+$), 156.0 (2, $[C_4H_8ON_6]^+$), 142 (2, $[C_3H_5ON_6]^+$), 57 (100, $[C_4H_9]^+$).

IR (Diamond-ATR) **(63)**: $\tilde{\nu}$ = 2976 (m), 2935 cm^{-1} (w), 2873 cm^{-1} (w), 2092 (s), 1267 (m), 1192 (m), 1023 (m), 667 (m), 555 (m) cm^{-1}.

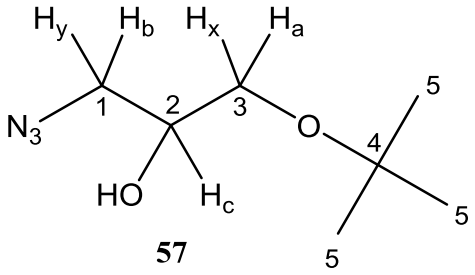

57

^{1}H-NMR (200.1 MHz, $CDCl_3$) **(63)**: δ = 1.21 (s, 9 H, 5-H), 2.9 (1 H, 2-OH), 3.31-3.68 (m, 5 H, 1-H_b, H_y, 3- H_a, H_x), 3.85-3.99 ppm (m, 1 H, 2-H_c).

^{13}C-NMR (50 MHz, $CDCl_3$) **(63)**: δ = 27.2 (q, C-5), 53.4, 53.8 (t, C-1), 65.7 (t, C-3), 69.4, 69.8 (d, C-2), 73.4 ppm (s, C-4).

MS (GC/MS: Method 2) (64) (EI, 70 eV): *m/z* (%) = 173.1 (2, $[M]^+$), 117.0 (10, $[C_3H_7O_2N_3]^+$), 57 (100, $[C_4H_9]^+$).

IR (diamond-ATR) **(64)**: $\tilde{\nu}$ = 3412 (w), 2976 (m), 2932 cm^{-1} (w), 2874 cm^{-1} (w), 2092 (s), 1268 (m), 1192 (m), 1023 (m), 877 (m), 554 (m) cm^{-1}.

15.4.7: 1,2-Diamino-3-*tert*-butoxy propane (58)

824 mg (5.6 mmol) of **57** was dissolved in 10 mL of methanol and the solution was added to a solution of 1.42 g (5.6 mmol) $Na_2S(H_2O)_9$ in 10 mL of H_2O. The reaction mixture was heated at 55 ^oC for 36 h. 10 mL of saturated NaCl solution was added to the resulting colourless mixture and it was extracted 5 times with 20 mL diethyl ether. The organic layer was dried over Na_2SO_4 and evaporated to yield (710 mg, 4.86 mmol, 92 %) **58** as a thick yellow liquid.

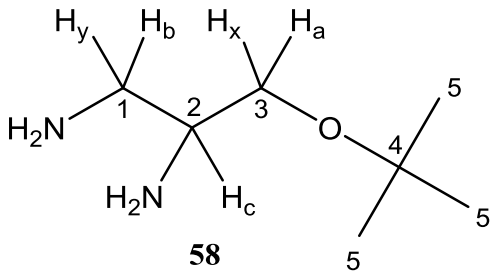

58

^{1}H-NMR (200.1 MHz, C_3D_6O): δ = 1.15 (s, 9 H, 5-H), 2.8-3.81 ppm (m, 5 H, 1-H_b, H_y, 3-H_a, H_x, 2-H_c).

^{13}C-NMR (50 MHz, C_3D_6O): δ = 27.6 (q, C-5), 49.4 (t, C-1), 64.9 (d, C-2), 72.9 (t, C-3), 76.4 ppm (s, C-4)

MS (GC/MS: Method 2) (EI, 70 eV): *m/z* (%) = 116 (50, $[M^+-CH_4N]^+$), 90 (15, $[C_3H_{10}ON_2]^+$), 72 (35, $[C_3H_8N_2]^+$), 60 (50, $[C_2H_8N_2]$), 57 (100, $[C_4H_9]^+$).

IR (diamond-ATR): $\tilde{\nu}$ = 3356-3275 (w), 2972 (m), 2931 (w), 2872 cm^{-1} (w), 1633 (w), 1389 (m), 1195 (s), 1021 (s) cm^{-1}.

15.4.8: 1-(9,9-Dimethyl-8,10-dioxolan-6-methyl)-4-phenyl-1*H*-1,2,3-triazole (60)

Procedure 1

In a round bottomed flask equipped with a mechanical stirrer 1 g (0.0064 mol) of **51** and 0.784 g (0.007 mol) of phenylacetylene were suspended in a 5 mL of 1:1 solution of *tert*-butanol and water. To the suspension 0.42 mL of 0.3 M $CuSO_4$ solution in water and 0.64 mL of 1 M sodium ascorbate solution in water were added, and the mixture was stirred for 20 h. The resulting mixture was cooled in an ice bath and 20 mL of water was added. A whitish-

yellow coloured powder precipitated. The powder was filtered off and washed thrice with ice cold water and dried to obtain 893 mg of greenish-white crude product. The product was several times reprecipitated in methanol to obtain 435 mg (0.016, 34 %) of **67** as analytically pure white amorphous powder.

Procedure 2

In a round bottomed flask 54 mg of Cu powder (Jennesen-45 micron) and 30 mg of activated charcoal were placed and 85 mg (0.54 mmol) of **51** dissolved in 1 mL of dioxane and 1 mL of triethylamine were added and well agitated in an ultrasonic sound bath. To the reaction mixture 1 mL of phenyl acetylene was added dropwise and the reaction mixture was stirred overnight. The resulting product mixture was filtered through a celite pad to remove the catalyst and the charcoal. Excess reactants were evaporated under vacuum and the resulting powder was washed twice with 5 mL of water and was filtered to obtain 103 mg (0.39 mmol, 72 %) of **67** as analytically pure white amorphous powder (m.p. 110-112 ^{o}C)

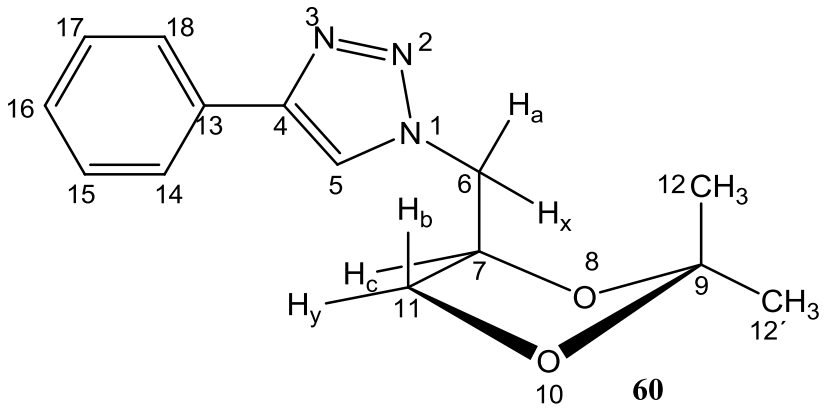

60

^{1}H-NMR (200.1 MHz, $CDCl_3$): δ = 1.41 (s, 3 H, 12-H), 1.45 (s, 3 H, 12´-H), 3.67-3.71 (dd, 1H, 6-H_a, $^{2}J_{Ha,Hx}$ = 9.1 Hz, $^{3}J_{Ha,Hc}$ = 5.83), 4.03-4.07 (dd, 1H, 6-H_x, $^{2}J_{Ha,Hx}$ = 8.72 Hz, $^{3}J_{Hx,Hc}$ = 6.2), 4.38-4.54 (m, 3 H, 11-H_b, H_y, 7-H_c), 7.35-7.52 (m, 3 H, 15-H, 16-H, 17-H), 7.87 (d, 1 H, 14-H, $^{3}J_{14\text{-}H,\ 15\text{-}H}$ = 2 Hz), 7.91-7.92 (d, 1 H, 18-H, $^{3}J_{18\text{-}H,\ 17\text{-}H}$ = 2 Hz), 7.96 ppm (s_b, 1 H, 5-H).

^{13}C-NMR (50.1 MHz, $CDCl_3$): δ = 25.21 (q, C-12), 26.69 (q, C-12´), 52.2 (t, C-6), 66.4 (t, C-11), 74.1 (d, C-7), 110.2 (s, C-9), 120.9 (d, C-5), 125.7 (d, C-14), 125.8 (d, C-18), 128.1 (d, C-16), 128.8 (d, C-15, 17), 130.5 (s, C-13), 147.7 ppm (s, C-4).

MS (GC/MS: Method 2) (EI, 70 eV): *m/z* (%) = 259.2 (100, $[M]^+$), 244.1 (80, $[C_{13}H_{14}N_3O_2]^+$), 230.1 (35, $[C_{12}H_{12}N_3O_2]^+$), 144.1 (55, $[C_8H_6N_3]^+$), 116.1 (75, $[C_6H_{12}O_2]^+$), 102 (40, $[C_5H_{10}O_2]^+$), 77.1 (25, $[C_6H_5]^+$), 43.0 (80, $[C_2H_3O]^+$).

IR (diamond-ATR): $\tilde{\nu}$ = 3145 (w), 2992 (w), 2950 (w), 1462 (w), 1376 (m), 1041 (m), 1023 (s), 833 (s) cm^{-1}.

Elemental analysis:

Calculated: C 64.85, H 6.61, N 17.20; found: C 64.85, H 6.31, N 17.77

15.4.9: 1,1'-(8-*tert*-butoxypropane-6,7-diyl)-bis-(4-phenyl-1*H*-1,2,3-triazole) (61)

In a round bottomed flask 100 mg of Cu powder (Jennesen-45 micron) and 100 mg of activated charcoal were placed and a solution of 990 mg (0.5 mmol) of **56** dissolved in 5 mL of dioxane and 1.2 g of triethylamine was added. The reaction mixture was well agitated in a ultrasonic sound bath. To the reaction mixture 1.2 g (0.012 mol) of phenylacetylene was added dropwise, it was stirred overnight. The resulting product mixture was filtered through a celite pad to remove the catalyst and excess reactants were evaporated under vacuum. The resulting powder was washed twice with 10 mL of water and was filtered off to obtain 1.67 g (0.4 mmol, 83 %) of analytically pure white amorphous powder (m.p. 165 ^oC).

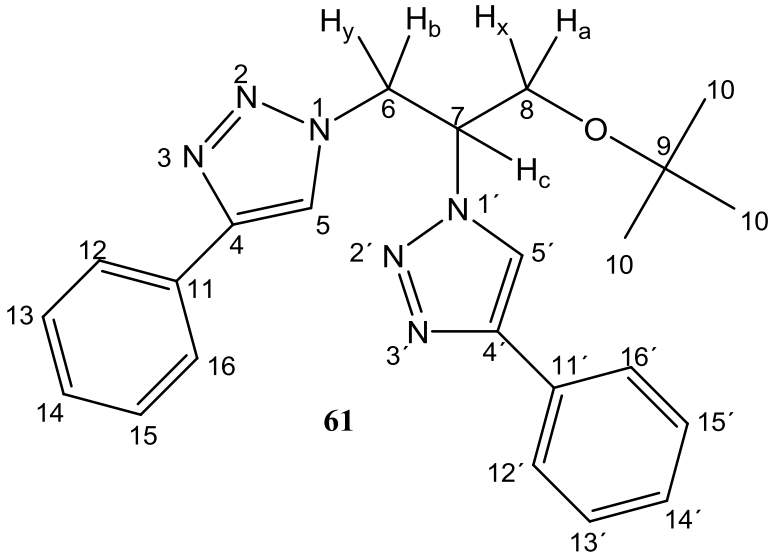

61

^{1}H-NMR (400.1 MHz, $CDCl_3$): δ = 1.18 (s, 9 H, 5-H), 3.7-3.83 (dd, 1 H, 6-H_a, $^2J_{Ha,Hx}$ = 9.65 Hz, $^3J_{Ha,Hc}$ = 5.86), 3.89-3.93 (dd, 1 H, 6-H_x, $^2J_{Ha,Hx}$ = 9.64 Hz, $^3J_{Hx,Hc}$ = 5.16), 5.0-5.15 (m, 1 H, 7-Hc), 5.16-5.25 (m, 2 H, 8-H_a, H_x), 7.27-7.41 (m, 6 H, 13H-15-H, 13´-15´-H), 7.54 (s_b, 2

H, 5-H, 5´-H), 7.6-7.7 (d, 2 H, 12-H, 12´-H, $^{3}J_{12\text{-H, }13\text{-H}}$ = 7 Hz), 7.7-7.8 ppm (d, 2 H, 16-H, 16´-H, $^{3}J_{16\text{-H, }15\text{-H}}$ = 8 Hz)

^{13}C-NMR (100.1 MHz, $CDCl_3$): δ = 27.30 (q, C-10), 50. 63 (t, C-8), 61.5 (d, C-7), 61.8 (t, C-6), 74.3 (s, C-9), 125.7 (d, C-12, 12´, 16, 16´), 128.2 (d, C-13, 15, 13´, 15´), 128.3 (d, C-13, 15, 13´, 15´), 128.7, 128.8 (d, C-14, 14´), 130 (s, C-4,C-4´), 130.2 ppm (s, C-11, C-11´)

MS (GC/MS: Method 2) (EI, 70 eV): *m/z* (%) = 402.0 (35, $[M]^+$), 317.0 (40, $[C_{18}H_{17}N_6]^+$), 287 (75, $[C_{15}H_{21}ON_5]^+$), 259 (100, $[C_{15}H_{21}ON_3]^+$), 202 (25, $[C_7H_{18}ON_6]^+$), 173 (20, $[C_{10}H_{11}N_3]^+$), 159 (25, $[C_9H_9N_3]^+$), 144 (25, $[C_8H_6N_3]^+$), 116 (85, $[C_7H_{16}O]^+$), 57.8 (95, , $[C_4H_9]^+$).

IR (diamond-ATR): $\tilde{\nu}$ = 3084 (w), 2971 (m), 2937 (w), 2879 (w), 1464 (w), 1352 (m), 1221 (m), 1087 (s) cm^{-1}.

Elemental analysis:

Calculated: C 68.63, H 6.51, N 20.88; found: C 68.38, H 6.51, N 21.07

15.5: Experiments from Chapter 11

15.5.1: 1,2,3-Tris-(diethylaminomethoxy)propane (65)

9.2 g (0.1 mol) of glycerol **(2)** was placed in a 100 mL round bottomed flask, 24 g (0.33 mol) of diethyl amine **(64)** was added and the mixture was stirred well to dissolve the compound. The flask was cooled in an ice bath and 9.9 g (0.33 mol) paraformaldehyde **(63)** was slowly introduced during 10 min while care was taken to maintain the temperature below 30 ^{o}C. The reaction was allowed to warm to the room temperature and when a clear solution had formed 13 g of potassium carbonate was added to the mixture during a period of 90 min. The mixture was allowed to stir overnight and it was filtered and washed twice with 100 mL diethyl ether to obtain a product mixture of 42.3 g, further purification of which was performed by distilling off the side product **66** at 30 ^{o}C and 0.2 mbar (lit.[24p] 166-169 ^{o}C) to obtain 33.8 g (0.09 mol, 96 %) (lit.[164] 11 %) of **65** as a colorless oil.

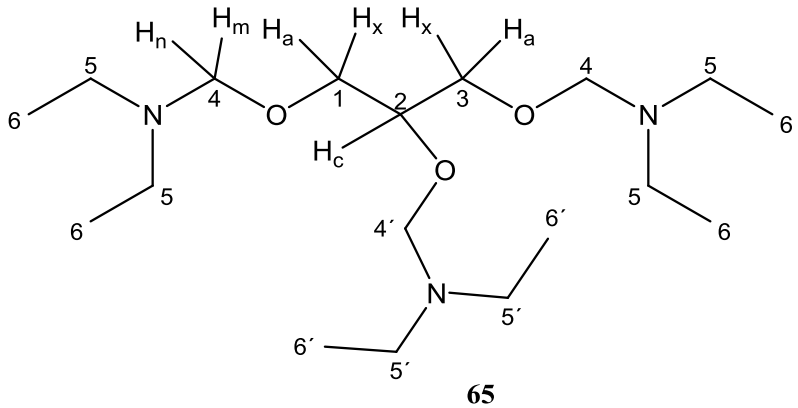

65

^{1}H-NMR (400.1 MHz, $CDCl_3$): δ = 1.05-1.09 (m, 18 H, 6-H, 6´-H), 2.54-2.62 (m, 12 H, 5-H, 5´-H), 3.41-3.61 (m, 5 H, 1, 3-H_a, H_x, 2-H_c), 4.15 and 4.22 (s, 4 H, 4-H_m, H_n), 4.38 ppm (s, 2 H, 4´-H_m, H_n).

^{13}C-NMR (101 MHz, $CDCl_3$): δ = 12.3 (q, C-6´), 13.0 (q, C-6), 45.0, 45.2 (t, C-5´, C-5), 68.7 (t, C-1), 71.7 (t, C-3), 75.8 (d, C-2), 83.9 (t, C-4´), 84. 6 (t, C-4), 85.8 ppm (t, C-4).

MS (GC/MS: Method 2) (EI, 70 eV): *m/z* (%) = 275 (2, $[M^+-C_4H_{10}N]$), 261 (5, $[C_{13}H_{29}O_3N_2]^+$), 231 (2, $[C_{12}H_{27}O_2N_2]^+$), 176 (20, $[C_8H_{20}O_2N_2]^+$), 160 (35, $[C_8H_{18}O_2N]^+$), 146 (15, $[C_7H_{16}O_2N]^+$), 102 (45, $[C_5H_{12}ON]^+$),85 (100, $[C_5H_{11}N]^+$).

IR (diamond-ATR): $\tilde{\nu}$ = 2968 (m), 2932 (w), 2872 (w), 2842 (w), 2805 (w), 1469 (w), 1378 (m), 1205 (m), 1064 (s) cm^{-1}.

15.5.2: 1,2-Bis-(diethylaminomethoxy)-3-*tert*-butoxy propane (67)

14.6 g (0.1 mol) of **14** was placed in a 100 mL round bottomed flask, 15.2 g of diethyl amine **(64)** (0.26 mol) was added, and the mixture was stirred well. The flask was cooled in an ice bath and 6.5 g (0.26 mol) paraformaldehyde **(63)** was slowly introduced during 10 min while care was taken to maintain the temperature below 30 ^{o}C. The reaction was allowed to warm to the room temperature and when a clear solution had formed 13 g of potassium carbonate was added to the reaction mixture during a period of 90 min. The mixture was stirred overnight and was filtered and washed twice with 100 ml diethyl ether to obtain a product mixture of 35.8 g. Further purification was performed by removing the side product **66** at 30 ^{o}C and 0.2 mbar (lit.[24p] 166-169 ^{o}C) to obtain 94 % (30.6 g, 0.09 mol) of **67** as a colorless oil.

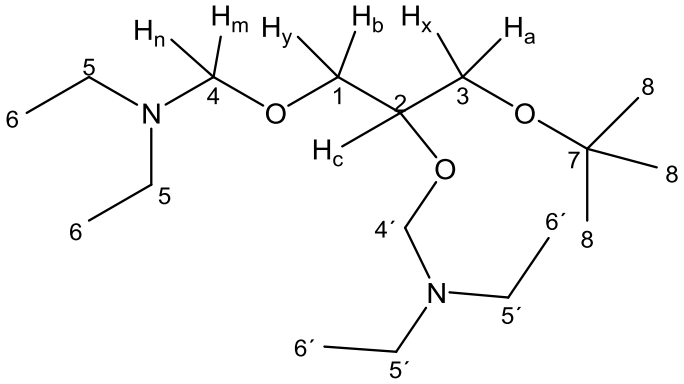

67

^{1}H-NMR (200.1 MHz, $CDCl_3$): δ = 0.72-0.79 (m, 12 H, 6-H, 6´-H), 0.86 and 0.87 (s, 9 H, 8-H), 2.35-2.42 (m, 8 H, 5-H, 5´-H), 2.95-3.8 (m, 5 H, 3-H_a, H_x, 1-H_b, H_y, 2-H_c), 4.071-4.076 (d, 2 H, 4-H_m, H_n), 4.09-4.10 ppm (d, 2 H, 4´-H_m, H_n).

^{13}C-NMR (50 MHz, $CDCl_3$): δ = 11.4 (q, C-6´), 12.3 (q, C-6), 26.6 (q, C-8), 43.9, 44.3 (t, C-5´, C-5), 68.2 (t, C-1), 69.2 (t, C-3), 75.4 (d, C-2), 76.3 (d, C-2), 83.2 (t, C-4´), 83. 8 (t, C-4), 85.3 ppm (t, C-4).

MS (GC/MS: Method 2) (EI, 70 eV): *m/z* (%) = 173 (2, $[M^+-C_4H_{10}N]$), 147 (5, $[C_7H_{14}O_3]^+$), 117 (2, $[C_7H_{17}O]^+$), 100 (20, $[C_6H_{12}O]^+$), 57 (100, $[C_4H_{10}]^+$).

IR (diamond-ATR): $\tilde{\nu}$ = 2971 (m), 2932 (w), 2872 (w), 2842 (w), 2805 (w), 1469 (w), 1378 (m), 1205 (m), 1076 (s) cm^{-1}.

15.5.3: 2,2-Dimethyl-(4-diethylaminomethoxymethy)-1,3-dioxolane (68)

A mixture of 13.2 g (0.1 mol) **26** and 7.6 g of **64** (0.13 mol) was placed in a round bottomed flask. The flask was cooled in an ice bath and 3.9 g (0.13 mol) of **63** was slowly introduced during a period of 10 min while care was taken to maintain the temperature below 10 ^{o}C. The reaction was allowed to warm to room temperature, and when a clear solution had formed 13 g of potassium carbonate was slowly introduced during 90 min. The reaction mixture was allowed to stir overnight. The product mixture was filtered, and was dissolved in diethyl ether and dried over Na_2SO_4. The solvent was evaporated to obtain 24.3 g of crude product. Further purification was performed by distilling off the side product **66** at 30 ^{o}C and 0.2 mbar (lit.[24p] 166-169 ^{o}C) to obtain 21.2 g (0.09 mol, 98 %) of **68** as a colorless oil.

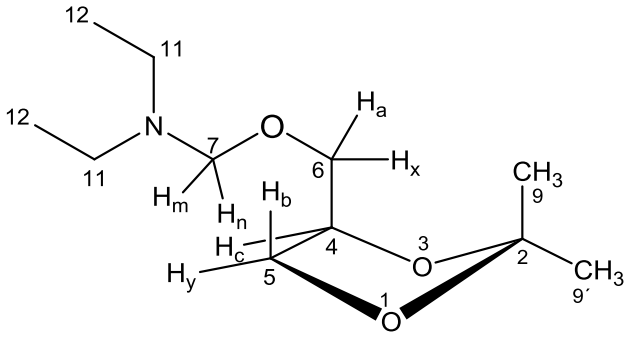

68

^{1}H-NMR (400.1 MHz, $CDCl_3$): δ = 1.04-1.08 (m, 6 H, 12-H), 2.69-2.74 (m, 4 H, 11-H), 1.35-1.36 (s, 3 H, 9-H), 1.41-1.43 (s, 3 H, 9´-H), 3.40-3.44 (dd, 1 H, 6-H_a, $^2J_{Ha,Hx}$ = 10.09 Hz, $^3J_{Ha\text{-}anti\text{-}Hc}$ = 5.91), 3.47-3.51 (dd, 1 H, 6-H_x, $^2J_{Ha,Hx}$ = 10.09, $^3J_{Hx\text{-}syn\text{-}Hc}$ = 5.17 Hz), 3.74-3.77 (m, 1 H, 5-H_b), 4.02-4.06 (m, 1 H, 6-H_y), 4.1-4.27 (m, 1 H, 4-H_c), 4.24 ppm (d, 2 H, 7-H_m, H_n).

^{13}C-NMR (101 MHz, $CDCl_3$): δ = 13.0 (q, C-9), 25.1 (q, C-11), 26.6 (q, C-11´), 45.1 (t, C-8), 66.8 (t, C-6), 68.7 (t, C-5), 74.8 (d, C-4), 85. 0 (t, C-7), 109.0 ppm (s, C-2).

MS (GC/MS: Method 2) (EI, 70 eV): *m/z* (%) = 216.3 (2, $[C_{11}H_{22}O_3N]^+$), 202.2 (5, $[C_{10}H_{20}O_3N]^+$), 188.2 (2, $[C_9H_{18}O_3N]^+$), 172.1 (2, $[C_8H_{14}O_3N]^+$), 159.1 (20, $[C_7H_{14}O_3N]^+$), 145.1 (15, $[C_7H_{15}O_2N]^+$), 117.1 (40, $[C_6H_{13}O_2]^+$), 101 (20, $[C_5H_{11}O]^+$), 86.1 (100, $[C_5H_{12}N]^+$), 72 (10, $[C_4H_{11}O]^+$), 43.1 (100, $[C_4H_9]^+$)

IR (diamond-ATR): $\tilde{\nu}$ = 2971 (m), 2933 (w), 2873 (w), 1455 (w), 1372 (m), 1212 (m), 1054 (s) cm^{-1}.

15.6: Experiments from Chapter 12

15.6.1: 1,3,5-Trisbutylperhydro-1,3,5-triazine (73)

A mixture of 13.2 g (0.1 mol) **26** and 7.6 g of **71** (0.1 mol) was placed in a round bottomed flask. The flask was cooled in an ice bath and 3.14 g (0.1 mol) of **63** was slowly introduced during a period of 10 min while care was taken to maintain the temperature below 10 ^oC. The reaction mixture was allowed to warm to room temperature and when a clear solution had formed 13 g of potassium carbonate was slowly introduced to the reaction mixture within 90 min. The reaction was allowed to stir overnight and was extracted with diethyl ether. The solvent was evaporated to obtain 19.6 g of crude product. Further purification was performed

by column chromatography using diethyl ether (Rf=0.43) to obtain 8.24 g (0.03 mol, 97 % with respect to formaldehyde) of **73** as a yellow oil.

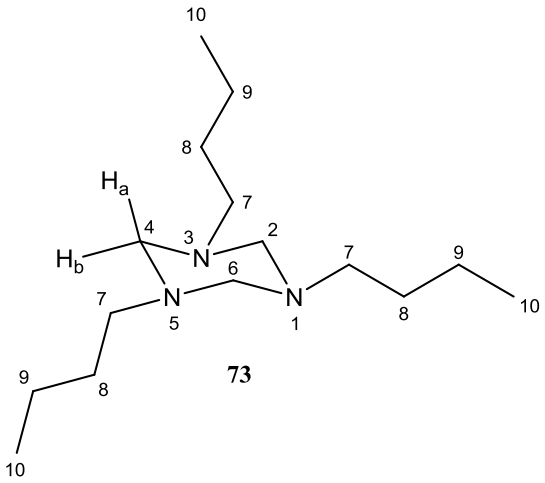

73

^{1}H-NMR (200 MHz, $CDCl_3$): δ = 0.80-0.87 (t, 9 H, 10-H, $^{3}J_{9\text{-}10}$ = 7.07 Hz), 1.20-1.40 (m, 12 H, 9-H, 8-H), 2.29-2.36 (t, 6 H, 7-H, $^{3}J_{7\text{-}8}$ = 7.83 Hz), 3.22 ppm (sb, 6 H, 2,3,6-H_a, H_b).

^{13}C-NMR (100.1 MHz, $CDCl_3$): δ = 13.96 (q, C-10), 20.63 (t, C-9), 29.73 (t, C-8), 52.52 (t, C-7), 74.7 ppm (t, C-2,4,6).

MS (GC/MS: Method 2) (EI, 70 eV): *m/z* (%) = 253 (10, $[M]^+$), 170 (50, $[C_{10}H_{21}N_2]^+$), 98 (50, $[C_6H_{12}N]^+$), 86 (100, $[C_5H_{12}N]^+$), 84 (100, $[C_5H_{10}N]^+$), 75 (10, $[C_4H_{11}O]^+$), 57.1 (100, $[C_4H_9]^+$).

IR (diamond-ATR): $\tilde{\nu}$ = 2956 (s), 2929 (s), 2864 (m), 2790 (mb), 1464 (m), 1370 (m), 1191 (s), 1109 (s) cm^{-1}.

These analytical data are in good agreement with those reported in the literature.[204-206]

15.6.2: 1,3,5-Triphenylperhydro-1,3,5-triazine (77)

A mixture of 13.3 g (0.1 mol) **26** and 14.02 g of **75** (0.15 mol) was placed in a round bottomed flask. The flask was cooled in an ice bath and 4.70 g (0.16 mol) **63** was slowly introduced during a period of 30 min while the temperature was kept below 10 ^{o}C. The reaction mixture was allowed to warm to room temperature and when a clear solution had formed 20.7 g of potassium carbonate was slowly introduced to the reaction mixture in a period of 90 min. The reaction mixture was allowed to stir overnight and was extracted thrice with 50 mL of diethyl ether. The compound was dried over Na_2SO_4 and the solvent was

evaporated to obtain 19.6 g of crude product. Further purification was performed by column chromatography using diethyl ether (Rf=0.26) to obtain 14.8 g (0.04 mol, 95% with respect to formaldehyde) of **77** as a white amorphous solid.

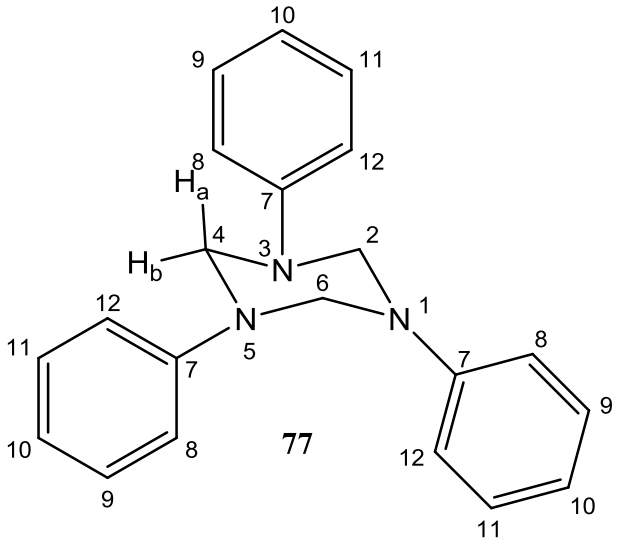

^{1}H-NMR (200 MHz, $CDCl_3$): δ = 4.88 (sb, 6 H, 2,3,6-H_a, H_b), 6.81-6.90 (t, 3 H, 10-H, ^3J =7.22 Hz), 6.98-7.03 (d, 6 H, 8-H, 12-H, ^3J =7.75 Hz), 7.15-7.25 ppm (m, 6 H, 9-H, 11-H).

^{13}C-NMR (100.1 MHz, $CDCl_3$): δ = 68.5 (t, C-2,4,5), 117.6 (d, C-8, C-12), 120.9 (d, C-10), 129.1 (d, C-9, C-11), 148.8 ppm (s, C-7).

MS (GC/MS: Method 2) (EI, 70 eV): *m/z* (%) = 210 (50, $[M^+ - C_7H_8N]$), 105 (100, $[C_7H_7N]^+$), 77 (80, $[C_6H_5]^+$).

IR (diamond-ATR): $\tilde{\nu}$ = 3092 (w), 3068 (w), 3036 (w), 2849 (w), 1594 (m), 1494 (m), 1201 (s), 1127 (s) cm^{-1}.

These analytical data is agrees with those reported in the literature.[204-206]

15.6.3: 1,2,3-Tris-(chloromethoxy)propane (78)

In a three necked flask fitted with a drying tube 18.4 g (0.2 mol) of glycerol **(2)** and 24 g (0.8 mol) of **63** were suspended in 170 mL of dry dichloromethane. Dry HCl was slowly bubbled through the suspension until a clear solution was observed (app. 100 min). The clear solution was stirred for 2 h under extremely dry conditions. Excess HCl was removed under reduced pressure and the resulting product mixture was dried over calcium chloride. The solvent was

evaporated to obtain 50.4 g (0.21 mol, 105 %) (due to the presence of dissolved HCl) of a yellow oil. The yellow oil was distilled by fractional distillation at 40 mbar pressure to produce three fractions, 4.85 g (100 ^{o}C, mixture), 12.2 g (160 ^{o}C, 78 %) (based on GC analysis) and 6.24 g (180 ^{o}C, 86 %) (based on GC analysis), The last two fractions (18.44 g) were collected together and redistilled at 160 ^{o}C, 34-40 mbar to obtain 6.84 g (0.029 mol, 14 %) of a **80** as a colorless oil. (The compound **80** was observed to be highly hygroscopic and decomposed during distillation)

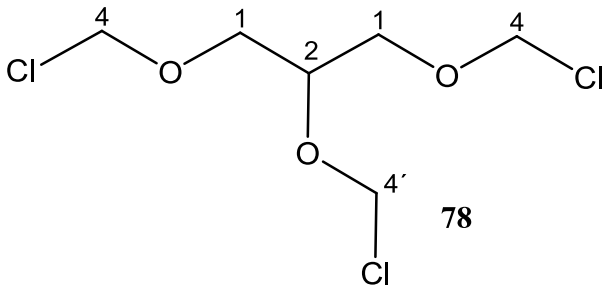

78

The boiling point of the compound is in good agreement with that reported in the literature (also see Chapter 12.3).[207, 208]

15.7: Experiments from Chapter 13

15.7.1: (2,2-Dimethyl-1,3-dioxolane)-4-methoxy-*N*-ethylcarbamate (85)

In a round bottomed flask 2.65 g (0.02 mol) of **26** was dissolved in 50 mL of dichloromethane. To the solution 1 mL of triethylamine was added followed by 710 mg (0.01 mol) of ethylisocyanate **(84)**. The reaction mixture was stirred overnight (10-12 h) under nitrogen and the solvent was evaporated under vacuum to obtain 3.9 g (0.019 mol, 95 %) of thick colourless oil. The crude product was purified by column chromatography using diethylether (R_f=0.71) to obtain 2.18 g (0.01 mol, 50 %) of **85** as an analytically pure product.

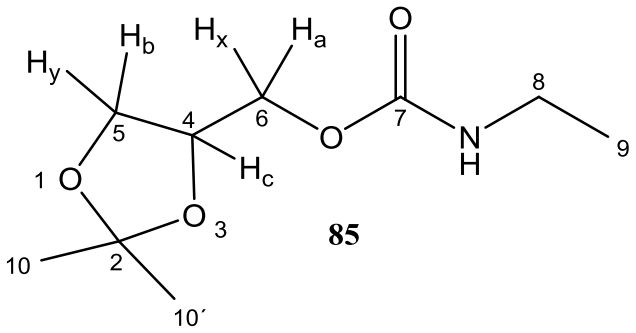

85

^{1}H-NMR (200 MHz, $CDCl_3$): δ = 0.80-0.91 (t, 3 H, 9-H, $^{3}J_{8,9}$ of 7.25 Hz), 1.37 (s, 3 H, 10-H), 1.44 (s, 3 H, 10´-H), 3.15-3.28 (m, 2 H, 8-H), 3.54-3.83 (m, 2 H, 6-H_a, H_x), 4.01-4.34 (m, 3 H, 4-H_c, 5-H_b, H_y), 4.9 ppm (s_b, 1 H, N-H).

^{13}C-NMR (75 MHz, $CDCl_3$): δ = 14.8 (q, C-9), 25.0 (q, C-10), 26.4 (q, C-10´), 35.6 (t, C-8), 64.8 (t, C-6), 66.0 (t, C-5), 73.8 (d, C-4), 109.4 (s, C-2), 155.8 ppm (s, C-7).

MS (GC/MS: Method 2) (EI, 70 eV): *m/z* (%) = 188 (100, $[M^+-CH_3]$), 144 (10, $[CH_2NH]^+$), 101 (80, $[C_5H_{11}O]^+$), 86.1 (5, $[C_5H_{12}N]^+$), 72 (50, $[C_3H_6ON]^+$), 44 (70, $[C_2H_6N]^+$).

IR (diamond-ATR): $\tilde{\nu}$ = 3345 (w), 2984 (m), 2938 (w), 2883 (w), 1710 (s), 1530 (m), 1241 (s), 1215 (m), 1155 (s) cm^{-1}.

Elemental analysis:

Calculated: C 53.19, H 8.43, N 6.89); found: C 52.50, H 8.59, N 6.88)

15.7.2: 3-*tert*-Butoxy-propyl-2-ol-1-*N*-ethylcarbamate (86)

In a round bottomed flask 1.48 g (0.01 mol) of **14** was dissolved in 50 mL of benzene. To the solution 0.1 mL of triethylamine was added, followed by 1.42 g (0.02 mol) of **84**. The reaction mixture was stirred for 24 h under nitrogen at room temperature and the solvent was evaporated under vacuum to obtain 2.163 g (0.09 mol, 98 %) as a viscous colorless liquid. The crude product was subjected to column chromatography using diethylether (R_f=0.48) to obtain in quantitative yield analytically pure **86** as a colorless oil.

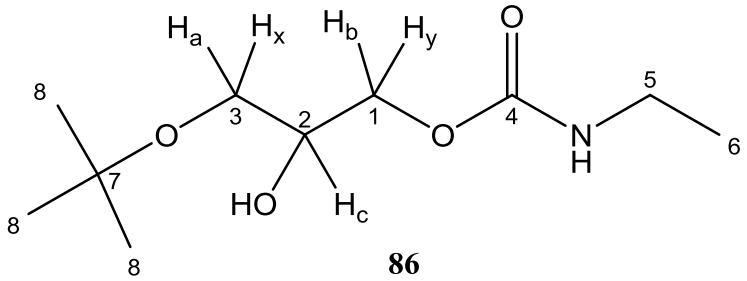

86

^{1}H-NMR (200 MHz, $CDCl_3$): δ = 1.10-1.18 (t, 3 H, 6-H, $^{3}J_{8,9}$ of 7.24 Hz), 1.10 (s, 9 H, 8-H), 2.39 (s_b, 1 H, O-H), 3.16-3.27 (m, 2 H, 5-H), 3.32-3.46 (m, 2 H, 1-H_b, H_y), 3.85-3.95 (m, 1 H, 2-H_c), 4.04 to 4.22 (m, 2 H, 3-H_a, H_x), 4.79 ppm (s_b, 1 H, N-H).

^{13}C-NMR (75 MHz, $CDCl_3$): δ = 15.7 (q, C-6), 27.9 (q, C-8), 36.4 (t, C-5), 63.0 (t, C-1), 66.8 (d, C-2), 70.1 (t, C-3), 73.9 (s, C-7), 156.6 ppm (s, C-4).

MS (GC/MS: Method 2) (EI, 70 eV): *m/z* (%) = 146 (50, $[M^+-C_3H_6NO]$), 132 (50, $[C_4H_6NO_4]^+$), 90 (100, $[C_3H_6NO_2]^+$), 72 (50, $[C_3H_7NO]^+$), 57 (90, $[C_4H_9]^+$).

IR (diamond-ATR): $\tilde{\nu}$ = 3332 (m), 2960 (m), 2932 (m), 2872 (w), 1695 (s), 1535 (s), 1251 (s), 1194 (m), 1148 (s), 1081 (m) cm^{-1}.

Elemental analysis:

Calculated: C 54.77, H 9.65, N 6.39); found: C 54.14, H 9.85, N 6.31

15.7.3: 3-*tert*-Butoxy-propyl-1,2-bis-(*N*-ethylcarbamate) (87)

Procedure 1

In a round bottomed flask 1.48 g (0.01 mol) of **14** was dissolved in 15 mL of benzene. To the solution 100 mg of pyridine was added, followed by 1.42 g (0.02 mol) of **84**. The reaction mixture was stirred for 5 d under nitrogen and the solvent was evaporated under vacuum to obtain 2.85 g of a thick colourless liquid. The crude product was purified by column chromatography with diethylether to obtain 940 mg (0.004 mol, 43 %) of **86** (R_f=0.48) as an analytically pure highly viscous colorless liquid and 580 mg (0.002 mol, 20 %) of **87** (R_f=0.56) as analytically pure solid (m.p. 92 ^oC).

Procedure 2

In a round bottomed flask 3 g (0.02 mol) of **14** was dissolved in 15 mL of benzene. To the solution 400 mg of dry $ZnCl_2$ was added, followed by 1.42 g (0.02 mol) of **84**. The reaction mixture was stirred overnight under nitrogen at 50 ^oC and the solvent was evaporated under vacuum to obtain 4.68 g of a viscous liquid; 2 g of the crude product was subjected to column chromatography using diethylether to obtain 400 mg (0.0018 mol, 21 %) of **86** (R_f=0.48) as an analytically pure thick colorless liquid and 730 mg (0.0025 mol, 28 %) of **87** (R_f=0. 56) as an analytically pure amorphous solid (m.p. 92 ^oC),

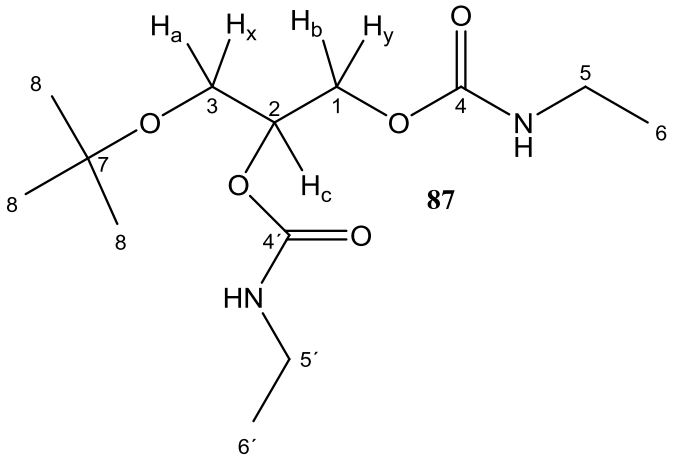

87

^{1}H-NMR (200 MHz, $CDCl_3$): δ = 1.14-1.27 (m, 15 H, 6-H, 6´-H, 8-H), 3.2-3.33 (m, 4 H, 5-H, 5´-H), 3.51-3.55 (m, 2 H, 1-H_b, H_y), 4.08-4.13 (m, 1 H, 2-H_c), 4.26-4.31 (m, 2 H, 3-H_a, H_x), 4.78 ppm (s_b, 1 H, N-H).

^{13}C-NMR (75 MHz, $CDCl_3$): δ = 15.17 (q, C-6, C-6´), 27.2 (q, C-8), 35.7 (t, C-5, C-5´), 60.5 (t, C-1), 63.8 (d, C-2), 67.4 (t, C-3), 73.2 (s, C-7), 155.7, 156.1 ppm (s, C-4, C-4´).

MS (GC/MS: Method 2) (EI, 70 eV): *m/z* (%) = 217 (30, $[M^+-C_3H_6NO]$), 188 (50, $[C_9H_{18}O_3N]^+$), 132 (100, $[C_4H_6NO_4]^+$), 88 (50, $[C_3H_6NO_2]^+$), 72 (50, $[C_3H_7NO]^+$), 57 (90, $[C_4H_9]^+$).

IR (diamond-ATR): $\tilde{\nu}$ = 3332 (m), 2960 (m), 2932 (m), 2872 (w), 1691 (s), 1532 (s), 1247 (s), 1339 (m), 1192 (s), 1150 (m) cm^{-1}.

Elemental analysis:

Calculated: C 53.78, H 9.03, N 9.65; found: C 53.90, H 9.15, N 9.70

15.7.4: Propane-1,2,3-tris-(*N*-ethylcarbamate) (88)

Procedure 1

In a round bottomed flask 920 mg (0.01 mol) of glycerol **(2)** was dissolved in 15 mL of benzene. To the solution 1 mL of triethylamine was added followed by 2.13 g (0.03 mol) of **84**. The reaction mixture was stirred for 72 h under nitrogen. A white precipitate was formed in the reaction mixture which was filtered off. The filtered solid was dissolved in warm chloroform. The impurities were filtered off and the filtrate was evaporated to obtain 1.15 g

(0.003 mol, 37 %) of the desired product **88** as a white amorphous solid melting at 127-130 °C

Procedure 2

In a round bottomed flask 1.84 g (0.02 mol) of glycerol **(2)** was dissolved in 15 mL benzene. To the solution 320 mg of dry $ZnCl_2$ was added followed by 4.26 g (0.06 mol) of ethylisocyanate **(84)**. The reaction mixture was stirred overnight under nitrogen at 50 °C. A white solid precipitated which was filtered off. The thus collected solid was dissolved in warm chloroform and filtered to remove impurities. The solvent from the filtrate was evaporated to obtain 5.98 g (0.019 mol, 98 %) **88** as white amorphous solid melting at 127-130 °C.

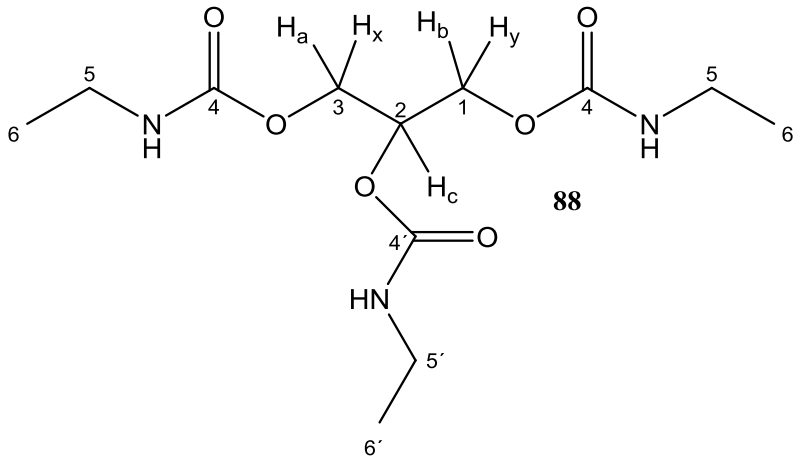

88

^{1}H-NMR (400.1 MHz, $CDCl_3$): δ = 1.10-1.13 (t, 6 H, 6-H, $^3J_{8,9}$ = 7.25 Hz), 1.11-1.14 (t, 6´ H, $^3J_{8,9}$ = 7.24 Hz), 3.15 = 3.23 (m, 6 H, 5-H, 5´-H), 4.18 (sb, 4 H, 1-H_b, H_y, 3-H_a, H_x), 5.13 ppm (s_b, 4 H, 2-H_c, N-H).

^{13}C-NMR (100.1 MHz, $CDCl_3$): δ = 14.92 (q, C-6), 14.95 (q, C-6´), 35.8 (t, C-5), 62.9 (t, C-1, C-3), 70.1 (d, C-2), 155.4 (s, C-4), 155.9 ppm (s, C-4´).

MS (EI, 70 eV): *m/z* (%) = 328 (100, $[M^+ + Na]$), 217 (50, $[C_9H_{17}O_4N_2]^+$).

IR (diamond-ATR): $\tilde{\nu}$ = 3331 cm^{-1} (m), 2959 cm^{-1} (m), 2932 (m), 2872 (w), 1691 (s), 1534 (s), 1250 (s), 1148 (m) cm^{-1}.

Elemental analysis:

Calculated: C 47.2, H 13.76, N 13.76, found: C 44.70, H 7.43, N 13.21

15.8: Experiments from Chapter 14

15.8.1: *cis*-9-Octadecenoic hydrazide (105) and *n*-octadecenoic hydrazide (106)

10 g (33.6 mmol) of RME **(94-98)** and 60 mL of hydrazine monohydrade **(90)** were placed in a round bottomed flask. The reaction mixture was heated for 6 h at 140 ^{o}C. The resulting product mixture was allowed to cool down and stirred overnight at room temperature. A yellowish white solid separated during this period. The liquid part of the product mixture was decanted and the solid was dissolved in dichloromethane and further filtered to separate the sparingly soluble solid. The organic layer was washed twice with H_2O, dried over $MgSO_4$ and evaporated to yield 9.2 g (91 %) of the crude product mixture. The mixture was taken in a separating funnel and heated to 60 ^{o}C. The 7.4 g (0.025 mol, 76 %) of low melting compound **105** separated out, leaving 1.7 g (5.6 mmol, 17 %) of **106** in the separating funnel.

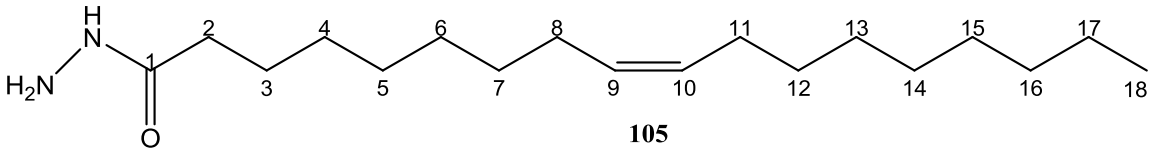

105

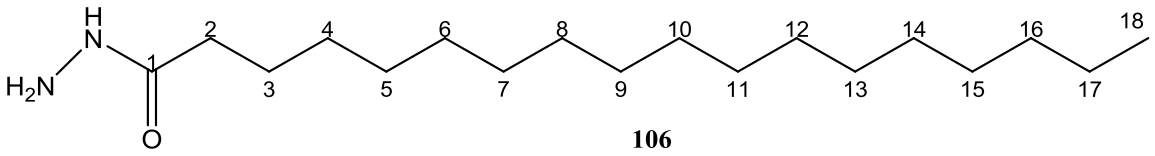

106

105:

^{1}H-NMR (200.1 MHz, $CDCl_3$): δ = 0.84-0.91 (t, 3 H, 18-H), 1.25-1.30 (t, 18 H, 4,5,6,7,12,13,14,15,16-H), 1.6-1.92 (qi, 2 H, 3-H), 1.99-2.18 (qi, 4 H, 8-H, 11-H), 2.7-2.8 (t, 2H, 2-H), 4.88 (s, 2 H, NH_2), 5.31-5.37 (m, 2 H, 9-H, 10-H), 6.93 ppm (s, 1 H, NH).

^{13}C-NMR (50.1 MHz, $CDCl_3$): δ=14.7 (q, C-18), 23.2 (t, C-17), 26.1 (t, C-16), 27.8 (t, C-15), 29. 7 (t, C-14), 29. 8 (t, C-13), 29. 9 (t, C-12, C-7), 30. 1 (t, C-6), 30.3 (t, C-5), 30.37 (t, C-11, C-8), 32.5 (t, C-3), 35.1 (C-2), 130.3 (d, C-10), 130.6 (d, C-9), 173 ppm (s, C-1).

MS (GC/MS: Method 2) (EI, 70 eV): *m/z* (%) = 296 (5, $[M]^+$), 265 (20, $[C_{18}H_{33}O]^+$), 41 (60, $[C_3H_6]^+$).

IR (diamond-ATR): $\tilde{\nu}$ = 3317 (m), 3295 (m), 3919 cm^{-1} (s), 2850 (s), 1629 (s), 1534 (m), 1379 (w) cm^{-1}.

106:

^{1}H-NMR (200.1 MHz, $CDCl_3$): δ = 0.84-0.90 (t, 3 H, 18-H), 1.25 (s, 28 H, 17 to 4-H), 1.63-1.97 (qi, 2H, 3-H), 2.02-2.18 (t, 2H, 3-H), 3.89 (s, 2H, NH_2), 6.71 ppm (s, 1H, NH)

^{13}C-NMR (50.1 MHz, $CDCl_3$): δ = 14.4 (q, C-18), 23.6 (t, C-17), 26.3 (t, C-16), 27.6 (t, C-15), 29. 8 (t, C-14), 29. 9 (t, C-13), 30.0 (t, C-12, C-7), 30.1 (t, C-6), 30.3 (t, C-5), 30.36 (t, C-11, C-8), 32.5 (t, C-3), 35.2 (C-2), 173.3 ppm (s, C-1).

MS (GC/MS: Method 2) (EI, 70 eV): *m/z* (%) = 298 (20, $[M]^+$), 267 (20, $[C_{18}H_{33}O]^+$), 87 (80, $[C_6H_{15}]^+$), 74 (100, $[C_2H_5N_2O]^+$),41 (100, $[C_3H_6]^+$).

IR (diamond-ATR): $\tilde{\nu}$ = 3317 (m), 3290 (m), 3200 cm^{-1} (w), 2957 (s), 2849 (s), 1628 (s), 1534 (m), 1339 (m), 1329 (m) cm^{-1}.

These analytical data are in good agreement with those reported in the literature.[241-246]

15.8.2: Reduction of RME on Pd/C (107)

In a 25 mL hydrogenation flask 5 g (17 mmol) of RME **(94-98)** was dissolved in 10 mL of diethylether and 500 mg of a Pd/C catalyst was added. The mixture was stirred under hydrogen with a magnetic stirrer for 12 h. The catalyst was filtered off and the solvent was evaporated to obtain 4.8 g (16.1 mmol, 96 %) of the colourless solid **107** melting at 30-35 °C.

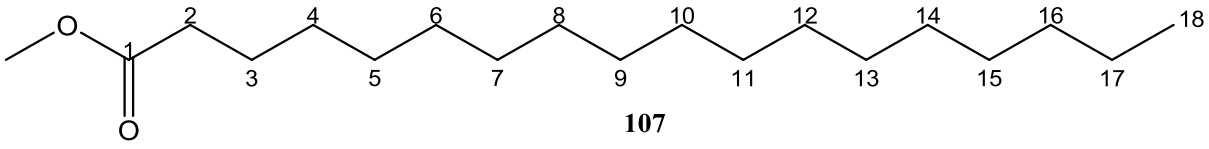

107

^{1}H-NMR (200.1 MHz, $CDCl_3$): δ = 0.85-0.92 (t, 2 H, 18-H), 1.27 (s, 28 H, 4 to17-H), 1.44-1.66 (qi, 2 H, 3-H), 2.2-2.3 (t, 2H, 3-H), 3.67 ppm (s, 3H, Me-H)

^{13}C-NMR (50.1 MHz, $CDCl_3$): δ = 14.0 (q, C-18), 22.7 (t, C-17), 24.9 (t, C-16), 29.7 (t, C-14-4), 31.9 (t, C-3), 34.1 (t, C-2), 51.3 (q, C-CH_3), 174 ppm (s, C-1).

MS (GC/MS: Method 2) (EI, 70 eV): *m/z* (%) = 217 (30, $[M^+-C_3H_6NO]$), 188 (50, $[C_9H_{18}O_3N]^+$), 132 (100, $[C_4H_6NO_4]^+$), 88 (50, $[C_3H_6NO_2]^+$), 72 (50, $[C_3H_7NO]^+$), 57 (90, $[C_4H_9]^+$).

IR (diamond-ATR): $\tilde{\nu}$ = 2952 (s), 2917 (s), 2849 (s), 1740 (s), 1213 (m) cm^{-1}.

These analytical data are in good agreement with those reported in the literature.[250]

15.8.3: Stearic hydrazide (106) from 107

In a 50 mL round bottomed flask 3 g (10 mmol) of **107** was placed, 15 mL of $N_2H_4.H_2O$ was added and the mixture refluxed for 6 h and stirred overnight at room temperature. A white solid precipitated which was filtered off and washed with 10 mL of dist. H_2O and twice with 5 mL dichloromethane. Upon drying and evaporation of the solvent 2.69 g (9 mmol, 90 %) of hydrazide **106** melting at 104-110 ^oC was obtained.

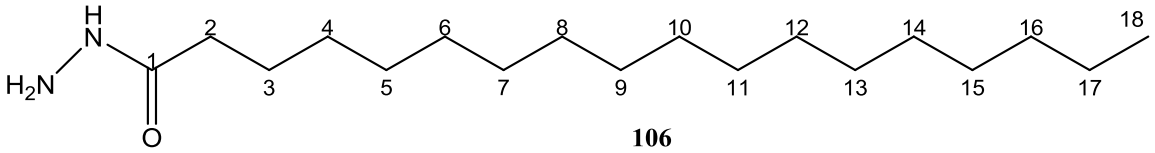

106

The analytical data agree with the data reported above (15.8.1).

Chapter 16 References

Chapter 1

[1] R. Christoph, B. Schmidt, U. Steinberner, W. Dilla, R. Karinen, *Ullmann's Encyclopedia of Industrial Chemistry Published by Wiley-VCH, Weinheim*. **2006**.

[2] M. Pagliaro, R. Ciriminna, H. Kimura, M. Rossi, C. D. Pina, *Angew. Chem. Int. Ed*., **2007**, *46*,2–20, *Angew. Chem.* **2007**, *119(24)*, 4516-4522.

[3] Physical properties of glycerine and its solutions, *Glycerine Producers Association, New York*. **1963**.

[4] D. J. Anneken, S. Both, R. Christoph, G. Fieg, U. Steinberner, A. Westfechtel, *Ullmann's Encyclopedia of Industrial Chemistry*. **2006**.

[5] http://journeytoforever.org/biodiesel_glycerin.html

[6] http://www.theglycerolchallenge.org/

[7] http://www.frost.com/prod/servlet/market-insight-top.pag?docid=70283330

[8] A. R. Carr, R. E. Townsend, W. L. Badger, *Ind. Eng. Chem.* **1925**, *17*, 643-646

[9] L. W. Bosart, A. O. Snoddy, *Ind. Eng. Chem.* **1927**, *19*, 506-510.

[10] L. W. Bosart, A. O. Snoddy, *Ind. Eng. Chem.* **1928**, *20*, 1377-1379.

[11] A. M. Comey, C. F. Bakus, *Ind. Eng. Chem.* **1910**, *2*, 11-16.

[12] B. C. McEwen, *J. Chem. Soc.* **1923**, *123*, 2279.

[13] D. F. Stedman, *Trans. Faraday soc.* **1928**, *24*, 289-289.

[14] A. Richardson, *J. Chem. Soc.* **1886**, *49*, 761-765.

[15] J. B. Segur, K. Oberstar, *Ind. Eng. Chem.* **1951**, *43*, 2117-2120.

[16] M. L. Sheeley, *Ind. Eng. Chem.* **1932**, *24*, 1060-1064.

[17] W. M. Jackson, J. S. Drury *Ind. Eng. Chem.* **1959**, *51*, 1491-1494.

[18] H. J. Masson, W. F. Hamilton, *Ind. Eng. Chem.* **1928**, *20*, 813-816.

[19] O. Dean, H. Allen, Z. Karl, H. Kevin, *WO942305.* **2000**, *EP1006174*, **2002**.

[20] B. Gutsche, *Fett/Lipid.* **1997**, *99*, 418–427.

[21] http://www.cartage.org.lb/en/themes/Reference/dictionary/Biologie/G/13.html **(05/2010)**

[22] F. T. Tymstra, *Shell Dev. Co., US 2 605293*. **1952**.

[23] K. B. Cofer, *Shell Dev. Co., US 2 810 768*. **1957**.

[24] H. D. V. Finch, A. D. Benedictis, *Shell Dev. Co., US 2 779 801*. **1957**.

[25] M. Wyszogrodzka, K. Möws, J. Wodzin´ska, B. Plietker, R. Haag, *Eur. J. Org. Chem.* **2008**, *1*, 53–63.

[26] K. B. Sharpless, K. Akashai, *J. Am. Chem. Soc*. **1976**, *98*, 1986-1987.

Chapter 2

[27] A. Radich, *Biodiesel Performance, Costs, and Use, Energy Information Administration (EIA).* Anonymous, European Biodiesel Standard DIN EN 14214, Beuth-Verlag, Berlin, **2003**. [www.beuth.de]

[28] W. Körbitz, *Renewable Energy*, **1999**, *16*, 1078-1083.

[29] a) W. R. Nitske, C. M. Wilson, *Rudolf Diesel, Pioneer of the Age of Power*, University of Oklahoma Press, Norman, Oklahoma, **1965**. Historical prospective on vegetable oil based fuels *Industrial Oils, 12,* **2001**. b) R. Diesel, *Die Entstehung des Dieselmotors, Verlag von Julius Springer, Berlin*, **1913**.

[30] G. Knothe, J. V. Gerpen, J. Krahl, *The Biodiesel Handbook, AOCS press*, **2005**

[31] Western Biofuels, http://www.westernbiofuelsinc.com/

[32] European biodiesel board-statistics, http://www.ebb-eu.org/ **(05/2010)**

[33] M. Bloch, L. Bournay, D. Casanave, J. A. Chodorge, V. Coupard, G. Hillion, D. Lorne, *Oil & Gas Science and Technology, Rev. IFP,* **2008**, *63*,405-417.

[34] J. Krahl, A. Munack, D. Bockey, *Landbauforschung Völkenrode,* **2007**, *57,* 415-418.

[35] D. Bockey**,** *Biodiesel in Germany 2006: Market Trends and Competition***,** *Union for Promoting Oil and Protein Plants.* http://www.biofuelstp.eu/downloads/070329_document_Biodieselreport2006.pdf **(05/2010)**

[36] a) H. Tschöke, G. Braungarten, U. Pitze, *Oil dilution of a passenger car diesel engine in operation with blended diesel fuel B10*, Promotion report-22010007 (07Nr100), **2009**, b) M. J. Thornton, T. L. Alleman, J. Luecke, R. L. McCormick, *Presented at the 2009 SAE International Powertrains, Fuels, and lubricants meeting,* **2009**

[37] http://www.researchandmarkets.com/reports/338596/338596.htm **(05/2010)**

[38] http://www.ufop.de/1299.php,www.power-technology.com/features/feature58850/ **(05/2010)**

[39] M. Johnston, T. Holloway, *Environ. Sci. Technol.*, **2007**, *41(23)*, 7967-7973.

[40] J. Rathbauer, D. Bacovsky, H. Prankl, M. Wörgetter, W. Körbitz, *Local and innovative Biodiesel new feedstock blending recipes for improved fuel properties,*

http://www.blt.bmlf.gv.at/vero/veroeff/0886_Local_and_innovative_biodiesel.pdf **(05/2010)**

[41] http://www.biodiesel.org/markets/pre/WilliamsColdFlowTestingReport.pdf **(05/2010)**

[42] http://www.astm.org/Standards/D6371.htm **(05/2010)**

[43] http://edition.cnn.com/2007/WORLD/asiapcf/11/08/greenpeace.palmoil/index.html **(08/2007)**

[44] H. Iki, Y. Iguchi**,** A. Koyama**,** Applicability of hydrogenated palm oil for automotive fuels, *16th Soudi arabia-Japan Joint Symposium, November 5-6,* **2006**

[45] L. Canoira, R. Alcantara, S. Torcal, N. Tsiouvaras, E. Lois, D. M. Korres, *Fuel* **2007**, *86*, 965–971.

[46] N. U. Soriano, Jr., P. V. Migo, M. Matsumura, *Eur. J. Lipid Sci. Technol.* **2005**, *107*, 689–696.

[47] N. U. Soriano Jr., P. V. Migo, K. Sato, M. Matsumura, *Fuel* **2006**, *8*, 25–31.

[48] E. H. Pryde, D. E. Anders, H. M. Teeter, J. C. Cowan, *J. Org. Chem.* **1959**, *25*, 618-621.

[49] E. H. Pryde, *J. Org. Chem.* **1966**, *35*, 412-419.

[50] R. G. Ackman, M. E. Retson, L. R. Gallay, F. A. Vandenhuvel, *Can. J. Chem.* **1961**, *39*, 1956-1963.

Chapter 3

[51] R. L. McCormick, *Environ. Sci. Technol*. **1997**, *31*, 1144-1150.

[52] M. Pagliaro, R. Ciriminna, H. Kimura, M. Rossi, C. D. Pina, *Angew. Chem. Int. Ed.* **2007**, *46*, 2–20, *Angew. Chem.* **2007**, *119*, 4516-4522.

[53] W. Dabelstein, A. Reglitzky, A. Schütze, K. Reders, Automotive Fuels, *Ullmann's Encyclopedia of Industrial Chemistry*. **2007**

[54] http://inventors.about.com/library/weekly/aacarsgasa.htm **(05/2010)**

[55] http://www.aboutmycar.com/category/car_history/creation_history/n-otto-four-stroke-engine-invention-1176.htm **(05/2010)**

[56] http://library.thinkquest.org/C006011/english/sites/ottomotor.php3?v=2 **(05/2010)**

[57] http://www.keveney.com/otto.html **(05/2010)**

[58] www.schoolscience.co.uk

[59] T. C. Schmidt, H. A. Duong, M. Berg, S. B. Haderlein, *Analyst.* **2001**, *126*, 405–413

[60] http://www.refiningonline.com/engelhardkb/crep/tcr4_29.htm **(05/2010)**

[61] http://hubpages.com/hub/Fuels-With-High-Octane-Number **(05/2010)**

[62] http://www.astm.org/Standards/D2700.htm **(05/2010)**

[63] http://files.asme.org/ASMEORG/Communities/History/Landmarks/5519.pdf **(05/2010)**

[64] www.ems.psu.edu/~boehman/facilities.html **(05/2010)**

[65] http://library.thinkquest.org/C006011/english/sites/diesel.php3?v=2 **(05/2010)**

[66] DOE Fundamentals handbook, *Mechanical science*, *Department of energy, USA* Volume 1&2, **1993**

[67] Encyclopedia Britannica inc. **2007**, (www.britannica.com)

[68] http://rb-kwin.bosch.com. (keyword: CRS) **(05/2010)**

[69] W. W. Irion, O. S. Neuwirth, Oil refining, *Ullmann's Encyclopedia of Industrial Chemistry*. **2005**.

[70] T. Yonei, K. Hashimoto, M. Arai, M. Tamura, *Energy Fuels.* **2003**, *17*, 725-730.

[71] http://www.astm.org/Standards/D976.htm **(05/2010)**

Chapter 4

[72] http://www.innovatia.com/Design_Center/rktprop2.htm **(05/2010)**

[73] M. Votsmeier, T. Kreuzer, G. Lepperhoff, Automobile Exhaust controll, *Ullmann's Encyclopedia of Industrial Chemistry*. **2005**

[74] http://www.stealth316.com/2-safcii-adjust.htm (emission curves from Tayota motor sales literature) **(05/2010)**

[75] http://www.epa.gov/oms/invntory/overview/pollutants/hydrocarbons.htm **(05/2010)**

[76] http://www.epa.gov/otaq/invntory/overview/pollutants/carbonmon.htm **(05/2010)**

[77] http://cdiac.ornl.gov/ **(05/2010)**

[78] http://www.umweltbundesamt-daten-zur-umwelt.de/umweltdaten/public/document/downloadImage.do?ident=17876 **(05/2010)**

[79] http://www.who.int/mediacentre/factsheets/fs313/en/ **(05/2010)**

[80] J. S. Evans, S. K. Wolff, K. Phonboon, J. I. Levy, K. R. Smith, *Chemosphere*. **2002**, *49*, 1075-1091.

[81] http://www.epa.gov/oms/invntory/overview/pollutants/pm.htm **(05/2010)**

[82] http://www.epa.gov/oms/invntory/overview/pollutants/nox.htm **(05/2010)**

[83] S. Fearnando, C. Hall, S. Jha, *Energy and Fuels.* **2006**, *20*, 376-382.

[84] Allied Environmental Technologies Inc., *The Formation of NOx*. **2005**. http://www.alentecinc.com/papers/NOx/The%20formation%20of%20NOx_files/The%20formation%20of%20NOx.htm **(05/2010)**

[85] http://202.185.100.7/homepage/fluent/html/ug/node624.htm. **(05/2010)**

[86] C. P. Fenimore, Formation of Nitric Oxide in Premixed Hydrocarbon Flames, *In 13th Symp. (Int'l.) on Combustion*,. The Combustion Institute. **1971**, 373.

[87] S**.** Archer, A. K. Gupta, *37th lntersociety Energy Conversion Engineering Conference.* **2002**, 364-369.

[88] http://202.185.100.7/homepage/fluent/html/ug/node625.htm **(05/2010)**

[89] J. Song, V. Zello, A. L. Boehman, F. J. Waller, *Energy and Fuels*, **2004**, *18*, 1282-1290.

[90] J. Li, J. O. Chae, S. B. Park, S. B. Paik, *SAE Tech. Paper No. 970322*. **1997**.

[91] R. B. Poola, D. E. Longman, K. Callaghan, R. Sekar, *SAE Tech. Paper No. 2000-01-0228.* **2000**.

[92] T. Ullman, R. Mason, D. Montalvo, *Coordinating Research Council, Southwest Research Institute, Santiago, TX*. **1990**.

[93] R. L. McCormick, J. D. Ross, M. S. Graboski, *Environ. Sci. Technol*. **1997**, *31*, 1144–1150.

[94] G. Labeckas, S. Slavinskas, *Energy Conversion and Management*. **2006**, *47*, 1954–1967.

[95] R. L. McCormick, J. R. Alvarez, M. S. Graboski, *NOx solutions for Biodiesel, National energy research laboratory*. **2003**.

[96] R. L. McCormick, M. S. Graboski, T. L. Alleman, A. M. Herring, K. S. Tyson, *Environ. Sci. Technol.* **2001**, *35 (9)*,1742-1747.

Chapter 5

[97] http://www.dieselnet.com/standards/eu/ld.php **(05/2010)**

[98] T. Johnson, *Platinum Metals Rev.* **2008**, *52 (1)*, 23–37

[99] http://www.platinumrecoveries.com/news/autocatalysts.php **(05/2010)**

[100] http://www.aecc.eu/en/Technology/Catalysts.html **(05/2010)**

[101] http://www.catalysis.nsk.su/envicat/rnd/3.htm **(05/2010)**

[102] I. Chorkendorff, J. W. Niemantsverdriet, *Concepts of Modern Catalysis and Kinetics.* **2003,** 382-383.

[103] http://www.motorspain.com/28-08-2007/varios/tecnologia/cientificos-espanoles-descubren-como-mejorar-los-catalizadores **(05/2010)**

[104] H. J. Borg, J. M. Reijerse, R. A. van Santen, J. W. Niemantsverdrieta, *J. Chem. Phys*. **1994**, *101 (11)*, 10052-10063.

[105] C. P. Vinod, J. W. N. Hans, B. E. Nieuwenhuys, *Applied Catalysis A: General*. **2005**, *291*, 93–97

[106] M. J. P. Hopstaken, J. W. Niemantsverdrieta, *J. Chem. Phys*. **2000**, *113 (13)*, 5457-5465.

[107] K. Walker, *J. R. Agric. Soc. Engl*, **1994**, *155*, 43-44.

[108] http://www.chevron.com/prodserv/fuels/bulletin/diesel/L2_6_8_rf.htm **(05/2010)**

[109] http://www.amc.edu.au/research/areas/marine.engines/projects/ **(05/2010)**

[110] http://www.ammoniapro.com/Ammonia%20Library/ **(05/2010)**

[111] C. Dossi, A. Fusi, S. Recchia, R. Psaro, G. Moretti, *Microporous and Mesoporous Materials*. **1999**, *30 (11)*, 165-175.

[112] C. Ciardelli, I. Nova, E. Tronconi, B. Konrad, D. Chatterjee, K. Ecke, M.Weibel, *Chemical Engineering Science*. **2004**, *59*, 5301–5309.

[113] T. Beutel, J. Srkny, G.D. Lei, J. Y. Yan, W. M. H. Sachtler, *J. Phys. Chem*. **1996**, *100*, 845-851

[114] NAIAS Detroit 2007: Volkswagen continues BLUETEC offensive **(05/2010)**

[115] N. U. Zhanpeisov, S. Higashimoto, M. Anpo, *Int. J. Quant. Chem*. **2001**, *84*, 677–685.

[116] http://www.greencarcongress.com/2008/03/johnson-matthey.html **(05/2010)**

[117] www.findadblue.com **(05/2010)**

[118] M. Imanari, T. Koshikawa, H. Akihiro, F. Masayuki, *US 4833113*. **1988**.

[119] J. W. Byrne**,** *Engelhard Corporation, US 4961917*. **1990**.

[120] Johnson Matthey emission control technologies, http://ect.jmcatalysts.com/ (> technologies>SCR catalyst>Ammonia-SCR) **(05/2010)**

[121] G. Stephen Jr., S. Iretskaya, *WO 2008085265, US 2008166282*. **2008**.

[122] a) S. Fernando, C. Hall, S. Jha, *Energy and Fuel*, **2006**, *20 (1)*, 376-382, b) N. V. Heeb, P. Schmid, *Environ. Sci. Technol*. **2010,** *44*, 1078–1084.

Chapter 6

[123] http://www.efoa.org/index.html **(05/2010)**

[124] R. L. McCormick, J. D. Ross, M. S. Graboski, *Environ. Sci. Technol*. **1997**, *31*, 1144–1150.

[125] a) E. C. Zabetta, M. Hupa, K. Saviharju, *Ing. Eng. Chem. Res.* **2005**, *44*, 4552-4561, b) J. K. Arand, L. J. Majio, D. P. Teixeria, *US 4325924 A*, **1982**.

[126] R. K. Lyon, *US 3900554*, **1975**.

[127] a) T. R. Brogan, *US 4335084*, **1982**. b) J. R. Gladden, *US 4403473*, **1983**, c) M. Atsukawa, N. Ukawa, K. Matsumoto, *US 4302431*, **1981**, d) J. T. Leach, *US 4981660*, **1991**. e) H. Kobayashi, L. E. Bool, *US 6702569 B2*, **2004**, f) B. P. Breen, R. W. Glickert, *US 6030204*, **2000**, g) M. M. Johonson, *US 3049872*, **1962**, i) J. M. Valentine, *US 5535708*, **1996.**

[128] a) D. R. Poole, W. M. Graven, *J. Am. Chem. Soc.* **1961,** *83*, 283-286, b) W. Weissman, *US 5947080*, **1999**.

[129] a) A. J. Reiter, S. C. Kong, *Energy & Fuels*, **2008**, *22(5)*, 2963-2971, b) E. R. Stephens, R. N. Pease, *J. Am. Chem. Soc.* **1950,** *72*, 1188-1190, c) M. Farber, A. J. Darnell, *J. Chem. Phys.*, **1954**, *22*, 1261-1263, d) G. E. Moore, K. E. Shuler, S. Silverman, R. Herman, *J. Phys. Chem.*, **1956**, *60*, 813-814, e) C. P. Fenimore, G. W. Jones, *J. Phys. Chem.*, **1961**, *65*, 298-303, f) T. Itoh,Y. Matsuya, H. Maeta, M. Miyazaki, K. Nagata, A. Ohsawa, *Chem. Pharm. Bull.*, **1999**, *47(6)*, 819-823, g) J. A. Miller, M. D. Smooke, R. M. Green, R. J. Kee, *Combustion and Flame*, **1981**, *43*, 81-84, h) J. A. Miller, C. T. Bowman, *Prog. Energy, Combustion and Science*, **1989**, *15 (4)*, 287-338, i) D. M. Dramlic, z. J. Grsic, M. M. Popovic, *Journal of Environmental Protection and Ecology*, **2002**, *3(2)*, 519-526, j) R. P. Lindstedt, F. C. Lockwood, M. A. Selim, *Combustion Science and Technology*, **1994**, *99*, 253-276, k) D. L. Baulch, C. J. Cobos, R. A. Cox, C. Esser, P. Frank, J. A. Kerr, R. W. Warnatz, *J. Phys. Chem*, **1992**, *21*, 411-420.

Chapter 7

[130] www.dieselnet.com **(05/2010)**

[131] a) A. Martyr, M. A. Plint, *Engine testing*. **2006**, 337-338. b) Dr. W. Peter, *EP:1893987-B1*

Chapter 8

[132] M. S. Malinovskii, V. M. Vvedenskii, *Zhurnal. Obshchei. Khimii*. **1953**, *23*, 219-20

[133] V**.** P. Guptha, *US 5476971*. **1995**.

[134] C. Dewattines, H. Hinnekens, *EP 649 829 B1*. **1995**.

[135] R. Wessendorf, G. Wilfried, *EP 718270 A2*. **1996**.

[136] A. Behr, L. Obendorf, *Chemie Ingenieur Technik*. **2001**, *73(11)*, 1463-1467.

[137] E. Breitmaier, *Structural Elucidation By NMR In Organic Chemistry*, John Wiley & Sons. **1993**, 54-56.

[138] X. Han, X. Chen, R. W. Gross, *J. Am. Chem. Soc.* **1991**, *113*7, 104-7109.

[139] I. Pascher, *Curr. Opin. Struct. Biol*. **1996**, *6 (4)*, 439-448

[140] H. Hirschmann, *J. Biol. Chem*. **1960**, *235(10)* 2762-2767

[141] R. S. Cahn, C. K. Ingold, V. Prelog, *Experientia*. **1956**, *12*, 81-86

Chapter 9

[142] E. Fischer, *Ber. Dtsch. Chem. Ges.* **1894**, *27*, 3189-3232.

[143] M. S. Newman, M. Renoll, *J. Am. Chem. Soc.* **1945**, *67 (9)*, 1621-1621.

[144] K. D. Thiele, M. A. Kausemaker, *WO 2005010131 A1*. **2005.**

[145] G. M. Clode, *Chem. Rev.* **1979**, *79*, 491-513.

[146] W. J. Baumann, *J. Org. Chem*., **1971**, *36 (19)*, 2743-2747

[147] W. E. Willy, G. Binsch, E. L. Eliel, *J. Am. Chem. Soc.* **1970**, *92*, 5394-5402.

[148] R. U. Lemieux, J. D. Stevens, R. R. Fraser, *Can. J. Chem*, **1962**, *40*, 1955-1957.

[149] M. Anteunis, F. Alderweireldt, *Bull. Soc. Chim. Belges.* **1964**, *73*, 889-893.

[150] A. Espinosa, M. A. Gallo, J. Campos, A. Entrina, E. Camacho, *Magn. Res. Chem*. **1986**, *24*, 754-757.

[151] A. Espinosa, M. A. Gallo, J. Campos, A. Entrina, E. Camacho, *Magn. Res. Chem.* **1988**, *26*, 108-110.

[152] D. M. Clode, *Chem. Rew*. **1979**, *79 (6)*, 491-513 *and references therein.*

[153] A. Barker, E. J. Bourne, R. M. Pinkard, M. Stacey, D. H. Whiffen, *J. Chem. Soc.* **1958**, 3232-3238.

[154] H. Hibbert, S. Hill, *J. Am. Chem. Soc.* **1923**, *45 (17)*, 734.

[155] H. Adkins, A. E. Broderick, *J. Am. Chem. Soc.* **1928,** *50 (2)*, 499-502.

[156] T.H. Fife, L. K. Jao, *J. Org. Chem*. **1965**, *30*, 1492-1495.

[157] R. B. Tuner, D. E. Nettleton. Jr, M. Perelman, *J. Am. Chem. Soc.* **1958**, *80 (6)*, 1430-1433

[158] D. J. Triggel, B. Bellieu, *Can. J. Chem*. **1962**, *40*, 1201-1206.

[159] A. Mucci, L. Schemetti, L. Brasili, L. Malmusi, *Magn. Res. Chem.* **1995**, *33*, 167-173.

[160] D. J. Pasto, F. M. Klein, T. W. Doyle, *J. Am. Chem. Soc.* **1967**, *89 (17)*, 4368-4374.

[161] N. Baggett, J. M. Duxburry, A. B. Foster, J. M. Webber, *Carbohyd. Res.* **1966**, *2*, 216-219

[162] H. K. Garner, H. J. Lucas, *J. Am. Chem. Soc.* **1950**, *72 (12)*, 5497-5501.

[163] J. G. Pritchard, P. C. Lauterbur, *J. Am. Chem. Soc.* **1961**, *83*, 2105-2110.

[164] C. H. Green, D. G. Heller, *J. C. S. Perkin Trans-II*. **1973**, *14*, 1966-1973.

[165] C. H. Green, D. G. Heller, *J. C. S. Perkin Trans-II*. **1973**, *3*, 243-252.

[166] C. H. Green, D. G. Heller, *J. C. S. Perkin Trans-II*. **1975**, *2*, 190-193.

[167] P. Chochrek, J. Frelek, M. Kwit, J. Wicha, *J. Org. Chem*. **2009**.

[168] G. Snatzke, *Angew. Chem. Int. Ed. Engl*. **1979**, *18*, 363-377, *Angew. Chem.***1979**, *91*, 380-393

[169] M. Anteunis, D. Danneels, *Org. Magn. Res*. **1975**, *7*, 345-348.

[170] G. W. Buchanan, J. B. Stothers, G. Wood, *Can. J. Chem*. **1973**, *51*, 3746-3751.

[171] R. J. Abraham, *J. Chem. Soc*. **1965**, 256-262.

[172] V. Tabacik, *Tet. Lett*. **1968**, *555*, 561-568.

[173] J. B. Lambert, *J. Amer. Chem. Soc*. **1967**, 89, 1836-1840.

[174] M. Lemaire, J. Bolte, *Tetrahedron Asymm*. **1999**, *10*, 4755-4762.

Chapter 10

[175] W. J. Pope, F. G. Mann, *Compt. rend*. **1924**, *176*, 2085-2086.

[176] M. M. Green, R. A. Gross, C. Crosby, F. C. Schilling, *Macromol*. **1987**, *20(5)*, 992-998.

[177] E. Baer, H. O. L. Fischer, *J. Am. Chem. Soc*. **1948**, *70 (2)*, 609-610.

[178] G. Pelletier, *Chem. Ind*. **1953**, 1034.

[179] F. S. Gibson, M. S. Park, H. Rapoport, *J. Org. Chem*. **1994**, *59*, 7503-7507

[180] B. A. Belinka. Jr, A. Hassner, *J. Org. Chem*. **1979**, *44*, 4712-4713.

[181] P. R. Rablen, R. W. Hoffmann, D. A. Hrovat, W. T. Borden, *J. C. S. Perkin Trans-II*. **1999**, 1719-1726.

[182] C. J. Nielsen, K. Kosa, H. Priebe, C. E. Sjøgren, *Spectrochimica Acta*. **1988**, *44A(4)*, 409-422.

[183] L. S. Sonntag, S. Sschweizer, C. Ochsenfeld, H. Wennemers, *J. Am. Chem. Soc*. **2006**, *128*, 14697-14703.

[184] J. B. Lambert, A. R. Vagenas, *Org. Mag. Res*. **1981**, *17 (4)*, 270-277.

[185] C. J. Nielsen, P. Klaeboe, H. Priebe, S. H. Schei, C. E. Sjøgren, *J. Mol. Struct*. **1986**, *141*, 161-172.

[186] N. Hadjililiadias, A. Doit, T. Theophanides, *Can. J. Chem*. **1972**, *50*, 1005-1007.

[187] A. Yokozeki, K. Kuchitsu, *Bull. Chem. Soc. Japan*. **1971**, *44*, 2926-2930.

[188] P. Bultinck, A. Goeminne, D. Von. De. Vondel, *J. Mol. Struct*. **1995**, *339*, 1-14.

[189] L. V. Lanshina, M. N. Rodnikova, K. T. Dudnikova, *J. Struct. Chem*, **1990**, *31 (4)* 684-687.

[190] M. N. Buslaeva, V. N. Kartsev, K. T. Dudnikova, *Zh. Fij. Khim*. **1982**, *56 (5)*, 1254-1255.

[191] J. Pernak, A. Skrzypczak, G. Lota, E. Frackwiak, *Chem. Eur. J*. **2007**, *13*, 3106-3112.

[192] F. Himo, T. Lovell, R. Hilgraf, V. V. Rostovtsev, L. Noodleman, K. B. Sharpless, V. V. Fokin, *J. Am. Chem. Soc*. **2005**, *127 (1)*, 210-216.

[193] L. Ciavatta, D. Ferri, R. Palombari, *J. Inorg. Nucl. Chem*. **1980**, *42*, 593-598.

[194] B. H. Lipshutz, B. R. Taft, *Angew. Chem. int. Ed*. **2006**, *45*, 82335-8238, *Angew. Chem*. **2006**, *118 (48)*, 8415-8418.

[195] H. G. Colemann, H. W. Host, *J. Am. Chem. Soc*. **1936**, *58*, 2310-2312.

[196] B. M. Trost, A. Bertogg, *Org. Lett*. **2009**, 11(3), 511-513.

[197] C. D. Hurd, F. L. Cohen, *J. Am. Chem. Soc.* **1931**, *53*, 1068-1077.

[198] K. Sonogashira, Y. Tohda, N. Hagihara, *Tett. Lett*. **1975**,*50*, 4467-4470.

[199] K. Sonogashira, Y. Tohda, N. Hagihara, *Synthesis*. **1977**, 777-778.

[200] D. Nightingale, F. Wordsworth, *J. Am. Chem. Soc*. **1945**, *67*, 1626-1629,

Chapter 11

[201] C. M. McLeod, G. M. Robinson, *J. Chem. Soc.* **1921**, *119*, 1470-1476.

[202] G. M. Robinson, R. Robinson, *J. Chem. Soc*. **1923**, *123*, 532-543.

[203] T. D. Stewart, J. G. Aston, *J. Chem. Soc.* **1926**, *48*, 1642-1655.

Chapter 12

[204] J. Barluenga, A. M. Bayon, G. Asensio, *J. Chem. Soc., Chem. Commun*. **1983**, *24*, 1109-1110, *ibid.* **1984**, *24*, 427-429.

[205] L. E. Overman, T. Osawa, *J. Am. Chem. Soc*. **1985**, *107*, 1698-1701

[206] J. Barluenga, A. M. Bayon, P. Campos, *J. Chem. Soc. Perkin Trans. I*. **1988**, 1631-1636

[207] T. Shono, S. Kashimura, *J. Am. Chem. Soc*. **1982**, *104*, 5753-5757, and references therein.

[208] J. Lichtenberger, L. Martin, *Bull. Soc. Chim. Fr*. **1947**, 468-476.

Chapter 13

[209] G. Höfle, W. Steglich, H. Vorbrüggen, *Angew.Chem.* **1978**, *90*, 602-615. *Angew. Chem. Int. Ed. Engl.* **1978**, *17*, 569–583

[210] G. Höfle, W. Steglich, *Angew. Chem. Int. Ed. Engl.* **1969**, *8*, 981–986, *Angew.Chem.* **1969**, *81*, 1001-1006

[211] M. Matzner, R. P. Kurkjy, R. J. Cotter, *Chem.Rev.* **1964**, *64***,** 645-652.

[212] W. M. Kraft, *J. Am. Chem. Soc.* **1948**, *70*, 3569-3574.

[213] BASF, *DE 2910132*. **1979**.

[214] Bayer, *DE 2819826*. **1978**.

[215] P. Jäger, C. N. Rentzea, H. Kieczka, Carbamates and Carbamoyl chlorides, *Ullmann's Encyclopedia of Industrial Chemistry*. **2005**.

[216] B. M. Bhanage, S. Fujita, *Green Chem.* **2004**, *6*, 78-80.

[217] D. Chaturvedi, S. Ray, *Monatshefte für Chemie*. **2006**, *137*, 127–145.

[218] D. Chaturvedi, S. Ray, A. Kumar, *Tetrahedron Letters.* **2003**, *44*, 7637–7639.

[219] T. L. Davis, J. McFarnum, *J. Am. Chem. Soc.* **1934**, *56*, 883-885.

[220] D. S. Tarbell, R. C. Mallatt, J. W. Wilson, *J. Am. Chem. Soc.* **1942**, *64*, 2229-2230.

[221] C. Spino, M. A. Joly, C. Godbout, M. Arbour, *J. Org. Chem.* **2005**, *70*, 6118-6121.

[222] C. Len, D. Postel, G. Ronco, P. Villa, *Phosphorus, Sulphur and Silicon*. **1998**, *133*, 41-59.

[223] T. L. Davis, J. M. Farnum, *J. Am. Chem. Soc*. **1934**, *56*, 883-886.

[224] C. Cox, T. Lectka, *J. Org. Chem.* **1998**, *63*, 2426-2427.

[225] D. M. Soignet, G. J. Boudreaux, R. J. Berni, R. R. Benerito, *Applied Spectroscopy*. **1974**, *28 (4)*, 350-353.

[226] P. R. Rablen, *J. Org. Chem.* **2000**, *65*, 7930-7937.

[227] P. M. Quan, *J. Org. Chem.* **1968**, *33 (10)*, 3937-3938.

[228] M. Oki, H. Nakanishi, *Bull. Chem Soc. Jpn.* **1971**, *44 (11)*, 3148-3151.

[229] J. C. Carter, I. R. Devia, *Spectrochem. Acta*. **1973**, *29 (4)*, 623-632.

[230] H. S. Randhawa, K. G. Rao, C. N. R. Rao, *Spectrochem. Acta*. **1974**, *30 (10)*, 1915-1922.

[231] C. P. Lewis, Anal. Chem. **1964**, *36 (1)*, 176-180.

[232] R. A. Perry, D. L. Siebers, *Nature*, **1986**, *324*, 657-658. Also see Non-catalytic NO*x* removal from gas turbine exhaust with cyanuric acid in recirculating reactor http://www.biofuels.coop/archive/nox_reducer.pdf

[233] a) B. G. Wicke, K. A. Grady, J. W. Ratcliffe, *Nature*, **1989**, *338*, 492-493.b) B. Dorofeeva, O. G. Tarakanov, *Journal of structural chemistry*, **1987**, *27 (4)*, 539-544, c) A. Orzeszko, A. Kolbrecki, *Journal of Applied Polymer Science*, **1980**, *25*, 2969-2973

Chapter 14

[234] H. Paulson, D. Stoye, *The Chemistry of Functional groups*. **1970**, 525-600

[235] P. A. S. Smith, *Org. Reactions*. **1946**, *3*, 366.

[236] F. L. Scott, J. B. Aylward, *Tetrahydron Letters*. **1965**, 6 (13), 841-847.

[237] I. T. Barnish, M. S. Gibson, *J. Chem. Soc.* **1965**, 2999-3001.

[238] E. C. Kornfeld, G. B. Kline, M. J. Mann, R. G. Jones, R. B. Woodward, *J. Am. Chem. Soc.* **1956**, *78*, 3087-3114.

[239] E. D. Nicolides, *J. Org. Chem*. **1967**, *32*, 1251-1253.

[240] R. L. Hinman, *J. Am. Chem. Soc.* **1956**, *78*, 2463-2467.

[241] F. Aylward, C. V. N. Rao, *J. appl. Chem.* **1956**, *6*, 248-252.

[242] C. R. Scholfield, E. P. Jones, j. Nowakowska, E. Selke, H. J. Dutton, *J. Am. Oil Chemists Soc*. **1961**, *38*, 208-209.

[243] *Ibid.*, **1960**, *37*, 579-582.

[244] E. D. Bitner, H. J. Dutton, *J. Am. Oil Chemists Soc*. **1968**, *45*, 603-606.

[245] F. Aylward, M. Sawistowaska, *J. Chem. Soc.* **1964**, 1435-1441.

[246] F. Aylward, C. V. N. Rao, *J. appl. Chem.* **1957**, *7*, 134-137.

[247] a) E. W. Scmidt, Hydrazine and its derivatives, *John Wiely & Sons*. **1983**, 708-712, b) S. Yashodai, S. Govindarajan, *Thermochemica Acta*, **1999**, *338*, 113-123, c) H. W. Lucien, *Journal of Chemical and Engineering Data*, **1961**, *6 (4)*, 584-586

[248] K. Klepacova, D. Mravec, M. Bajus, *Applied Catalysis. A*. **2005**, *249*, 141-147.

[249] R. S. Karinen, A. O. I. Krause, *Applied Catalysis. A*. **2006**, *306*, 128-133.

[250] Commercially available product Sigma Aldrich CAS No.: 112-61-8

List of abbreviations

ASG	Analytic-Service Gesellshaft-mbH
ASTM	American Society of Testing and Materials
A/F ratio (λ)	Air to Fuel Ratio (equivalence ratio)
BTL	Biomass-to-Liquid Transformation
CFPP	Cold Filter Plugging Point
CFR	Cooperative Fuel Research
CRT	Continuously Regenerating Trap
CRFI	Common Rail Fuel Injection System
DPFs	Diesel Particulate Filters
DIPE	Di-isopropyl Ether
DI	Direct Injection Engine
ETBE	Ethyl *tert*-butyl ether
EHN	2-Ethylhexyl nitrate
EPA	Environmental Protection Agency
EGR	Exhaust Gas Recirculation
ESC	European Stationary Cycle
ELR	European Load Response
FAME	Fatty Acid Methyl Ester
FEW	Fuel Water Emulsion
FBC	Fuel Borne Catalyst
HC	Unburned or Partially Oxidized Hydrocarbons
HVO	Hydrogenated Vegetable Oils
IPA	Isopropyl Alcohol
IDI	Indirect Injection Engines
IBA	Isobutyl Alcohol
LNTC	Lean NO*x* Trap Catalyst
LEA	Low Excess Air
MTBE	Methyl *tert*-butyl ether
MON	Motor Octane Number
NMVOC	Non Methane Volatile Organic Compounds
NMHC	Non-Methane Hydrocarbons
OBC	On Board Computer

PM	Particulate Matter
PMP	Particle Measurement Programme
RME	Rapeseed oil Methyl Ester
RON	Research Octane Number
RAPH	Reduced Air Preheat
SME	Soybean oil Methyl Ester
SNCR	Selective Non-Catalytic Reduction
SCR	Selective Catalytic Reduction
TSP	Total Suspended Particles
TAME	*Tert*-amyl methyl ether
TBA	*Tert*-butyl alcohol
TWC	Three-Way Catalytic Converter
vTI	Johann Heinrich von Thünen-Institut
VOCs	Volatile Organic Compounds
WHO	World Health Organization
WSI	Water-Steam Injection